

THE AEGEAN EARTHQUAKE and TSUNAMI OF 30 OCTOBER 2020

A FIELD REPORT BY EEFIT



THE AEGEAN EARTHQUAKE and TSUNAMI OF 30 OCTOBER 2020

Dr Yasemin Didem AKTAS, Epicentre, University College London

Aisling O'KANE, Cambridge University

Dr Ali Tolga OZDEN, Canakkale Onsekiz Mart University

Anil KÖŞKER, Middle East Technical University

Ahsana PARAMMAL VATTERI, Epicentre, University College London

Bahar DURMAZ, Izmir University of Economic

Danai KAZANTZIDOU-FIRTINIDOU, National Kapodistrian University of Athens

Dave COTTON, Atkins

Dr Diana CONTRERAS, Newcastle University

Enrica VERRUCCI, Epicentre, University College London

Eser ÇABUK, Middle East Technical University

Fatma Sevil MALCIOGLU, Boğaziçi University

Dr Ioanna IOANNOU, Epicentre, University College London

Jacob BLACK, Imperial College London

Jonas CELS, University College London

Dr Marco BAIGUERA, Epicentre, University College London

Maria KONTAE, Epicentre, University College London

Mariana ASINARI, Mott Macdonald

Dr Marianna ERCOLINO, Greenwich University

Martha ESABALIOGLOU, independent

Matthew FREE, Arup

Panagiotis DERMANIS, University of Patras

Dr Paul BURTON, University of East Anglia

Rohollah ROSTAMI, Glasgow Caledonian University

Dr Sean WILKINSON, Newcastle University

Valentina PUTRINO, Epicentre, University College London

EXECUTIVE SUMMARY

On 30 October 2020 at 2:51 pm Turkey and 1:51 pm Greece time, a $M_w=6.9$ earthquake hit the Aegean coasts of Turkey and Greece. The epicentre (37.879°N 26.703°E) was 14 km northeast of Avlakia in the Greek Island of Samos and some 25 km southwest of Izmir, Seferihisar Doganbey. The event's magnitude has been announced as 6.6 by the AFAD and 7.0 by the USGS. Notably, the event triggered a tsunami that affected a significant coastline between Alaçatı to Gümüldür in Turkey and the northern coasts of Samos. The event was followed by more than 4000 aftershocks with up to $M_w=5.2$.

The worst affected area in Turkey was the Bayraklı and Bornova districts in Izmir, located some 70 km away from the epicentre. This is where the death toll, and building and infrastructure damage was concentrated: 116 out of the total 119 casualties took place here, and almost all of the 17 collapsed buildings were located here. In these two districts alone around 200 buildings were heavily damaged. The reasons behind such a high ground motion intensity in Bayraklı (estimated as XIV), despite peak ground accelerations (PGA) lower than what the service and design codes suggest are several: The soil amplification given soft soil conditions ($V=100$ m/s) combined with poor construction practices, non-compliant design to building codes and post-occupancy modifications on the structures. Samos island was significantly affected with almost 2000 buildings deemed as unsafe for use. There were 2 fatalities due to the collapse of old abandoned buildings, few injuries and extensive damage to a number of churches.

The mission launched by the Earthquake Engineering Field Investigation Team (EEFIT) for this event was carried out the 16th November and the 17th December, inclusive of five-day field investigations in Izmir and its surroundings (30 Nov-4 Dec), and 8 days in Samos (2-3 Dec & 7-11 Dec). The team was composed of 20 members and a support crew of 4. The mission covered multiple aspects of the event in the form of five working groups in seismotectonics, geotechnics, structures, tsunami, and relief, response and recovery. In addition to these, a team focussed on data analysis and representation including social media analysis, in support of the other sub-teams.

The earthquake hit during the global COVID pandemic. This mission therefore adopted an unconventional strategy, and combined field and remote survey methods for assessing damage to buildings, critical infrastructure, and geotechnical structures. This hybrid strategy was achieved through a large remote team supported by two local field crews in Turkey and Greece. One of the main objectives of this mission was to assess this hybrid model's usability for future missions and investigate the extent in which other data sources can be used for remote reconnaissance in support of field work.

Other mission objectives were to carry out a systematic analysis of the impact of earthquake and tsunami over the affected areas in both countries; to develop an understanding as to how the EEFIT Mobile App can be tailored to address the specificities of this event; and to develop a multi-stakeholder understanding of the event and of its impacts through a public survey and interviews with various professionals in Turkey and in Greece.

A summary of key findings/messages is given below.

Seismic hazard mapping:

- The regional seismotectonic structures have the capacity to achieve an earthquake half magnitude larger with "heavily damaging" ground shaking intensity (VIII), and an engineering peak ground acceleration with 10% probability exceedance over 50-years (i.e. a 475-year occurrence on average) of 0.45g.

Damage and casualties:

- The structural damage observed in Turkey is concentrated almost exclusively in Bayraklı and Bornova districts of the city of Izmir. It is mostly attributed to noncompliant design and workmanship, exacerbated by the site amplification effects leading to elevated seismic demand levels in mid-rise buildings. The collapse and heavy damage in these 8-10 storey buildings led to a high death toll (116 out of 119).
- The structural damage observed in Samos, Greece, is dispersed throughout the island and is predominantly attributable to the age and the poor maintenance of buildings. A notable portion of the damaged buildings were abandoned. Casualties were much lower here (2 out of 119)

thanks to the low-rise building stock and a lower population density (around 60 times lower than that of Izmir).

Assessment of disaster response:

- The Aegean Earthquake was a disaster amid the ongoing COVID pandemic, and both countries lacked an earthquake emergency plan suitably tailored to these conditions.
- It has been claimed by our health professional interviewee that the event caused a significant spike in COVID cases in Izmir, which however is hard to verify due to Turkey's lack of region/city specific statistics on the COVID-cases and resulting losses of life.
- In Samos a targeted and effective response involving multiple stakeholders was deployed. In Turkey, there was strong civic action and good cooperation between NGOs and public bodies for recovery beyond the immediate physical needs - an approach first used following the 24 Jan 2020 Elazığ Earthquake, and further developed in the 26 March 2020 Van Earthquake.
- Our public survey showed that in both countries the tsunami awareness was lower than the awareness of seismic risk. In Samos the tsunami early warning system has been proved effective in alerting the coastal populations to the hazard. In Turkey the tsunami led to 1 (out of 119) casualty.

Learnings for future hybrid EEFIT missions:

- **Data availability:** The extent to which alternative, reliable data sources exist and can be used for remote assessment seems to be highly country-dependent. During this mission, we were able to find more data and data sources for Greece than for Turkey. Reasons for this variation may include varying awareness of disaster risk across countries, or differing ways/levels of engaging with social media in the event of a disaster. Another important factor governing the availability of data representative of the overall damage levels seems to be how dispersed damage is. In case of localised dramatic damage (Turkey), the damage bias in remote data sources is much higher than when the damage levels are more even and more scattered across the affected area (Samos).
- **Advantages over fully remote missions:** A hybrid approach to reconnaissance activities bringing together remote and field survey strategies emerges as a powerful alternative in the way forward: Teaming up with a local field crew helps overcome difficulties intrinsic to conventional missions, including language barrier for the team on-site and lack of familiarity with the building stock or the organisational structure in a given country.
- **Communication:** Communication is critical for ensuring efficient information flow between remote and field teams, hence spotting and solving potential problems on time. In this mission, this was achieved through two daily briefings and a messaging platform which helped to stay in touch at all times. Weekly all team meetings, and a separate messaging platform for the whole team also proved beneficial for efficient communication.
- **Preparatory desk-study:** Before deploying field crews, it is beneficial to have a preparatory period (in our case 2 weeks) to all data pertinent to the event. This preparation helped us to review the EEFIT app; plan the mission itinerary and priorities; and train remote and field teams on the damage assessment process, classification of damage as well as primary and secondary structural systems.
- **Remote assessment of field-data:** In our mission, the remote assessment of data collected in the field improved their quality by completing key information which were not recorded during the field assessment. While the discrepancy between the field and remote assessment of data obtained from the field was found to be relatively small, in certain cases an accurate description of the damage mechanism and the structural system required a few iterations.
- **EEFIT Mobile App:** Overall the EEFIT Mobile app is found to be a powerful and indispensable tool for this mission and undoubtedly it will be for the future hybrid reconnaissance activities. It is important however to tailor the contents of the app before every deployment to make sure it is suitable to the specificities of the event/location in terms of building stock characteristics and expected damage. When the Spatial Data Infrastructure (SDI) is completed, data organisation and mapping, which still was a time-consuming job in this mission, will be much easier.

CONTENTS

1.	INTRODUCTION.....	1
1.1.	Team.....	2
1.2.	Mission Diary.....	2
1.3.	Report structure.....	2
	References.....	3
2.	SEISMOTECTONICS.....	4
2.1.	Introduction.....	4
2.2.	Regional Geology and Tectonics.....	4
2.3.	Geodetic.....	5
2.4.	Local Geology.....	6
2.5.	Regional Seismicity.....	8
2.6.	Seismological Interpretation of Event.....	10
2.7.	Field Observations.....	12
2.8.	Seismic Hazard in Greece and Turkey.....	13
2.8.1.	Earthquake magnitude and return periods.....	15
2.8.2.	“Bands” and evolution of zones and zonation.....	16
2.8.3.	Seismic Hazard Maps Greece, the Aegean and Turkey.....	19
2.8.4.	Maximum Magnitude.....	23
2.8.5.	Deaggregation and Perceptibility.....	26
2.8.6.	Hazard Summary and Perspective on the Aegean Sea 2020 Earthquake.....	28
2.9.	Characterization of Strong Ground Motions.....	29
2.9.4.	Characteristics of Strong Ground Motion Networks.....	29
2.9.5.	Database & Processing of Waveforms.....	31
2.9.6.	Engineering Parameters.....	31
2.9.7.	Comparison with GMPEs.....	33
2.9.8.	Selected Ground Motion Prediction Equations.....	33
2.9.9.	Variation of Peak Ground Motion Parameters.....	34
2.10.	Comparison with Hazard Section and Codes.....	34
2.10.4.	Seismic Hazard and Codes of Greece.....	34
2.10.5.	Seismic Hazard and Codes of Turkey.....	36
2.11.	Summary and Conclusions.....	39
	References.....	39
3.	GEOTECHNICAL OBSERVATIONS AND SITE RESPONSE.....	45
3.1.	Introduction.....	45
3.2.	Co-seismic environmental effects.....	45
3.2.1.	Ground cracks.....	46

3.2.2. Landslides and rock falls	47
3.2.3. Liquefaction	50
3.3. Geotechnical Failures	51
3.3.1. Performance of Samos's Ports.....	51
3.4. Geotechnical Setting of Izmir Bay	53
3.5. Summary and Conclusions.....	56
References.....	56
4. DAMAGE ASSESSMENT AND OBSERVATIONS	58
4.1. Fieldwork Itinerary Planning.....	58
4.2. Fieldwork: Approach and Limitations	60
4.3. Damage Assessment Tools: EEFIT Mobile App.....	61
4.4. Remote Data Sources	62
4.5. Damage Data Processing	65
4.5.1. Key Information	65
4.5.2. Misclassification Error	65
4.6. Damage Observations: Samos	66
4.6.1. Building Stock and Code Evolution	66
4.6.2. Damage Statistics	67
4.6.3. Damage Patterns to Reinforced Concrete Buildings.....	69
4.6.4. Damage Patterns to Load Bearing Masonry Buildings	71
4.6.5. Damage Patterns to Cultural Heritage	73
4.7. Damage Observations: Izmir.....	76
4.7.1. Building Stock and Code Evolution	76
4.7.2. Damage Statistics	77
4.7.3. Damage Patterns to Reinforced Concrete Buildings.....	80
4.7.4. Damage Patterns to Masonry Cultural Heritage Structures.....	84
4.8. Masonry/Timber Vernacular Typology Common to Turkey and Greece	86
4.9. Conclusions.....	88
References.....	89
5. TSUNAMI	91
5.1. Tsunami Terminology.....	91
5.2. Past Tsunamis in the Aegean Sea.....	91
5.3. The 30 th October 2020 tsunami characteristics	92
5.4. International tsunami surveys	95
5.5. General observations obtained through field survey	96
5.6. EEFIT Mobile App	96
5.7. Observations from Siğacık and Akarca	96
5.8. Observations from Samos island	98
5.9. Summary	98
References.....	99
6. RELIEF, RESPONSE AND RECOVERY OBSERVATIONS	100

6.1.	Methods and Sources of Information	100
6.2.	Economic Aftermath	101
6.2.1.	Turkey	101
6.2.2.	Samos	102
6.3.	Risk Transfer Mechanism	102
6.3.1.	Turkey	102
6.3.2.	Samos	103
6.4.	Casualties.....	104
6.4.1.	Turkey	104
6.5.	Emergency Response: Search and Rescue (SAR)	104
6.5.1.	Turkey	104
6.5.2.	Samos	105
6.6.	Medical Response.....	107
6.6.1.	Turkey	107
6.6.2.	Samos	108
6.7.	Temporary Shelters and Aid Distributions	109
6.7.1.	Turkey	109
6.7.2.	Samos	112
6.8.	Recovery	114
6.8.1.	Turkey	114
6.8.2.	Samos	114
6.9.	Compound disasters - impacts of the COVID-19 pandemic.....	115
6.10.	Public Survey	116
6.10.1.	Residential building stock and impact of damage.....	116
6.10.2.	Occupancy rates at the time of the event	117
6.10.3.	Risk perception and risk transfer.....	117
6.10.4.	Preparedness for a seismic event or tsunami.....	119
6.10.5.	Earthquake response	120
6.10.6.	Tsunami response and early warning	120
6.10.7.	Disaster causes and preventability	121
6.10.8.	Additional respondent input.....	121
7.	SOCIAL MEDIA ANALYSES.....	124
7.1.	Data Sources.....	124
7.2.	LastQuake App	125
7.2.1.	Language	126
7.2.2.	Intensity.....	127
7.2.3.	Sentiment Analysis (SA)	129
7.2.4.	Topic Analysis	132
7.3.	Twitter.....	136
7.3.1.	Sentiment Analysis.....	136
7.3.2.	Most retweeted Tweets	137

EEFIT

7.3.3. Most liked Tweets.....	138
7.4. Conclusions and recommendations	140
References.....	141

ACKNOWLEDGEMENTS

EEFIT team on the Aegean Earthquake mission is very grateful to many in the UK, Turkey and Greece, who offered extremely generous help and assistance throughout.

We gratefully acknowledge the support of many UK universities and companies to the mission: University College London (team leader Dr Yasemin D Aktas, tsunami sub-team lead Dr Marco Baiguera, Relief, Response, Recovery sub-team lead Jonas Cels, Data Analysis and Representation sub-team lead Dr Ioanna Ioannou, Maria Kontoe, Enrica Verrucci and Valentina Putrino), Greenwich University (Structures sub-team co-lead Marianna Ercolino), Glasgow Caledonian University (Geotechnics sub-team lead Rohollah Rostami), Middle East Technical University (Eser Çabuk and Anil Köşker), Cambridge University (Aisling O’Kane), Imperial College London (Jacob Black), Bogazici University (Fatma Sevil Malcioglu), National Kapodistrian University of Athens (Danai Kazantzidou-Firtinidou), Çanakkale 18 Mart University (Ali Tolga Ozden), Newcastle University (Social Media sub-team lead Dr Diana Contreras and Dr Sean Wilkinson), University of Porto (Humberto Varum), Cambridge Architectural Research (Bahar Durmaz), Arup (Seismotectonic sub-team lead Matthew Free), Atkins (Structures sub-team co-lead David Cotton), Mott Macdonald (Mariana Asinari).

We are also indebted to the following individuals and organisations who supported and contributed to the mission:

Prof Ahmet Yakut, the director of the Middle East Technical University (METU) Earthquake Engineering Research Centre who linked us to Eser Çabuk and Anil Köşker for the Turkey fieldwork; Mustafa Erdik, Ioannis Kalogeras and Theodoros Tsapanos who provided access to significant material; Sude Kilic (World Human Relief), Mehmet Sarica (IDEMA), Ilker Kahraman (Izmir Provincial Coordination Board and Turkish Chamber of Architects Izmir Branch), Mert Aksoy (Lokman Hekim Saglik Vakfi), Eylem Ayatar (Turkish Chamber of Structural Engineers Izmir Branch) Ferdi Golcuk (Fire Department of Izmir Metropolitan Municipality), an anonymous health professional from Ege University Hospital; Yercizenler, EMRC; Burcak Basbug Erkan, Emily So, Erdal Safak, Mauricio Morales Beltran (owner of the top cover photo); Duncan Gordon; Ali Osman Durmaz; Mete Isikoglu; Arda Yalamac; Mert Torun; Erdem Kazaz; Spyros Efthymiopoulos; Ioannis Stamoulis (Regional Fire Service of North Aegean), Dimitrios Malliaros (Civil protection Directorate of North Aegean Region), Alexandros Tatouris (Civil Protection Department of Regional Unit of Samos), Thekla Thoma (Preparedness and Aid Provision Department, Earthquake Planning and Protection Organisation), Gerassimos Papadopoulos (International Society for the Prevention & Mitigation of Natural Hazards), Georgios Kaviris (National Kapodistrian University of Athens), Antonios Pomonis (World Bank), Maria Kleanthi (Natural Disaster Rehabilitation Directorate, Ministry of Infrastructure and Transport), Aris Konstantaras (“Mikres diadromes” youtube channel), Burcu Erdogan Gundogdu; Kemal Gulcen; Nilufer Sariaslan; Canay Dogulu; Laure Fallou, Matthieu Landès, Rémy Bossu from the Euro-Mediterranean Seismological Centre (EMSC); Canakkale Olay Gazetesi; Gazete Duvar; Izmir Metropolitan Municipality and Learning from Earthquakes Team.

EEFIT would like to acknowledge the on-going support of corporate sponsors: AECOM, AIR Worldwide Ltd, Arup, Atkins, Mott MacDonald, Guy Carpenter & Co Ltd, Sellafeld Ltd, and Willis Towers Watson.

The team also thanks the reviewers who greatly contributed to the refinement of this report.

1. INTRODUCTION

(authored by: YDA)

The 30 October 2020 earthquake hit the Aegean coastline of Turkey and Greece at 2:51 pm Turkey and 1:51 pm Greece time with magnitude 6.9, and triggered a tsunami between Alaçatı and Gümüldür in Turkey. The epicentre (37.879°N, 26.703°E) was 14 km northeast of Avlakia in Greek Island of Samos and some 25 km southwest of Izmir, Seferihisar Doganbey. Notably, the event triggered a tsunami that affected a significant coastline between Alaçatı to Gümüldür in Turkey and northern coasts of Samos, roughly between Karlovasi and Vathy. The event was followed by thousands of aftershocks with up to Mw=5.2 (BO KRDAE, 2021). The reported depth for the earthquake varied between 10 and 21 km.

The event caused 2 casualties and 19 injuries in Samos. A total of 400 families are estimated to have been displaced in the aftermath of the event. The estimated loss so far, including overall state expenditure is €117M.

The worst affected area in Turkey was the Bayraklı and Bornova districts in Izmir, a metropolitan city around 65 km away from the epicentre and with an average population density nearly 60 times that of Samos. These districts were where the death toll, and building and infrastructure damage was concentrated: 116 out of a total of 119 casualties due to this event took place here in the collapsed buildings. As of January 7, Compulsory Earthquake Insurance payout for the affected properties in and around Izmir was reported as approximately 224 million TL (Turkish Liras) (DASK, 2020).

Reasons for deploying a mission for this event were:

- The concentrated dramatic damage in Turkey, which was indicative of prominent issues with the design and construction of some building stocks;
- The rare incident of a tsunami in the Aegean region;
- That it took place during an ongoing pandemic, making the event a compound hazard.

Unlike the conventional earthquake reconnaissance practices, which mainly rely on fieldwork, this mission used a hybrid approach due to the COVID pandemic related travel restrictions. This model has previously been used during the EEFIT&LfE mission deployed for the March 2020 Zagreb Earthquake (So et al., 2020). Even though this hybrid model still benefits from a field crew recruited locally to collect field data, it relies heavily on a remote team seeking remote data for assessment of damage to buildings and infrastructure, while at the same time coordinating the fieldwork and conducting the desk studies. How this hybrid model compares to the conventional fieldwork-based reconnaissance activities is an open question pertinent to the earthquake engineering research and practice in case similar global circumstances may prevail in the future, or simply to achieve reconnaissance outcomes with fewer resources, quicker or with better efficiency, if this former proves to be the way forward.

Therefore, the mission objectives for the 2020 Aegean Earthquake and Tsunami were determined as follows:

- Combine field and remote survey strategies for assessment of damage to buildings and critical infrastructure and geotechnical structures;
- Train and deploy small local field crews on the damage assessment tools developed in the Learning from Earthquakes (LfE) project, namely the EEFIT Mobile App;
- Investigate the extent to which other data sources can be used for remote reconnaissance in support of fieldwork;
- Conduct a systematic and comparative analysis of the impact of earthquake and tsunami over a wide geographic area;
- Develop an understanding as to how the EEFIT Mobile App can be tailored to address the specificities of this event;
- Develop an understanding of how the lockdown restrictions and additional pressures induced by the ongoing pandemic affected the response and recovery operations;
- Develop a multi-stakeholder understanding of the event and of its impacts.

EEFIT

The purpose of this report is to share the immediate preliminary outcomes of this mission and discuss the potentials and limitations of running a hybrid reconnaissance activity with specific emphasis on the Aegean Earthquake and Tsunami.

1.1. Team

The team selected for this mission was 26 individuals from industry (5) and academia (21, 11 of whom are students).

The team benefitted from local field crews to complement the remote team's activities - the Turkey field crew was recruited through the help of Prof Ahmet Yakut, the director of the Middle East Technical University (METU) Earthquake Engineering Research Centre (EERC). The Greece field crew on the other hand was recruited on a volunteering basis.

The team has been organised under 7 main sub-working area as shown below, with a substantial support group:

SEISMOTECTONICS: Matthew Free (Arup), Aisling O'Kane (Cambridge University), Fatma Sevil Malcioglu (Boğaziçi University), Paul Burton (University of East Anglia), Rohollah Rostami (Glasgow Caledonian University)

STRUCTURES: Marianna Ercolino (Greenwich University), David Cotton (Atkins), Danai Kazantzidou-Firtinidou (NKUA), Jacob Black (Imperial College London), Maria Kontoe (UCL), Mariana Asinari (Mott Macdonald), Ahsana Parammal Vatteri (UCL)

TSUNAMI: Marco Baiguera (UCL)

Field Crew: Martha Esabalioglou (independent), Panagiotis Dermanis (University of Patras), Eser Cabuk (METU), Anil Kosker (METU).

GEOTECHNICS: Rohollah Rostami (Glasgow Caledonian University)

RELIEF, RESPONSE, RECOVERY: Jonas Cels (UCL), Ali Tolga Ozden (Canakkale On Sekiz Mart University), Danai Kazantzidou-Firtinidou (National Kapodistrian University of Athens)

DATA REPRESENTATION & ANALYSIS: Ioanna Ioannou (UCL), Marco Baiguera (UCL), Danai Kazantzidou-Firtinidou (National Kapodistrian University of Athens)

SOCIAL MEDIA ANALYSIS: Diana Contreras (Newcastle University)

SUPPORT: Bahar Durmaz (Izmir University of Economics & CAR), Enrica Verrucci (UCL), Sean Wilkinson (Newcastle University), Valentina Putrino (UCL)

Team leader: Yasemin D Aktas

1.2. Mission Diary

The mission officially started on 16 November 2020. The first two weeks were used for an intensive desk study to collate all related information and remote data sources and recruit local field crews, train them, and set out itineraries. The fieldwork has been carried out in 3 instalments (Turkey between 30 Nov-4 Dec, and Greece between 2-3 and 7-11 Dec). The team also developed a blog site for daily updates on the field crews' activities: <https://eeftaegean.wordpress.com>. The mission lecture was delivered on 17 December 2020 (<https://www.istructe.org/resources/case-study/2020-eeftaegean-earthquake-mission/>).

1.3. Report structure

The report is organised in the form of 7 sections, as indicated in **Table 1**.

Table 1: Report structure

Chapter no	Chapter title	Authors
1	Introduction	YDA
2	Seismotectonics	PB, FSM, AOK, RR
3	Geotechnics	RR
4	Damage Assessment and Observations	YDA, MA, DC, ME, DK-F, II, VP, EV
5	Tsunami	MB
6	Relief, Response, Recovery	JC, TAO, DK-F
7	Social Media Analyses	DiC, SW

References

- BU-KRDAE. (2021, January 20). *Boğaziçi Üniversitesi Kandilli Rasathanesi ve Deprem Arastirma Enstitusu (KRDAE) Bolgesel Deprem-Tsunami Izleme ve Degerlendirme Merkezi (BDTIM)*. Retrieved from <http://udim.koeri.boun.edu.tr/zeqmap/osmap.asp>
- Cetin, K. O., Mylonakis, G., Sextos, A., & Stewart, J. P. (2020). *Seismological and Engineering Effects of the M 7.0 Samos Island (Aegean Sea) Earthquake*. HAEE 2020/02, Earthquake Engineering Assoc of Turkey, Earthquake Foundstion of Turkey, EERI, GEER-069. doi:<https://doi.org/10.18118/G6H088>
- DASK. (2021, January 7). *DASK (Dogal Afet Sigortalari Kurumu)*. Retrieved from DASK: <https://www.dask.gov.tr/>
- So, E., Babić, A., Majetić, H., Putrino, V., Verrucci, E., Contreras Mojica, D., . . . D'Ayala, D. (2020). *The Zagreb Earthquake of 22 March 202*

2. SEISMOTECTONICS

2.1. Introduction

A MW6.9 earthquake took place on October 30, 2020, in the Aegean Sea, which is one of the most seismically active regions in the world. This strong earthquake resulted in catastrophic damage in İzmir province in Turkey and Samos Island in Greece. This chapter presents the tectonic structure, geodetic interpretation, geology and seismicity of the region to provide the seismotectonic background of the Aegean Sea and its territories. It then focuses on the seismological interpretation of the event and ground surface deformations based on field observations. The mid-section covers the development of seismic hazard studies from past to present for the region and concludes with the hazard summary and perspective on the Aegean Sea Earthquake of 30 October 2020. In the final part of the chapter, strong ground motion records of the event give an insight into the engineering parameters. The variation of peak ground accelerations (PGAs) with respect to epicentral distances and soil conditions and their comparison with ground motion prediction models are presented. Following a description of the evolution of Greek and Turkish seismic codes, the spectral accelerations of closest station records are compared with design code spectra.

2.2. Regional Geology and Tectonics

(Authored by AOK)

The Aegean is one of the most rapidly deforming regions in the world and forms part of the Alpine-Himalayan Belt. The neotectonics of the region is governed by three major tectonic plates: the African, Arabian and Eurasian, in addition to two microplates: the Aegean and Anatolian (McKenzie, 1972). The region is dominated by both strike-slip and extensional motion. The northward subduction of the African plate beneath the Aegean and western Turkey causes extension in the overriding Aegean plate (Taymaz et al., 2007), within which the 30th October 2020 earthquake occurred. The second contributing factor is the strike-slip motion along both the North Anatolian and East Anatolian Fault Zones which cause an overall westward motion of Turkey relative to Eurasia (McKenzie, 1972; Jackson, 1994; Taymaz et al., 2007) (See **Figure 1**).

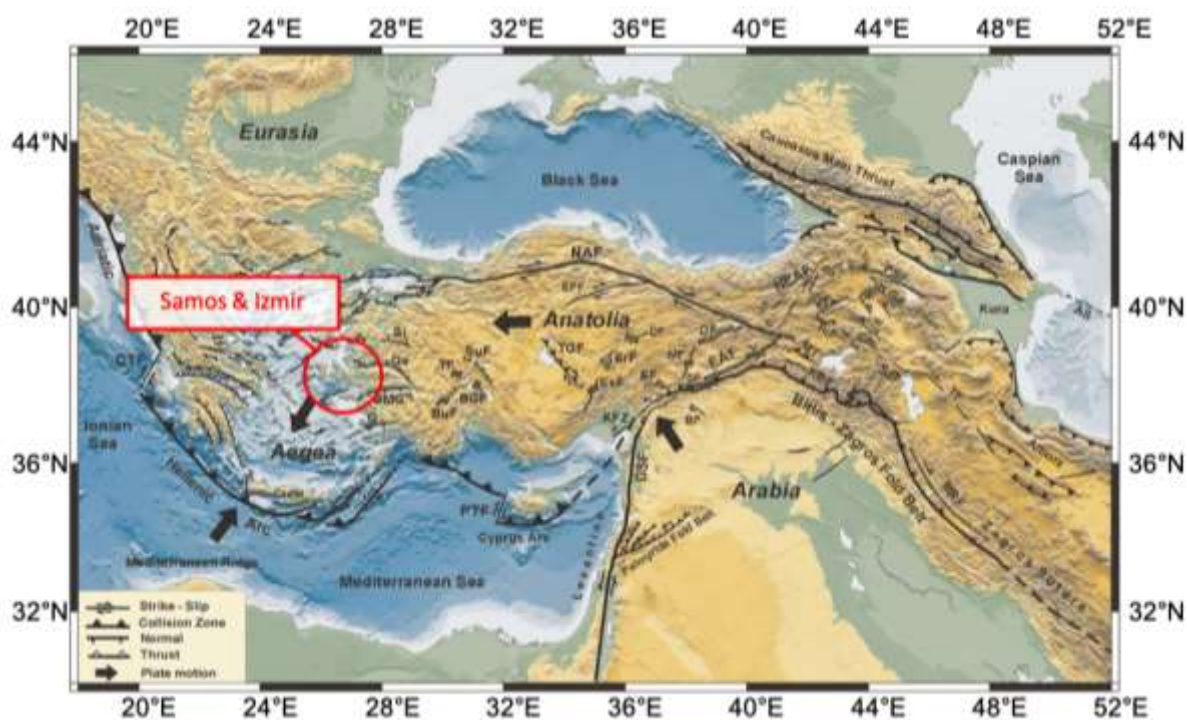


Figure 1: Topography map adapted from Taymaz et al. (2007) showing the regional tectonics across the Aegean and Anatolia. The study area has been circled in red.

2.3. Geodetic

(Authored by AOK)

Several authors have studied the strain rates across the Aegean and the surrounding region over the past century. McKenzie (1972) was the first to estimate the convergence rates of the wider region (Turkey) relative to Eurasia, to be ~ 70 mm/yr. Jackson and McKenzie (1988) followed suit by using the earthquakes between 1908 and 1981 to estimate the average velocities for both regions undergoing extension and shortening in the Aegean. They found that the N-S extensional rates were within the range of 20 – 60 mm/yr., whereas the shortening rates in the Hellenic Trench were much less at ~ 15 mm/yr. Africa and Eurasia are converging so this anomaly led to the conclusion that most of the convergence in the Hellenic Trench must be aseismic. McCluskey et al. (2000) carried out an extensive study using GPS measurements of the crustal motions for the period following Jackson and McKenzie (1988) between 1988-1997 and found that the average strain rates across the Aegean were ~ 30 mm/yr. to the southwest, relative to Eurasia. This is consistent with the findings of Nocquet (2012) ($\sim 30 - 40$ mm/yr. across the Aegean) who carried out a study using all available datasets, to assess the kinematics of the Mediterranean. Nocquet (2012) noted slightly higher strain rates at sites near Crete and the Southern Peloponnese. England et al. (2016) later measured the strain across the Southern Aegean to be ~ 43 mm/yr. **Figure 2** illustrates the latest measured GPS velocities relative to Eurasia from the Nocquet (2012) and England et al. (2016) catalogues.

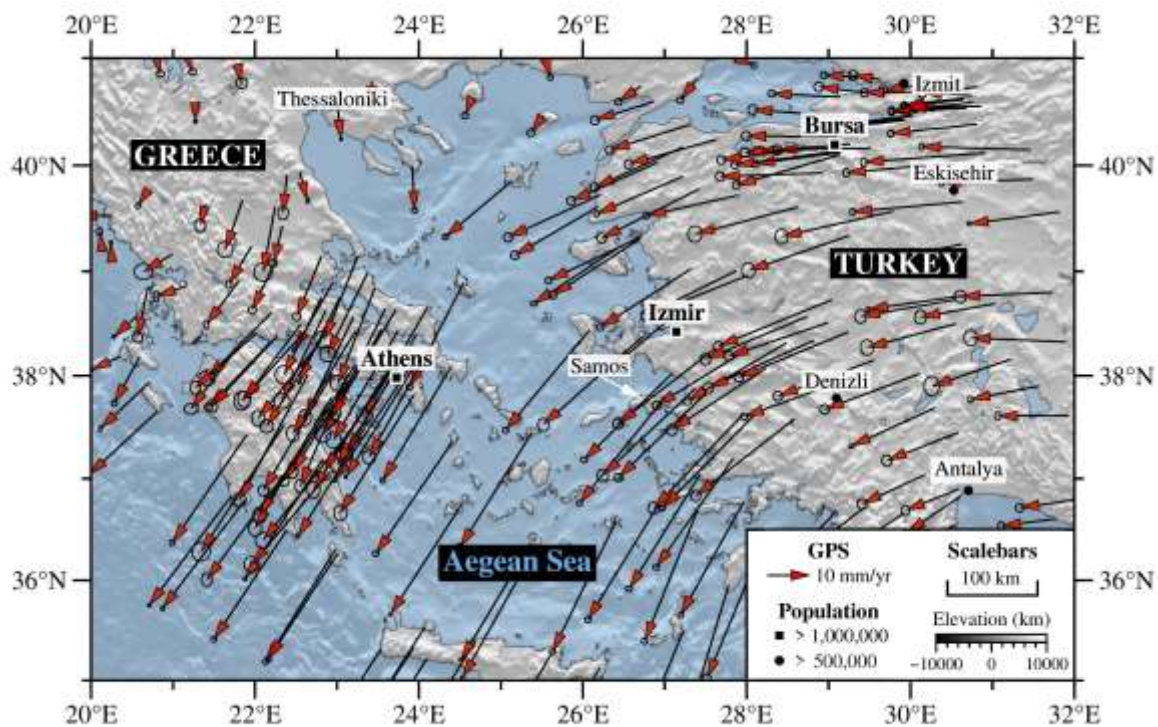


Figure 2: GPS velocities relative to Eurasia from Nocquet (2012) and England et al., (2016) catalogues.

Recently Weiss et al. (2020) calculated the surface velocities and strain for Anatolia from Sentinel-1 InSAR and GNSS Data, inclusive of the Eastern Aegean where the 30th October 2020 earthquake occurred. They have produced a strain rate model covering $\sim 800,000$ km² across Anatolia which maps areas of high strain including the North and Eastern Anatolia Faults, and the region west of Izmir which is relevant to our study (see **Figure 3**).

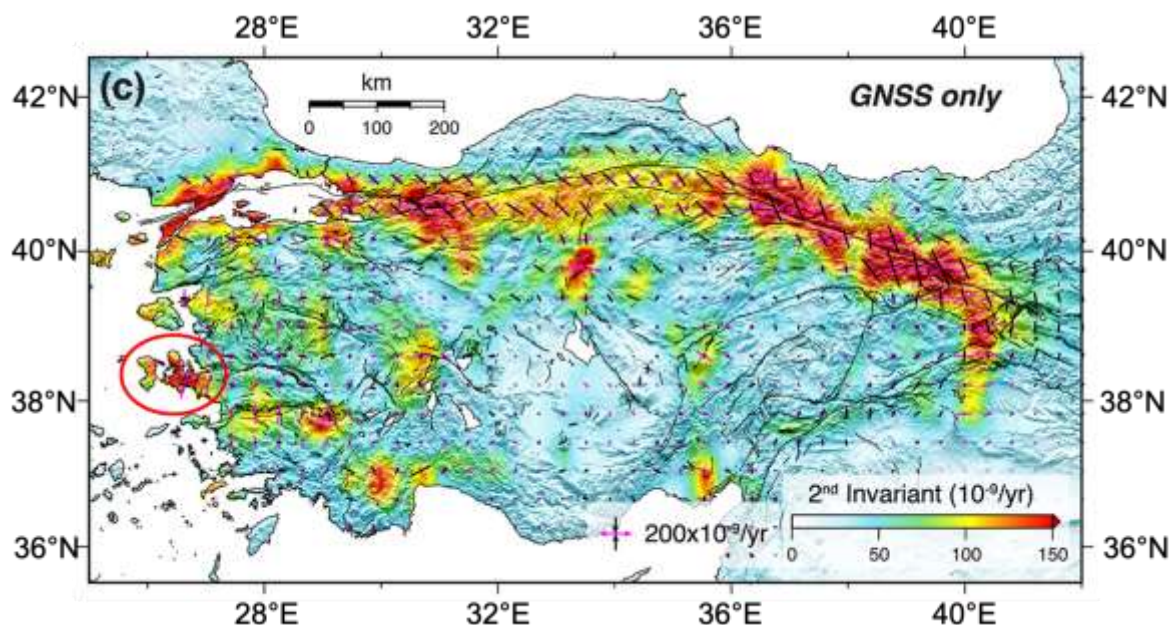


Figure 3: Map of Anatolia from Weiss et al. (2020) showing the second invariant of the strain rate tensor derived using GNSS data. In the West of the map, you can see that the region West of Izmir (circled in red) is an area of high strain.

2.4. Local Geology

(Authored by RR)

The island of Samos is a mountainous island located in the Aegean Sea, approximately 1.5 km from the West Anatolian coasts. The island is ~45 km long and has a surface area of 478 km², carved by steep cliffs and highly incised streams (Evelpidou et al. 2020). It is an extension of the Mycale range on the Anatolian mainland (Papadimitriou et al., 2020). The topographic gradient of Samos island decreases to the east and is very pronounced (Ring et al., 2007). The southeastern part of Samos is characterized by low, smooth relief with lagoons and extensive sand-gravel of coastal subsidence (Evelpidou et al. 2020). The geology map of Samos is shown in **Figure 4a** (Ring et al., 2007) – the main geological features consist of various metamorphic nappes, a non-metamorphic nappe, and a Miocene graben (Ring et al., 2007; Lekkas et al. 2020). These features expose an exceptionally complete nappe stack of the Central Hellenides (Ring et al., 2007), structurally below the Cycladic blueschist unit (Ring et al., 1999) and the non-metamorphosed Cycladic ophiolite nappe (Papadimitriou et al. 2020). Samos's active faults include Karlovasi fault, Marathokampos fault, Pythagorion fault, Vathy fault, and Northern Samos offshore fault.

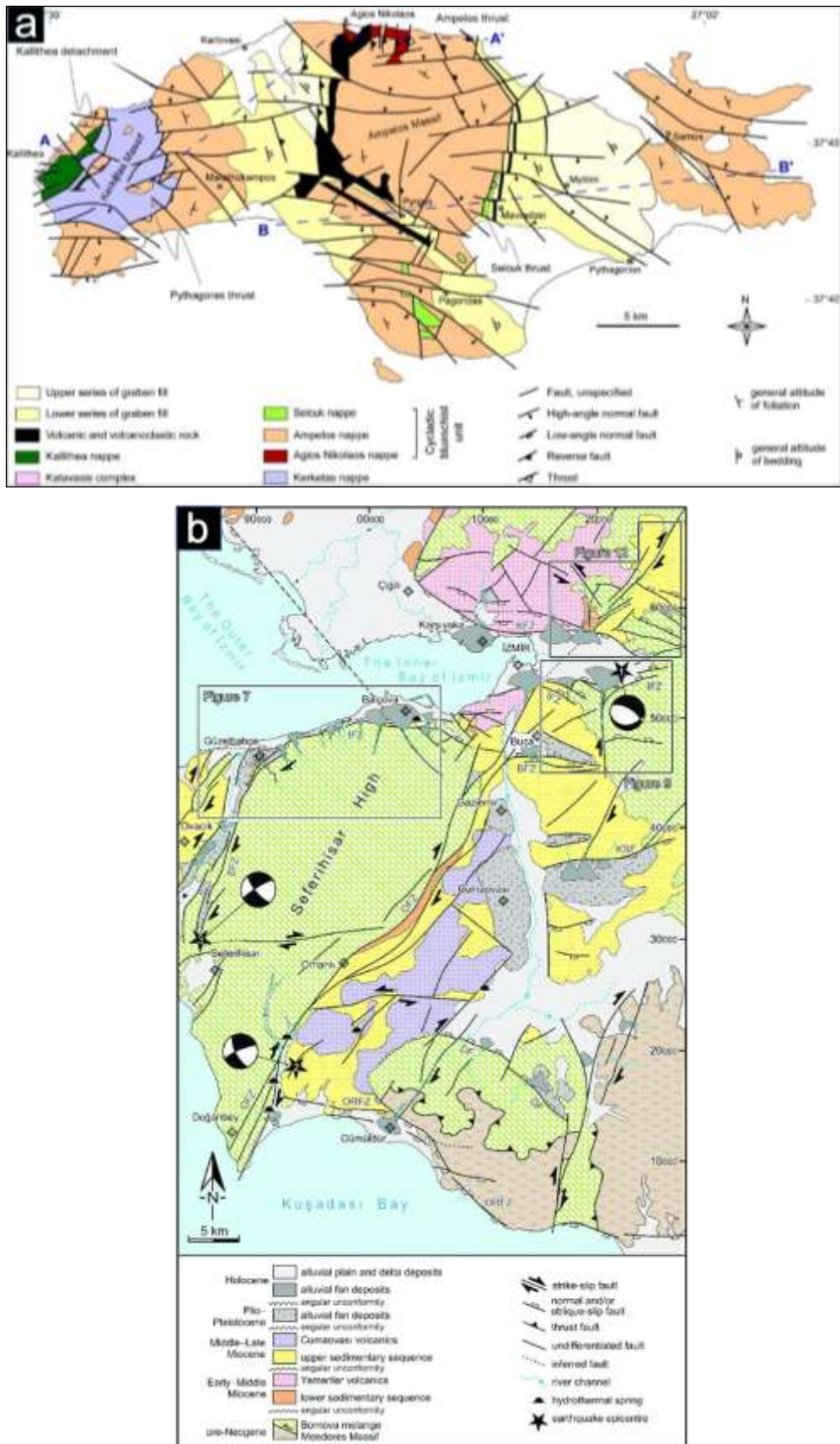


Figure 4: (a) Geological map for the Island of Samos (Ring et al., 2007) and (b) geology for the area SW of the city of Izmir (Uzel et al., 2009)

Figure 4b shows the variation in ground types across the region southeast of Izmir. Izmir metropolitan area is the third largest city of Turkey located along the eastern coast of the Aegean Sea at the western end of Turkey (Gök and Polat, 2014). The city is situated within Izmir Bay, which is covered by Plio-Quaternary terrestrial-marine deposits (Gök and Polat, 2014). This area is controlled by active faults in the West Anatolian Extensional Province (Gök, 2011). Much of the affected area (Bayraklı district) was built on these alluvial sediments and active normal faults: Izmir Fault (IF) and Karşıyaka Fault Zone (KFZ).

2.5. Regional Seismicity

(Authored by AOK)

The Aegean is one of the most seismically active regions in the world as demonstrated by its history of destructive earthquakes. It is an extensional back-arc area behind the Hellenic subduction and is dominated by strike-slip and normal faulting (McKenzie, 1978). The deformation in the Aegean is distributed over many active faults, both offshore and onshore Turkey and Greece (**Figure 5**). The seismicity is therefore frequent due to the large number of active structures, which mainly strike NE-SW or E-W across the region.

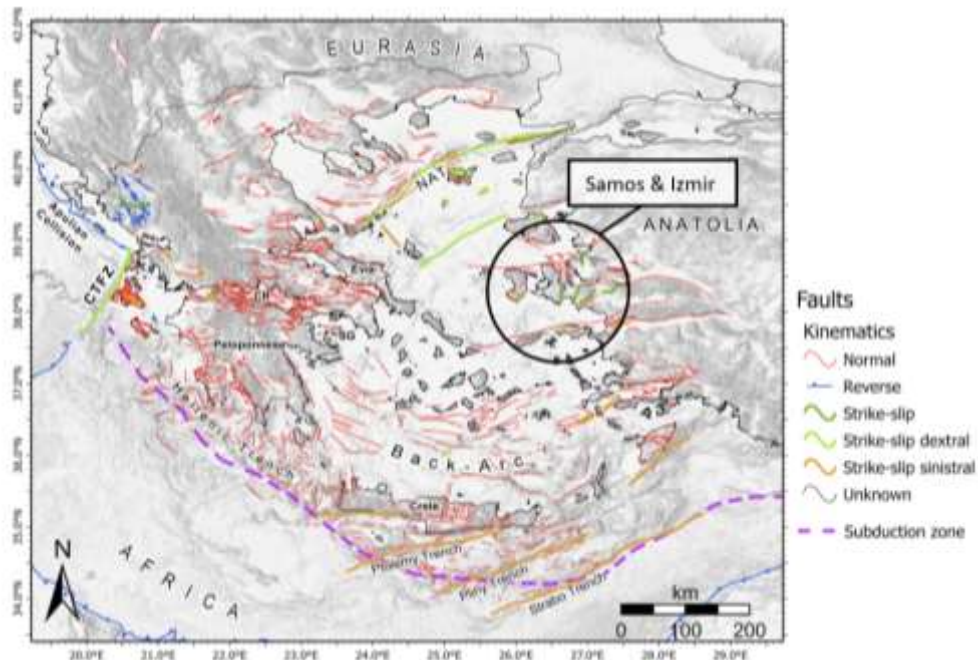


Figure 5: Active fault map from Kassaras et al. (2020) showing all the active structures across the Aegean and surrounding regions. The area local to the Aegean earthquake has been circled in black.

The seismicity of moderately sized earthquakes across the region is frequent and has been shown to be episodic in nature through periods of quiescence followed by a clustering of earthquakes (e.g., in 1969 (McKenzie, 1972) or on a more local scale in 2009 in Samos (Tan et al., 2014). Over the past century, there have been thousands of earthquakes across the Aegean (**Figure 6**).

For clarity, we have filtered the seismic data to only show the most destructive earthquakes which contribute to the seismic hazard (**Figure 7**). These events have sufficiently large moment magnitudes ($> M_w 5$) and occur within the crust at depths of < 35 km, as Jackson et al., (2008) defined the moho depth of the Aegean to be 25-35 km. **Figure 7** illustrates the spatial distribution of the crustal earthquakes and their mechanisms across the region. There is an aseismic region in the centre of the Aegean, surrounded by active belts on all sides. In mainland Greece and the eastern Aegean Greek Islands, normal faulting is the main mechanism of deformation, whilst in the Hellenic arc, thrust faulting dominates (as shown by the focal mechanisms on **Figure 7**). In the Northern Aegean, particularly along the North Aegean Trough, strike-slip faulting is the main type of rupture. The focal mechanisms illustrate transpressional stress along the Hellenic Arc and transtensional tectonics in the overriding Aegean plate (Kassaras et al., 2020).

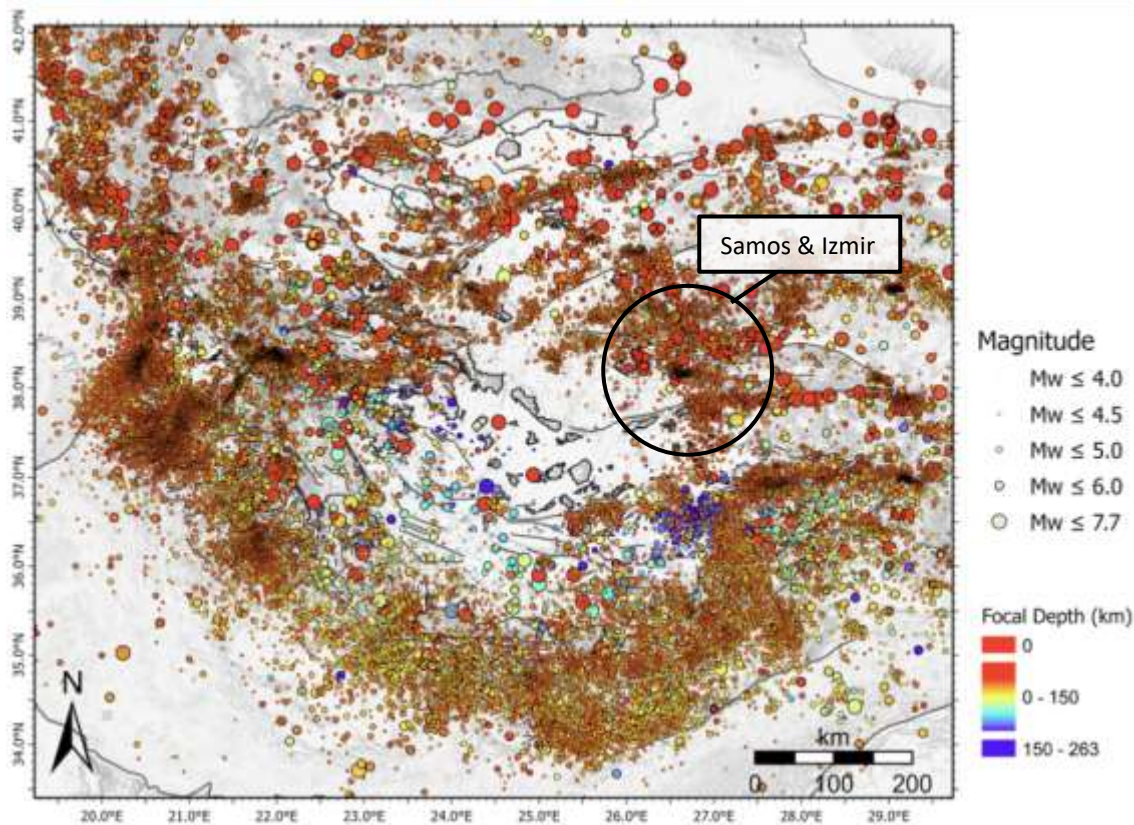


Figure 6: Seismicity map from Kassaras et al. (2020) showing the historical seismicity across the Aegean and surrounding regions. The region local to the Samos earthquake has been circled in black.

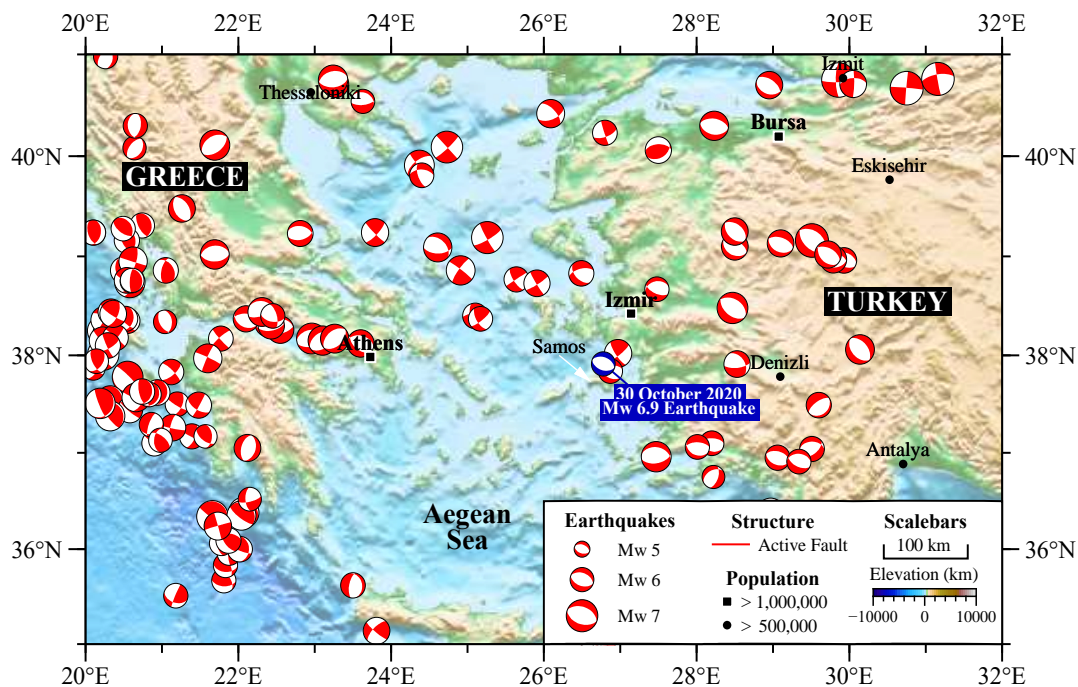


Figure 7: Focal mechanism map showing Aegean earthquake events from the Wimpenny and Watson (2020) global waveform-modelled catalogue for earthquakes that have been modelled using synthetic seismograms to constrain better point-source fault-plane solutions and focal depths. Note the focal mechanism for the recent 30th October 2020 earthquake in blue.

We also assessed the seismicity on a more local scale to the recent earthquake off the coast of Samos. **Figure 8** demonstrates the historical seismicity of the local region to Samos and Izmir, the regions

affected most by the earthquake. The map illustrates the active faults across the region with most faults trending NE-SW, with a few offshore striking E-W. Various authors (Mountrakis et al., 2003; Chatzipetros et al., 2013; Coskun et al., 2017) have carried out studies on the active faults within the Gulf of Kuşadası where the 30th October 2020 Aegean earthquake occurred. Whilst there are many faults spread across the Island of Samos and the surrounding area, Chatzipetros et al. (2013) identified the Karlovasi, Marathokampos, Pythagorion, Vathy and North Samos faults to be the active structures in the region. The Samos fault (located ~10 km north of Samos) was noted to dip 45 degrees to the North at a depth of 15 km (Eyidogan et al., 2020), consistent with the earthquake parameters of the 30th October 2020 event and has since been determined to be responsible for the earthquake. Lekkas et al. (2020) noted that the M_w 6.8 11th August 1904 Samos earthquake was similar to the 30th October 2020 event. Although the early seismic record for Samos is relatively unknown, Stiros (2000) noted that there were other devastating earthquakes in 200 BC, 47 AD and 1751, and at least six $> M_w$ 6 earthquakes in the 19th century, in addition to the most recent large earthquakes (1904 M_w 6.8, 1955 M_w 6.9).

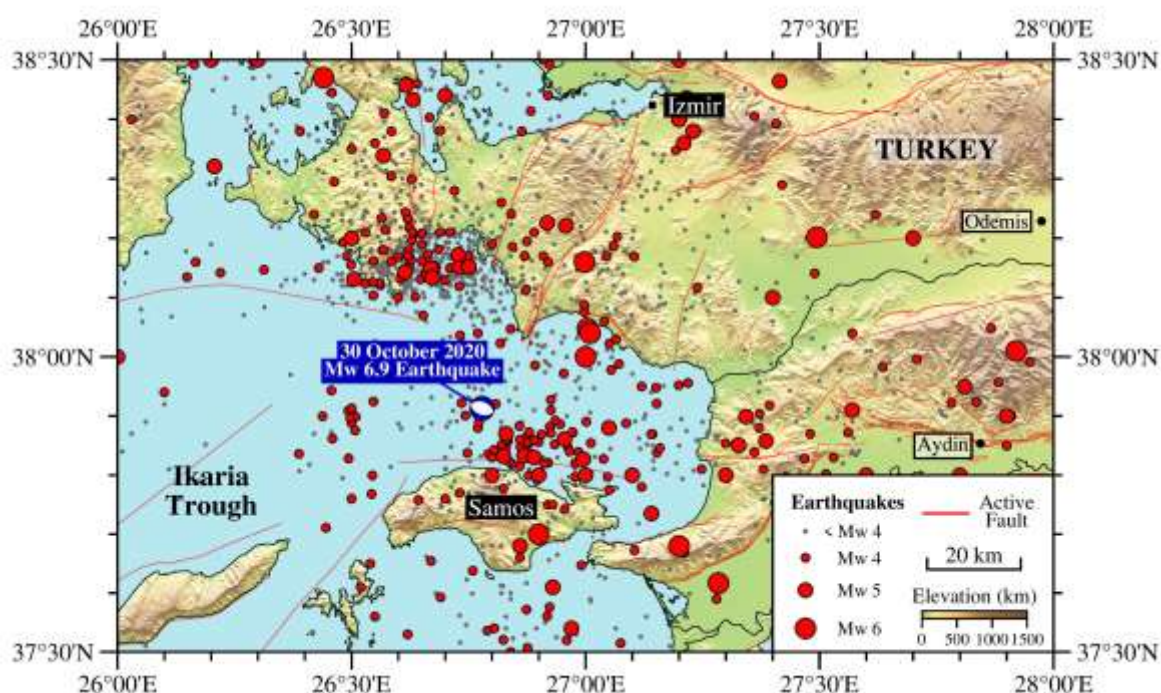


Figure 8: Seismicity map of the region local to the 30th October 2020 Samos earthquake. The map illustrates only crustal (<35 km) events from Dziewonski et al., 1981; Burton et al., 2004, Ekström et al., 2012 and the AFAD 1900-2020 earthquake catalogue (AFAD, 2020).

2.6. Seismological Interpretation of Event

(Authored by AOK)

On 30th October 2020 (11:51:27 UTC) a M_w 6.9 normal-faulting earthquake occurred ~35 km off the West coast of Turkey and ~10 km north of the Greek island of Samos in the Eastern Aegean (See **Figure 7** and **Figure 8**). Various techniques have been used to interpret the full effects of the earthquake. One such approach was performed by Professor James Jackson from the University of Cambridge who teleseismic body waveform modelled the event as a finite-duration rupture by conducting a joint inversion of long-period P and SH seismic waveforms using the Zwick et al. (1994) MT5 program, based on the McCaffrey and Abers (1988) and McCaffrey et al. (1991) algorithm. A centroid depth of ~7 km was determined, meaning that it is likely that the earthquake ruptured from the surface to 14 km in depth and had a fault length of ~33 km. The modelling determined a seismic moment of 3.2×10^{19} N m, equivalent to a moment magnitude of 7.0, in line with the findings of the USGS (USGS, 2020), GEOFON (GEOFON Data Centre, 2020) and CMT earthquake catalogues (Dziewonski et al. 1981; Ekström et al., 2012). The minimum-misfit solution (**Figure 9**) determined a normal-fault source with a strike, dip and rake of 291°, 44° and -88° respectively, suggesting the

EEFIT

earthquake was pure extension (with little to no strike-slip motion involved) and resulted in the uplift of Samos on the footwall side of the fault and subsidence on the hanging wall side, where Izmir and surrounding villages experienced significant damage. These parameters are consistent with the ~27-37 km long E-W trending Samos fault (Chatzipetros et al., 2013; Lekkas et al., 2020), located north of Samos Island and correlate with the earthquake parameters other authors have determined through fault modelling based on InSAR line of sight displacements and GNSS offsets (Ganas et al., 2020) and moment tensor inversion based on greens functions computed with the (Bouchon, 1979; 2003) frequency-wavenumber integration method Papadimitriou et al., 2020).

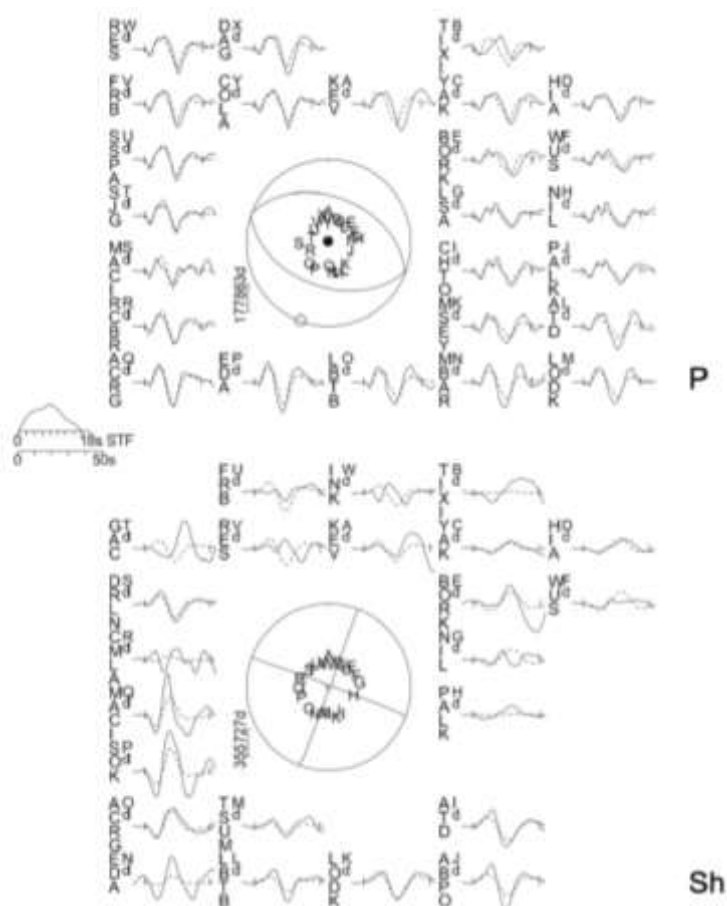


Figure 9: Minimum misfit solution determined from teleseismic body waveform modelling.

Ganas et al. (2020) reported that there were more than 750 aftershocks within the first couple of days after the Samos earthquake on 30th October 2020, with a moderate M_w 5.2 aftershock striking the region just three hours after the mainshock. Eyidogan et al. (2020) reported that this number had increased to 1,600 aftershocks by 27th November (see **Figure 10**). It was the distribution of aftershocks that helped indicate the length and location of the ruptured fault.

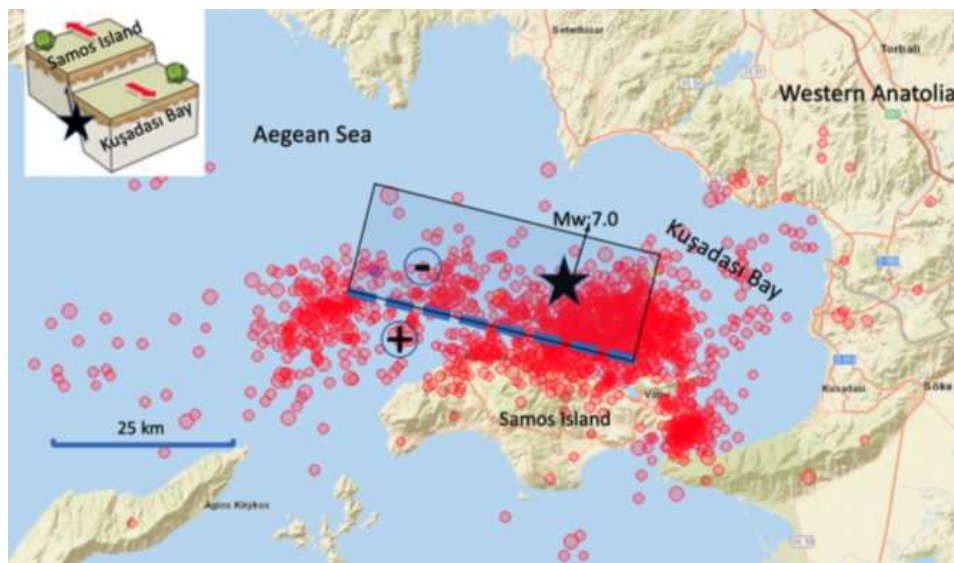


Figure 10: Map from Eyidogan et al. (2020) showing the distribution of aftershocks between 30th October and 27th November 2020.

2.7. Field Observations

(Authored by AOK)

Due to the high magnitude and shallow nature of the 30th October 2020 earthquake, the island of Samos and area SW of Izmir displayed the full effects of the high ground motions produced. One of the first observations was coseismic surface rupturing which was documented across the Island of Samos and along the Eastern coast of Chios island, Greece. Our EFFIT field team located some metre-scale ruptures in northern Samos (Latitude: 37.803591° / Longitude: 26.724584°) as well as some structural ground cracking with offsets of < 30cm. The ruptures are continuous for up to ~10 m and strike ~60° NE as expected, as this is parallel with the main strain direction and active faulting in the area, especially the >10 km long Karlovasi fault (Pavlidis et al., 2009). Lekkas et al. (2020) also report many metre-scale surface ruptures with centimetre-scale offsets in the nearby Agios Nikolaos, Agios Elias and Kontakaeika villages in NW Samos. The ruptures in the area of Agios Nikolaos strike 40-70° NE, consistent with our findings. The ruptures were semi-continuous for lengths < 1 km and caused vertical and horizontal offsets between 5 – 8 cm (see **Figure 11**).



Figure 11: Photographs from Lekkas et al. (2020) illustrating surface rupturing in the Agios Nikolaos area in NW Samos.

Lekkas et al. (2020) also documented the permanent coseismic uplift attributed to the 30th October 2020 earthquake (see **Figure 12**), which was easy to see along the rocky shoreline and port/harbour walls due to the old waterline left behind. This observation is not unique to the region as many studies have documented tectonic uplift and subsidence across the Gulf of Corinth (Jackson et al., 1982; McNeill and Collier, 2004), Ionian Islands (Pirazzoli et al., 1994), Euboea (Stiros et al., 1992), Rhodes (Pirazzoli et al., 1989), Crete (Tiberti et al., 2014) and the Cyclades (Evelpidou et al., 2014).

In the region local to the 30th October 2020 earthquake, Stiros et al. (2000) and Evelpidou et al. (2019) have previously documented the change in shorelines along the coast of Samos, which offered a good measurable indicator for the uplift attributed to the recent M_w 6.9 earthquake. Lekkas et al. (2020) noted between 8 and 35cm of uplift at various locations along the coast, many of which were comparable with the Stiros et al. (2000) measurements.



Figure 12: Photograph from Lekkas et al. (2020) illustrating 22 cm of coastal uplift in Punta, Samos, measured relative to values from Stiros et al. (2000).

2.8. Seismic Hazard in Greece and Turkey

(Authored by PB)

Seismic hazard material has developed over many years for Greece and Turkey, more so than for many countries. It has developed broadly and diversely. The purpose of this section is first to sample, display and demonstrate this diverse material, secondly, to draw conclusions on the diversity and reliability of current seismic hazard mapping, and finally, to focus on these maps in the region of the Aegean Sea 2020 earthquake near Samos and coastal mainland Turkey, to extract hazard parameters, and ultimately place the Aegean Sea 2020 earthquake into perspective within the capacity of the regional seismotectonics.

The popular urge to record, understand and hence protect against earthquake in a formal and scientific approach is usually held to point to Robert Mallet's initiative. His map of 1857 (**Figure 13**; Mallet, 1862) illustrates areas having experienced ground shaking ranging over levels of severity; by diluting a dye it indicates through differential shading those areas that have suffered slight, moderate and catastrophic damage caused by earthquake. This map is derived from accumulated, centralised, information on earthquake impacts i.e., a catalogue (Mallet, 1858, with R. Mallet & J. W. Mallet's world map) – a preliminary starting point for all seismic hazard analyses. The map ignores national frontiers. This map spans further than Greece, the Aegean and Turkey, extending well into western Europe.

Now take a scientific leap of faith over a century and half to the last map of **Figure 20**. At face value it appears little different in terms of the seismic "Bands" resolved. This is as it should be; they describe the same seismicity. They differ in underlying material content, and approach, as the discipline evolves. The map in **Figure 20** is extracted from R. T. Ministry of Interior, Disaster and Emergency Management Presidency, Department of Earthquake, and showcases their contemporary wealth of archived earthquake catalogue data, seismograph data and extensive earthquake strong ground motion observation network in Turkey today. The map embraces the need for: earthquake catalogues, understanding of now obvious "Bands" and zones and seismotectonic implications, maximum magnitudes, average recurrence times of earthquakes, recurrence rates of strong ground shaking (and

EEFIT

hence relationships between intensity and engineering strong ground motion parameters), direct observation of strong ground motion and hence ground motion prediction equations (GMPEs) describing the attenuation and dissipation of earthquake energy with distance, and statistical methodologies to forecast magnitude and ground motion with time histories and spectra. That is a long list of needs, however, unlike some studies, the cultures of Greece and Turkey have led to a wealth of diverse material leading to their national standards of earthquake defence.

There are two basic types of calculation from catalogues: Type1) seismicity or magnitude recurrence rates, and return periods (magnitude seismic hazard); Type2) ground shaking (conventionally seismic hazard for engineering parameters). These overlap considerably in their requirements and diversity, nevertheless each forms a chain-like calculation. The box in the text below poses a Schematic to assist and organise discussion.

There are overlaps between the chains of analysis, including starting point and general direction, and critical differences such as the need for establishing and selecting GMPEs, and the practical observational need for recording strong ground motion time histories in addition to seismograms of all the seismic phases. The links in the chains have varied lives, some are permanent subject to continual addition and improvement (catalogues), some become outmoded and are simply replaced (e.g. GMPEs), some become subject to alternative concepts and visualisations (e.g. tectonic models, statistical models, zonations) and some links in the chain are simply ephemeral realisations of a chain of analysis (this is particularly true of the outcomes sought, viz, the seismic hazard maps themselves).

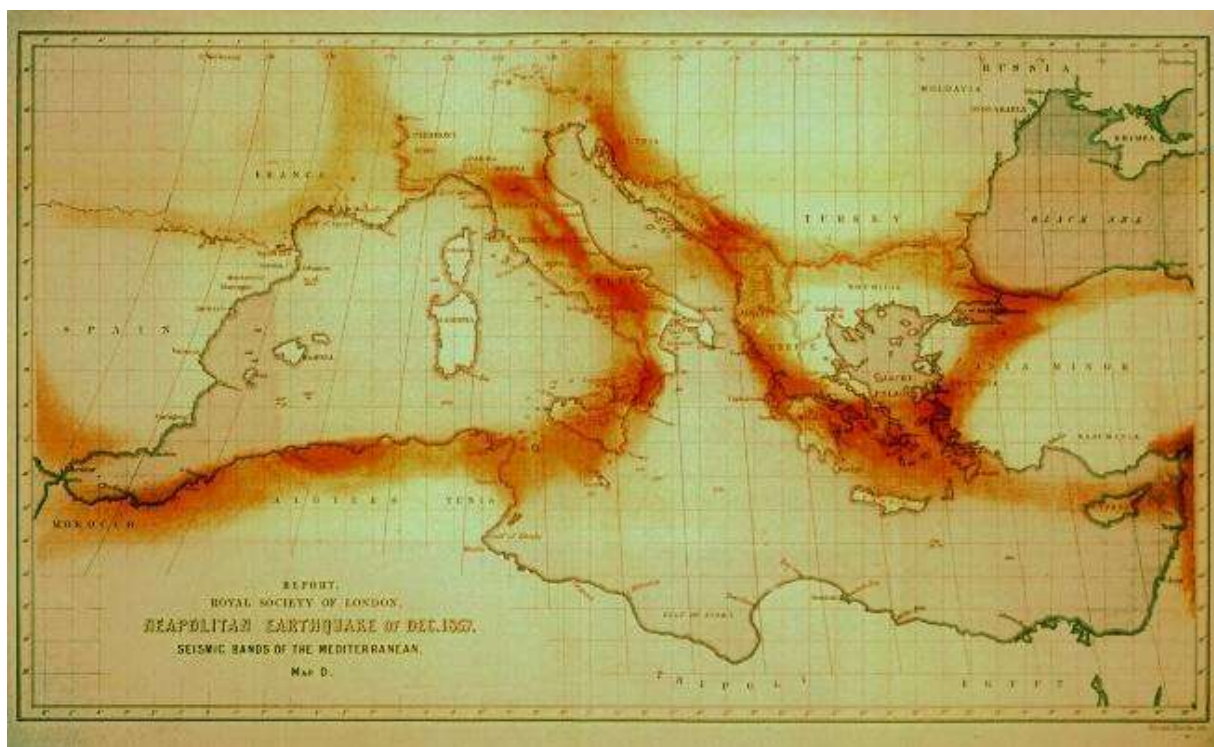


Figure 13: Mallet's (1862) map of 1857 depicts "Bands" around the Mediterranean that are defined by historical record of damage to buildings; it illustrates the modern idea of risk as it extends the earthquake hazard to damage and loss.

Schematic:

0) earthquake observation → homogenisation e.g. intensity/magnitude scale → earthquake catalogue → technical issues e.g. completeness

Type1) catalogue → technical completeness → statistics → Magnitude return periods

Maximum magnitude

Scenario earthquakes

Type2) catalogue → GMPEs → calculate ground shaking → statistics → Shaking repeat times

Spectra/SM histories

Building codes

With the above perspective, a representative selection of articles is considered to provide visual regional examples of related seismicity and seismic hazard maps, maximum magnitude, deaggregation and perceptibility. There is a wealth of diverse material for Greece and Turkey, with Greece having the highest seismicity in Europe. An attempt to tabulate papers with respect to catalogue used, GMPEs filtered and then selected, choice of statistics, zonations, statistics adopted, map and parameter outcomes...was not productive, given the plethora of material. Hence the selection of visual illustration with brief comment. However, this will be resolved by consideration and tabulation of values specific to Samos, and surrounding region of nearest Turkey; the coasts of both are nearly equidistant to the epicentre of the Aegean Sea 2020 earthquake.

2.8.1. Earthquake magnitude and return periods

The energy (E) in an earthquake or the magnitude (M) with their rate of recurrence provide short-hand descriptions of seismicity. Estimates have been calculated for Greece, the Aegean and Turkey many times over the years. **Figure 14** illustrates three maps; two of these provide contours for M100 and M475 respectively, calculated without zonation (Burton et al., 2004) and the third, more recent, illustrates M100 in clearly defined zones for Turkey (Bayrak et al., 2008). M100 represents estimates of the largest earthquake magnitude expected for a 100-year time span, M475 that for 475-years. There is a commonly understood equivalence between an occurrence with 90% probability of not being exceeded (p.n.b.e., or 10% probability of being exceeded, p.b.e.) in 50-years and M475. These maps suggest 100-year magnitude values of 6.5, 7.0 and a 475-year earthquake magnitude of 7.3 for the seismicity of Samos. A magnitude 6.9 Mw (moment magnitude) is far from unexpected for the vicinity of Samos.

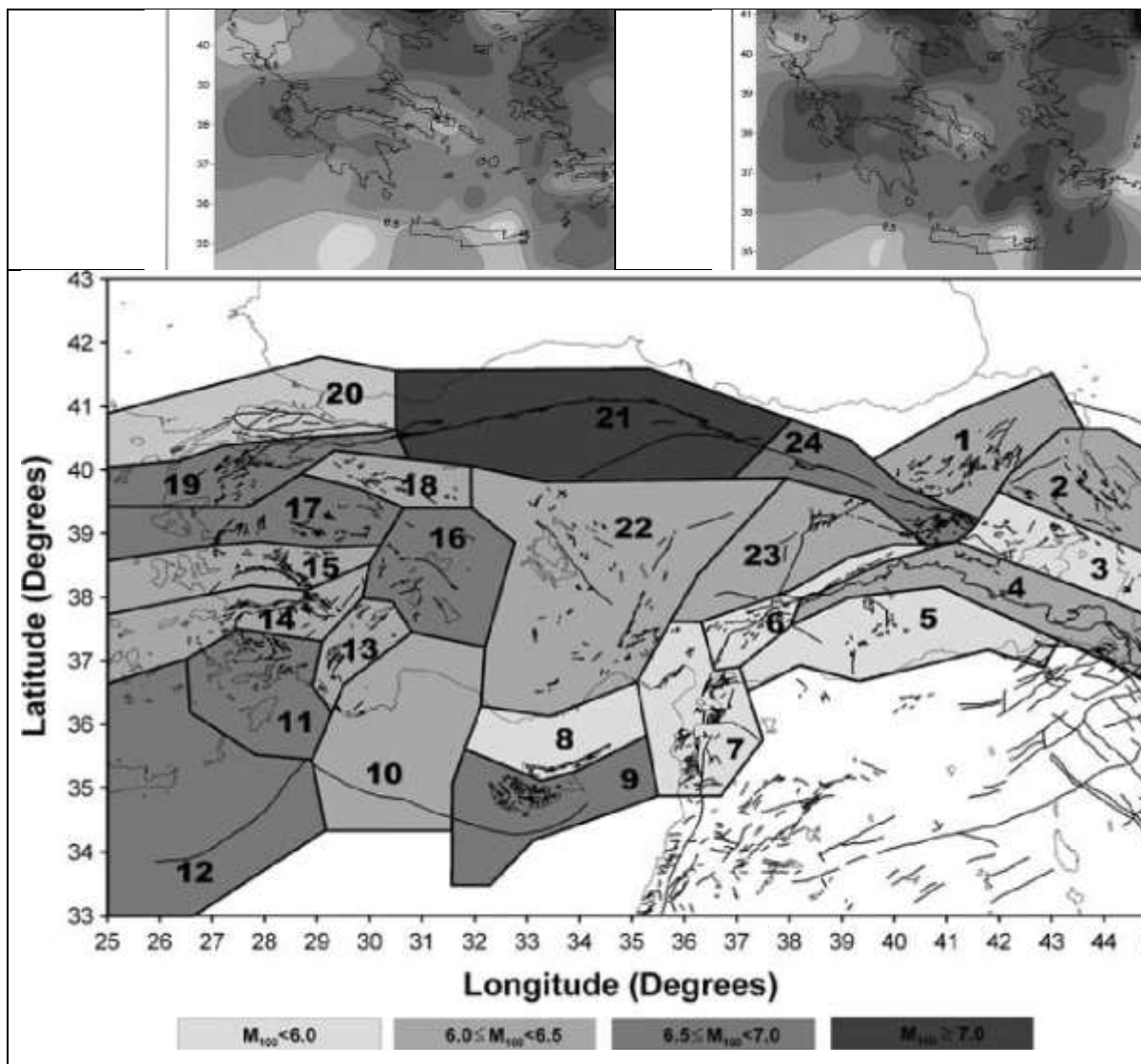


Figure 14: Earthquake magnitude return periods. (a) and (b) provide contours, without zonation, of the 100-year and 475-year earthquake respectively (the latter equivalent to 10% probability exceeded in 50 years (Burton et al., 2004) whereas Bayrak et al. (2008) illustrate the 100-year earthquake in 24 explicit zones in Turkey.

2.8.2. “Bands” and evolution of zones and zonation

“Bands” of seismicity in Greece, Aegean and Turkey are demonstrable in Mallet’s 1857 map and were based entirely on observations (of earthquake impact) in the field, these were not ephemeral, and these “Bands” became here to stay. What has changed and evolved in a century and half is an understanding of seismotectonics linking geology and seismicity profiles of a region, and hence a spectrum of approaches to zonation. Bayrak et al. (2008) sum up the challenge and the shortfall in three succinct sentences:

“A complete comprehension of the historical and instrumental seismicity, tectonics, geology, paleoseismology, and other neotectonics properties of the studying region are necessary for an ideal delineation of seismic source zones. But, for much of the world it is not always possible to compile detailed information in all these fields. Thus, seismic source zones are frequently determined with two fundamental tools; (1) a seismicity profile, and (2) the tectonic structure of the region under consideration”.

(Erdik et al., 1999).

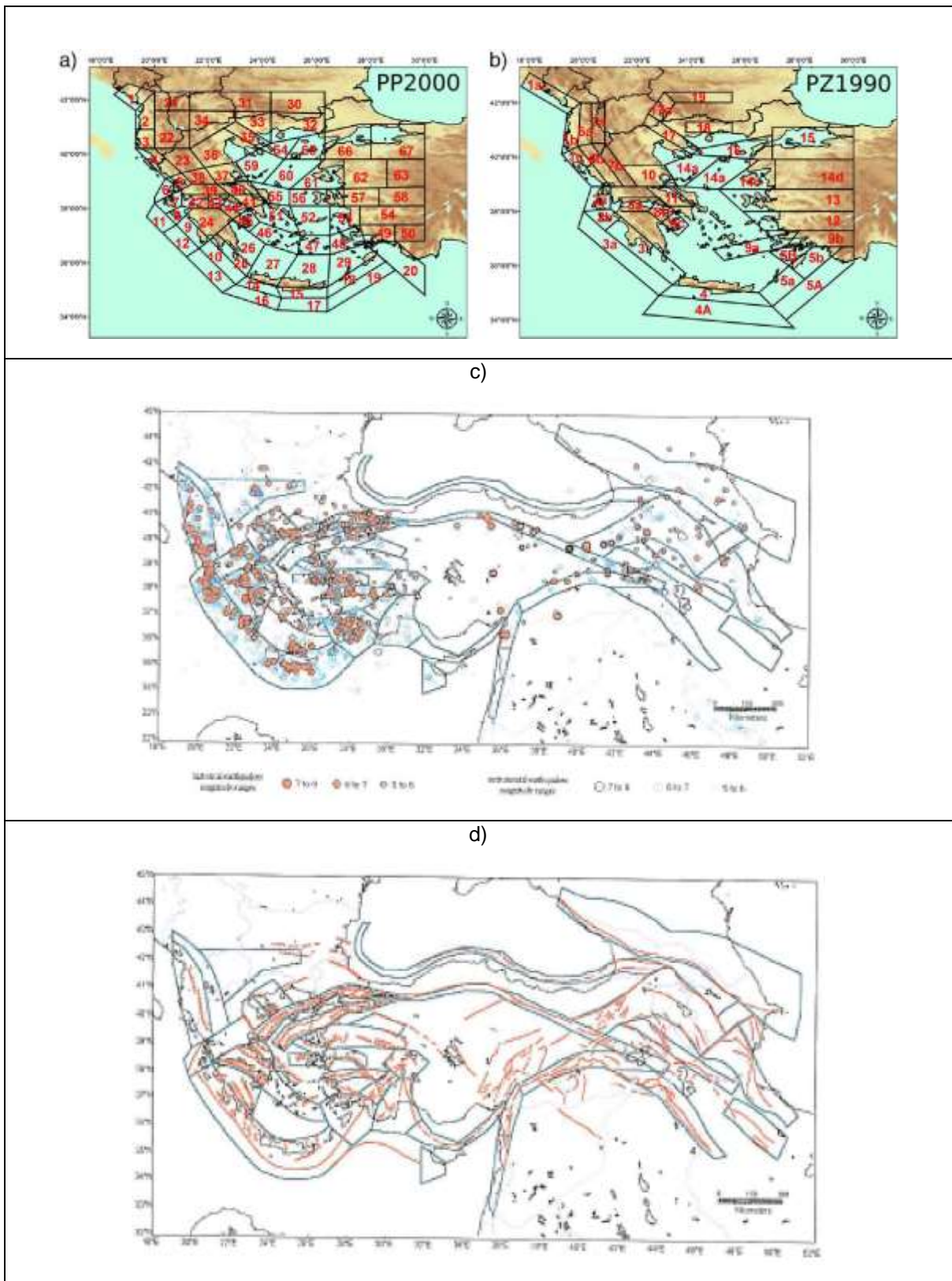


Figure 15: Traditional Zonation: Greece and Turkey. (a) and (b) are traditional Euclidean seismic zones for Greece developed by Papazachos with Papaioannou (1900, 2000). (c) and (d) Erdik et al.'s (1985, 1999) zones for Turkey founded on the axioms of (c) seismicity and (d) fault zones, together supporting each zone.

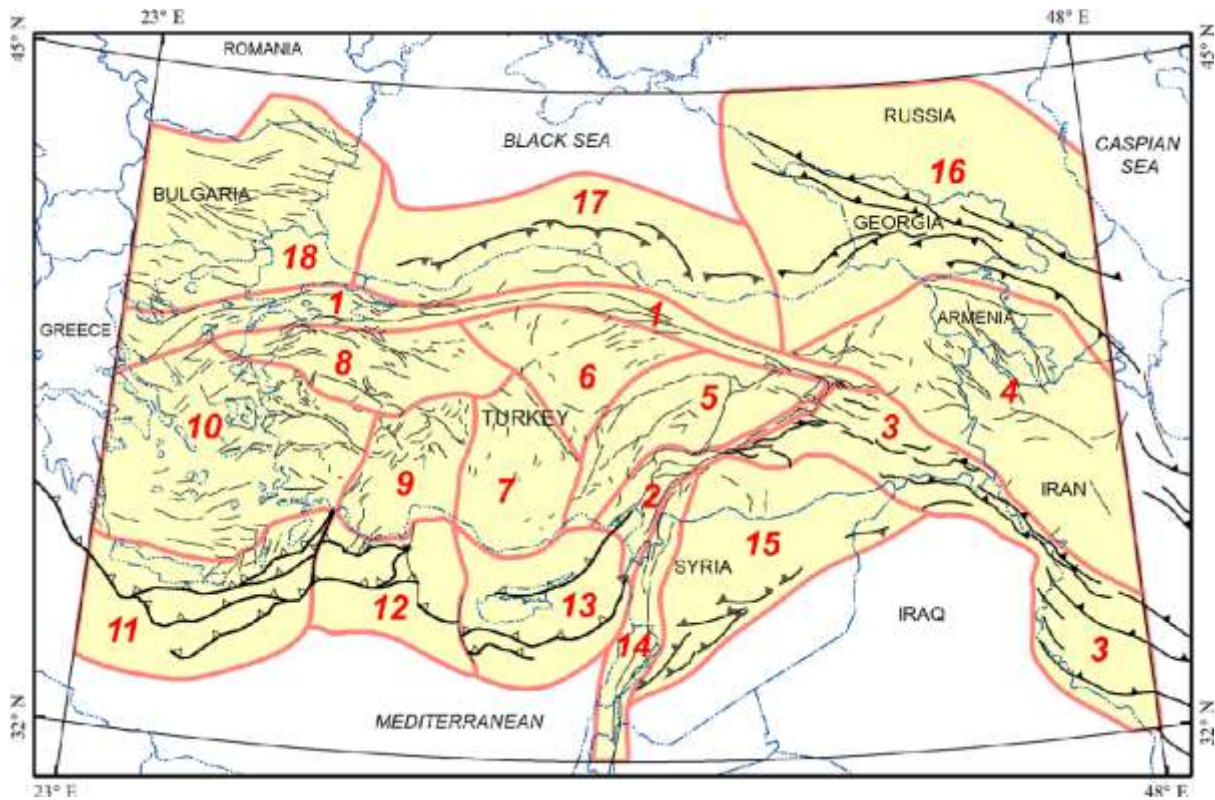


Figure 16: Recent zonation: Aegean and Turkey. 18 major zones adopted by Sesetyan et al. (2018) based on Duman et al.'s (2016) seismotectonic database.

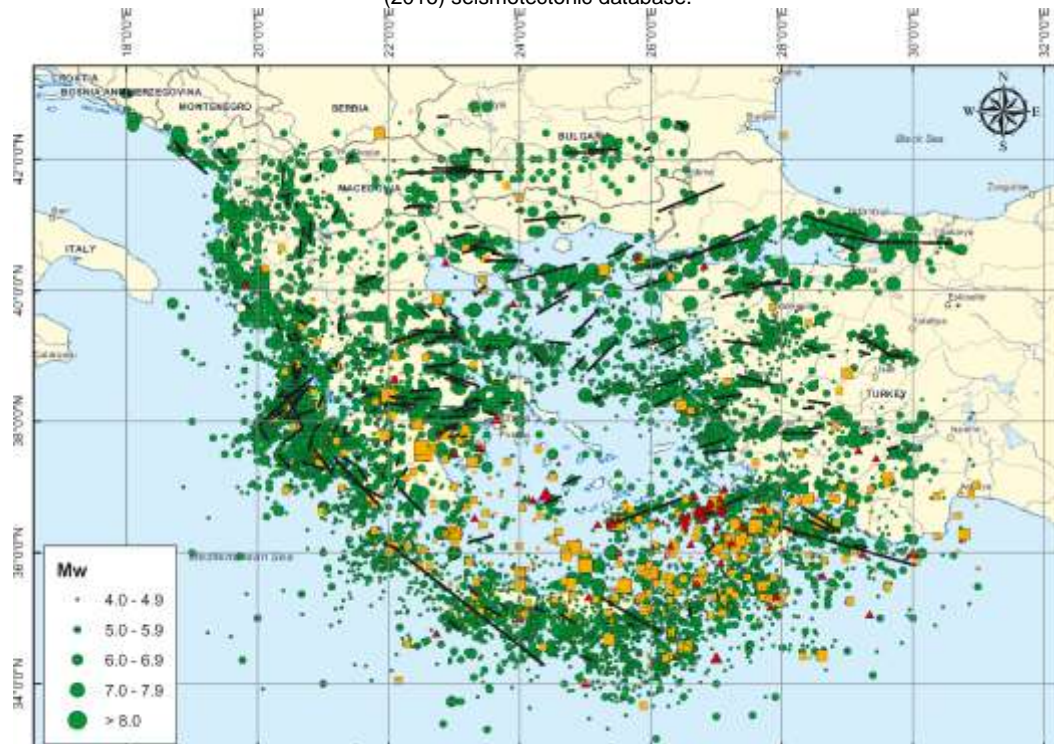


Figure 17: Seismicity and fault ruptures: Greece, the Aegean and W Turkey (Weatherill & Burton, 2009; fault ruptures calculated from length after Papazachos et al. (1999) catalogue).

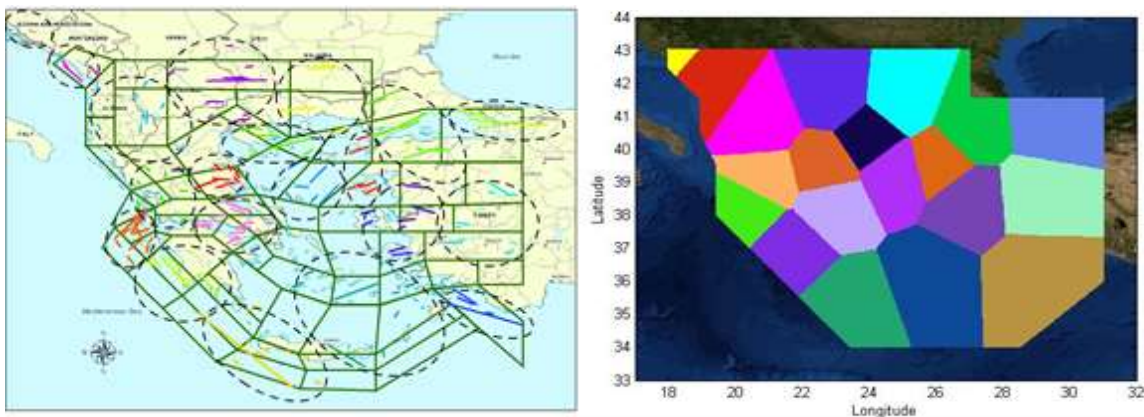


Figure 18: “Soft” zonation: Greece, Aegean and W Turkey. Ellipses indicate 27 earthquake clusters optimised using seismicity and fault zone data (Weatherill & Burton, 2009) with hard Euclidean zones of Papaioannou & Papazachos (2000) superimposed. Tessellation provides pseudo hard zone imagery.

Two long standing zonation models for Greece and Turkey are illustrated in **Figure 15**. Euclidean zones of seismicity were developed over decades by Papaioannou & Papazachos and then revised (1990, 2000) as in **Figure 15**. This zonation model is founded on an intensely researched earthquake catalogue (of historical and instrumental earthquake data) merged with geological information. Erdik et al. (1985, 1999) likewise produced a zonation model for Turkey. The two facets of Erdik et al.’s model, earthquakes in the derived zones, and tectonic features in the same zones, are shown in **Figure 15**. More recently Duman et al. (2016), as adopted and displayed in Sesetyan et al. (2018), have deduced a new model consisting of a set of 18 major seismotectonic zones which are defined by the earthquakes and fault zones with “similar characteristics” (see **Figure 16**). An example of the two main ingredients of zonation for Greece and Aegean, seismicity and faulting, are illustrated in **Figure 17** which includes strike and rupture lengths indicated by Papazachos et al. (1999). However, the hard geometry imposed by Euclidean zones is not an essential approach to its understanding. Groups of related earthquakes can be identified and brought together as clusters using Hartigan’s (1975) techniques. An outcome with 27 clusters, separate ellipses indicating clusters – but not boundaries, are shown in **Figure 18** (Weatherill & Burton, 2009) with Papaioannou & Papazachos (2000) Euclidean zones superimposed. Pseudo hard boundaries can be forced onto the clusters using tessellation to provide a traditional image.

2.8.3. Seismic Hazard Maps Greece, the Aegean and Turkey

The need to obtain engineering ground-motion parameters and provide these to assist with the design of earthquake resistant structures originally centred on linking intensity scale degrees with ground-motion or strong ground-shaking observations. Thus, Modified Mercalli and MSK Intensity scale degrees would be linked to the physically dimensioned peak ground acceleration $PGA \text{ cm s}^{-2}$. This need persists in ongoing reviewing of, for example, pre-instrumental historical earthquakes. There are many engineering ground-motion parameters now considered desirable, including, for example, peak ground velocity, displacement, Arias intensity and cumulative absolute velocity. There are also many ground motion prediction equations (GMPE) describing the attenuation of earthquake ground-motion from epicentre to point-of-interest. Even recently, Tselentis & Danciu (2008) examine the relationship between MMI and PGA etc. for Greece; one finding being a model that had lowest standard deviation of the MMI predictive model for PGA, another, that site effect (V_{s30}) has a little influence on the MMI prediction model for PGV. That said, **Figure 19** and **Figure 20** roll out six probabilistic seismic hazard maps (PSHA) for Greece and Turkey with PGA as the example engineering ground-motion parameter. These maps are outcomes from a variety of Type 2 methodologies and complexities (Schematic box above) and use a wide range of GMPEs in their construction of epicentre \rightarrow PGA at point-of-interest. In all cases, the outcome map of the methodology illustrated is cast at the 10% probability of exceedance level in 50-years, that is a PGA_{475} calculation similar to magnitude recurrence maps. In both **Figure 19** and **Figure 20**, the map depicted last is a recently produced map prepared by a Greek or Turkish team of analysts.

First, consider the extant seismic hazard mapping for Greece, Aegean and W Turkey. The methodology in the first map of **Figure 19** adopts an unzoned technique in which a matrix of points is constructed throughout the study area, ground-motions calculated and then analysed using extreme value statistics

to obtain PGA475 (Burton et al., 2003). The second map in **Figure 19** adopts the 27 earthquake clusters of **Figure 18** (soft-zonation), with fault control in addition supplied by strike and rupture lengths estimated from the Papazachos et al. (1999) data on rupture zones, and Monte Carlo probabilistic seismic hazard analysis (PSHA) (Ebel & Kafka, 1999) to determine multiple simulation of ground motion at a site (Weatherill & Burton, 2010); thus the two fundamental tools, or axioms, of Erdik et al. (1999) are in composite consideration.

The larger, third map, is drawn from Tselentis & Danciu (2010a) in **Figure 19**, and relies on 67 zones (Papaioannou & Papazachos, 2000) and quantifying the seismicity in each zone through the well-known Gutenberg-Richter “a” and “b” parameters determining frequency. The recent rapid increase in GMPEs available in Greece, due to improvement of the strong motion networks providing regional ground truth, is recognised, but the primary GMPE selected is that of Danciu & Tselentis (2007), accompanied by extensive discussion of the exact equations posed by other Authors for other engineering parameters.

It is difficult to see how the three maps of **Figure 19** could be more divergent in their methodologies or even selection of GMPEs. Inspection of the three maps for the vicinity of Samos yields PGA475 values of 400 cm s⁻², 400-500 cm s⁻² and 0.4-0.5 g (~390-490 cm s⁻²). Divergence of methodology, yet there is convergence of result.

Secondly, in **Figure 20**, we examine similarly the seismic hazard PGA for Turkey through three maps. The first map (Erdik et al., 1999) was created through the Global Seismic Hazard Programme (GSHAP, Giardini & Basham, 1993), a programme created to attempt to produce a world-scale, homogeneous PSHA map that would overcome transfrontier differences in available maps. The fundamental approach was the traditional one of Cornell (1968) and assumes zones each with uniform seismicity. Erdik et al. (1999) adopt 37 zones (illustrated in **Figure 15**), a Poisson model for earthquake occurrence, viz, the recurrence relationship for earthquakes is the Gutenberg-Richter:

$$\log N = a - bM$$

where N is the number of earthquakes of magnitude M or greater per unit time, and “a” and “b” are the classic regression parameters.

Three attenuation relationships, GMPEs, were adopted with equal weights. Sesetyan et al. (2018) have recently published the second map of **Figure 20**. They point out it is to be used in conjunction with updates of the national seismic design code, and to produce ground-motion parameters e.g., design spectra, required in the new Turkish Earthquake Design Code. There is a second part or sequel to Sesetyan et al. (2018) from Demircioglu et al. (2018) which presents additional models and conceptual approaches leading to additional PSHA maps. The example map in **Figure 20** adopts, and adapts, the 18 main seismotectonic domains of Duman et al. (2016) of **Figure 16** “which has been used as a guide” when delineating the source zones for modelling the hazard. The zonation model used in computation uses zone characteristics of maximum magnitude, focal depth distribution, predominant strike and slip angles, top and bottom depths to a zone, and recurrence parameters from the Gutenberg-Richter relationship. Logic trees are adopted to explore alternative possibilities for a parameter e.g. estimates of maximum magnitude. The final map of **Figure 20** might be considered definitive (but all seismic hazard maps are ephemeral); extracted from R. T. Ministry of Interior, Disaster and Emergency Management Presidency, Department of Earthquake, it demonstrates their contemporary wealth of archived earthquake data, and state-of-the-art analysis. It was extracted recently in November 2020 for this project and again depicts PGA475.

Inspection of these three maps at the nearest approach of mainland Turkey to the east Aegean island Samos, or Samos itself, yields PGA475 values of ~0.5 g, ~0.48 g and ~0.4 g. Once again, there is fundamental divergence of methodology, followed by convergence of result.

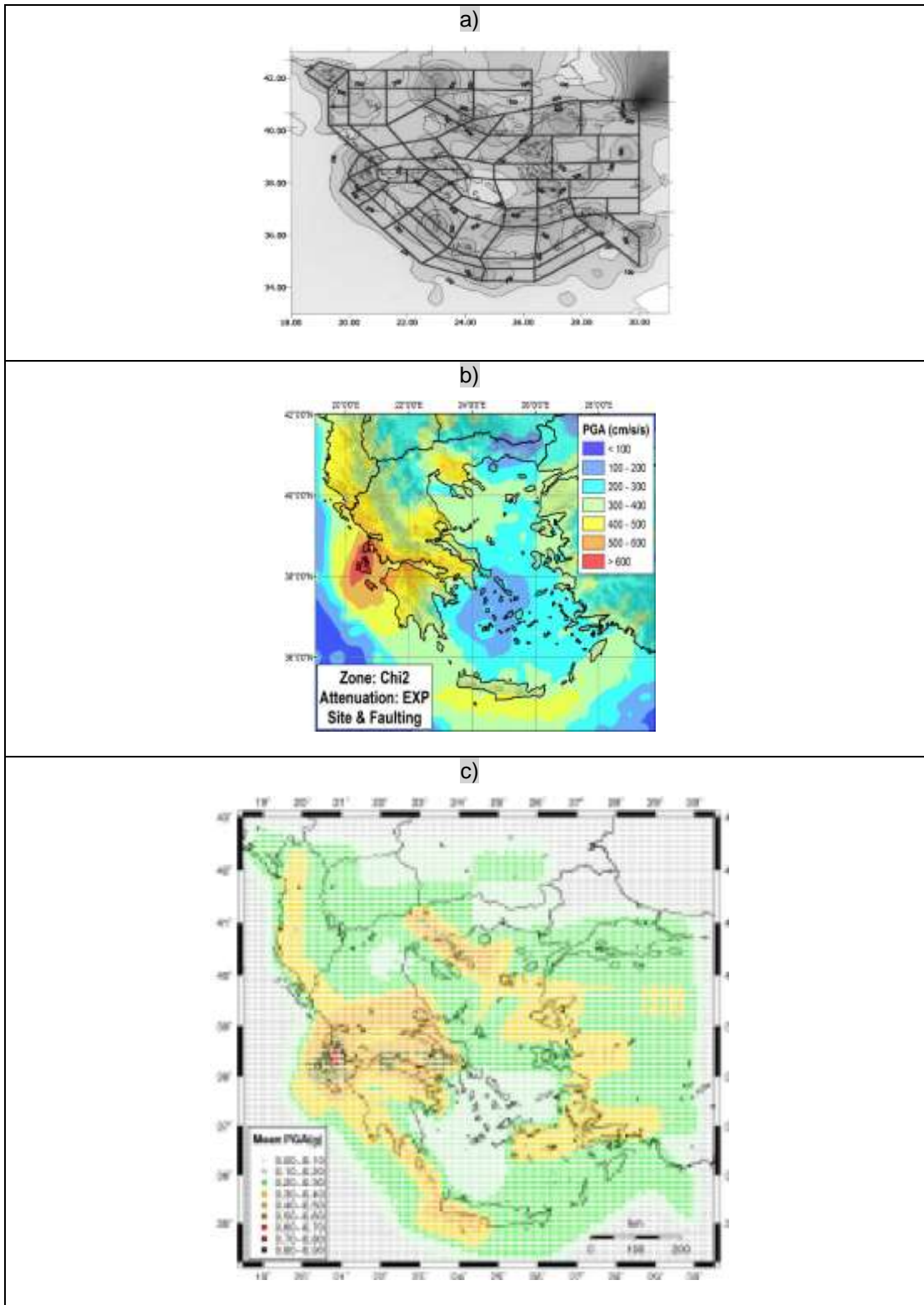


Figure 19: Recent seismic hazard mapping: Greece, the Aegean and Western Turkey. All three maps depict PGA with 10% probability exceedance in 50 years, viz, PGA475. (a) no-zonation method (Burton et al., 2003) with Papaioannou & Papazachos (2000) zones superimposed. (b) soft-zonation method using the 27 clusters of Figure 18 with Monte Carlo PSHA (Weatherill & Burton, 2010). (c) hard-zonation method of Tselentis & Danciu (2010) using Gutenberg-Richter PSHA and 67 Papaioannou & Papazachos (2000) zones.

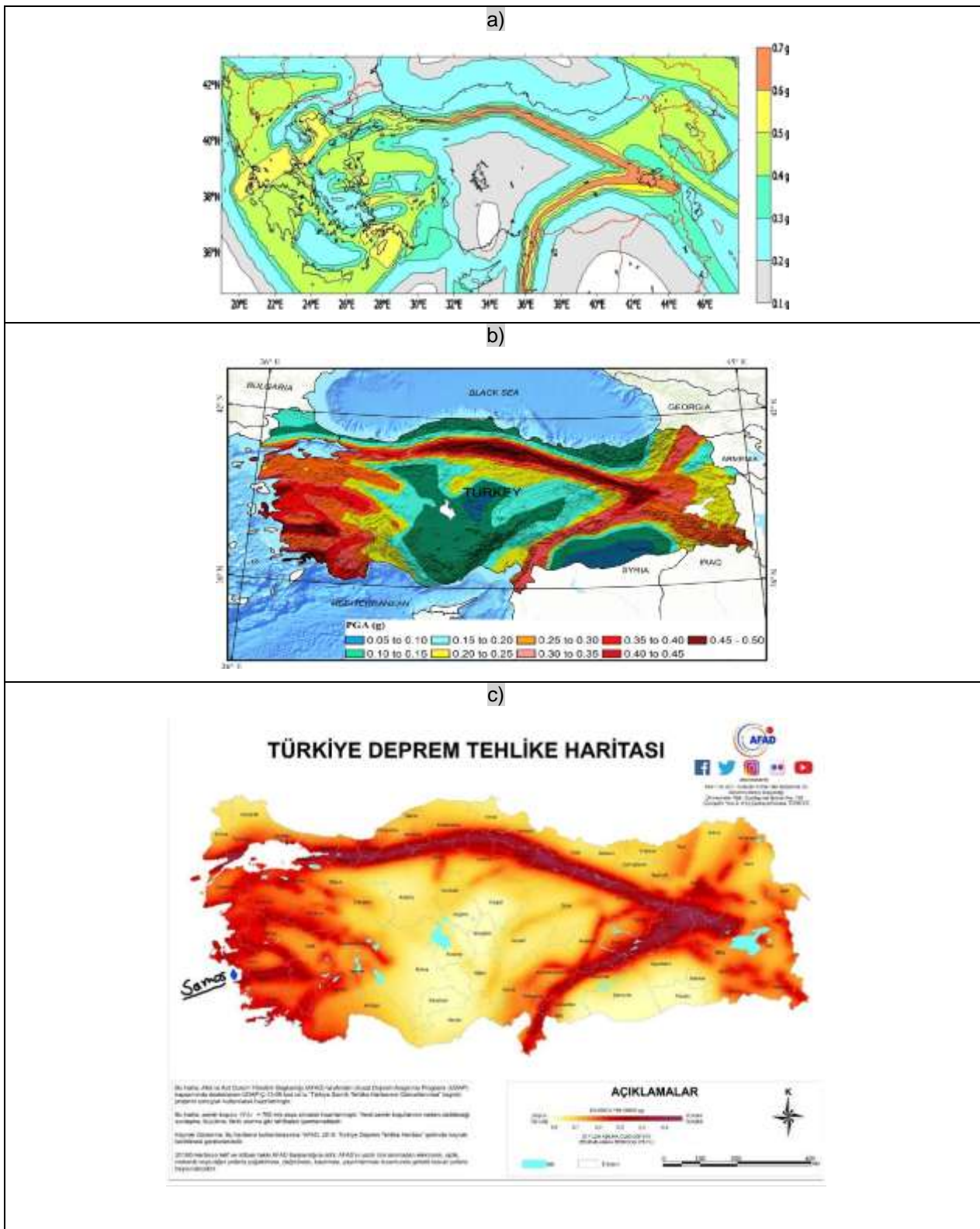


Figure 20: Recent seismic hazard mapping, Turkey. PGA with 10% probability exceedance in 50 years, PGA475. (a) hard-zonation method, 37 zones, with Gutenberg-Richter statistics, Erdik et al. (1999). (b) recent hard-zonation method, using 18 major zones of Figure 16 Sesetyan et al. (2018). (c) most recent map of R. T. Ministry of Interior, Disaster and Emergency Management Presidency, Department of Earthquake (downloaded November 2020).

2.8.4. Maximum Magnitude

Any study of the seismicity and seismotectonics of a region that is ultimately directed to protection of the people is insufficient, inadequate, without consideration of the largest earthquake that might be generated and consideration of its true rarity. Generation of the largest earthquake is directed by global tectonics imposing a finite strain rate into a finite fault system during the current tectonic regime (large faults created in a previous tectonic regime can be reactivated) – it may not have been observed in the earthquake catalogue.

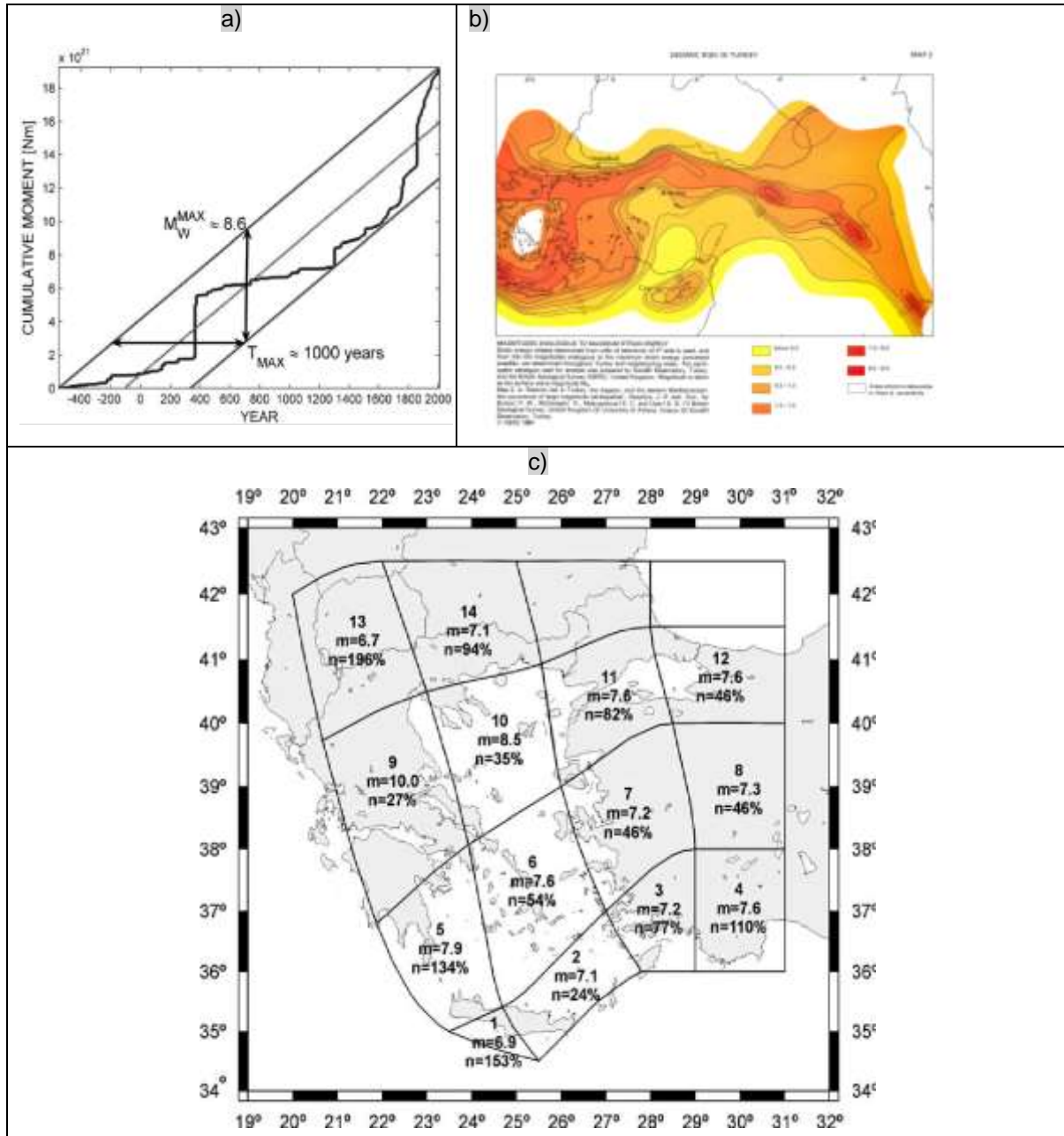


Figure 21: Maximum Magnitude M_{max} . (a) Staircase step-by-step release of energy released by earthquakes, M_{max} being estimated by the energy gap between the two outer lines and (b) M_{max} contoured for Turkey (Makropoulos & Burton, 1983; Burton et al., 1984). (c) M_{max} deduced by Koravos et al. (2003a) in large zones using seismicity and geodetic strain data.

The maximum magnitude earthquake, M_{\max} , is typically estimated using estimates of cumulative seismic energy accumulation and release, strain rates, geological estimates of fault length and statistics of earthquake recurrence rates that include an upper bound parameter (the “maximum considered earthquake” of the nuclear industry is a lesser earthquake). Such estimates of M_{\max} are usually backed up by identifying the largest earthquake that has been observed, which it must exceed. The graph in **Figure 21** depicts a staircase of abrupt releases of coseismic energy release or cumulative moment release, as can be calculated from an earthquake catalogue (after Weatherill & Burton, 2010, adapting Makropoulos & Burton, 1983); the larger steps in the staircase are the larger observed earthquakes. The energy step between the lower and upper parallel lines enveloping the entire process of energy release is the maximum possible quantity of energy that can be stored and conceivably released by the system, from which $M_{\max}(E)$ can be calculated simply. The older colour map (Burton et al., 1984) shows the outcome for all Turkey. A newer approach that in addition to evidence of the earthquake catalogue also incorporates geodetic data, measured strain rates, obtains results for 14 large zones spanning Greece, Aegean and western Turkey (Koravos et al., 2003a).

Additional approaches to M_{\max} determination are depicted in **Figure 22**. Bayrak et al. (2008) provide a map with 24 zones spanning Aegean and Turkey indicating what they consider to be the largest observed earthquake observed in each specific region. Estimates of the upper bound magnitude, made using extreme value statistics, are also provided by Bayrak et al. for the same set of zones; their map of regional values for M_{\max} (upper bound) is in **Figure 22** and a full set of parameter values is tabulated in their article. The large map extracted from Sesetyan et al. (2018) relies on calculation of characteristic mean magnitudes obtained from fault segment lengths (L) inside an individual source zone, using Wells & Coppersmith (1994) relationships between M and L , and a consideration of observed largest earthquakes. It should be noted that in practice, when calculating PSHA, Sesetyan et al. straddle their $M_{\max}(L)$ with 0.3 increments of magnitude in a logic tree assessment in attempt to embrace model (epistemic) uncertainties.

There are five maps representing a range of approaches to M_{\max} shown in **Figures 21-22**. Considering model zones that include Samos then, those in **Figure 21**, relying on cumulative coseismic energy release, and secondly, including geodetic strain, indicate $M_{\max}(E)$ of ~ 7.5 and ~ 7.2 . Similarly, in **Figure 22** values of M_{\max} based on maximum observed, upper bound statistics and mean fault length are $M_{\max}(\text{observed}) \sim 6.8$, $M_{\max}(\text{upper bound}) \sim 7.4 \pm 1.4$ and $M_{\max}(L) \sim 7.3$. All estimates of calculated M_{\max} exceed the observed maximum magnitude of Bayrak et al. (2008) and the magnitude of the recent 30 October 2020 Aegean Sea earthquake; as expected. This spread of M_{\max} values also demonstrates convergence. It is to be noted that region 14 of Bayrak et al. clearly confines the primary source hazard of the Buyuk and Kucuk Menderes grabens. Sesetyan et al. (2018) embrace the graben structures using two shallow crustal sources juxtaposed geometrically just East of Samos, never-the-less the two juxtaposed zones have identical M_{\max} in their map in **Figure 22**.

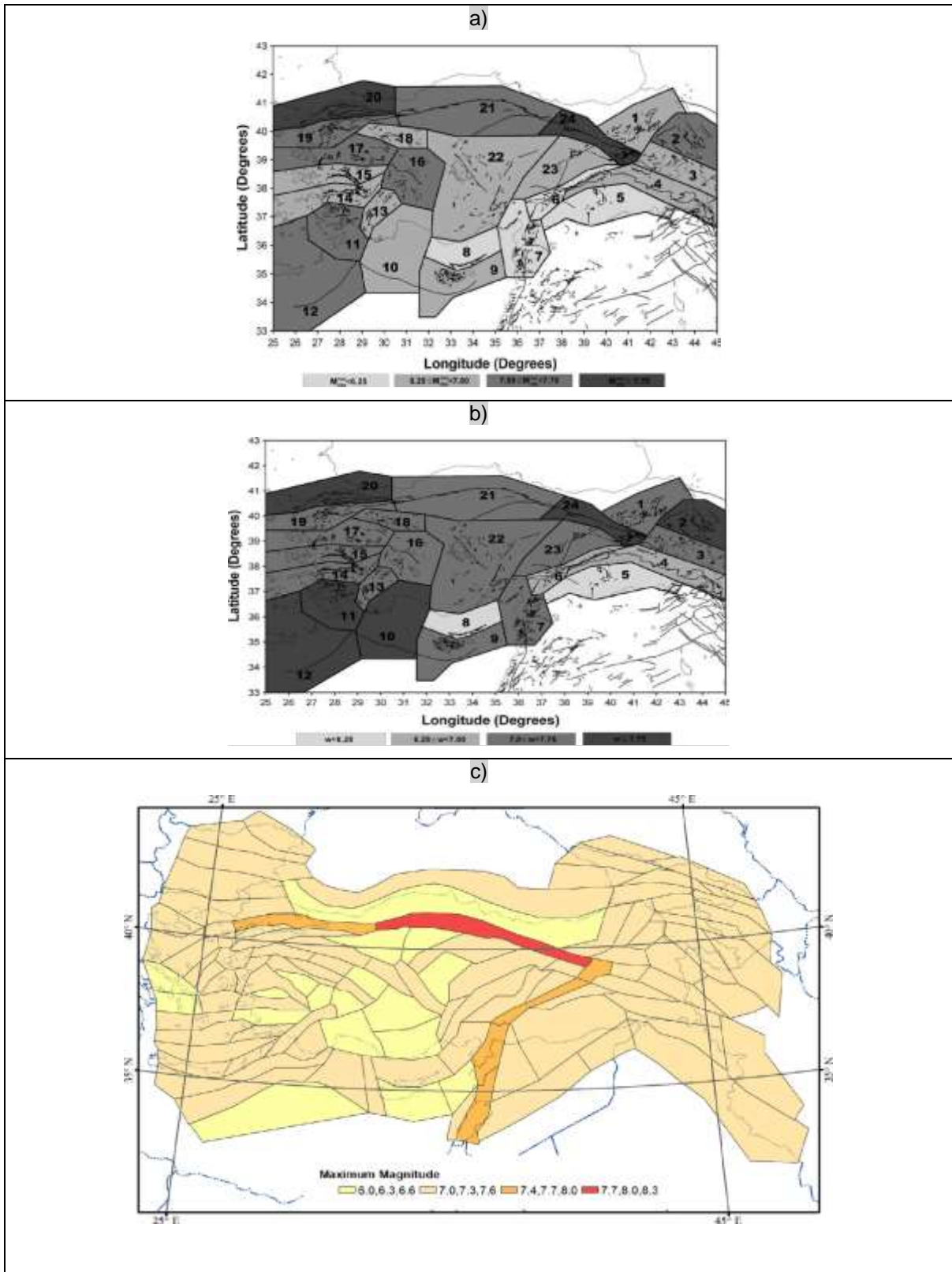


Figure 22: Maximum Magnitude M_{max} . Bayrak et al. (2008) adopt 24 zones and depict in (a) the largest observed earthquake and in (b) the upper bound magnitude determined using extreme value statistics. (c) Sesetyan et al. (2018) determine zone M_{max} values using fault segment lengths and Wells & Coppersmith (1994) relationships to estimate M_{max} .

2.8.5. Deaggregation and Perceptibility

There are needs for earthquake scenarios. These may not directly assist the structural engineer but certainly are needed by those sharing a common interest in the same hazard and ensuing risk, for instance: urban land use planners (Tsapanos, 2003), strategic lifeline planners, and insurers and reinsurers. The magnitude of any earthquake associated with population panic or building damage can be considered as scenario source to interact with vulnerability of the population and built environment (or natural environment, e.g. landslides) to identify impacts, but it is better to have a logic behind the selection of a scenario earthquake. A simple logic tree might point to the maximum earthquake, but this in some circumstances might be assessed as so rare that taking onboard a scenario value of its impact and \$losses might undermine a cost-benefit analysis.

A full PSHA aggregates all earthquake occurrences (all M) at all ranges, source-to-site distance (R) to obtain PSHA parameters (e.g. PGA) at the site-of-interest. Deaggregation, in principle, identifies the M - R pairing that contributes most pertinently to the exposure of the site-of-interest: simplistically, is it near, small earthquakes, or is it distant, larger earthquakes that have more impact? It is often used in assessing or designing complex or critical engineered structures (McGuire & Shedlock, 1981; Chapman, 1995). Tselentis & Danciu (2010b) deaggregate their existing PSHA for Greece (Tselentis & Danciu, 2010a; Tselentis et al., 2010). They deaggregate in terms of M - R (and a third parameter) and in relation to several PSHA parameters including PGA associated with the norm of 475-year return period (10% probability exceedance in 50-year). They map results on a dense point matrix throughout Greece, the Aegean and Western Turkey and the example in **Figure 23** illustrates the outcome in terms of mean magnitudes.

A conceptually different approach to the problem invokes perceptibility (schematic **Figure 23**), viz, the conditional chance of perceiving a magnitude M earthquake after it has occurred (Burton, 1978). The principle is that the probability of earthquake occurrence decreases with increasing magnitude, on the other hand, the chance of feeling an earthquake in a region increases with magnitude – felt area is larger for larger earthquakes. The conditional probability $P(x | M)$ determines perceptibility in terms of ground shaking $\geq x$ (intensity, PGA or PGV) given the annual probability of a magnitude M earthquake – the inevitable peak of the conditional probability curve is the most perceptible earthquake magnitude M_p . A scenario leading to design earthquakes for use with respect to anti-seismic urban dwelling in Crete, following similar methodology, has been developed by Tsapanos (2003). The three related maps of **Figure 23** illustrate two that apply to all Turkey and the Aegean and one to Greece, the Aegean and Western Turkey (Koravos et al., 2003b; Burton et al., 1984, 2004). The results of Koravos et al. (2003b) apply to 16 tectonic zones, usually large zones, constrained by geodetic crustal deformation rates, and the corresponding results for M_p are noted for each zone ($mp(x)$ in Koravos et al. notation) in **Figure 23**.

Inspection of the Tselentis & Danciu (2020) deaggregation map using PGA475 indicates a scenario earthquake magnitude ~ 6.4 for Samos. The three most perceptible earthquake scenario magnitudes are $M_p \sim 6.6$, ~ 6.5 and 7.2 ± 0.1 . The first three values of these four converge, the third is a relative outlier, probably dictated in result by the considerable geographic extent and seismotectonic coverage of its pertinent zone 3.

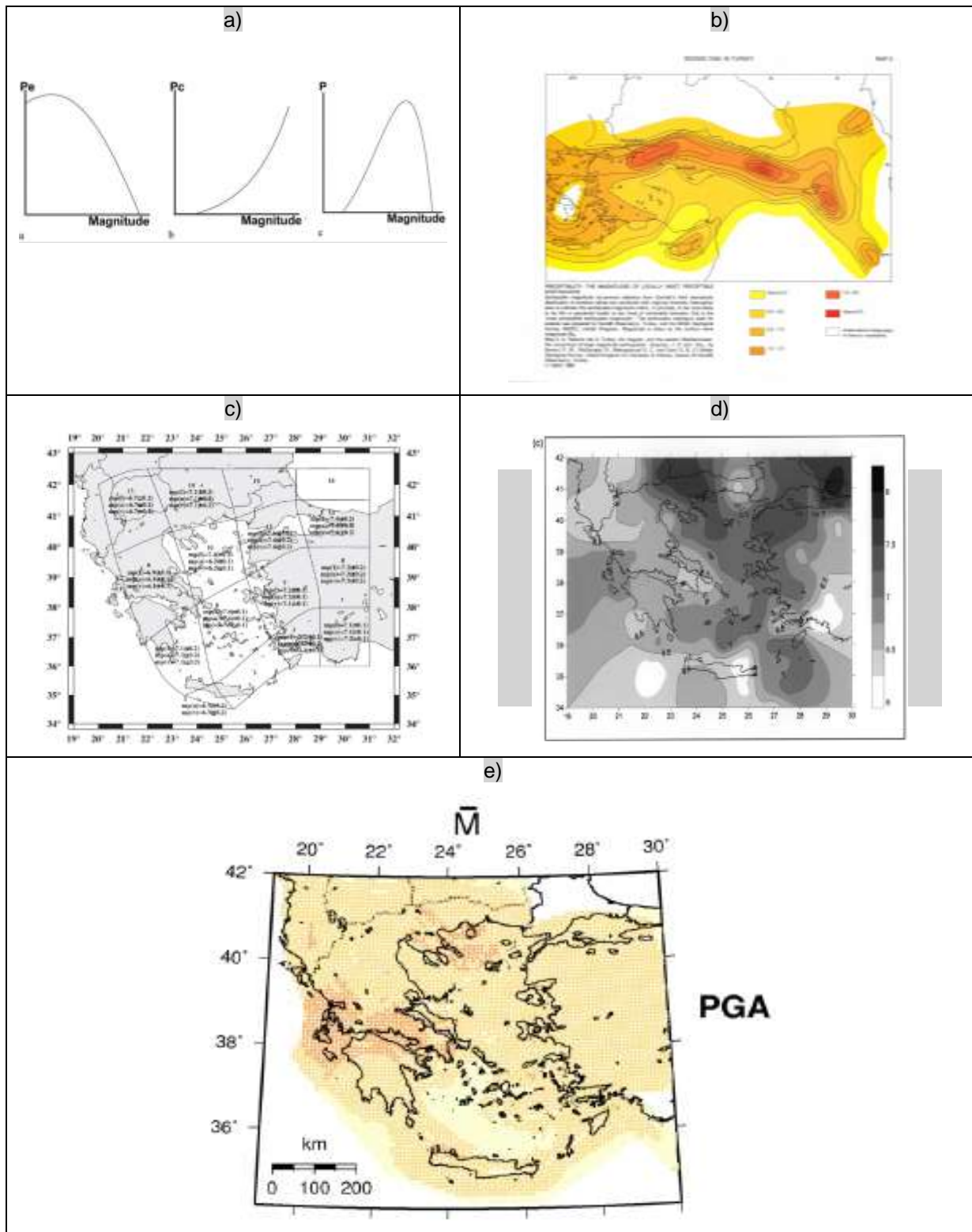


Figure 23: Most Perceptible Earthquake M_p and De-aggregation. With increasing magnitude, the probability of occurrence decreases but the probability of then experiencing strong shaking, e.g. $I = VII$, increases and their product in (a) shows a peak at M_p , the most perceptible earthquake, illustrated in (b) throughout Turkey (Burton et al., 1984). (c) Koravos et al. (2003b) adopt 16 zones spanning Greece, Aegean and W Turkey and constraints including geodetic deformation rates to calculate M_p . (d) M_p contoured without zonation throughout Greece, Aegean and W Turkey (Burton et al., 2004). (e) Tselentis & Danciu (2010) examine magnitude/range (source-site) pairings to identify the magnitude that causes most PGA exposure at a matrix of points over Greece, Aegean and Western Turkey.

2.8.6. Hazard Summary and Perspective on the Aegean Sea 2020 Earthquake

The earthquake of 30 October 2020 had shallow focal depth with epicentre about 14 km NNE of Neon Karlovasion, Samos, into the Aegean Sea. The distance further northwards to the Turkish mainland was only slightly greater (and Izmir about 40 km distance). It is already labelled the Aegean Sea earthquake; this is a vague label and as the island of Samos is the nearest landmass it serves to focus geographical attention. Throughout the above review, and what follows here as summary, is also relevant to the Turkish coast near the epicentre.

There is a difficulty in dealing with earthquake epicentres offshore through magnitude, it is at an offshore *point*, whereas elsewhere the PGA strong ground shaking is a propagating *field* effect observed on land. **Table 2** pulls together the estimates of PGA obtained from a diverse set of methodologies and maps, typically for PGA100 and PGA450, the latter is equivalent to the norm of largest occurrence expected over 50-year with 10% probability of exceedance. The parameters examining seismicity or magnitude recurrence adopt the examples of M100 and M475 by various methodologies and include different estimates of the maximum magnitude believed attainable, and scenario earthquake magnitudes arrived at from deaggregation of a PSHA and through assessment of the most perceptible earthquake. The estimates in **Table 2** are a sample of the material available, use only PGA to represent the available engineering ground motion parameters, and do not discuss the plethora of available GMPEs.

The magnitude parameters in **Table 2** have a hierarchy:

Scenario magnitude 6.5 < M100 6.75 < maximum observed 6.8 [superseded] < M475 7.3 < M_{max} (E or L) 7.35 < M_{max} (upper bound) 7.4

which follow a satisfyingly logical sequence. These are accompanied by an engineering ground motion PGA of 440 $cm\ s^{-2}$ (with range 392-490 $cm\ s^{-2}$) for the 475-year occurrence.

Table 2: Parameter results pertinent to Samos and coast of mainland Turkey gleaned from the available maps and varied methodologies reviewed in the text. PGA475 is chosen as a representative of engineering ground-motion. Seismicity is examined through results for 100-year and 475-year return period earthquakes, maximum magnitude by several methodologies (see text) and scenario magnitudes through deaggregation and most perceptible earthquake techniques.

Parameter	Values	Average	Range
Event magnitude	6.9 M_w	-	-
PGA475 in g or $cm\ s^{-2}$	400, 400-500, 0.4-0.5g, 0.5g, 0.48g, 0.4g	440	392-490
M100	7, 6.5	6.75	6.5-7.0
M475	7.3	7.3	7.3
M_{max} , Maximum magnitude: two from energy release considerations, one from fault length	7.5, 7.2, 7.3	7.3	7.2-7.5
M_{max} , Upper bound magnitude from statistical method	7.4	7.4	7.4
M_{max} , Maximum magnitude observed	6.8 (now superseded)	6.8	6.8
Scenario magnitude: two from perceptibility and one from de-aggregation techniques	6.6, 6.5, 6.4 [excluding 7.2 outlier]	6.5	6.4-6.6

Despite visiting and reviewing many hazard maps and seismicity maps spanning decades, it is now the case that Turkey does not use hazard zone mapping as such, instead the hazard values and spectra for a given location (identified as coordinates) are obtained from a dedicated web page (Erdik, pers. comm.).

The main lessons learned by reviewing some of the published material available as published maps, in addition to recognising the quantity of material now available, are:

- There is a great diversity of methodologies in the approach to PSHA. These spans individual links in the chain of calculation e.g. earthquake catalogues, zone models, GMPEs and statistical approaches.

- It is difficult to see how the methodologies reviewed could be more divergent. Divergence of methodology, yet there is convergence of results. This is a healthy scientific and reassuring outcome.
- Contemporary seismic hazard maps and magnitude recurrence maps are now ephemeral. A weakening or updated link in the model or chain of calculation can readily be replaced and a new map calculated.
- Today's maps are at best illustrations to help understanding. The present day "map" is now of such depth that it is a matrix of specialised material with calculations processed and held in a computer, where it may be consulted. Turkey is one of the leaders on this.

The Aegean Sea earthquake in perspective

The significance of the Aegean Sea 2020 magnitude 6.9 M_w earthquake should not be overstated; it is best seen as a timely reminder, a warning, of what may happen. Those who have close knowledge of the Buyuk Menderes graben (e.g. Gurer et al., 2009; Bayrak & Bayrak, 2012) in the West Anatolian extensional system are aware of the potential for greater impact. The above survey of hazard from magnitude and subsequent strong ground shaking events bears this out and puts this Aegean Sea earthquake into perspective. In terms of magnitude at 6.9 M_w , it is ~0.4 magnitude units less than the 475-year earthquake (**Table 2**), nearly half magnitude less, which puts the energy in a M475 earthquake around five times greater. The maximum magnitude M_{max} estimates ranging over 7.2-7.5 M_w from several methodologies indicate a M_{max} circa half-magnitude greater than this Aegean Sea event. At 6.9 M_w , the Aegean Sea earthquake is much closer to the 100-year event than the 475-year event (M100, M475, in **Table 2**). The epicentre of the earthquake was offshore with a shallow focus in the submarine unmapped graben system and so occurring at some distance before impacting Samos and mainland coast of Turkey – the graben system is readily observed on mainland Turkey. Six estimates of ground shaking through the engineering parameter PGA for 50-years with 10% probability of exceedance (PGA475, **Table 2**) have an average 440 $cm\ s^{-2}$ (0.45g) (range 392-490 $cm\ s^{-2}$) which is equivalent approximately to MSK/MM Intensity = VIII, briefly summarised in MSK as "heavily damaging". Although the Aegean Sea 2020 earthquake fell significantly short of these impact levels, the regional seismotectonics, in which it developed, has the capacity to achieve them.

2.9. Characterization of Strong Ground Motions

(Authored by FSM)

This section covers three main subjects; selection of the stations & main characteristics of the networks in the region, compilation and processing of the strong ground motion records and calculation/interpretation of several fundamental engineering parameters.

2.9.4. Characteristics of Strong Ground Motion Networks

The ORFEUS Data Centre provides access to strong ground motion waveforms from the European-Mediterranean & Middle-East region via Rapid Raw Strong Motion (RRSM) and Engineering Strong Motion (ESM) data portals. The detailed examination of the database in the accessed time period (November 2020) gave an insight into the networks that recorded the event. Within about 560 km of epicentral distances, 126 strong ground motion stations of 9 different networks from Greece and Turkey were triggered by the earthquake motions according to the ORFEUS database. Majority of data comes from Boğaziçi University Kandilli Observatory and Earthquake Research Institute (KOERI). National Observatory of Athens Seismic Network (HL) and ITSAK Strong Ground Motion (HI) follows the KOERI. Moreover, the University of Patras, Seismological Laboratory (PSLNET), Seismological Network of Crete, Corrinth Riff Laboratory (CRLNET), Hellenic Seismological Network, University of Athens, Seismological Laboratory, Aristotle University of Thessaloniki Seismological Network are the others that recorded the event. Also, it should be noted that 27% of these data are signed as "*bad quality record*" in the ORFEUS database.

Despite the convenience of the access to strong ground motion records in the ORFEUS, the lack of the largest local network of Turkey (AFAD), unexpected PGA values of some records from KOERI (such as GMLD station) and the lack of the stations in Samos (SMG1 & SAMA) led to the scanning of the local networks' databases rather than using only the ORFEUS database. The main intention for the analyses was to pick up all accelerograms recorded within 200 km of epicentral distances (R_{epi}). In this respect, four main networks were detected:

- The Ministry of Interior Disaster and Emergency Management Presidency (ERD or AFAD – in this study, it is referred to as AFAD),
- Boğaziçi University’s Kandilli Observatory and Earthquake Research Institute (KOERI),
- National Observatory of Athens Seismic Network (HL) and
- ITSAK Strong Ground Motion (HI).

Spatial distribution of networks in **Figure 24a** explicitly reveals that there are well-distributed stations to the east and the north of the epicentre operated mainly by AFAD and KOERI. One of the closest stations (Station code: GMLD) is about 20 km distant to the epicentre on the Turkish side operated by KOERI. Fortunately, two stations from Samos Island at similar distances gave a chance to obtain records from the -relatively near- south of the event, one of which is operated by ITSAK (Station code: SMG1) and the other is of NOA (Station code: SAMA). Also, strong ground motions were recorded at several stations from the Greek Islands in the relatively greater distances. However, the presence of the Aegean Sea is responsible for the lack of data in the west and south of the epicentre. Due to these facts, there is no near-field ($R_{epi} < 20$ km) record for this event. When considered the proximity of the fault to Samos and also high seismic activity in the region, increasing the number of stations in Samos should be recommended in order to be able to provide near field records for possible future earthquakes in the region (**Figure 24a&b**).

The total number of the stations used in this section is 101 with distances ranging from 20 km to 200 km. It should be mentioned that the epicentral distances were re-calculated separately in this study. In other words, they don’t refer to the values given in the databases. **Figure 24b** shows the statistical distribution of source to station distances based on their networks. At the closest distances, the presence of stations from all networks provides an opportunity to compare their engineering parameters. The great number of stations belongs to AFAD in the database, then KOERI ITSAK and NOA follow it. The detailed explanation about the database will be the subject of the next sections.

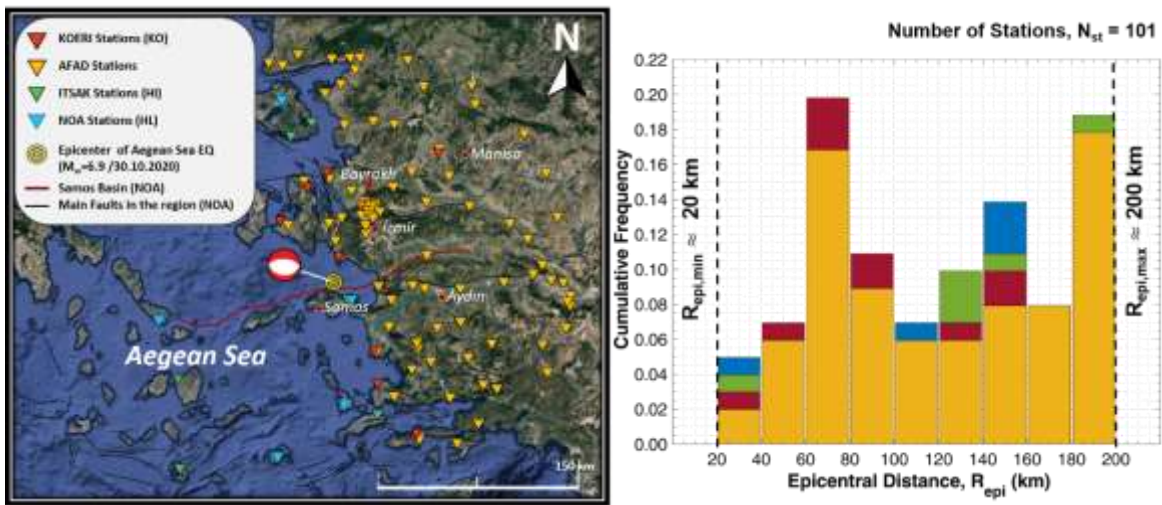


Figure 24: Characteristics of stations recording the 30/10/2020 Aegean Sea Earthquake within 200 km of epicentral distance (a) Epicenter of the event and spatial distribution of stations on the map, (b) Statistical distribution of epicentral distances based on networks (KOERI: Kandilli Observatory and Earthquake Research Institute, AFAD: The Ministry of Interior Disaster and Emergency Management Presidency)

Since the average shear wave velocity of stations for the upper 30 m depth ($V_{s,30}$) is an easiest and useful way to encapsulate the soil conditions into the interpretations and analyses, the distribution of $V_{s,30}$ values were examined in **Figure 25**. While the $V_{s,30}$ values of 16 stations of AFAD and 3 of ITSAK were not accessed, the majority of the stations are located on the soils between 360 – 800 m/sec of $V_{s,30}$ which is categorized as “Soil Class B” based on Eurocode 8 and described as “Deposits of very dense sand, gravel, or very stiff clay, at least several tens of metres in thickness, characterised by a gradual increase of mechanical properties with depth”. The stiffest ground type in EC8 is defined as “Rock or other rock-like geological formation, including at 5 m of weaker material at the surface” for soils with $V_{s,30}$ value greater than 800 m/sec. EC8 Soil Class C covers the soils between 180 – 360 m/sec of $V_{s,30}$ with the description of “Deep deposits of dense or medium-dense sand, gravel or stiff clay with thickness from several tens to many hundreds of metres”. Although there are other soil classes

softer than Soil Class C in the EC8, there are only very few stations corresponding these softer soils in our study. Hence, the soils with $V_{s,30} < 360$ m/sec was accepted as one class named as Soil Class C&D. Moreover, for each soil class, mean $V_{s,30}$ values were calculated as 980 m/sec, 532 m/sec and 263 m/sec for soil class A, B and C&D, respectively.

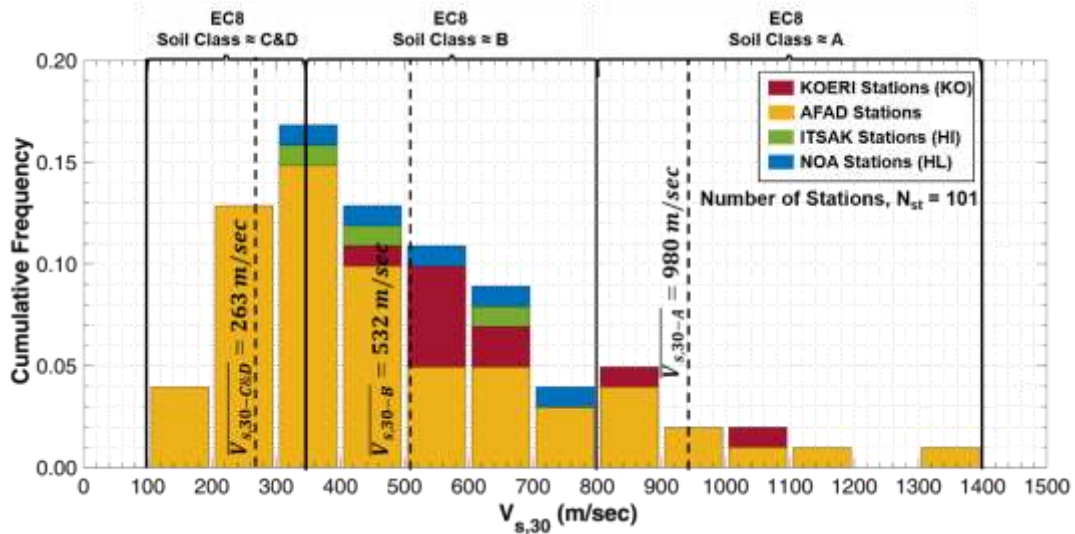


Figure 25: Distribution of average shear wave velocities of stations for the upper 30 m depth ($V_{s,30}$) ($\overline{V_{s,30}}$ corresponds to mean $V_{s,30}$ value).

2.9.5. Database & Processing of Waveforms

All raw acceleration waveforms were compiled from the stations of previously mentioned networks within Greece and Turkey. The rejection criteria for records are primarily based on the quality of the waveform and re-calculated epicentral distances. In the beginning, the records from 105 stations were evaluated but records from one station of NOA were eliminated since the mainshock could not be differentiated despite a filtering process. Also, re-calculated epicentral distances of three AFAD's stations were a little bit greater than 200 km, which is a limit distance for this study and thus these records were also excluded.

The KOERI recordings were obtained in terms of count and converted to raw accelerations by multiplying the count values with sensitivity factors reported at the KOERI-RETMC official website. Also, the unprocessed acceleration data of AFAD and NOA were accessed via their official websites. Firstly, to provide physically meaningful velocities and displacements, baseline corrections were performed on all raw acceleration time histories by subtracting the mean of whole time series via Matlab. The low-pass filter frequency limit was kept constant at 20 Hz for all traces, to obtain reliable information at the short periods. The high pass filter frequencies were identified by visual inspection of each velocity and displacement time histories. The selected high pass filter frequencies mainly vary between 0.1 Hz and 0.2 Hz similar to processed data recommended in the databases with the several minor exceptions. In order to perform the filtering process, Butterworth filter (4th order), the most widely used filter type in data processing of strong ground motions, was applied to these acceleration traces.

For ITSAK, we could access the only processed data whose selected high pass filter frequency vary from 0.05 to 0.22 Hz.

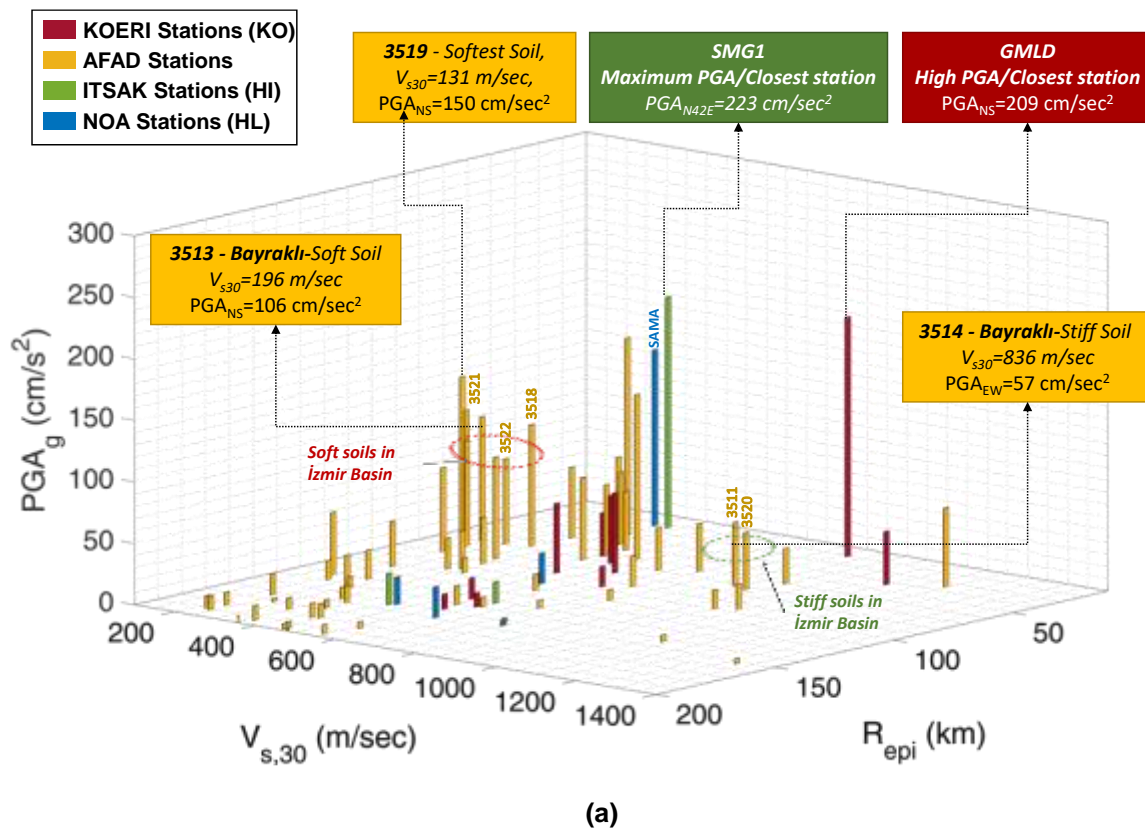
2.9.6. Engineering Parameters

In engineering studies, peak parameters of strong ground motions are still extensively utilized for describing the strong ground motions and may be a good indicator to determine the damage in the affected region. Despite the some geophysical and engineering limitations, i.e. it gives useful information mainly for the structures with periods shorter than 0.3 sec (Boore and Bommer, 2005 & Douglas, 2003), evaluation of peak ground accelerations (PGAs) may be one of the frequent solutions to understand the post-earthquake effects.

In this respect, in order to scrutinize the variations of ground motion observations on the surface, PGAs were correlated with soil conditions and epicentral distances (**Figure 26a**). It should be noted PGAs in

the figure refer to geometrical mean of peak values of two horizontal components. As expected, the highest peak values are observed at the closest distances (GMLD in Gümüldür and SMG1 in Samos) and the maximum PGA values for this database are detected as 223 cm/sec² from SMG1 station at approximately 20 km of distance to the epicentre, respectively. Although there is another station, SAMA, very close to the SMG1 in Samos, its PGA values are smaller than those of SMG1 and also GMLD but it should be remarked that there could not be reached exact $V_{s,30}$ value of the SAMA station. However, when considered the close distance of SAMA (≈ 500 m) to SMG1 ($V_{s,30} = 380$ m/sec) and the study of Kalogeras et al. (2020) was mentioned that the station is located on “soft rock”, $V_{s,30}$ value of SAMA was assumed as the lowest limit of the soft rock in EC8 classification, 360 m/sec.

Another striking point in the PGA distribution is the peak values of soft soil records. The 3519 station has the softest soil conditions with 131 m/sec of $V_{s,30}$ in the database. Although it is located at the intermediate distances (67 km), it exhibits high peak accelerations on the ground surface. Together with 3519, we detected a small cluster of soft soil stations positioned at similar distances in **Figure 26a**. This finding steered the discussion into the investigation of station locations. The locations of these soft soil stations at intermediate distances coincidence with the large damaged area in İzmir Basin (Bayraklı, Bornova & Karşıyaka – stations within red circles in **Figure 26b**). Also, the presence of several stations on the stiff soils in the same region, which is depicted with green circles in **Figure 26b**, allowed them to compare their peak values. As we turn back to **Figure 26a**, at similar distances, another cluster of stations, whose $V_{s,30}$ values vary between 800-900 m/sec, correspond to these green circles in **Figure 26b**. When the closest soft and stiff soil stations, 3513 and 3514, are taken into account, twofold PGA in the soft soil record may be seen as a basic indicator of soil amplification.



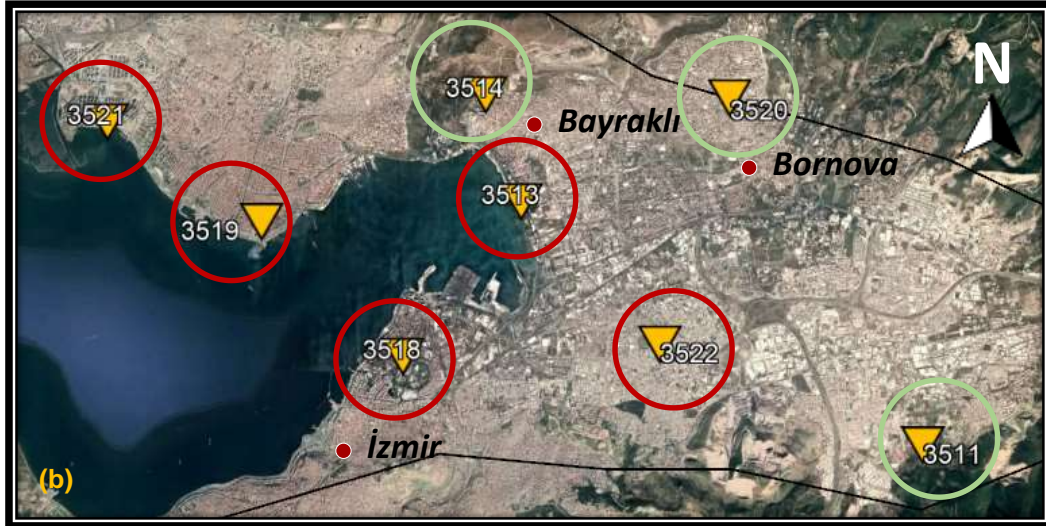


Figure 26: (a) Distribution of geometrical mean of peak ground accelerations (PGAs) and (b) Location of soft and stiff soil stations around the most damaged area in İzmir Basin (Red circles and green circles refer to the soft and stiff soils, respectively).

2.9.7. Comparison with GMPEs

The primary step of the engineering design of structures is the determination of the loading conditions. In the case of ground shaking, past events are the indispensable data to estimate the level of an imminent earthquake. In this context, ground motion prediction equations (GMPE), which establish mathematical relationships between source, path & site parameters and engineering variables such as peak attributes, spectral parameters or intensity measures, is one of the most common methods to predict the engineering parameters (Douglas, 2003).

In this section, an attempt has been made to compare observed data with empirically derived ground motion prediction equations (GMPEs) to evaluate their attenuation characteristics with distance.

2.9.8. Selected Ground Motion Prediction Equations

The geometric mean of ground motion parameters (PGAs) were compared with three commonly used ground motion prediction equations (GMPEs) for recent years. The selection criteria for GMPEs mainly depended on the compatibility of the database characteristics of GMPEs to main features of the Aegean Sea earthquake and the affected region. When regarded the main characteristics of the earthquake listed below, Boore et al., 2014 (BSSA14), Akkar et al., 2014 (ASB14) and Kale et al., 2015 (KAAH15) were chosen;

- **Moment magnitude (M_w):** All selected GMPEs cover the 6.9 of moment magnitude, which is announced by the majority of agencies for Aegean Sea Earthquake (30/10/2020).
- **Fault type (SoF):** All selected GMPEs propose options for different faulting mechanisms also including normal faults exhibited by the event as explained in previous sections.
- **Average shear wave velocity for the upper 30 m depth ($V_{s,30}$):** To be able to consider soil effects, stations were categorized based on EC8 as given in the previous section (**Figure 25**). For each class, the mean $V_{s,30}$ were assigned as a representative value for the interested soil class.
- **Region:** ASB14 and BSSA14 refer to Europe and Middle East region whereas KAAH15 consists of mainly Turkish and Iranian motions. Moreover, only BSSA14 and KAAH15 offer the region option. Regional values assigned for Turkey were selected in this study.
- **Distance:** The mutual distance parameter in three selected GMPEs is Joyner-Boore distance, which is defined as the shortest distance from the stations to the surface projection of the rupture surface of the event. While ASB14 and KAAH15 can be calculated up to 200 km of distances, BSSA14 allows estimating parameters for distances less than 400 km.

For the sake of brevity, the open forms of the selected GMPEs were not given in the report but could be accessed detailed information via the related references.

2.9.9. Variation of Peak Ground Motion Parameters

The geometric means of two horizontal PGAs are compared with selected GMPEs; ASB14, BSSA14 and KAAH15 for three soil classes in **Figure 27**. It is worth noting here that the observed values from the stations with unspecified $V_{s,30}$ are also shown in each soil classes with a marker depicted as a hexagram to give an insight on their probable soil conditions.

The observed PGAs are mainly in agreement with three empirically derived GMPEs with several exceptions. For the closest stations, PGAs are generally around the median values of GMPEs, whereas slight dispersions are seen in which the observed data exceed the two standard deviation ranges (2.3rd & 97.8th percentile predictions). With increasing distance (greater than 80-100 km for Soil Class B and C&D), the observed PGAs decay faster than those estimated from the empirical equations. Peak ground accelerations from the farthest stations at about 200 km distance seem overpredicted. In soil class C&D, PGAs of İzmir Basin stations located around 70 km distant are seen slightly above 84th percentile predictions.

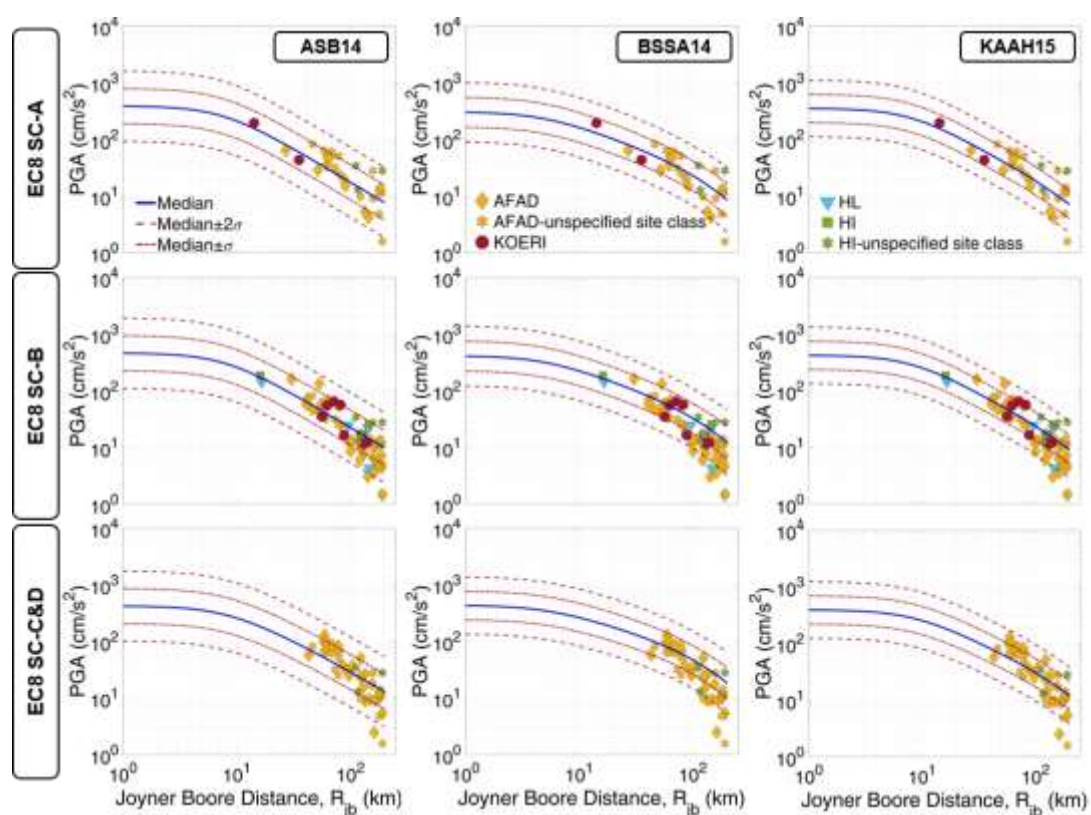


Figure 27: Comparison of PGAs with GMPEs; Akkar et al, 2014 (ASB14), Boore et al., 2014 (BSSA14), and Kale et al., 2015 (KAAH15), for the geometric mean of horizontal components and three soil classes.

2.10. Comparison with Hazard Section and Codes

The high seismic activity and complex tectonic structure of the Aegean region have produced severe earthquakes, which have resulted in economic, social and environmental consequences throughout history (Weatherill and Burton, 2010). These past earthquakes may give an insight for the expected ground motion levels, which present the loading conditions of structures, through seismic hazard assessments. In this part, we proceed to investigate the compatibility of observed data with the expected earthquake design loads in seismic codes of both countries.

2.10.4. Seismic Hazard and Codes of Greece

In 1928 and 1939, the first endeavours on seismic-resistant design codes were unveiled in Greece. In the late 1930s, Greece was encountered with the first seismic hazard map, “*Engineering Seismic Map of Greece*”. The review of the map in 1956 divided the territory of the country into five seismic hazard levels and three subcategories based on soil conditions. The spatial distribution of macroseismic results

of past earthquakes was the main basis of this map. In this hazard map, Samos was characterized by Seismic Zone III and IV and the maximum seismic coefficient was defined as 0.12g for the softest soils of Samos Island (Ansal et al., 2015). The seismic-resistant design code issued in 1959 (Royal Decrees 1959) was the first official attempt in Greece. Three seismic zones were defined and Samos fell into the moderate-to-high seismic zone proposing seismic coefficients between 0.06g (soft soils)-0.12g (stiff rocks). The 1978 and 1984 earthquakes in Thessaloniki and Alkionides, which resulted in severe damage and fatalities, underpinned the new “*Seismic Code for Building Structures*” (a decree of the Minister of the Environment) published in 1984. The seismic zones defined in the 1984 code includes three levels of seismic activity and Samos corresponds to Seismic Zone III referring to “*high earthquake activity*”. After the disastrous earthquake in Kalamata (1986), the studies for the code revision was started and in 1992, new seismic code provisions were promulgated. Similar to the zonation of the preceding seismic code, four earthquake levels were provided in the 1992 seismic code and Samos was labelled as Zone III with the 0.24g of a seismic coefficient for 10% probability of exceedance in 50 years (Manos, 1994). The high peak accelerations and destructive damages seen in the 1996 and 1999 earthquakes stimulated the preparedness of new Greek seismic code and hazard map. The first upgraded version of 1992 seismic code (EAK2000) was released in 2000 with the seismic hazard map defining four zones. For Samos, peak ground accelerations were identified as 0.24g (Seismic Zone III) (Ansal et al., 2015). EAK2000 was modified in 2003 with the incorporation of currently used official seismic hazard map of Greece. In this zonation map, peak ground accelerations with 10% probability of exceedance in 50 years (475 years of mean return period) were given for three seismic zones and Samos corresponds to Seismic Zone II with 0.24g of PGA (**Figure 28**).

In 2012, Eurocode 8 (EC8) began to be implemented together with the EAK2003 in Greece (Nikolaou and Gilsanz, 2015). Both seismic codes propose traditional elastic response spectra for four different soil types. However, as mentioned in Pitkalis et al., 2016, whereas peak design spectral accelerations were represented by a wider flat region for softer soils, this plateau value is constant for all soil types since soil amplification issues are not considered in EAK2003. However, soil amplifications are reflected in the design spectrum through a constant soil factor in EC8. Also, EC8 proposes elastic design spectra for two-levels of an earthquake, one of which, Type 1, consists of more energy in long period content and surface wave magnitude (M_s) should be greater than 5.5. For earthquakes with $M_s < 5.5$, Type 2 design spectra is proposed in EC8.

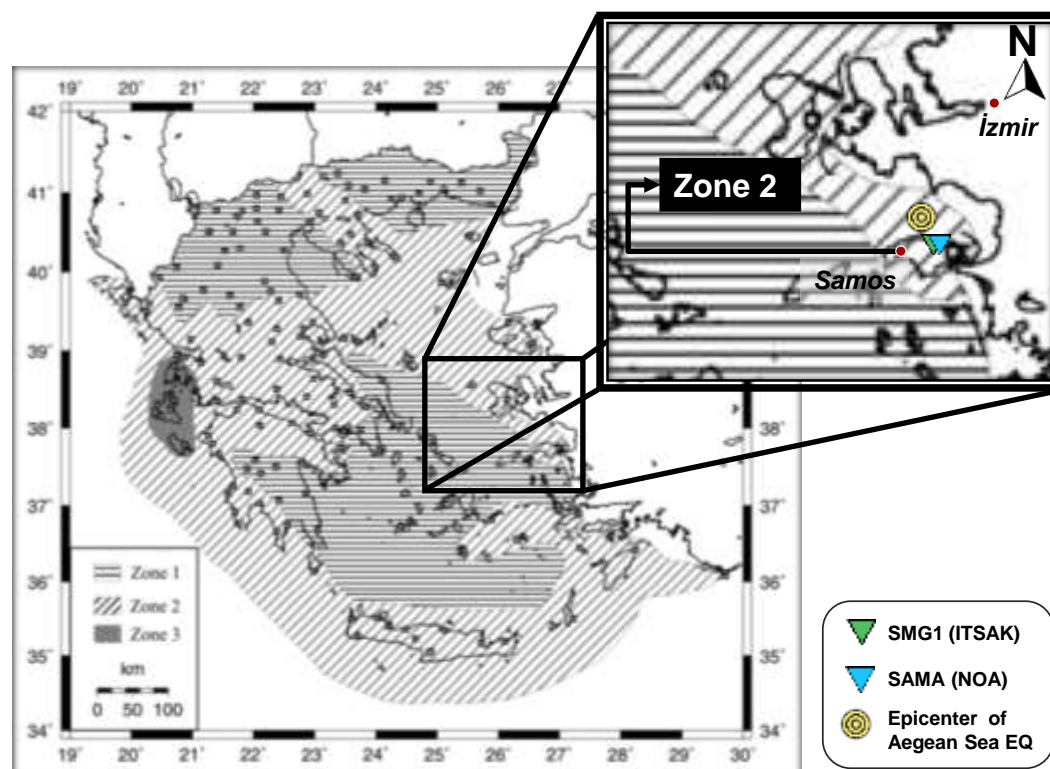


Figure 28: Current seismic hazard map of Greece in EAK 2000/2003 and close view to Samos Island (Modified from Tselentis& Danciu, 2010).

In this section, we exploit only the records of two closest stations in Samos; SMG1 and SAMA to compare with the elastic design spectra of currently used EAK2003 and EC8 seismic regulations. Other stations of Greek networks were excluded by virtue of not resulting in high spectral accelerations and for the sake of simplicity. In **Figure 29** the compatibility of elastic pseudo-spectral accelerations for both horizontal components of SMG1 and SAMA station records was investigated with the design spectra of EAK2003 and EC8 (for Type 1 Earthquake) for 5% damping ratios. As mentioned previously, the soil of SAMA station is labelled as “soft rock” and we assigned a $V_{s,30}$ value of 360 m/sec. Also, SMG1 is located on soil with 380 m/sec of $V_{s,30}$ value. In EAK2003, B and Γ type of soils covers 180 – 360 m/sec according to Pitikalis et al., 2004. So, we especially focused on these soil categories and highlighted the aforementioned lines bolder in **Figure 29**. Both horizontal components of records reach the peak spectral accelerations at the period of about 0.5 sec. Spectral accelerations around this period exceed the design spectra of all soil classes in EAK2003 except for the longitudinal component of SAMA.

As for EC8, design spectra of corresponding to all soil classes seems under the spectral accelerations of N42E components of SMG1 at around 0.5 sec while its N48W component slightly exceeds the corresponding design spectrum to Soil Class B. Only transverse component of SAMA records surpasses the design spectra in EC8 regardless of the soil classes. This result reveals that the design conditions of both codes do not meet the observed spectral quantities of Aegean Sea earthquake, especially for medium-rise reinforced concrete buildings.

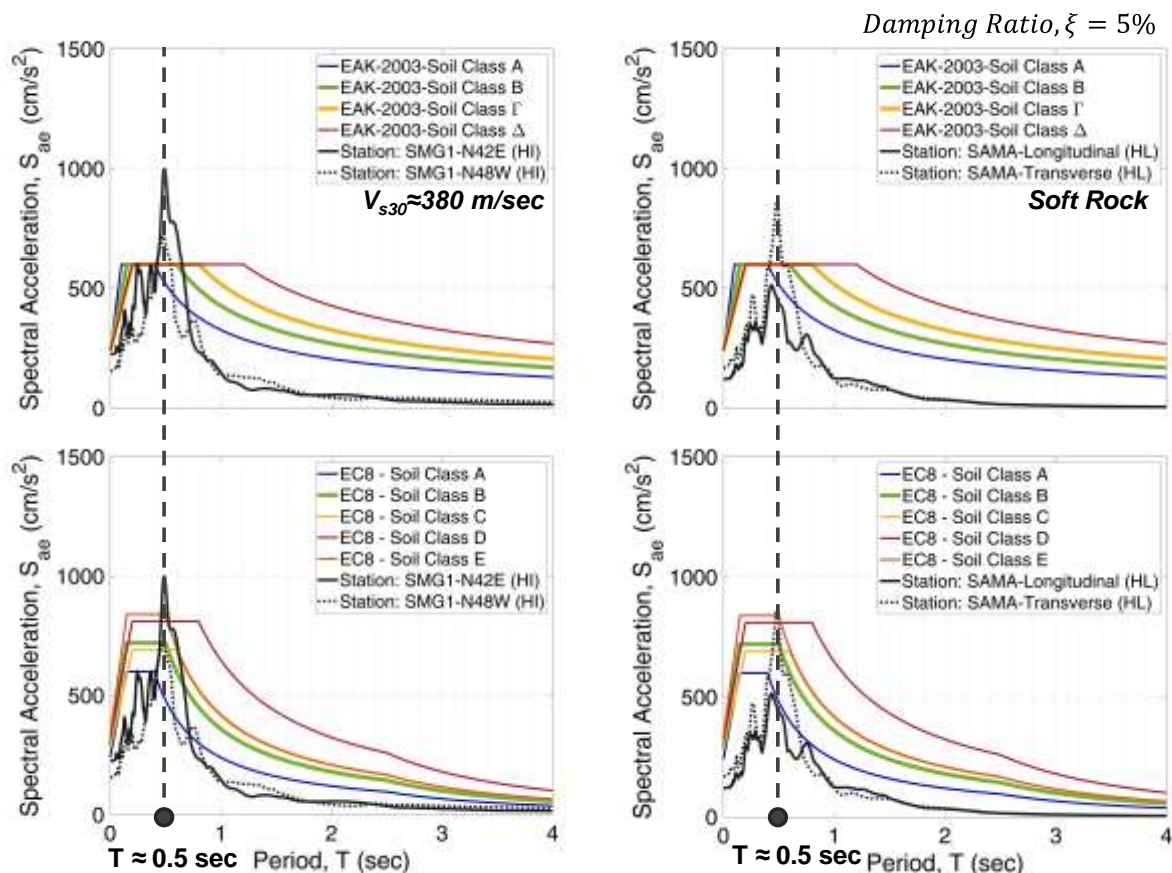


Figure 29: Comparison of the elastic acceleration response spectra of the recorded ground motions at the two stations in Samos Island against the design spectra recommended in EAK2003 and EC8 (Dashed line refers to the peak spectral accelerations).

2.10.5. Seismic Hazard and Codes of Turkey (Authored by FSM)

The first seismic zonation studies for Turkey date back to the 1930s. Sieberg’s studies with limited data were materialized in the first unofficial seismic zonation map of Turkey in 1932 (Özmen, 2012). With the catastrophic consequences of great Erzincan earthquake ($M=7.9$) in 1939, the Turkish government realized the necessity of a seismic provision for the design of structures and one year later, the first official seismic code was released. In 1944, an earthquake ($M7.2$) struck Bolu province in Turkey and

in the same year, legislation named “*Measures to Be Put into Effect Prior and Subsequent to Ground Tremors*” was made compulsory to mitigate the destructive consequences before an earthquake. One year later, the first seismic zonation map was officially released considering three seismic zones and İzmir province composed of the less and high seismic hazard regions (Soyluk and Harmankaya, 2012). In 1947, this map underwent a revision. The last two seismic zonation maps encapsulated the main principles of seismic risk and seismic activity in the region (Akkar et al., 2018). The seismic code was also updated in 1949 and then in 1953 (Soyluk and Harmankaya, 2012). In 1963, another modification of the seismic zonation map was released and divided the territory into four zones based on macroseismic intensity (MSK intensity scale) levels and major areas of İzmir were put into the high seismic hazard zones and a small part of İzmir was defined as moderate seismic hazard (Zone 2). Until 1972, the 1968 earthquake code, which includes the first implementation of a design spectrum concept for the seismic design loads, was utilized for the seismic design of buildings. As a result of the re-evaluation of earthquake catalogues, iso-seismal maps of past events and macroseismic intensities, in 1972, seismic zones of Turkey increased to five levels of seismic hazard. In this map, the whole İzmir province was marked as a high level of seismic hazard (Zone I) and appended the seismic code released in 1975 (Akkar et al., 2018). The 1975 seismic provision proposed an inelastic design spectrum by considering the ductile design concept. The seismic zonation map published in 1996 was underlined by PGA levels estimated through probabilistic seismic hazard analysis (PSHA) for 475 years of the mean return period. This map offered five seismic regions with the corresponding effective peak accelerations. For İzmir, the effective peak acceleration in the map refers to 0.4g (Seismic Zone I). In 1997, the seismic code was modified with the same name of the previous seismic provision. Two years after this revision, a densely populated region of Turkey was shattered by two disastrous earthquakes; 17th August Kocaeli (M_w 7.4) and 12th November Düzce (M_w 7.2). After these earthquakes, the rehabilitation needs of existing buildings led to the review of the 1997 seismic code. In 2007, a new code was released entitled “*Specifications for Buildings to be Built in Earthquake Areas*” (Soyluk and Harmankaya, 2012).

With the advent of earthquake engineering, the studies of currently used Turkish Seismic Code was initiated and officially enforced in 2019 (having been published in 2018). When compared to the previous code, one of the major amendments was made in the definition of earthquake design loads. Rather than a seismic zonation map, a georeferenced based contour map (**Figure 30**) is presented and gives PGA, PGV and spectral accelerations for different earthquake ground motion levels. To construct the design spectrum, firstly, spectral accelerations for the periods of 0.2s and 1.0 s are identified for a specific coordinate for referenced stiff soil sites from interactive Turkish earthquake hazard maps. Then, these spectral accelerations are altered based on soil conditions of the site (Sucuoğlu, 2018).

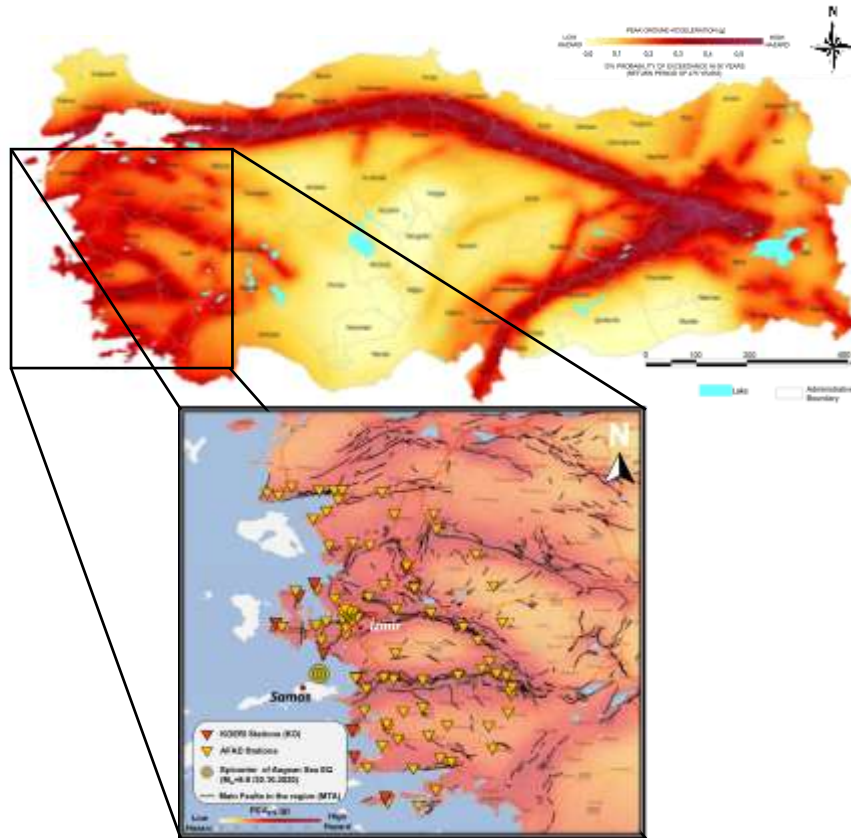


Figure 30: Turkish earthquake hazard map for design basis earthquake (475 years of mean return period) (2018) and a closer view to an area with a radius of 200 km from the Aegean Sea earthquake (30.10.2020) epicentre (Modified from AFAD, 2018).

Figure 31 compares the 5% damped acceleration response spectra of two horizontal components of the ground motion recorded at the closest station in Turkey (GMLD) against design spectra of two outdated (1975 & 2007) and one currently used (2018) Turkish seismic codes for design basis earthquake (475 years return period). It should be mentioned again that the 1975 Turkish seismic code proposes an inelastic response spectrum. In this respect, since we couldn't fulfil a meaningful comparison between inelastic and elastic response spectra, the design code spectra should be exaggerated by the ductility reduction factors with the intention of construction of equivalent elastic design spectra or vice versa (personal communication of Prof. Nuray Aydınoğlu, 2020). Herein, the ductility reduction factor was selected as 6 proposed for “Ductile frame-wall systems” in 1998, 2007 and 2018 Turkish seismic codes.

Similar to the comparison of closest records from Greece, **Figure 31** demonstrates a mismatch between the response spectral accelerations and corresponding design spectra recommended by three seismic regulations. Given that the $V_{s,30}$ value of the station location is designated as Soil Class I, 1975 design spectra are exceeded at the periods of 0.1 and 0.6 sec. In 2007, these exceedances occur at the periods around 0.6 sec for Soil Class 2 while spectral accelerations within a large range of period between 0.5 and 1.4 sec surpass the design spectra of 2018 seismic code. However, according to METU/EERC Report, (2020), this relatively large ground shaking does not lead to heavy structural damages in Gümüldür thanks to correct application of construction rules and convenient soil/rock foundation

conditions.

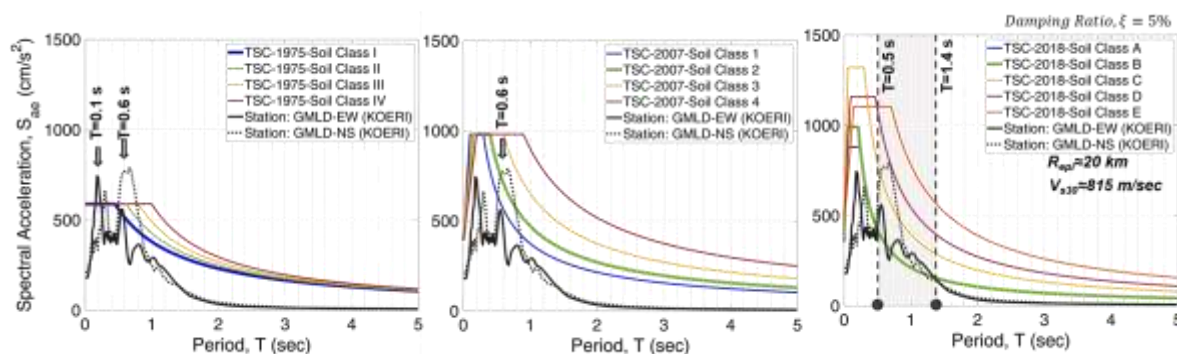


Figure 31: Comparison of the acceleration response spectra of the recorded ground motions at the closest station (GMLD) in Izmir, Turkey against the design spectra recommended in 1975, 2007 and 2019.

2.11. Summary and Conclusions

The development and evolution of seismic hazard mapping in Greece and Turkey is rich and diverse, but today's maps are ephemeral because modern computers and databases allow rapid updating. The present day "map" has become a matrix of specialised material and calculation held in a computer, which may be consulted. Turkey is one of the leaders on this. The significance of the Aegean Sea 2020 6.9 M_w earthquake should not be overstated: its magnitude is closer to the 100-year event than to the 475-year event. The regional seismotectonics in which the Aegean Sea earthquake developed has capacity to achieve a maximum magnitude 7.4 M_w , a "heavily damaging" intensity VIII and an engineering PGA for 50-years with probability 10% of exceedance of 0.45g (392-490 cm s^{-2}).

The well distributed strong ground motion networks in the east and north of the epicentre and stations in the nearest island Samos gave an opportunity to establish the link between earthquake phenomenon and its effects. As expected, maximum peak ground accelerations (PGA) were detected in the closest stations. Furthermore, records from the most damaged area, Bayraklı and surroundings exhibit relatively high PGAs. Recently generated ground motion prediction equations (GMPEs) provide identical results with the observed data especially for close distances. However, at further distances, the observed PGAs tend to decay faster than the estimations. PGAs of İzmir Basin stations located around 70 km away are seen slightly above 84th percentile predictions. All of the acceleration response spectra derived from the closest station records commonly surpass the design spectra proposed by both Greek and Turkish codes at around 0.5 second periods.

References

- Ansal, A., Tönük, G., Papatheodorou, K. K., Ntouros, K., Tzanou, H., Issam, S., Konstantinidis, A., Erdik, M., Demircioğlu, M.B., Şeşetyan, K., İlhan, O., Aksoy, H., Kırca, V.Ş.Ö., Çelik, G., Klimis, N., K. Makra, S. Skias, I. Markou, B. Margaris, N. Theodulidis, C. Papaioannou, A. Savvaidis, M. Rovithis, K. Konstantinidou, E. Tsiras, V. Nenov, L. Tofan, Ghe. Marmureanu, M.J.Adler, M.Lungu, Z. Prefac, A. Sidorenko, E. Zasavitsky, O. Bogdevich, O. Bujor, A. Belinschi, K. Stepanova, O. Rubel, (2015). A Scientific Network for Earthquake, Landslide & Flood Hazard Prevention – SciNetNatHaz, Black Sea Cross Border Cooperation.
- Akkar, S. and Özen, Ö., (2005). Effect of peak ground velocity on deformation demands for SDOF systems. *Earthquake Engineering & Structural Dynamics*, Volume 34, Issue 13. <https://doi.org/10.1002/eqe.492>
- Akkar S., Sandıkkaya M. A. and Bommer J. J, (2014), Empirical ground-motion models for point- and extended-source crustal earthquake scenarios in Europe and the Middle East. *Bulletin of Earthquake Eng* 12: 359. <https://doi.org/10.1007/s10518-013-9461-4>
- Akkar, S., Azak, T., Çan, T. et al. (2018). Evolution of seismic hazard maps in Turkey. *Bull Earthquake Eng* 16, 3197–3228. <https://doi.org/10.1007/s10518-018-0349-1>
- Bayrak, Y., Ozturk, S., Cinar, H., Koravos, G. Ch., & Tsapanos, T.M., 2008. Regional variation of the w – upper bound magnitude of GIII distribution in and around Turkey: tectonic implications for earthquake hazards, *Pure appl. Geophys.*, **165**, 1367-1390.

- Bayrak, Y., & Bayrak, E., 2012. An Evaluation of Earthquake Hazard Potential for Different Regions in Western Anatolia Using the Historical and Instrumental Earthquake Data, *Pure and Applied Geophysics*, **169**, 1859-1873, doi:10.1007/s00024-011-0439-3
- Boğaziçi University Kandilli Observatory and Earthquake Research Institute (KOERI) – RETMC, <http://www.koeri.boun.edu.tr/sismo/2/deprem-verileri/sayisal-veriler/> (accessed by 02/12/2020)
- Boore, D. M. and Bommer, J. J., (2005). Processing of strong-motion accelerograms: needs, options and consequences. *Soil Dynamics and Earthquake Engineering*, 25(2):93-115. <https://doi.org/10.1016/j.soildyn.2004.10.007>
- Boore D. M, Stewart J. P., Seyhan E., and Atkinson G. M. (2014), NGA-West2 Equations for Predicting PGA, PGV, and 5% Damped PSA for Shallow Crustal Earthquakes. *Earthquake Spectra*: August 2014, Vol. 30, No. 3, pp. 1057-1085. <https://doi.org/10.1193/070113EQS184M>
- Bouchon, M., 1979. Discrete wave number representation of elastic wave fields in three-space dimension, *J. Geophys. Res.*, **84**, 3609–3614.
- Bouchon, M., 2003. A review of the discrete wavenumber method, *Pure Appl. Geophys.*, **160**, 445–465.
- Burton, P. W., Xu, Y., Qin, C., Tselentis, G. A., & Sokos, E. (2004). A catalogue of seismicity in Greece and the adjacent areas for the twentieth century. *Tectonophysics*, **390**(1-4), 117-127.
- Burton, P.W., 1978. Perceptible earthquakes in the United Kingdom, **54**, *Geophys. J. R. astr. Soc.*, 475– 479.
- Burton, P.W., 1979. Seismic risk in Southern Europe through to India examined using Gumbel's third distribution of extreme values, *Geophys. J. R. astr. Soc.*, **59**, 249-280.
- Burton, P.W., McGonigle, R., Makropoulos, K.C., & Ucer, S.B., 1984. Seismic risk in Turkey, Aegean and the eastern Mediterranean: the occurrence of large magnitude earthquakes, *Geophys. J. R. astr. Soc.*, **78**, 475–506.
- Burton, P.W., Xu, Y., Tselentis, G.-A., Sokos, E., & Aspinall, W., 2003. Strong ground acceleration seismic hazard in Greece and neighbouring regions, *Soil Dynamics & Earthquake Eng.*, **23**, 159-181.
- Burton, P.W., Qin, C., Tselentis, G-A. & Sokos, E., 2004. Extreme earthquake and earthquake perceptibility study in Greece and its surrounding area, *Natural Hazards*, **32**, 277-312.
- Chapman, M. C., 1995. A probabilistic approach to ground motion selection for engineering design, *Bull. seism. Soc. Am.*, **85**, 937–942.
- Chatzipetros, A., Kiratzi, A., Sboras, S., Zouros, N., & Pavlides, S. (2013). Active faulting in the north-eastern Aegean Sea Islands. *Tectonophysics*, **597**, 106-122.
- Cornell, C. A., 1968. Engineering Seismic Risk Analysis, *Bull. seism. Soc. Am.*, **58**, 1583-1606.
- Coskun, S., Dondurur, D., Cifci, G., Aydemir, A., Gungor, T., & Drahor, M. G. (2017). Investigation on the tectonic significance of Izmir, Uzunada Fault Zones and other tectonic elements in the Gulf of Izmir, western Turkey, using high resolution seismic data. *Marine and Petroleum Geology*, **83**, 73-83.
- Cox, W. (2020). Demographia World Urban Areas: 16th Annual Edition. Demographia.
- Danciu, L., & Tselentis, G.-A., 2007. Engineering Ground-Motion Parameters Attenuation Relationships for Greece, *Bull. seism. Soc. Am.*, **97**, 162-183.
- Demircioglu, M.B., Sesetyan, K., Duman, T. Y., Can, T., Tekin, S., & Ergintav, S., 2018. A probabilistic seismic hazard assessment for the Turkish territory: part II - fault source and background seismicity model, *Bull. Earthquake Eng.*, **16**, 3399-3438.
- Disaster and Emergency Management Authority (AFAD), 1900 – 2020 Earthquake Catalog (M >= 4.0), <https://deprem.afad.gov.tr/depremkatalogu/> (accessed by 01/11/2020).
- Disaster and Emergency Management Authority (AFAD), Turkish National Strong Motion Network (TNSMN), <https://tadas.afad.gov.tr/> (accessed by 02/11/2020)
- Disaster and Emergency Management Authority (AFAD), (2019). Earthquake Hazard Map of Turkey.
- Douglas, J., (2003). Earthquake ground motion estimation using strong-motion records: a review of equations for the estimation of peak ground acceleration and response spectral ordinates. *Earth-Science Reviews* **61** (2003) 43–104. [https://doi.org/10.1016/S0012-8252\(02\)00112-5](https://doi.org/10.1016/S0012-8252(02)00112-5)
- Duman, T.Y., Can, T., Emre, O., Kadirioğlu, F.T., Basturk, N.B., Kilic, T., Arslan, S., Ozalp, S., Kartal, R.F., Kalafat, D., Karakaya, F., Azak, T.E., Ozel, N.M., Ergintav, S., Akkar, S., Altınok, Y., Tekin, S., Cingoz, A., & Kurt, A.I., 2016. Seismotectonics database of Turkey, *Bull. Earthquake Eng.*, doi:10.1007/s10518-016-9965-9.
- Dziewonski, A. M. TA Chou, Wondhouse J H. (1981), Determination of earthquake source parameters from waveform data for studies of global and regional seismicity. *J Geophys Res*, **86**(2), 825-2.
- EAK (2003) Greek seismic code, Earthquake planning & protection organization, Athens–Greece, (in Greek).

- Ebel, J.E., & Kafka, A.L., 1999. A Monte Carlo Approach to Seismic Hazard Analysis, *Bull. seism. Soc. Am.*, **89**, 854-866.
- Ekström, G., Nettles, M., & Dziewoński, A. M. (2012). The global CMT project 2004–2010: Centroid-moment tensors for 13,017 earthquakes. *Physics of the Earth and Planetary Interiors*, *200*, 1-9.
- EN, 2004. Eurocode 8: Design of structures for earthquake resistance - Part 1: General rules, seismic actions and rules for buildings, European Standard EN 1998-1:2004. Brussels, Belgium: European Committee for Standardisation.
- England, P., Houseman, G., & Nocquet, J. M. (2016). Constraints from GPS measurements on the dynamics of deformation in Anatolia and the Aegean. *Journal of Geophysical Research: Solid Earth*, *121*(12), 8888-8916.
- Erdik, M., Demircioğlu, M. B., Cüneyt, T., 2020, Forensic analysis reveals the causes of building damage in İzmir in the Oct. 30 Aegean Sea earthquake, Temblor, <http://doi.org/10.32858/temblor.139>
- Erdik, M., Doyuran, V., Akkas, N., & Gulkan, P., 1985. A probabilistic assessment of the seismic hazard in Turkey, *Tectonophysics*, **117**, 295-344.
- Erdik, M., Biro, Y., Onur, T., Sesetyan, K., & Birgoren, G., 1999. Assessment of earthquake hazard in Turkey and neighboring regions, *Annali di Geofisica*, **42**, 1125–1138.
- European Infrastructure for seismic waveform data, <https://www.orfeus-eu.org/data/strong/> (accessed by 05/11/2020).
- Evelpidou, N., Melini, D., Pirazzoli, P. A., & Vassilopoulos, A. (2014). Evidence of repeated late Holocene rapid subsidence in the SE Cyclades (Greece) deduced from submerged notches. *International Journal of Earth Sciences*, *103*(1), 381-395.
- Evelpidou, N., Pavlopoulos, K., Vouvalidis, K., Syrides, G., Triantaphyllou, M., Karkani, A., & Paraschou, T. (2019). Holocene palaeogeographical reconstruction and relative sea-level changes in the southeastern part of the island of Samos (Greece). *Comptes Rendus Geoscience*, *351*(6), 451-460.
- Eyidoğan, H. (2020) Report on the seismological characteristics and effects of the 30 October 2020 Samos-Kuşadası Bay earthquake (Mw7. 0) in the western Aegean Sea. Researchgate, https://www.researchgate.net/profile/Haluk_Eyidogan/publication/.
- Ganas, A., Elias, P., Briole, P., Tsironi, V., Valkaniotis, S., Escartin, J., ... & Efstathiou, E. (2020). Fault responsible for Samos earthquake identified. Temblor.
- Ganas, Athanassios (2019): NOAFAULTS KMZ layer Version 2.1 (2019 update). Zenodo. Dataset. <https://doi.org/10.5281/zenodo.3483136>
https://figshare.com/articles/NOAFAULTS_KMZ_layer_Version_2_1_2019_update_/11501277/1
- GEOFON Data Centre. (2020). GEOFON Earthquake Info. GEOFON Extended Virtual Network (GEVN). [Analysis performed manually by Saul, J.] <http://geofon.gfz-potsdam.de/eqinfo/event.php?id=gfz2020vimx>.
- Giardini, D., & Basham, P., 1993. The Global Seismic Hazard Assessment Program (GSHAP), *Annali di Geofisica*, **36**, 3-13.
- Gök, E., 2011. Investigation of earthquake hazard and seismic site characteristic in the examples of Bursa and Izmir (Doctoral dissertation, DEÜ Fen Bilimleri Enstitüsü).
- Gök, E., Chávez-García, F.J. and Polat, O., 2014. Effect of soil conditions on predicted ground motion: Case study from Western Anatolia, Turkey. *Physics of the Earth and Planetary Interiors*, *229*, pp.88-97.
- Grzegorz, K., (2020). StemBar (<https://www.mathworks.com/matlabcentral/fileexchange/28513-stembar>), MATLAB Central File Exchange. Retrieved December 14, 2020.
- Gürer, Ö., Sarica-Filoreau, N., Özburan, M., Sangu, E., & Dogan, B., 2009. Progressive development of the Büyük Menderes Graben based on new data, western Turkey, *Geol. Mag.*, **146**, 652–673, doi:10.1017/S0016756809006359
- Hartigan, J.A., 1975. *Clustering Algorithms*, John Wiley and Sons, New York.
- Hellenic Strong Motion Network (HUSN), National Observatory of Athens- Institute of Geodynamics, <https://accelnet.gein.noa.gr> (accessed by 06/12/2020).
- Institute of Engineering Seismology and Earthquake Engineering Research and Technical Institute (ITSAK), <http://www.itsak.gr/en/db/data/sm/after2000> (accessed by 01/12/2020).
- Jackson, J. A., Gagnepain, J., Houseman, G., King, G. C. P., Papadimitriou, P., Soufleris, C., & Virieux, J. (1982). Seismicity, normal faulting, and the geomorphological development of the Gulf of Corinth (Greece): the Corinth earthquakes of February and March 1981. *Earth and Planetary Science Letters*, *57*(2), 377-397.

- Jackson, J., & McKenzie, D. (1988). Rates of active deformation in the Aegean Sea and surrounding regions. *Basin Research*, 1(3), 121-128.
- Jackson, J. (1994). Active tectonics of the Aegean region. *Annual Review of Earth and Planetary Sciences*, 22(1), 239-271.
- Jackson, J., McKenzie, D., Priestley, K., and Emmerson, B. (2008). New views on the structure and rheology of the lithosphere. *Journal of the Geological Society*, 165(2):453–465.
- Kale Ö., Akkar S., Ansari A., Hamzehloo H., (2015), A Ground-Motion Predictive Model for Iran and Turkey for Horizontal PGA, PGV, and 5% Damped Response Spectrum: Investigation of Possible Regional Effects. *Bulletin of the Seismological Society of America*; 105 (2A): 963–980. <https://doi.org/10.1785/0120140134>
- Kalogeras, I. Melis, N.S. and Kalligeris, (2020). The earthquake of October 30th, 2020 at Samos, Eastern Aegean Sea, Greece. Preliminary Report, National Observatory of Athens, Institute of Geodynamics Earthquake Engineering & Structural Dynamics.
- Kassaras, I., Kapetanidis, V., Ganas, A., Tzanis, A., Kosma, C., Karakonstantis, A., ... & Papadimitriou, P. (2020). The New Seismotectonic Atlas of Greece (v1. 0) and Its Implementation. *Geosciences*, 10(11), 447.
- Koravos, G.Ch., Main, I.G., Tsapanos, T.M., & Musson, R.M.W., 2003a. Maximum earthquake magnitudes in the Aegean area constrained by tectonic seismic moment release rates, *Geophys. J. Int.*, **152**, 94– 112.
- Koravos, G.Ch., Main, I.G., Tsapanos, T.M., & Musson, R.M.W., 2003b. Perceptible earthquakes in the broad Aegean area, *Tectonophysics*, **371**, 175-186.
- Lekkas, E., Mavroulis, S., Gogou, M., Papadopoulou, G.A., Triantafyllou, I., Katsetsiadou, K.N., ... & Kranis, H. (2020). The October 30, 2020 Mw 6.9 Samos (Greece) earthquake. *Newsletter of Environmental, Disaster and Crises Management Strategies*, 21, ISSN 2653- 9454.
- Mallet, R., 1858. *Fourth report upon the facts and theory of earthquake phenomena*, Report of the 28th Meeting (Leeds) of the British Association for the Advancement of Science, p1-136.
- Mallet, R., 1862. *Great Neapolitan Earthquake of 1857. The first principles of observational seismology, Vol 2, Map D (Seismic Bands of The Mediterranean)*, Report, Royal Society of London.
- Makropoulos, K.C., & Burton, P.W., 1983. Seismic risk of circum-Pacific earthquakes. I: Strain energy release, *Pure appl. Geophys.*, **121**, 247-267.
- Manos G.C. (1994) Greece. In: Paz M. (eds) *International Handbook of Earthquake Engineering*. Springer, Boston, MA. https://doi.org/10.1007/978-1-4615-2069-6_17
- McCaffrey, R., & Abers, G. (1988). Syn3: A program for inversion of teleseismic body waveforms on microcomputers.
- McCaffrey, R., Abers, G., & Zwick, A. (1991). Inversion of teleseismic body waves, in *Digital Seismogram Analysis and Waveform Inversion*. W. Lee (ed.), IASPEI Software Library, chapter 3: IASPEI Software Library, Vol. 3, Menlo Park, USA.
- McClusky, S., Balassanian, S., Barka, A., Demir, C., Ergintav, S., Georgiev, I., ... & Kastens, K. (2000). Global Positioning System constraints on plate kinematics and dynamics in the eastern Mediterranean and Caucasus. *Journal of Geophysical Research: Solid Earth*, 105(B3), 5695-5719.
- McGuire, R. K., & Shedlock, K. M., 1981. Statistical uncertainties in seismic hazard evaluations in the United States, *Bull. seism. Soc. Am.*, **71**, 1287-1308.
- McKenzie, D. (1972). Active tectonics of the Mediterranean region. *Geophysical Journal International*, 30(2), 109-185.
- McKenzie, D. (1978). Active tectonics of the Alpine—Himalayan belt: the Aegean Sea and surrounding regions. *Geophysical Journal International*, 55(1), 217-254.
- McNeill, L. C., & Collier, R. L. (2004). Uplift and slip rates of the eastern Eliki fault segment, Gulf of Corinth, Greece, inferred from Holocene and Pleistocene terraces. *Journal of the Geological Society*, 161(1), 81-92.
- Middle East Technical University Earthquake Engineering Research Center (METU EERC), (2020). The October 30, 2020 İzmir-Seferihisar Offshore (Samos) Earthquake (Mw=6.6) Reconnaissance Observations and Findings, Report No: METU/EERC 2020-03, November, Ankara.
- Mountrakis, D., Kiliyas, A., Vavliakis, E., Psilovikos, A., & Thomaidou, E. (2003). Neotectonic map of Samos island (Aegean Sea, Greece): implication of geographical information systems in the geological mapping. In *4th European Congress on Regional Geoscientific Cartography and Information Systems, Bologna, Italy* (pp. 11-13).
- Nikolaou, S. and Gilsanz, R., (2015). Learning from Structural Success rather than failures. *Structure Magazine*, p.25-31, March.

- Nocquet, J. M. (2012). Present-day kinematics of the Mediterranean: A comprehensive overview of GPS results. *Tectonophysics*, 579, 220-242.
- Özmen, B., (2012). Türkiye deprem bölgeleri haritalarının tarihsel gelişimi. *Türkiye Jeoloji Bülteni* 55(1):43–55 (in Turkish).
- Papadimitriou, P., Kapetanidis, V., Karakonstantis, A., Spingos, I., Kassaras, I., Sakkas, V., ... & Voulgaris, N. (2020). First Results on the Mw= 6.9 Samos Earthquake of 30 October 2020. *Bulletin of the Geological Society of Greece*, 56(1), 251-279.
- Papaoiannou, Ch.A., & Papazachos, B.C., 2000. Time-independent and time-dependent seismic hazard in Greece based on seismogenic sources, *Bull. seism. Soc Am.*, **90**, 22- 33.
- Papazachos, B.C., 1990. Seismicity of the Aegean and surrounding area, *Tectonophysics*, **178**, 287–308.
- Papazachos, B.C., Papaoiannou, C.A., Papazachos, C.B., & Savvidis, A.S., 1999. Rupture zones in the Aegean region, *Tectonophysics*, **308**, 205–221.
- Pavlidis, S., Tsapanos, T., Zouros, N., Sboras, S., Koravos, G., & Chatzipetros, A. (2009). Using active fault data for assessing seismic hazard: a case study from NE Aegean Sea, Greece. In *Earthquake Geotechnical Engineering Satellite Conference XVIIth International Conference on Soil Mechanics & Geotechnical Engineering 2e3* (Vol. 10, p. 2009).
- Pirazzoli, P. A., Montaggioni, L. F., Saliege, J. F., Segonzac, G., Thommeret, Y., & Vergnaud-Grazzini, C. (1989). Crustal block movements from Holocene shorelines: Rhodes island (Greece). *Tectonophysics*, 170(1-2), 89-114.
- Pirazzoli, P. A., Stiros, S. C., Laborel, J., Laborel-Deguen, F., Arnold, M., Papageorgiou, S., & Morhangel, C. (1994). Late-Holocene shoreline changes related to palaeoseismic events in the Ionian Islands, Greece. *The Holocene*, 4(4), 397-405.
- Pitilakis, K., Gazepis, C. and Anastasiadis, A., (2004). Design Response Spectra and Soil Classification for Seismic Code Provisions. 13th World Conference on Earthquake Engineering, Vancouver, B.C., Canada, August 1-6, 2004, Paper No. 2904.
- Pitilakis, K., Riga, E. and Roumelioti, Z., (2016). The urgent need for an improvement of the Greek seismic code based on a new seismic hazard map for Europe and a new site classification system. Book Chapter in Jubilee volume, Andreas Anagnostopoulos, 50 years of service at the National Technical University of Athens. Publisher: TsotrasEditors: Michael Kavvadas.
- Ring, U., Okrusch, M. & Will, T. 2007. Samos Island, Part I: metamorphosed and non-metamorphosed nappes, and sedimentary basins. In: (Eds.) Gordon Lister, Marnie Forster, and Uwe Ring, Inside the Aegean Metamorphic Core Complexes, Journal of the Virtual Explorer, Electronic Edition, ISSN 1441-8142, volume 27, paper 5, doi:10.3809/jvirtex.2007.00180.
- Sesetyan, K., Demircioglu, M.B., Duman, T., Can, T., Tekin, S., Azak, E.T., & Zulfikar, F.O., 2018. A probabilistic seismic hazard assessment for the Turkish territory—Part I: the area source model, *Bull. Earthquake Eng.*, **16**, 3367-3397, doi:10.1007/s10518-016-0005-6.
- Sieberg, A., (1932). *Erdbebengeographie*, vol Band IV, Lieferung 3. Verlag von Gebrüder Borntraeger, Berlin.
- Soyluk, A. and Harmanakaya, Z.Y., (2012). Examination of earthquake resistant design in the education of architecture. *Proc Soc Behav Sci* 51:1080–1086.
- Specification for structures to be built in disaster areas, 1975. Ministry of Public Works and Settlement Government of Republic of Turkey.
- Specification for structures to be built in disaster areas, 2007. Ministry of Public Works and Settlement Government of Republic of Turkey.
- Specifications for buildings to be built in seismic areas (Turkish Building Earthquake Code),2018. Ministry of Public Works and Settlement, Ankara, Turkey
- Stiros, S. C., Arnold, M., Pirazzoli, P. A., Laborel, J., Laborel, F., & Papageorgiou, S. (1992). Historical coseismic uplift on Euboea island, Greece. *Earth and Planetary Science Letters*, 108(1-3), 109-117.
- Stiros, S. C., Laborel, J., Laborel-Deguen, F., Papageorgiou, S., Evin, J., & Pirazzoli, P. A. (2000). Seismic coastal uplift in a region of subsidence: Holocene raised shorelines of Samos Island, Aegean Sea, Greece. *Marine Geology*, 170(1-2), 41-58.
- Sucuoğlu, H. (2018). New Improvements in the 2018 Turkish Seismic Code. *International Workshop on Advanced Materials and Innovative Systems in Structural Engineering: Seismic Practices (IWAMISSE)*, İstanbul.
- Tan, O., Papadimitriou, E. E., Pabucçu, Z., Karakostas, V., Yörük, A., & Leptokarpoulos, K. (2014). A detailed analysis of microseismicity in Samos and Kuşadası (Eastern Aegean Sea) areas. *Acta Geophysica*, 62(6), 1283-1309.

- Taymaz, T., Yilmaz, Y. & Dilek, Y. (2007). The geodynamics of the Aegean and Anatolia: introduction. *Geological Society, London, Special Publications*, 291(1), 1-16.
- Tiberti, M. M., Basili, R., & Vannoli, P. (2014). Ups and downs in western Crete (Hellenic subduction zone). *Scientific reports*, 4, 5677.
- Tsapanos, T.M., 2003. A seismic hazard scenario for the main cities of Crete island-Greece, *Geophys. J. Int.*, **155**, 403-408.
- Tselentis, G-A., & Danciu, L., 2008. Empirical Relationships between Modified Mercalli Intensity and Engineering Ground-Motion Parameters in Greece, *Bull. seism. Soc. Am.*, **98**, 1863-1875.
- Tselentis, G-A., & Danciu, L., 2010a. Probabilistic seismic hazard assessment in Greece – Part 1: Engineering ground motion parameters, *Nat. Hazards Earth Syst. Sci.*, **10**, 25–39.
- Tselentis, G-A., & Danciu, L., 2010b. Probabilistic seismic hazard assessment in Greece – Part 3: deaggregation, *Nat. Hazards Earth Syst. Sci.*, **10**, 51-59.
- Tselentis, G-A., Danciu, L., & Sokos, E., 2010. Probabilistic seismic hazard assessment in Greece – Part 2: Acceleration response spectra and elastic input energy spectra, *Nat. Hazards Earth Syst. Sci.*, **10**, 41–49.
- Tselentis, G-A., & Danciu, L., (2010). Probabilistic seismic hazard assessment in Greece – Part 1: Engineering ground motion parameters, *Nat. Hazards Earth Syst. Sci.*, **10**, 25–39.
- United Nations, Department of Economic and Social Affairs, Population Division (2019). World Population Prospects 2019: Data Booklet. ST/ESA/SER.A/424.
- United States Geological Survey. (2020). Search Earthquake Catalog, <https://earthquake.usgs.gov/earthquakes/search/> (accessed by 01/11/2020).
- Weatherill, G. and Burton, P.W., (2010). An alternative approach to probabilistic seismic hazard analysis in the Aegean region using Monte Carlo simulation. *Tectonophysics* Volume 492, issues 1-4, p.253–278. <https://doi.org/10.1016/j.tecto.2010.06.022>
- Weatherill, G., & Burton, P.W., 2009. Delineation of shallow seismic source zones using K-means cluster analysis, with application to the Aegean region, *Geophys. J. Int.*, **176**, 565-588, doi: 10.1111/j.1365-246X.2008.03997.x.
- Weiss, J. R., Walters, R. J., Morishita, Y., Wright, T. J., Lazecky, M., Wang, H., ... & Yu, C. (2020). High-resolution surface velocities and strain for Anatolia from Sentinel-1 InSAR and GNSS data. *Geophysical Research Letters*, 47(17), e2020GL087376.
- Wells, D.L., & Coppersmith, K.J., 1994. New Empirical Relationships among Magnitude, Rupture Length, Rupture Width, Rupture Area, and Surface Displacement, *Bull. seism. Soc. Am.*, **86**, 974-1002.
- Wimpenny, S. & Watson, C.S., 2020. gWFM: A global catalog of moderate magnitude earthquakes studied using teleseismic body waves, *Seismol. Res. Lett.*, 92(1), 212–226.
- Zwick, P., McCaffrey, R., & Abers, G. (1994). MT5 program.

3. GEOTECHNICAL OBSERVATIONS AND SITE RESPONSE

(Authored by RR)

3.1. Introduction

This chapter presents the main findings from a geotechnical survey carried out during the EEFIT mission in the areas affected in Turkey and Samos Island (Eastern Aegean Sea, Greece) by the Mw 6.9 30 October 2020 earthquake. In this context, field investigations and desk reconnaissance studies were performed to characteristics of affected areas with respect to their geological and geotechnical properties. The aim of this survey was twofold: to locate and characterise the impact of seismic effects on the natural environment (e.g., ground cracks, landslides, rock falls and soil liquefaction, etc.) and to identify the possible geotechnical failures (e.g., collapse of quay walls and retaining walls, etc.). It further provides preliminary assessment regarding the site response of Bayraklı district where most heavily damaged buildings are located. Although no significant geotechnical effects in the form of foundation failures and liquefaction-induced lateral spreading were reported in this region, the deep alluvial deposits of soil, groundwater table at 1-3 m depth, and a significant amplification of the rock acceleration for this region may have been contributed in the seismic behaviour of these structures.

3.2. Co-seismic environmental effects

In this section, secondary environmental effects caused by the ground response to the seismic shaking including ground cracks, landslides, rock falls, and soil liquefaction are presented. For initial assessing regional seismic hazard and the geological/geotechnical properties in and around the study area, the information of geological and USGS maps were evaluated. **Figure 32** shows the geological map of the region (Coskun et al. 2017).

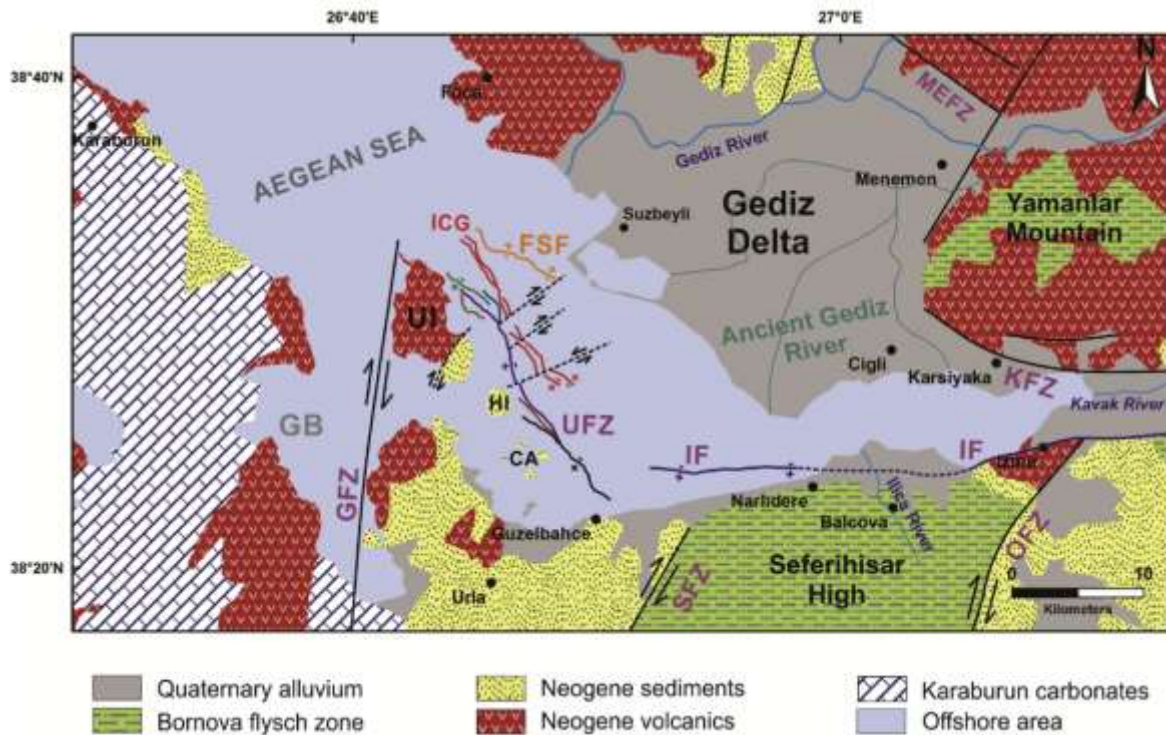


Figure 32: Geological map and fault lines of the region around the Gulf of Izmir. UFZ: Uzunada Fault Zone, IF: Izmir Fault Zone, ICG: Izmir Central Graben, FSF: FocaSuzbeyli Fault, OFZ: Orhanli (Tuzla) Fault Zone, GFZ: Gulbahce Fault Zone, GB: Gulbahce Bay, MEFZ: Menemen Fault Zone, SFZ: Seferihisar Fault Zone, KFZ: Karsiyaka Fault Zone, UI: Uzun Island, HI: Hekim Island, CA: Cicek Archipelago. Coskun et al. (2017).

Izmir region is located in northern coast of İzmir Bay and the main active faults of study area, which are the Izmir (IF), Gulbahce (GFZ), Orhanli (OFZ-it is also known as the “Tuzla Fault”), Seferihisar (SFZ)

and Karsiyaka Fault Zones (KFZ) in the onshore part of Gol and surrounding region (Coskun et al. 2017). The potential area of environmental effects such as landslides and liquefaction were also investigated by maps released by USGS after the event (**Figure 33** from <https://earthquake.usgs.gov/earthquakes/eventpage/us7000c7y0/ground-failure/summary>).

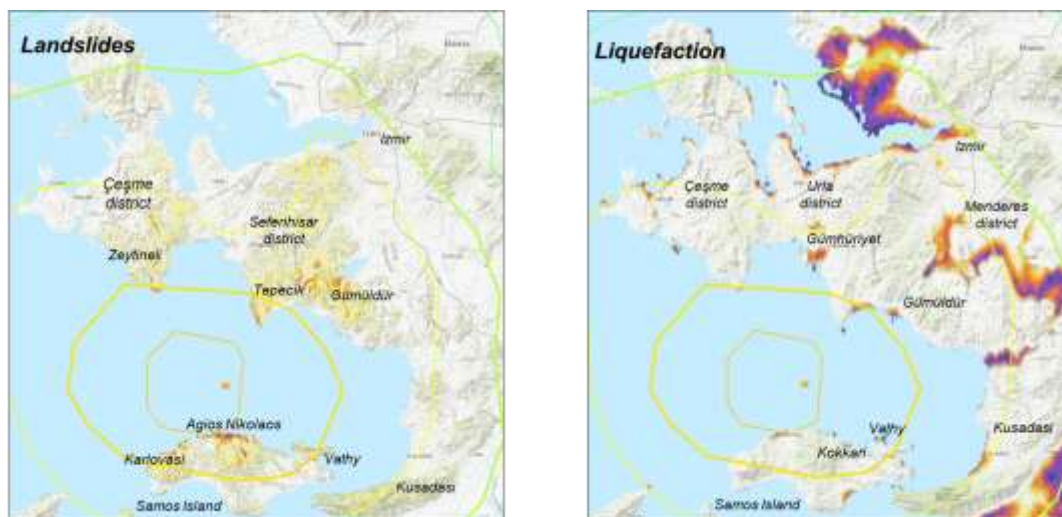


Figure 33: Landslides and liquefaction hazard maps released by USGS after the event (USGS, 2020)

Despite these ground failures predictions by the USGS (2020), the initial reports after earthquake indicate low levels of landslides and liquefaction around and to the south of Izmir (e.g. Vadaloukas et al., 2020; METU EERC, 2020) – an observation in broad agreement with the USGS predictions. On the Samos island, various co-seismic effects were noticed on both built and natural environments, including soil liquefaction, ground cracks and rock falls (Lekkas, et al. 2020). Extensive damage was observed in the quay walls of the Karlovasi, Kokkari and Vathy ports. Further details on these secondary coseismic effects are provided in the following subsections.

3.2.1. Ground cracks

Figure 34 shows some ground cracks observed in some of the northern settlements of Samos, Karlovasi (**Figure 34a**), Kokkari (**Figure 34b**) and in the area of the village of Agios Konstantinos (**Figure 34c&d**). These cracks affected buildings in the village of Agios Konstantinos. Similar observations were also reported by the HAEE reconnaissance team: they stated that buildings were likely affected by lateral spreading failure mechanism towards the seafront in the neighbourhood in Karlovasi (Vadaloukas et al., 2020).

These coseismic surface ruptures were reported in the northwestern part of the Karlovasi basin and affected by the major flat in this area, which is Hydroussa fault (Mavroulis et al 2021).

Moreover, some cracks were observed along the Vathy-Karlovasi road (**Figure 35a&b**), and roads network in the area of Agios Nikolaos (**Figure 35c&d**). Some additional effects were observed on the Vathy-Karlovasi road close to Karlovasi (**Figure 35e**). This area is located to the northeast, and composed of schists of the Ampelos nappe (Papadimitriou et al. 2020). The E–W-striking and N-dipping ruptures were reported in this location (Mavroulis et al 2021), which cut through the roads shown.



Figure 34: The observed ground cracks in a) Karlovasi, b) Kokkari and c) and d) at the village of Agios Konstantinos (source: <https://www.youtube.com/watch?v=E5lv20MwagI&t=1s>)



Figure 35: Road cracks observed in the area of (a) Vathy-Karlovasi road (Vadaloukas et al., 2020), (b, c) Agios Nikolaos (Lekkas et al. 2020), and (d) the main road Vathy-Karlovasi close to Karlovasi (photo taken by Manolis Thralvalos)

3.2.2. Landslides and rock falls

The landslide induced failures of slopes and permanent ground deformations and severe damage to the road often triggered by earthquakes. The landslides can be classified in the soft original ground, failure along the boundary between the fill and the original ground, due to shallow slips and without slippage due to seismic motion (Bhattacharya et al. 2020). One of the most severe environmental effects due to this earthquake was the disrupted rockslide and toe along the main artery in the northern part of the island. **Figure 36** shows rock slope failures generated along the coastal slopes in Avlaxia area which temporarily blocked the road networks after the earthquake, which might be attributed to the high and steep slopes of this site (Mavroulis et al 2021).

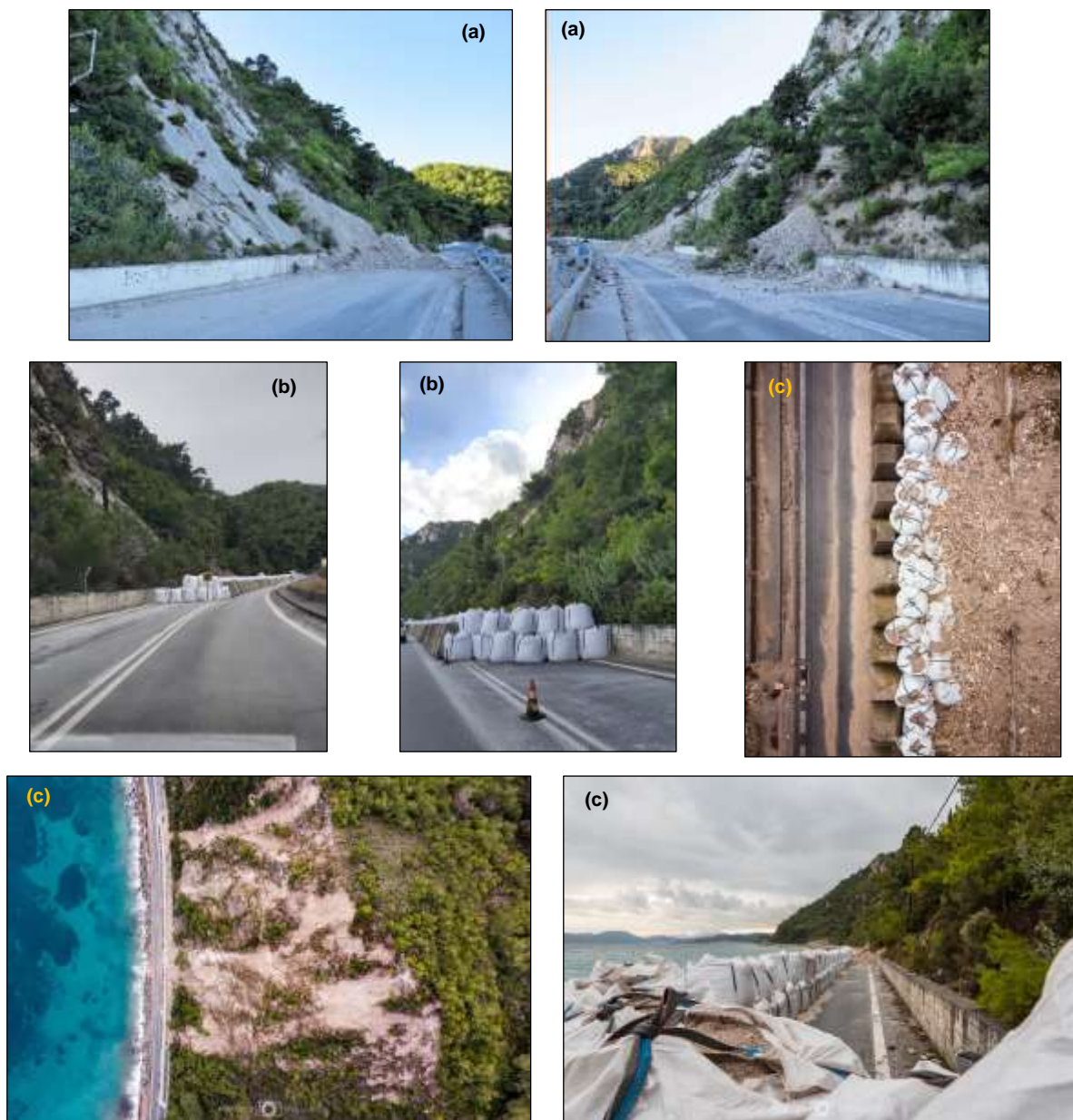


Figure 36: Landslides were generated along coastal slopes in Avlakia area a) immediately after the earthquake (31.10.2020) (Lekkas et al. 2020), b) large concrete block in order to protect the road from further slope failures (15.11.2020) and c) slope failures 45 days after earthquake (16.12.2020) (photos taken by Manolis Thravalos) (37°47'48.0"N, 26°51'27.7"E).

However, the road was re-secured within a few days using large concrete blocks (**Figure 36b**) placed along the toe of the affected area (Lekkas et al. 2020). Nonetheless, some further slope failures (**Figure 36c**) followed and affected these temporary restraining measures.

Rockfalls triggered by this earthquake were identified in several other sites as shown in **Figure 37**. The Hellenic Association of Earthquake Engineering (HAEE) reconnaissance team reported sandy marls and marly limestones very close to a residential building in the Kokkari region (Vadaloukas et al., 2020) (see **Figure 37a**). **Figure 37b** shows another rockfall along the road near the Tsambou beach (Vadaloukas et al., 2020). A limited number of rockfalls were also observed in Turkey, as also reported by the report by the METU/EERC (2020) (**Figure 37c**) (METU EERC, 2020). The damage proxy map (**Figure 38**) clearly shows most of the ground deformations concentrated on the road close to the Potami village (**Figure 38a**) and road close to Agios Nikolaos and Koumeika (**Figure 38b**), as also confirmed by Lekkas et al. (2020). Furthermore, Bayraklı District Cicek Neighbourhood was observed to pose favourable conditions for the generation of slope movements, mainly rockfalls (**Figure 39**).

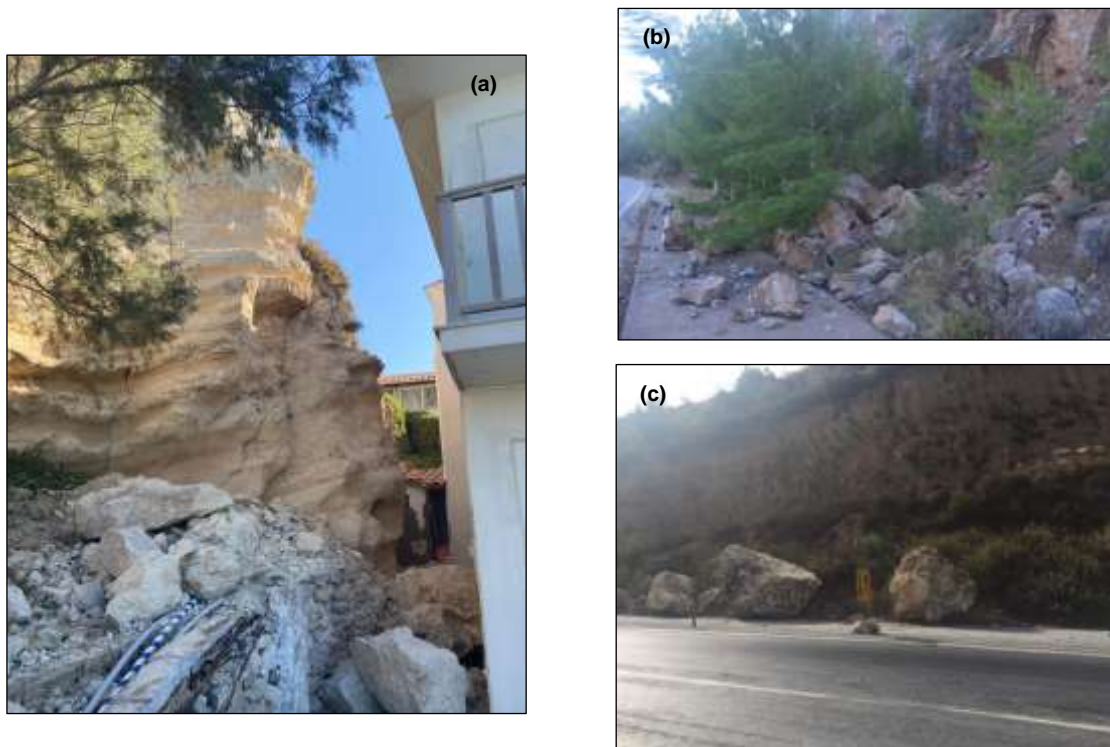


Figure 37: Rock falls (along with a large crack on the rock slope with future failure potential) were observed in a) in the Kokkari region (Samos Island, HAEE, 2020), b) near Tsambou beach (Samos Island, HAEE 2020), and c) Kuşadası (Turkey, 37.897341, 27.368394) (METU/EERC 2020)



Figure 38: Damage Proxy Map (DPM) of Potami close to Karlovasi and Kontakeika (from the Advanced Rapid Imaging and Analysis (ARIA) Centre for Natural Hazards, <https://aria-share.jpl.nasa.gov/20201030-Samos-Izmir-EQ/DPM/>). The colour grading from yellow to red indicates increasingly higher ground deformation.

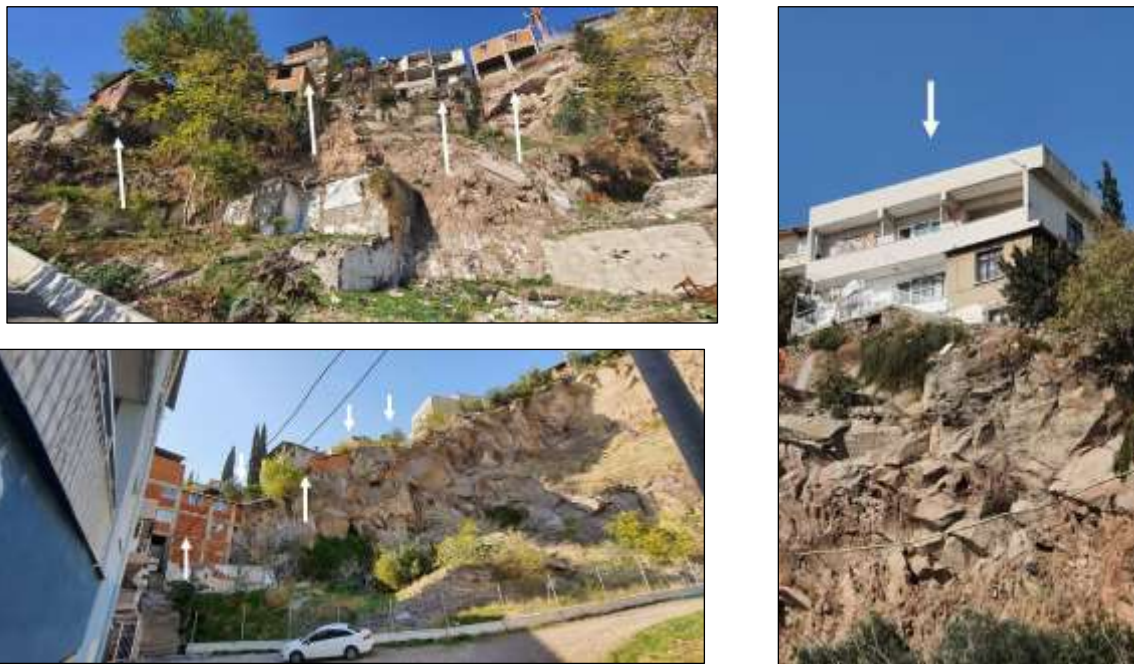


Figure 39: Potential area for rockfalls in Bayraklı District (TMoEU 2020)

3.2.3. Liquefaction

The initial reports mention post-earthquake soil liquefaction manifesting as sand boils at various locations, as also suggested by the USGS maps (**Figure 33**). However no liquefaction induced damages were reported in Izmir (METU/EERC, 2020).



Figure 40: Soil liquefaction in the form of sand boils in Malagari (source: photo on the left after Lekkas et al. 2020) and photos on the courtesy of Dr. A. Ganas)

Although not strictly a form of ground failures, sand boils are indicative of excess pore pressure, which indicates liquefaction potential (Rostami et al. 2020). Sand boils were observed along the shores of İcmeler and Gülbahçe districts (METU/EERC, 2020). Adverse effects of liquefaction were reported and damage appeared in the form of sand boils, sand ejecta and lateral spreading in Malagari located to the north-west of Vathy (**Figure 40**). The liquefaction phenomenon may also be responsible for the significant damage in the quay walls of the Vathy and Karlovasi ports (Lekkas et al. 2020), which is further discussed in the next section.

3.3. Geotechnical Failures

In this event, the most significant effect of failures after the earthquake was observed in Samos's main ports. This section presents the observations made in Karlovasi, Kokkari and Vathy ports, which experienced very severe damage. A few safety wall failures observed along Izmir province (Cetin, et al. 2020). However, there are no retaining wall damage reported for Turkey (METU/EERC, 2020).

3.3.1. Performance of Samos's Ports

Figure 41 shows the damage on the Pythagoreio port located on the southwest of Samos island. From the figure, it can be seen that this port suffered from cracks to the quay walls and horizontal displacement of the quay walls towards the sea.

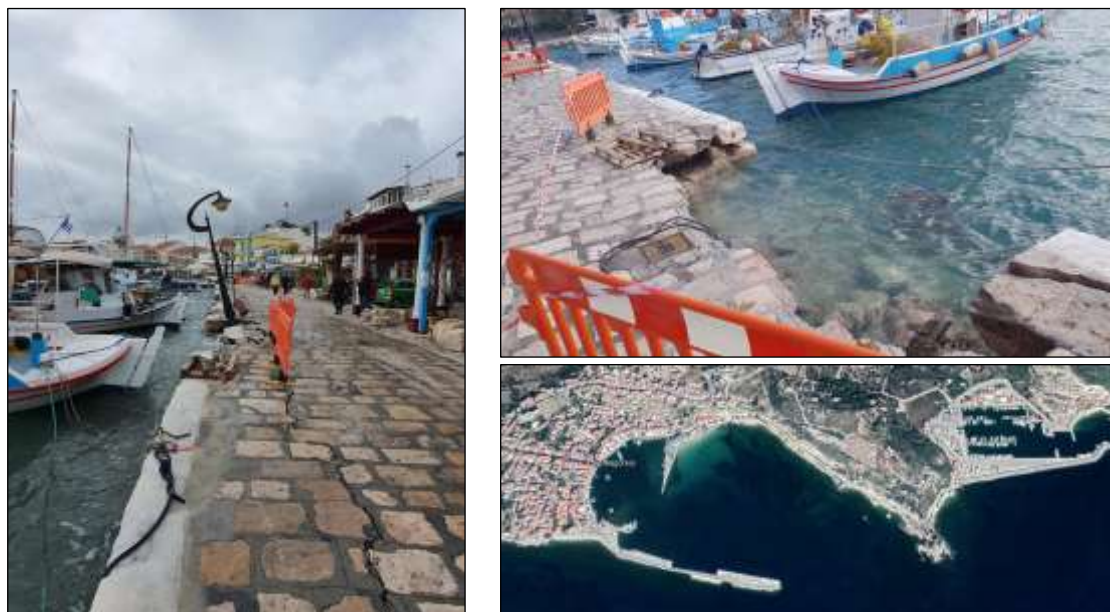


Figure 41: Damage was observed on Pythagoreio port

The Karlovasi and Vathy ports are situated in north Samos, and Kokkari (smaller port) is located between these two ports. In ports of Karlovasi and Vathy, there are two facilities: the eastern port and the western port. The western port of Vathy is known as the “Malagari” port and the eastern port of Karlovasi is a new port. More details on these ports can be found in Cetin et al. (2020). **Figure 42-44** show the extensive cracks and deformation that observed in these ports.



West



East



Figure 42: Significant damage was observed on Karlovasi ports of Samos.



(photo by Manolis Thravalos)



Figure 43: Significant damage was observed on Kokkari ports of Samos



Figure 44: Significant damage was observed on Vathy ports of Samos (Lekkas et al., 2020)

The level of failures observed at the block-type gravity quay wall structures in these areas might be due to a combination of the dynamic consolidation of the back-fill soil material, cracks on the surface, the near-surface liquefaction and displacements, and horizontal spread of the soil to the sea.

3.4. Geotechnical Setting of Izmir Bay

Izmir city is located along the eastern coast of the Aegean Sea at the western end of Turkey. The city is situated within the Izmir Bay. The most severe damage to structures is concentrated on the 7-12 story residential buildings Bayraklı district in Izmir. This section aims to present a preliminary assessment of the site response of Bayraklı area and geotechnical phenomena at play in this outcome. **Figure 45** shows the geological features and fault lines as well as the location of IzmirNET strong motion stations (Gök and Polat, 2014). It is seen that the majority of the affected area is located on a typical alluvial basin and threatened by the normal faults: Izmir Fault (IF) and Karşıyaka Fault Zone (KFZ).

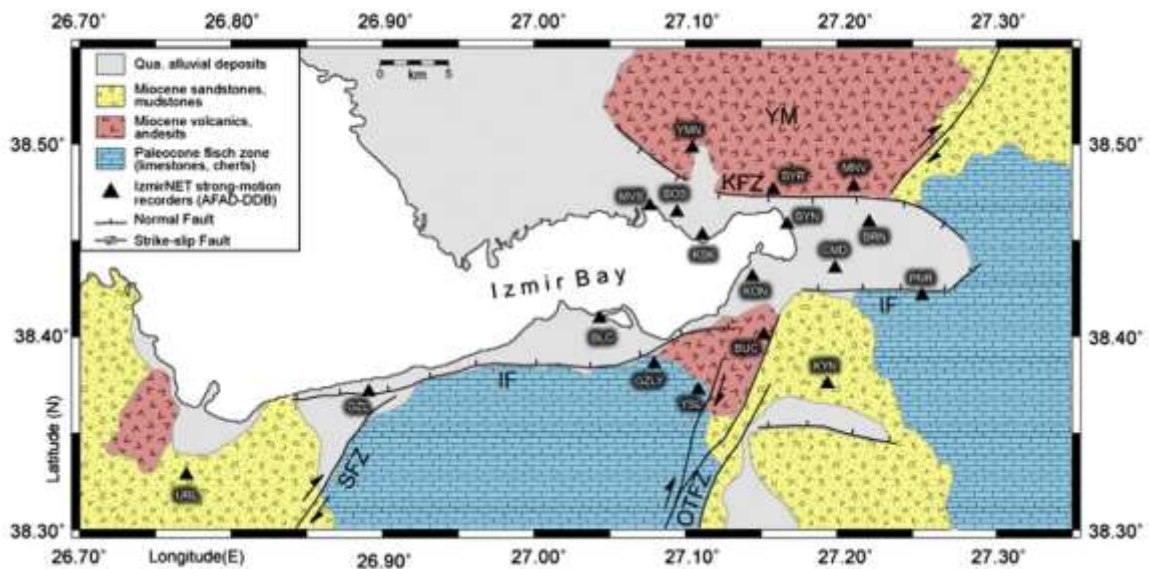


Figure 45: Geological features, fault Lines and location of IzmirNET stations (Gök and Polat, 2014)

Deep alluvial soil layers lying beneath the residential structures at Bayraklı lead to higher amplitude values of Pseudo Relative Velocity (PSV) at 1 s period, as illustrated in **Figure 46** for the city of Izmir for an expected M6.5 earthquake (Gök et al., 2014).

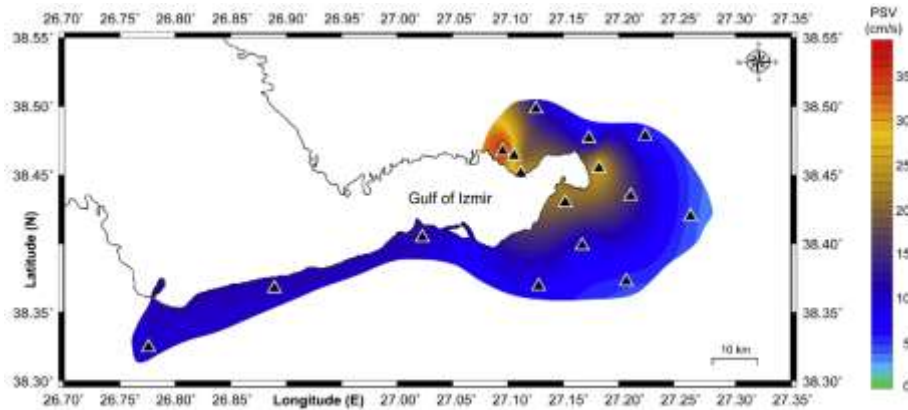


Figure 46: The distribution of amplitude values of PSV at 1 s period in the city of Izmir for the expected M6.5 earthquake (Gök et al., 2014)

The soil and SPT-count profile as well as the 1D P and S-Wave velocities of the deep alluvial soil in Bayraklı area are shown in **Figure 47**. These point out a low strength of soil, which is influential on the building response during the seismic event.

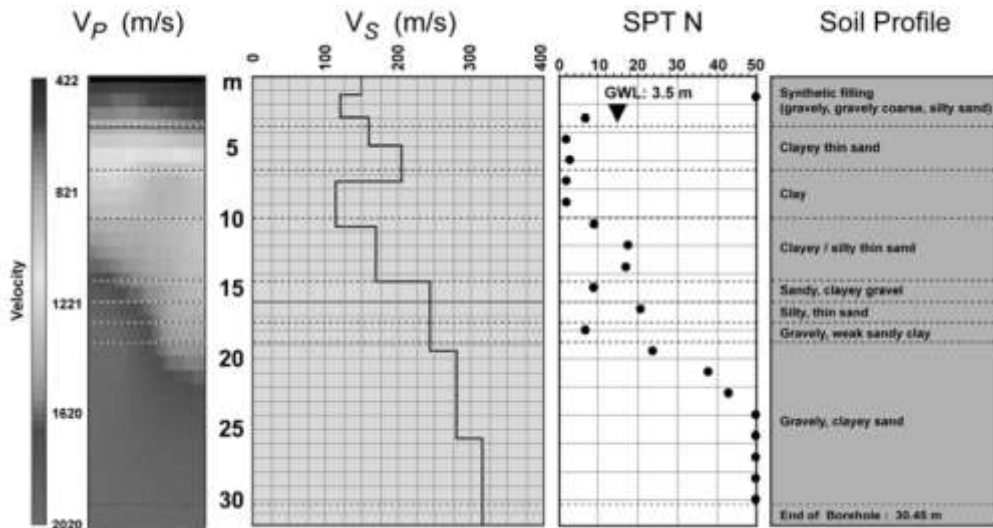


Figure 47: Typical soil properties of Bayraklı close to Station 3513 (Gök, 2011)

In order to further assessing the effects of site conditions, we considered the strong ground motion of stations 3513 and 3514 (**Figure 26**), which are both located in Bayraklı region close to the observed structural failures, on soil ($V_{s30}=196$ m/s) and rock ($V_{s30}=836$ m/s) sites respectively (**Figure 48**). The corresponding frequency distribution graphs was also studied: The peak ground acceleration (PGA) was measured as 106 cm/s^2 and 57 cm/s^2 for Bayraklı soil and rock sites (**Figure 48**). From the frequency domain plots, it is seen that the motion intensities are much higher for Station 3513, confirming that a significant amplification is expected in this region.

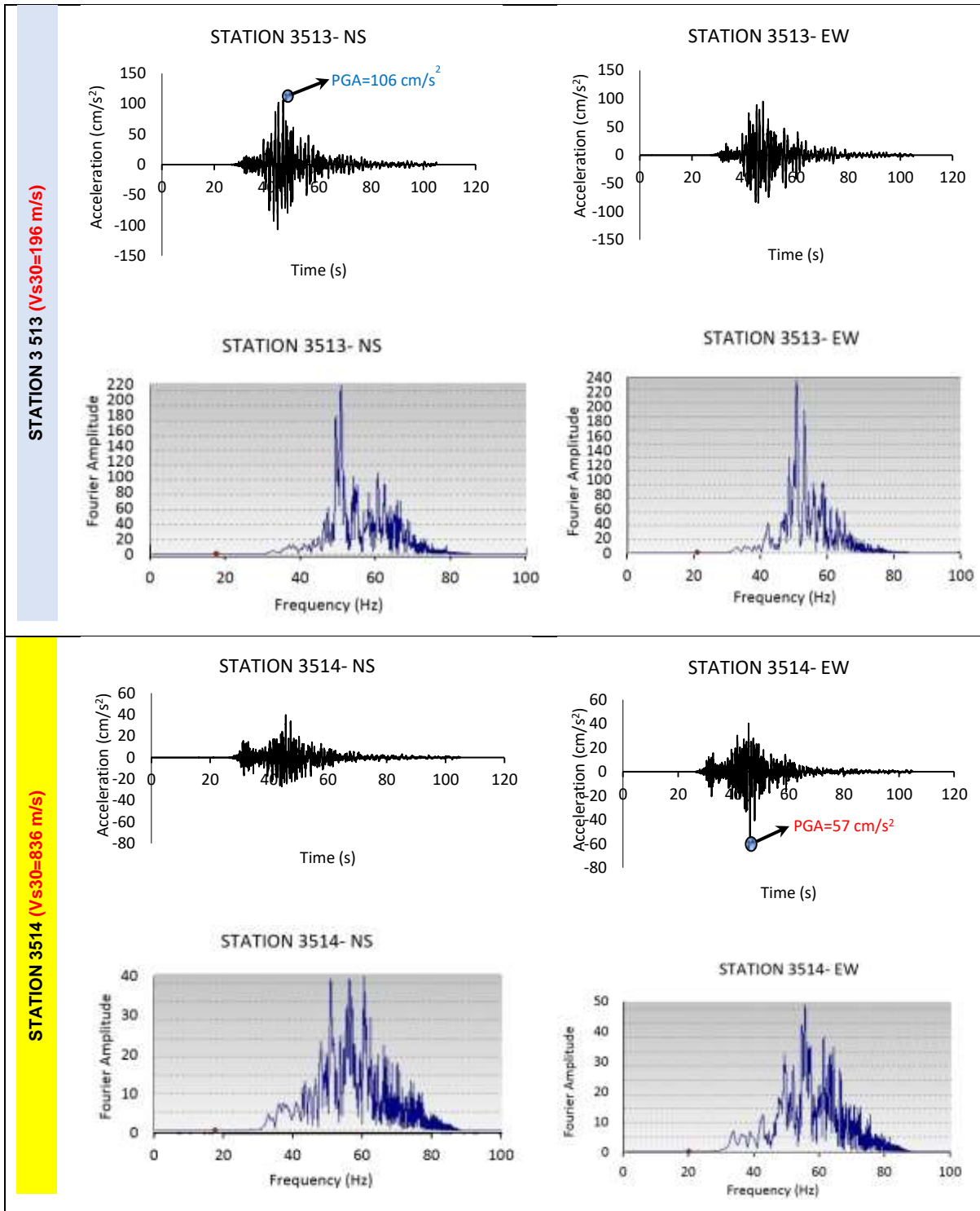


Figure 48: Recorded ground motion of stations 3513 and 3514 and the corresponding frequency

As mentioned before, 17 building with the 7-12 storeys residential were collapsed or heavily damaged in Bayraklı district during this earthquake. This can be related to potential of soil-structure resonance (Stanko et al. 2017). Therefore, seismic amplification spectra around Bayraklı (**Figure 49a&b**) and the ratios of the horizontal and vertical acceleration spectra (H / V relationships) of the Buca, Bayraklı and Karşıyaka station records, incorporating the Vs30 values provide the round amplification (Erdik et al., 2020) were examined (ITU, 2020). It is observed that large amplifications about 6 was formed in period values around 2.5 seconds for soil site at Bayraklı station, where the most severe damage to structures were reported. **Figure 49** also presents the comparison of the acceleration response spectra of Bayraklı

stations with the current and earlier versions of Turkish Seismic Codes at these locations (Erdik et al. 2020). It can be seen that records for soft soil (up to 0.35g) are much larger than those for the rock site (0.14g), however the spectrum values obtained for soft soil conditions still remain lower than the design values. Based on this data, we understand that the ground motion amplification in soft soil can be a significant contributor to the damage of these structures during earthquake on October 30,2020.

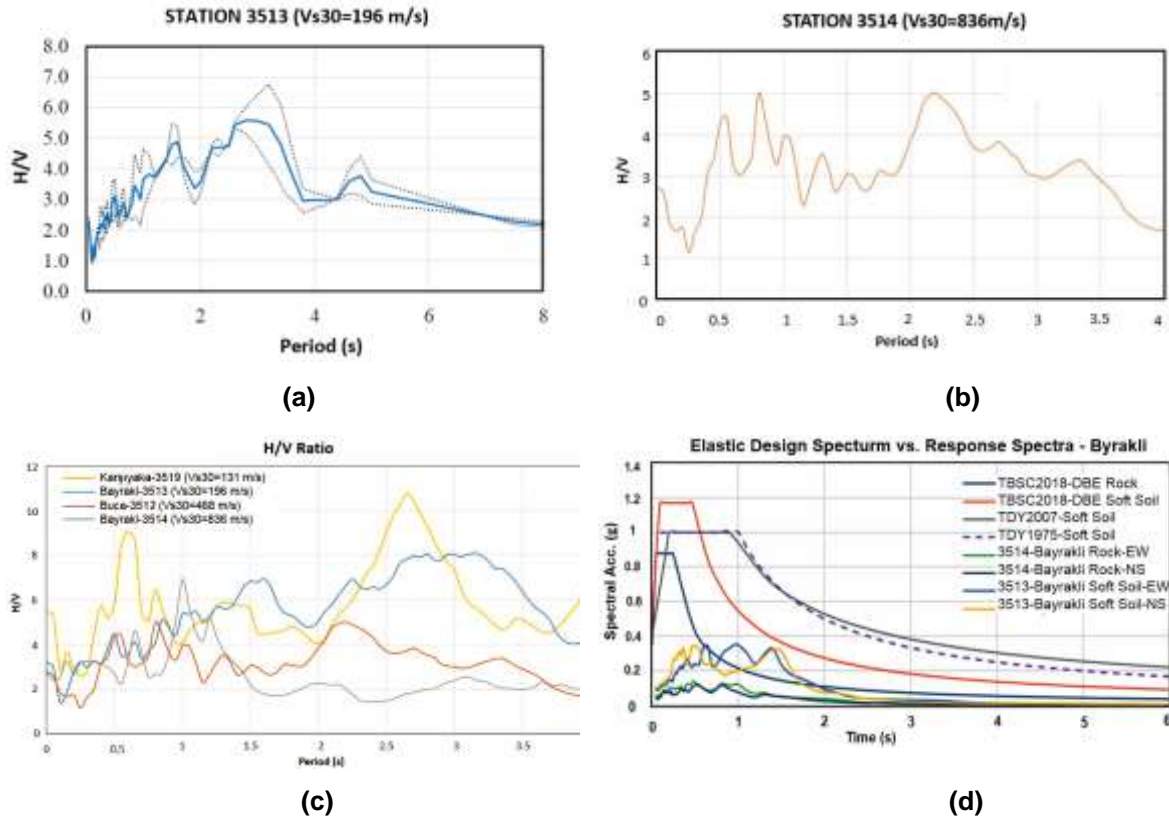


Figure 49: (a) and (b) The amplification spectra for stations 3513 and 3514 (ITU Report, 2020) and (c) the ratios of the horizontal and vertical of the acceleration spectra (H / V) graph for Buca, Bayraklı and Karşıyaka stations and d) comparison of the acceleration response spectra of the recorded ground motion at the two stations against the DBE level spectra of current and earlier versions of Turkish Seismic Codes at these locations (adapted from Erdik et al. 2020)

3.5. Summary and Conclusions

This chapter presented geotechnical damage observed after this seismic event. Various ground failures have been observed in form of ground cracks, landslides, rock falls, and soil liquefaction. A limited number of environmental effects were reported for Izmir area. Most of the secondary co-seismic effects observed in the north part of Samos were ground cracks and rockslides. This island witnessed severe damage on Port facilities in Karlovasi, Kokkari and Vathy. A unique feature of this earthquake was the heavy damage observed in the 7-12 story residential buildings in Bayraklı, a district located at about 65-70 km to the N-NE of the earthquake epicentre. It could be argued that the deep alluvial deposits of soil, groundwater table at 1-3 m depth, the highest ground acceleration (around 106 cm/s²) and a significant amplification of the rock acceleration for this region may have been contributed in the seismic behaviour of these structures.

References

- Bhattacharya, S., Orense, R.P. and Lombardi, D., 2019. Seismic design of foundations: concepts and applications. ICE Publishing.
- Cetin, K. O., et al. (2020). Seismological and Engineering Effects of the M 7.0 Samos Island (Aegean Sea) Earthquake. <https://doi.10.18118/G6H088>. <https://www.designsafe-ci.org/community/news/2021/january/recon-report-m7-samos-island-earthquake-oct-2020/>.
- Coskun, S., Dondurur, D., Cifci, G., Aydemir, A., Gungor, T. and Drahor, M.G., 2017. Investigation on the tectonic significance of Izmir, Uzunada Fault Zones and other tectonic elements in the Gulf

- of Izmir, western Turkey, using high resolution seismic data. *Marine and Petroleum Geology*, 83, pp.73-83.
- Erdik, M., Demircioğlu, M. B., Cüneyt, T., 2020, Forensic analysis reveals the causes of building damage in İzmir in the Oct. 30 Aegean Sea earthquake, *Temblores*, <http://doi.org/10.32858/temblor.139>.
- Gök, E., 2011. Investigation of earthquake hazard and seismic site characteristic in the examples of Bursa and Izmir (Doctoral dissertation, DEÜ Fen Bilimleri Enstitüsü).
- Gök, E., Chávez-García, F.J. and Polat, O., 2014. Effect of soil conditions on predicted ground motion: Case study from Western Anatolia, Turkey. *Physics of the Earth and Planetary Interiors*, 229, pp.88-97.
- Gök, E. and Polat, O., 2014. An assessment of the microseismic activity and focal mechanisms of the Izmir (Smyrna) area from a new local network (IzmirNET). *Tectonophysics*, 635, pp.154-164.
- İTÜ (2020). 30 Ekim 2020 İzmir Depremi Değerlendirme Raporu, İstanbul Teknik Üniversitesi, Page 31.
- Lekkas E, Mavroulis S, Gogou M, Papadopoulos GA, Triantafyllou I, Katsetsiadou K-N, Kranis H, Skourtsos , E., Carydis P, Voulgaris N, Papadimitriou P, Kapetanidis V, Karakonstantis A, Spingos I, Kouskouna V, Kassaras I, Kaviris G, Pavlou K, Sakkas V, Evelpidou N, Karkani E, Kampolis I, Nomikou P, Lambridou D, Krassakis P, Fouvelis M, Papazachos C, Karavias A, Bafi D, Gatsios T, Markogiannaki O, Parcharidis I, Ganas A, Tsironi V, Karasante I, Galanakis D, Kontodimos K, Sakellariou D, Theodoulidis N, Karakostas C, Lekidis V, Makra K, Margaris V, Morfidis K, Papaioannou C, Rovithis E, Salonikios T, Kourou A, Manousaki M, Thoma T , Karveleas N (2020). The October 30, 2020 Mw 6.9 Samos (Greece) earthquake. *Newsletter of Environmental, Disaster and Crises Management Strategies*, 21: 2653-9454.
- Mavroulis, S.; Triantafyllou, I.; Karavias, A.; Gogou, M.; Katsetsiadou, K.-N.; Lekkas, E.; Papadopoulos, G.A.; Parcharidis, I. Primary and Secondary Environmental Effects Triggered by the 30 October 2020, Mw = 7.0, Samos (Eastern Aegean Sea, Greece) Earthquake Based on Post-Event Field Surveys and InSAR Analysis. *Appl. Sci.* 2021, 11, 3281. <https://doi.org/10.3390/app11073281>
- Middle East Technical University Earthquake Engineering Research Center (METU EERC), (2020). The October 30, 2020 İzmir-Seferihisar Offshore (Samos) Earthquake (Mw=6.6) Reconnaissance Observations and Findings, Report No: METU/EERC 2020-03, November, Ankara.
- Rostami, R., Mickovski, S.B., Hytiris, N. and Bhattacharya, S., 2020. The Dynamic Behaviour of Pile Foundations in Seismically Liquefiable Soils: Failure Mechanisms, Analysis, Re-Qualification. In *Earthquakes*. IntechOpen. DOI: 10.5772/intechopen.94936.
- Stanko, D., Markušić, S., Strelec, S. and Gazdek, M., 2017. HVSR analysis of seismic site effects and soil-structure resonance in Varaždin city (North Croatia). *Soil Dynamics and Earthquake Engineering*, 92, pp.666-677.
- TMoEU (2020) 30 Ekim 2020 İzmir Depremi Afeti; TMoEU.
- U.S. Geological Survey (2020). Earthquake Hazards Program accessed November 11, 2020, at URL <https://earthquake.usgs.gov/earthquakes/eventpage/us7000c7y0/executive>.
- Vadaloukas, G., Vintzileou, E., Ganas, A., Giarlelis, C., Ziotopoulou, K., Theodoulidis, N., Karasante, I., Margaris, B., Mylonakis, G., Papachristidis, A., Repapis, C., Psarropoulos, P. N., and Sextos, A. G. (2020). Samos Earthquake of 30th October, 2020. Preliminary Report of the Hellenic Association for Earthquake Engineering, Athens, Greece. <https://doi.org/10.13140/RG.2.2.22609.76644>.

4. DAMAGE ASSESSMENT AND OBSERVATIONS

As this mission had to take place during the global COVID pandemic, the traditional EEFIT model which relies on in-situ data collection by the whole team was not feasible. In this mission, we adopted a hybrid approach bringing together (1) a large remote team working on remote data acquisition and analysis of damage levels, as well as other aspects of the earthquake such as the background information on damage levels, the seismology of the region, ground motions etc through desk study, and (2) small field crews doing in-situ damage assessment under the coordination of the remote team.

4.1. Fieldwork Itinerary Planning

(Authored by YDA)

The itineraries of the local field crews have been carefully planned to ensure good use of limited time and resources we had in the field.

Our main compass in planning the *Turkey* fieldwork was the extent of coverage and outcome of the comprehensive damage assessment work that the Turkish Ministry of Environment and Urbanisation (TMoEU) carried out within a rather short amount of time following the event. This database is accessible at <https://hasartespit.csb.gov.tr/#/>, and is summarised and mapped in **Figure 50** and **51**. As seen, the coverage levels are pretty low apart from Bornova, Bayraklı and Karşıyaka districts, where all of the dramatic collapses and almost all heavy damages were observed. While more than 90,000 buildings were damage assessed in total in these districts, the number of assessed buildings can be as low as 1 in some others. Further, the TMoEU focussed entirely on city of Izmir, and did not extend to the neighbouring cities which were also affected. The observed damage levels are mainly rather low or non-existent: when the buildings that could not be assessed for some reason are ruled out, of all records found in the TMoEU database 95.4% is labelled as no-damage and 4.1% as little damage, which once again shows that damage is very limited and concentrated.

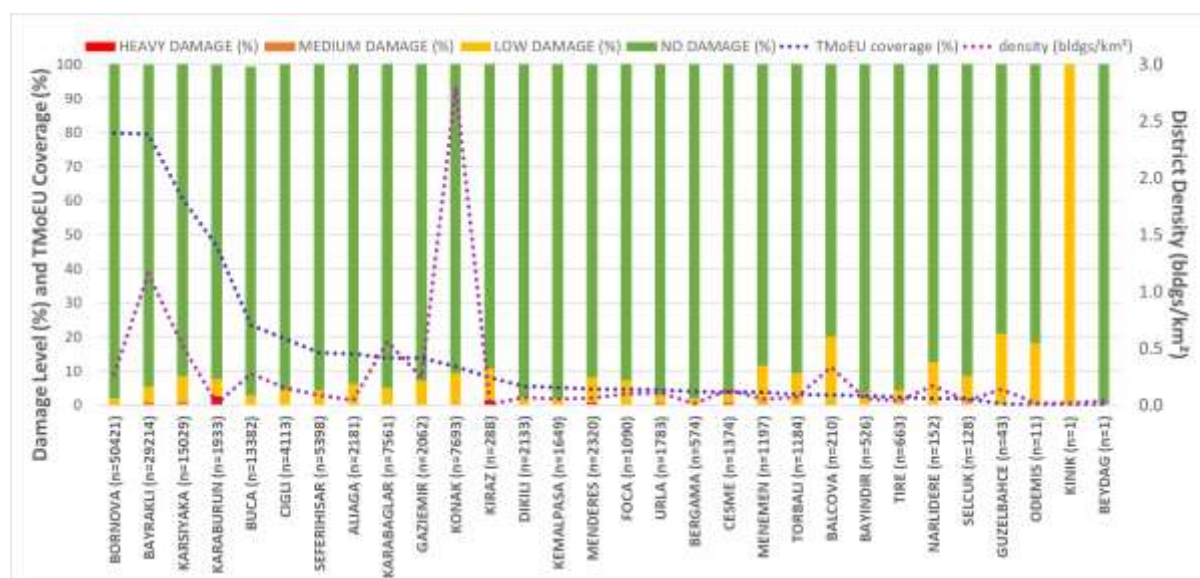


Figure 50: The extent of coverage of individual districts in Izmir by the TMoEU. This plot has been produced using the data on the TMoEU database at <https://hasartespit.csb.gov.tr/#/> as of 15 December 2020. All datapoints labelled as “no access to the property” and “not assessed” have been filtered out while calculating the coverage levels. The district densities were calculated using the district surface area and number of building information available at the Izmir Metropolitan Municipality’s GIS database, <https://kentrehberi.izmir.bel.tr/izmirkentrehberi>. It should be noted that, as the ministry’s damage-assessed building numbers for certain neighbourhoods are higher than the number of buildings in those neighbourhoods as reported by the municipality’s GIS database, we understand the number of buildings reported here might underestimate the actual number of buildings, especially for less central districts, where unregistered buildings activities seem commonplace. The rather high coverage percentage recorded in Karaburun might be attributed to this.

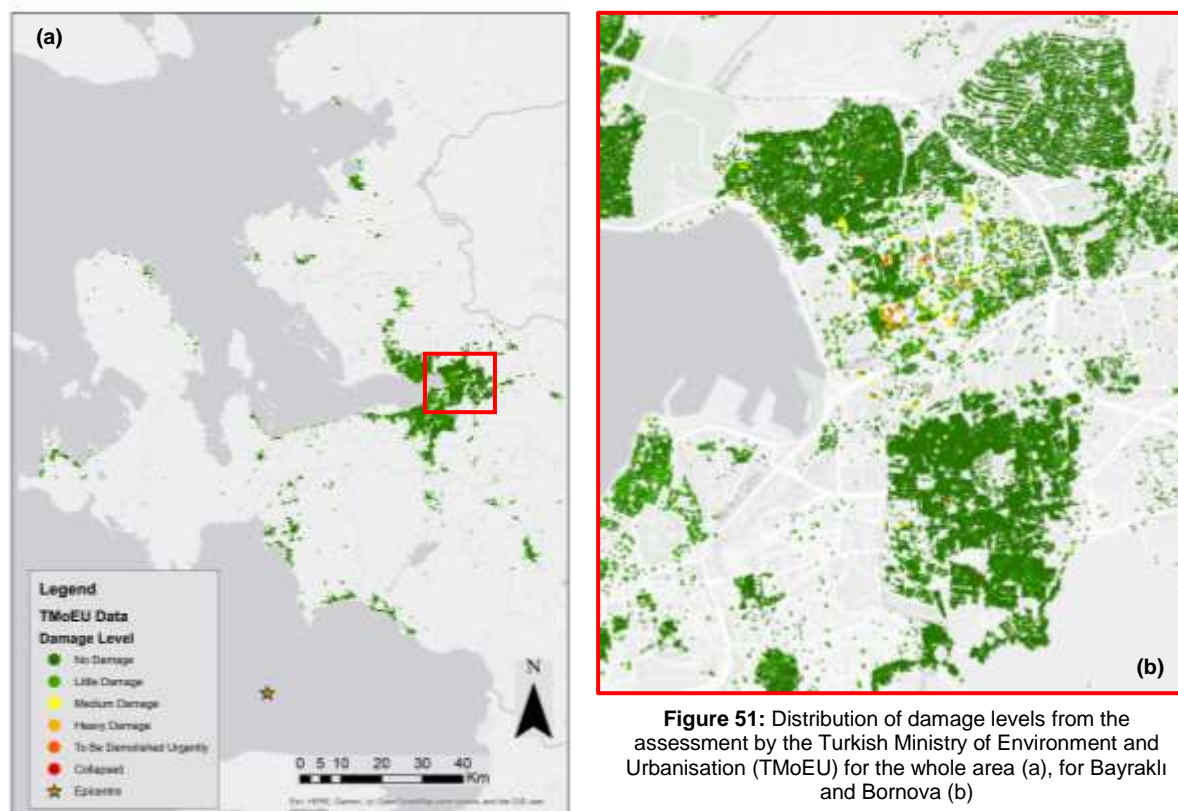


Figure 51: Distribution of damage levels from the assessment by the Turkish Ministry of Environment and Urbanisation (TMoEU) for the whole area (a), for Bayraklı and Bornova (b)

By the time the EEFIT Mission to the Aegean Earthquake and Tsunami planning was underway, the extensive and concentrated damage in Bayraklı and Bornova had been extensively documented and investigated by the TMoEU and other research groups, and detailed information as to the causes and consequences of damage were released. Therefore, to avoid duplication, the fieldwork of the EEFIT mission focussed less covered/studied areas in order to produce a comprehensive view of intensity and distribution of damage over the affected areas.

Based on the considerations discussed above and practicalities around travel ease, the Turkey fieldwork itinerary was finalised as shown in **Figure 52**. Day 1 was dedicated to Kuşadası, which is a town of Aydın province, and had not been covered at all by the TMoEU despite being one of the closest locations to the epicentre. It was also considered beneficial for the field crew to start from a less urban and less dense location, while the team is mastering and gaining experience with the EEFIT Mobile App. Field crew also spent a few hours in Selçuk in the evening. Day 2 was dedicated to Sığacık and Akarca, the two locations most adversely affected by the tsunami, as well as to Seferihisar which offers many examples of vernacular building typologies. Day 3 was dedicated to the southwest districts of the city of İzmir, namely, Guzelbahce, Narlidere, Balcova, Karabağlar and Buca. Day 4 was dedicated entirely to Konak for being the densest district in İzmir, yet very little covered by the TMoEU. Additionally, Konak has many public, and monumental and residential historic buildings. Day 5 was dedicated mainly to Çiğli, which is home to the largest industrial area in the whole region, the İzmir Atatürk Organised Industrial Area. On Day 5, our field crew also spent some time in Karşıyaka and Bayraklı to sample some of the heavy damage cases.

A total of 302 buildings were field-assessed in Turkey for earthquake impact (n=280) and for the combined impact of earthquake and tsunami (n=22) (**Figure 52**).



Figure 52: Turkey fieldwork itinerary (30 Nov-4 Dec). The numbers preceding EQ and EQ&T indicate the number of buildings assessed in a given location for earthquake impact, and for the combined impact of earthquake and tsunami, respectively. As such a total of 309 buildings were field-assessed in Turkey. An additional 23 pictures on tsunami consequences were sent through to the remote team.

Our *Samos* fieldwork itinerary, on the other hand, followed a less pre-determined pattern and was informed by where our field crew members were based in Samos. As such a total of 218 buildings were field-assessed in the most adversely affected northern part of Samos for earthquake impact (n=193) and for the combined impact of earthquake and tsunami (n=25) (**Figure 53**).



Figure 53: Samos fieldwork itinerary (2-3 Dec shown in pink, 7-11 Dec shown in purple). The numbers preceding EQ and EQ&T indicate the number of buildings assessed in a given location for earthquake impact, and for the combined impact of earthquake and tsunami, respectively. As such a total of 215 buildings were field-assessed in Samos. Additionally, a total of 101 buildings were pictured to send to the remote team for assessment.

4.2. Fieldwork: Approach and Limitations

(Authored by YDA)

In both Turkey and Greece fieldwork, the field crews were instructed:

- Not to cherry-pick damage: The mission has been planned on the premise that we can learn as much from the no/little damage cases as we can from the damaged buildings. As the primary objective of the mission was to produce a comprehensive view of the damage within the affected area, the field efforts were focussed such that their led to outcomes complementary to the previous works', rather than a repetition of these.
- To target a good cross-section of structural systems, age and occupancy types: The mission also aimed to address the diversity of the building stocks in both countries by sampling engineered and non-engineered buildings, residential and public buildings, monumental and civil historic structures and vernacular typologies.
- To take safety above all: In all EEFIT missions safety of the field crew is of first and foremost importance however the fact that the Aegean mission fieldwork had to be carried out during an ongoing pandemic and under related restrictions pushed us to take additional precautions. The field crews were instructed not to enter buildings to rule out any contact with the virus, and therefore most field-assessed buildings were assessed only from outside (unless the assessed buildings were collapsed/damaged in a way to expose indoors). This limitation may manifest as a potential underestimation of overall damage levels in our study (See discussions in Section 4.9).

4.3. Damage Assessment Tools: EEFIT Mobile App

(Authored by VP, EV)

In the context of rapidly changing post-disaster scenarios, geolocated data about damage are high-valuable and, at the same time, highly perishable - due to the need of the response teams to progress rapidly towards a "return to normalcy". Once collected, disaster data must be managed and stored efficiently to avoid data loss and to be analysed by different actors at different times. The way the data is managed and distributed to its users affects its suitability for use in the decision-making process that follows a disaster, and also the possibility to compare multiple events and they have unfolded over time.

A Spatial Data Infrastructure (SDI) is the best suited technology to achieve these objectives. An SDI is an infrastructure aimed at supporting the data management (including storage), discovery, access, and easy retrieval and reuse of the geographic data collected, and can be designed to support very varied users' needs. Unlike storage devices, the use of metadata (i.e, data about the data) assists in the classification of the data and, in turn, promotes the integration of data coming from disparate sources and thus limiting - if not eliminating - the need for parallel and costly data collection campaigns. Altogether, these characteristics make an SDI an ideal tool for use in the Disaster Risk Reduction and Response field.

As part of the Learning from Earthquake UK project, an SDI and a data collection app are being developed to support the data needs of the Earthquake Engineering Field Investigation Team (EEFIT). The Earthquake Engineering Field Investigation Team (EEFIT) is a joint venture between industry and universities, conducting field investigations following major earthquakes. Data are usually collected by team members deployed to the affected areas, which are trained to collect data following protocols that have built and improved on during the decades in which EEFIT has remained active. In the past decade, EEFIT has responded to the technological advancement in data collection by introducing new ways to collect geolocated digital data. From the lessons learned from past missions, new data needs have emerged and these are now being addressed with the development of the standardised forms for digital data collection in the EEFIT app and of the SDI.

The EEFIT App aims to

- Collect series of non-repeated data following a tier-based approach. On the basis of the time the user can spend on-site the app allows gathering homogenized data sets aiming to assess as many buildings as possible, to allow for quantitative analysis and to understand the performance of buildings
- Communicate with the SDI, allowing to safely storing the geolocated data coming from the assessments
- Minimize the number of extra tools the user needs while on the field: the functionalities of the app are deemed to be sufficient to conduct a comprehensive assessment.

- Work seamlessly both online and offline allowing the user to access their collected data from the dashboard

The EEFIT Mobile App deployed during the Aegean Mission incorporated damage data collection for tsunami assessment within the existing earthquake damage assessment flowchart.

The structure of the submissions output coming from the EEFIT Mobile App served as a baseline to conduct remote assessment of the data collected from the field or sourced from elsewhere (see Section 4.4 on remote data sources), thus allowing to assess data sourced elsewhere and from other photographic repositories and reconcile the obtained results.

The EEFIT Spatial Data Infrastructure is designed with a user's needs-centred approach to accommodate data collected in reconnaissance and recovery missions as well as training. Since missions can occur without internet connectivity, the SDI is designed to work on two complementary systems. The offline local SDI is hosted on a laptop computer which is carried during mission times. It is used to upload all the data that are collected during the mission, so that “no data is left behind” and that perishable information about the data are collated into a centralised place at the time of collection. Once uploaded the data are analysed by ad-hoc scripts so that key metadata can be extracted automatically. For the uploaded photos, the typical metadata include the time of capture, the resolution, information about the collecting device, and geolocation. The metadata and the data volunteered by the data collector at the moment of upload are used to build a database of information linked to the collected data and to map the data that have a geolocation. The local SDI is supported and augmented by a cloud-based SDI, which enriches the information available in the local SDI by adding a further layer of data richness. This is achieved by integrating the data collected with the EEFIT app and other apps that EEFIT may use to collect data. The EEFIT app *de facto* replaces the need for paper forms, which were used in the past. The integration of the SDI and the EEFIT app allows the user to collect disaster data at ease and to be guided in this process by the workflows that have been designed in the EEFIT app forms, so that the data collected are standardised and can be easily compared. Once uploaded, the “data to maps” process is performed automatically by the SDI.

The SDI has 3 components: An Uploader - which consists of a set of easy forms that can be accessed both offline and online to upload data to either the local SDI or the Cloud-based SDI, a Metadata Extractor which analysed the data and populates a database, and a Mapper that uses the data in the database to produce daily maps of what has been observed in the field. When there is no internet connectivity, the users will be able to see the locations that have been visited during daily deployments in the form of a trail of dots. Each of the dots represents the place where the geolocated data have been collected (e.g. geolocated picture of damaged building). If internet connectivity is present, the user will be able to download the data collected with the EEFIT app by accessing the app dashboard online. Once these data are also uploaded, new data attributes will be linked to the collected data.

4.4. Remote Data Sources

(Authored by YDA)

All data sources explored for remote assessment are listed in **Table 3** along with a brief description of the data type/content, its use and some brief notes on their strength and limitations.

Table 3: Remote data sources explored in this mission

	Data type/content	Its use in this mission	Notes
Pictures by our field crews of buildings that were not field-assessed	Georeferenced images of buildings and infrastructure, as well as other observations significant from a seismotectonic and geotechnical point of view.	Remotely assessed (n=74 so far)	These extra pictures were very helpful to maximise the benefit of having a crew on the ground. Some villages were not field-assessed, but only photographed (e.g. Lekka). The field pictures also did not focus on damage.

Turkish Ministry of Environment and Urbanisation (TMoEU) database	Images of individual buildings, along with their addresses and damage categories assigned during the TMoEU's field assessment.	A small subset remotely assessed (n=24 so far)	This informed the team on the coverage levels and damage distributions within Izmir, and hence the Turkey fieldwork itinerary. Remotely assessing a small subset of this database allowed us to pass judgement on how aligned our and the ministry's damage assessment outcomes were.
Twitter	Images and tweets related to the event resulting damage, relief, response, and early recovery activities.	Not used.	Very hard to obtain visual and descriptive information which is used for individual building damage assessment and otherwise. This limitation is due firstly to the sheer size of Twitter data and lack of georeferencing and enough visual context in some occasions.
Euro-Mediterranean Seismological Centre (ESMC)	Reports of intensity in the modified Mercalli (MMI) scale by citizens. Images and commentaries describing damage levels.	A small subset remotely assessed (n=2)	Like in Twitter, this also yields little material that can be used for individual building assessment. They are often isolated damage pictures without context or repeated appearance of the few heavy damage cases. From 61 georeferenced pictures of damage, only 2 were used.
Youtube	Videos	Remotely assessed (n=154 from a single channel)	We benefitted from a particular channel ("Mikres diadromes") featuring several villages in Samos following the event, which was used to damage assess individual buildings seen in the video. Some of the videos offered also Unmanned Aerial Vehicle (UAV) shots, which were particularly helpful in identifying the damage to the roofs, which is normally not easy to assess both in the field and remotely.
Facebook	Pictures and commentary from various groups	Remotely assessed (n=9)	It is challenging to find suitable groups and even when these are identified leads to little usable material for individual building damage assessment.
Izmir Provincial Coordination Board	Georeferenced pictures and commentary on building damage	Not used for formal damage assessment, but used to further our understanding of the heavy damage/collapse cases.	Often isolated damage pictures without context, or focusses on the same dramatic damage cases
News websites	Pictures of damage to buildings or geotechnical structures. Nongeoreferenced. Seldom accompanied by address.	Not used for formal damage assessment, but were extensively referred to to develop a general picture of the damage distribution and extent, especially in case of heritage structures in Samos.	Strong focus on a few dramatic damage cases.
Individuals donating their archives	Georeferenced pictures of the damage to buildings	Not used yet for formal damage assessment.	By the time this report is being written, these pictures are still being filtered to identify material to include in the database.

EEFIT

	or geotechnical structures		
Other reconnaissance reports	Pictures of damage to buildings or geotechnical structures	Not used for formal damage assessment.	Not yielded much material due to repetition of a few damage cases, lack of context for a whole building assessment and lack of georeference/address.

The damage assessment made based on the remote data sources listed in **Table 3** is mapped in **Figure 54**. We also benefitted from Google Street View images to check the pre-earthquake damage level as well as to double check the reported georeference information for certain cases. Izmir Metropolitan Municipality has also kindly donated their archive of pre-earthquake pictures of urban strips or individual buildings. These were not georeferenced, however were groups based on district and sometimes neighbourhood, were occasionally used to differentiate pre- and post- damage on a building when this is not easy to judge from the post-earthquake pictures. Other explored options for remote data acquisition included the CCTV imagery, however it was not available for the affected areas in this particular event.



Figure 54: Assessments done remotely using various data sources as of Dec 2020.

Except for the pictures sent to the remote team by our field crew, the main limitation of using remote data sources was the strong focus on damage. None of the mentioned data sources documented no or little damage cases, and especially in case of Turkey it was almost entirely focussed on Bayraklı and Bornova. The georeferencing was done through the image metadata, which in often cases needed to be checked and verified, as these were frequently incorrect or insufficient to locate a building. Difficulties associated with relying on the image metadata were discussed by So et al. (2020). In case of this particular mission, we managed to find a few more alternative sources for more diverse and comprehensive data for remote damage assessment for Samos than for Turkey. While this might to some extent indicate that the Samos citizens are more widely and efficiently engaged with social media, it can also be explained by the fact that the damage in Samos is more dispersed throughout the island as opposed to the dramatic collapse and damage cases in Turkey which monopolised the attention by the media and citizens alike, hence narrowing the diversity and increasing damage-bias.

4.5. Damage Data Processing

(Authored by II)

This mission brought together a team of engineers who collected and processed data regarding the building characteristics and the assessment of their sustained damage. The key challenges in processing the damage data were the following:

- a. To clarify which key information should be recorded.
- b. How to ensure negligible misclassification errors in recording the building characteristics and assessing the level of damage sustained by each building.

4.5.1. Key Information

The data were collected through the app in the field and the same fields were used to record information in the remote assessment, as well. The team decided to focus on collecting information on the building characteristics and damage descriptors depicted in **Table 4**. A problem that the team faced was that the app has 447 fields which can be completed either by selecting from a dropdown menu, adding pictures or by writing a free text. In the field, the user is not required to complete all of them for each structure. Instead, a subset of these fields needs to be completed depending on how long the user spends assessing the structure both externally and internally. From the 520 buildings surveyed in the field, 74% of which were surveyed as the team was either driving or dedicated between 3-5 minutes assessing the structure. A further 14% of data are based on a 5 to 7 minute assessment of the building. The data were overwhelmingly based on the external assessment of the buildings. This meant that not all required information was recorded. For example, if the team assesses a building while driving, the entry includes the location of the building, a picture of the building and damage level in the EMD98 scale. To complete key missing data which were not recorded in the field, the field data were also assessed remotely by team members which aimed to complete as many fields of **Table 4** as possible based on the photographic evidence provided.

Table 4: Key building characteristics and damage descriptors aimed to be recorded from each building.

Building Characteristic	Damage Description
Primary Structural System	Level of EMS98 scale
Floor material	
Roof material	
Number of stories above the ground	
Presence of basements	Earthquake induced hazard
Occupancy	Peril
Location	

4.5.2. Misclassification Error

To ensure the high quality of the data, care was taken to reduce as much as possible the error in recording wrong information regarding the building characteristics or its sustained damage. To ensure

small misclassification errors, guidance and training was provided in all team members with plenty of examples. The remote assessments of the field data were also used as an opportunity to reconsider the provided information for each building and not to simply rely on the judgement of the field team, who completed key fields often in a rush. The comparison of the overall distribution of damage based on remote and field assessment of the field surveyed data depicted in **Figure 55** shows that the two types of assessment yielded similar results for moderate or extreme damage (i.e., \geq DG2). However, notable differences can be seen for no or slight damage states (i.e., DG0 or DG1). In particular, the remote assessment classified by substantially more buildings as having suffered no damage than the field assessment. This can be attributed to the difficulty in depicting hairline cracks through pictures. For this reason, the distribution of damage presented in the following two sections is based on the damage assessment conducted in the field which is considered more reliable.

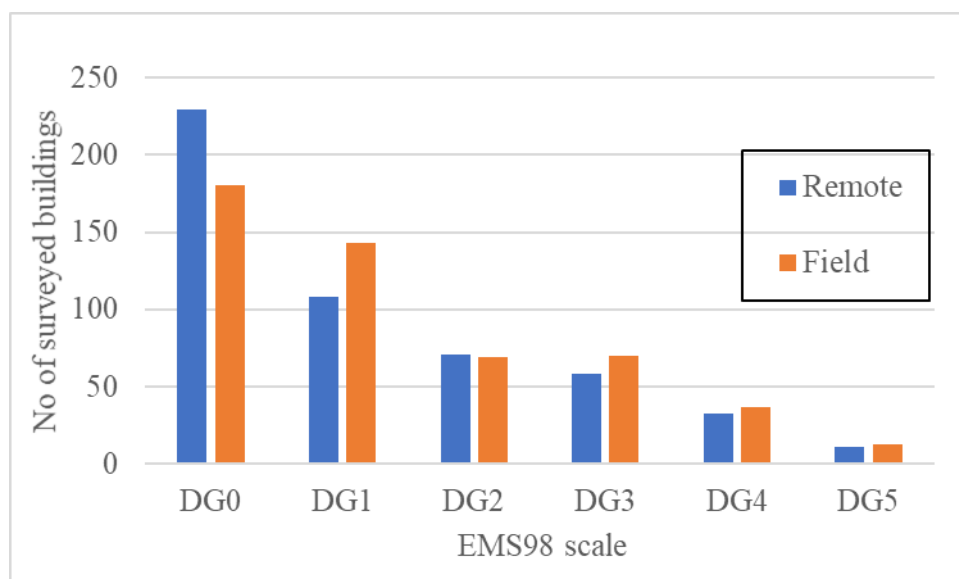


Figure 55: Overall distribution of damage based on the field and remote assessment of the field surveyed buildings.

4.6. Damage Observations: Samos

(Authored by DK-F, MA & II)

4.6.1. Building Stock and Code Evolution

The total number of buildings in Samos as of 2011 is 27.388, which corresponds to 1:1.2 ratio of population to buildings (EL.STAT, 2011); a clear indication of second homes and touristic buildings only occupied during the summer season. The most common typology in 1940's was load-bearing stone masonry, whereas Reinforced Concrete (RC) frames with masonry infill walls became more popular after 1960's. According to the 2011 building census (**Figure 56a**), RC structures represent the largest portion (44%) of the building stock; whereas 30% of the buildings are made of stone masonry. In particular, these structures are classified as vernacular typology, with either traditional masonry or *hımıř*, which will be discussed in Section 4.8.

Figure 56b shows the breakdown of the current RC structure stock based on the corresponding building code. According to EL.STAT. (2011) most of the buildings were designed between 1960-1985 following the Royal Decree on the Seismic Code for Building Structures (Gazette 1959), i.e. the first Greek seismic code. An update of the design code occurred in 1984 (MOD84, 1984) and significant seismic design provisions were included, such as 3D modelling of multi-story buildings, ductility requirements as well as displacement limitation requirements. In 1995 the New Greek Earthquake Resistant Design Code (NEAK 1995) introduced the probabilistic seismic acceleration design spectrum along with a new seismic hazard map with four zones. In particular, the dynamic spectral method became the most common analysis method and provisions by Eurocode 8 (CEN 1994) were also included, such as the behaviour factor depending on the ductility as well as the capacity design approach. The Greek seismic building code "EAK-2000" was reviewed in 2003 to include a new seismic hazard map. The country is currently divided into three seismic zones with soil classes, with a peak ground acceleration (PGA)

ranging from 0.16g to 0.36g (TR=475years). The most recent National Codes (EAK 2000, EKOS 2000) are used in parallel with the Eurocode 8 since 2011.

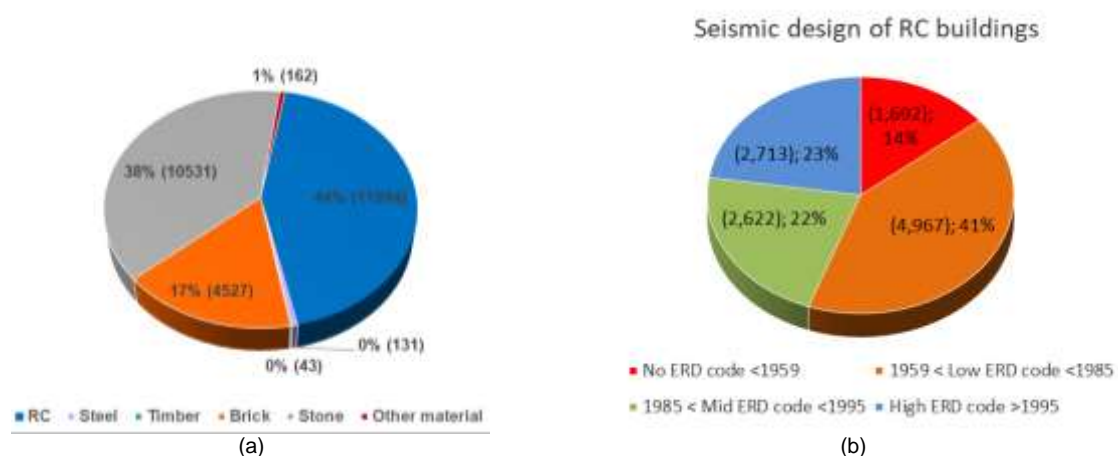


Figure 56: (a) Building stock distribution in Samos per construction material and (b) distribution of RC buildings in Samos per design code (EL.STAT. 2011)

4.6.2. Damage Statistics

In Samos, the damage sustained by 218 buildings was assessed by the team on the field using the app and 244 buildings were assessed remotely based on photographic evidence sent by field team members or found in alternative online sources such as the Facebook page of the two municipalities, EMSC and YouTube videos (i.e., mainly from the “Mikres Diadromes youtube channel”). Based on external reports (e.g. Lekkas et al., 2020; Vadaloukas et al., 2020), social media and news outlets as well as interviews with local authorities (Civil protection and Fire Brigade, see Section 6.1), the field work focused mainly on the worst affected north side of the island and surveyed buildings in Samos City, Vathy, Karlovassi and Kokkari. The field team surveyed both damaged and undamaged buildings in the selected area, avoiding biasing the sample by focusing only on the damaged buildings. By contrast, the remote assessment focused mainly on damaged buildings in a number of villages scattered across the island such as: Agii Theodoroi, Agios Konstantinos, Ampelos, Chora, Koumaradei, Koumeika, Konteika, Marathokampos, Mavratzei, Mesogios, Mili, Pagondas, Pandrosos, Pyrgos, Vourliotes. **Figure 57** shows the outcomes of the field assessments. The markers colour represents the damage state of the assessed buildings according to the EMS98 (Grünthal, 1998) as clarified in the pie chart of **Figure 58** which is based on the field data irrespective of the building occupancy and whether the building is abandoned or in use. Some first overall conclusions can be drawn from this pie chart: (1) approximately 40% of the surveyed buildings suffered slight or no damage; (2) approximately 20% of the buildings suffered extreme damage DG4 or DG5. In **Figure 58**(bottom) the distribution of damage for the primary structural systems recorded in the field is plotted. It can be noted that most surveyed buildings are vernacular (i.e. either masonry or hybrid masonry timber buildings) and that explains the high percentage of the damaged buildings.

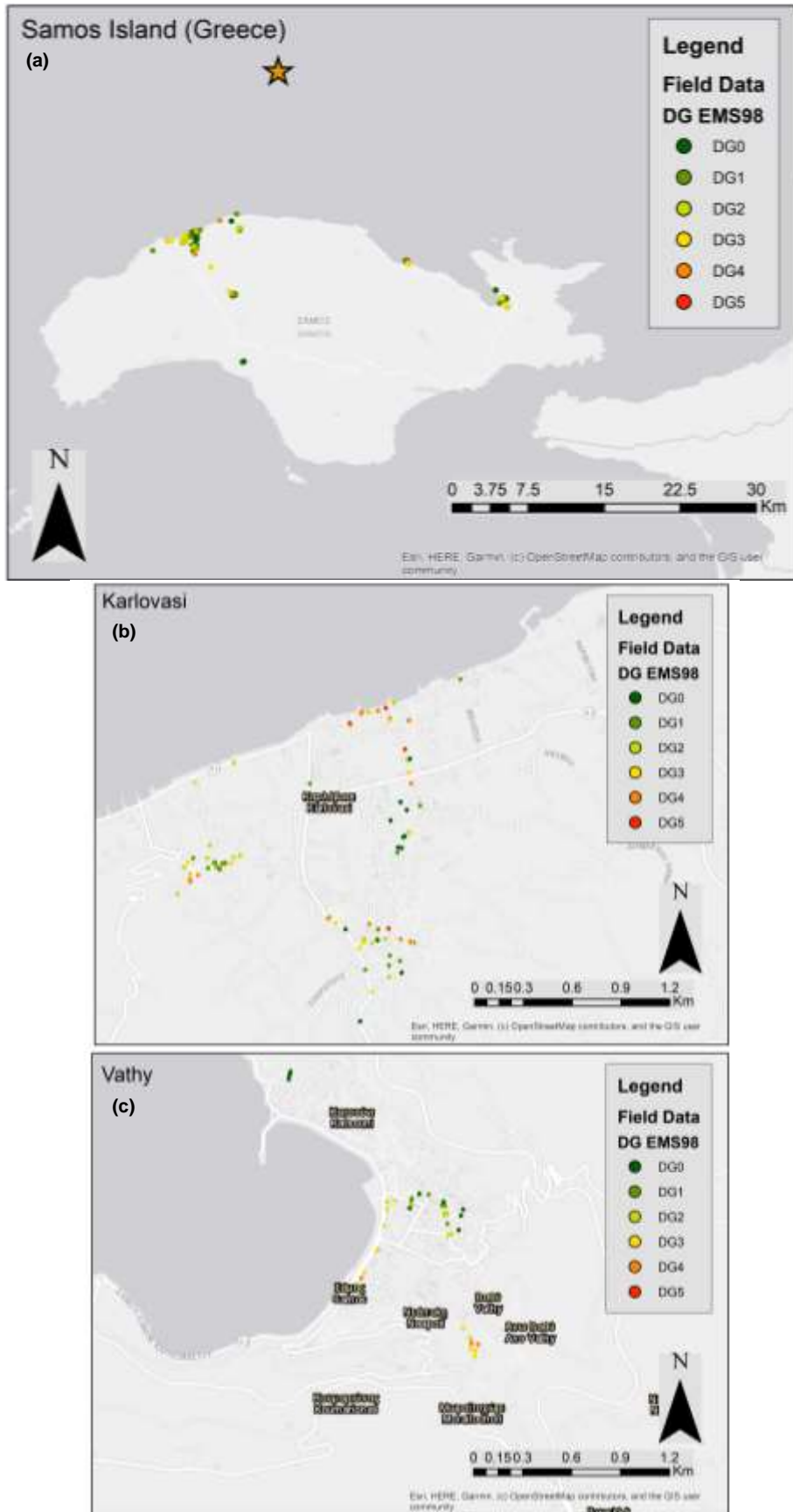


Figure 57: Distribution of field damage assessment throughout Samos (a) Karlovasi (b) and Vathy (c)

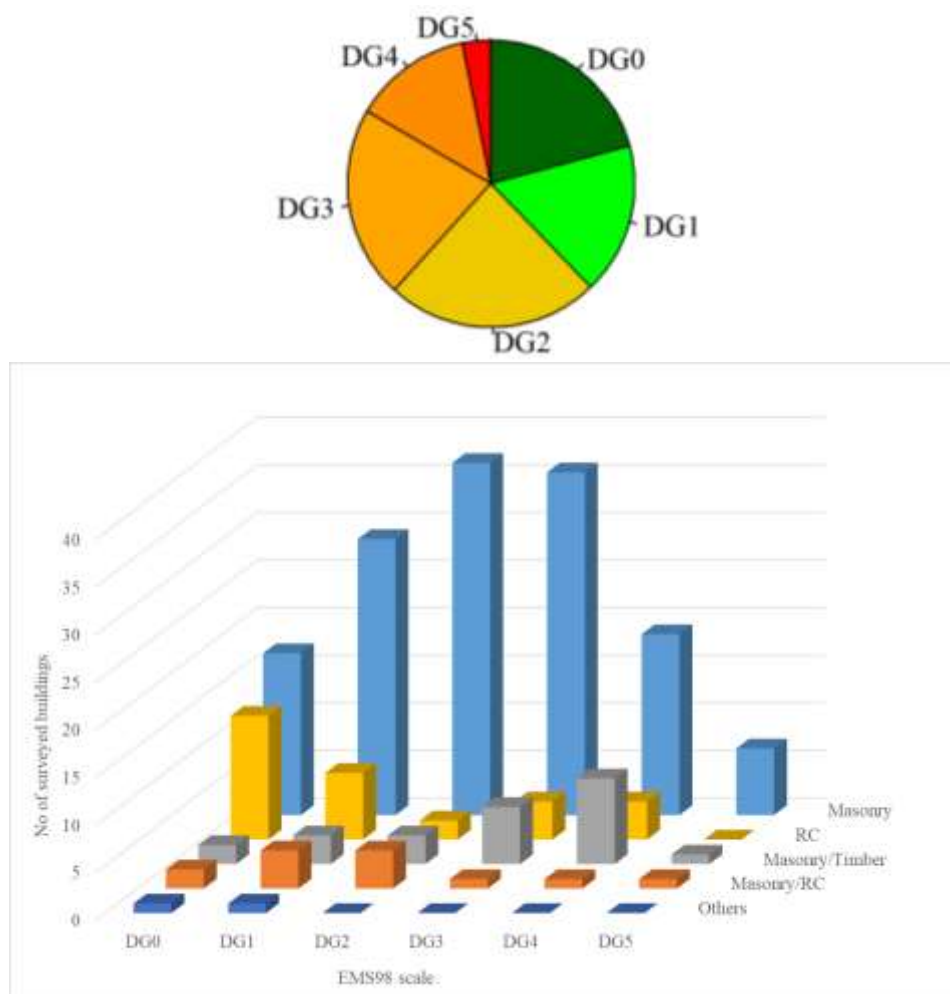


Figure 58: Overall damage grades distribution according to field assessments (top), distribution of damage for the primary structural system recorded (bottom).

4.6.3. Damage Patterns to Reinforced Concrete Buildings

Most RC examined here are either residential (single or multiple family dwellings) or dual occupancy with commercial use of the ground floor and dwellings (and less frequently offices) on the floors above. These represent the 14% of the field-assessed data and they have been mainly found in the urban settlements of Samos City, Vathy and Karlovassi. **Figure 59** presents the distribution of the damage grades for the assessed structures based on the field damage assessments. It can be noted that 33% of the surveyed RC buildings suffered moderate or more severe damage. The more severe damage grades were recorded in buildings designed with obsolete seismic codes.

The most common damage mechanism observed was the failure of infill walls, both in plane (**Figure 60a**) and out-of-plane (**Figure 60b**). In particular, significant separations from the frame as well as corner failures and diagonal shear cracks were observed. In some cases, localised or extended infill collapses were also recorded.

Approximately half of the surveyed buildings had some type of irregularity. Typical irregularities were found to buildings with dual occupancy: commercial activities and/or garage at the ground level with higher ceilings and/or large openings, and residential flats at the upper storeys with stiff infill masonry walls. Typical damage due to soft first storey (pilotis effect) was observed involving the structural elements as well as the beam-to-column joints (**Figure 61**) at the first storeys. Another source of irregularities was also observed at upper storeys where shear-failure of short columns was recorded (**Figure 62**).

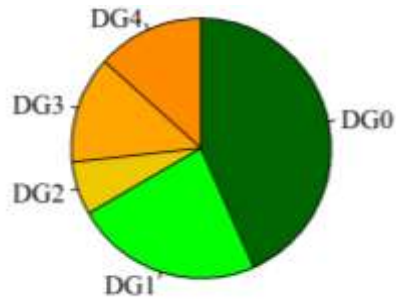


Figure 59: Distribution of the damage grade in RC buildings according to field assessment



Figure 60: Damage to infill walls in two RC buildings in Samos: (a) in plane and (b) out of plane failure



Figure 61: Five-storey building with soft first storey (pilotis) failure at the ground level in Karlovasi (Samos)



Figure 62: Four-storey building with short column failure in Samos

4.6.4. Damage Patterns to Load Bearing Masonry Buildings

The load bearing masonry buildings, typically but not exclusively built using local stone, was one of the structural typologies most affected by this event. The field damage assessment showed that only 32% of the surveyed buildings suffered slight or no damage. Common failure modes include, corner failures were registered at the intersection of the two orthogonal walls (**Figure 63**). Depending on the extent of the dislocation, this damage mechanism led to diverse damage grades and usability levels. This failure mode is often combined with vertical cracks along the two orthogonal walls which tend to get separated with cracks of different width (**Figure 63**). Horizontal cracks at the floor level were observed in a few cases, due to sliding between the timber floor and the bearing masonry wall underneath (**Figure 64**). Different extents of roof damage were also observed in many masonry structures (**Figure 65**).

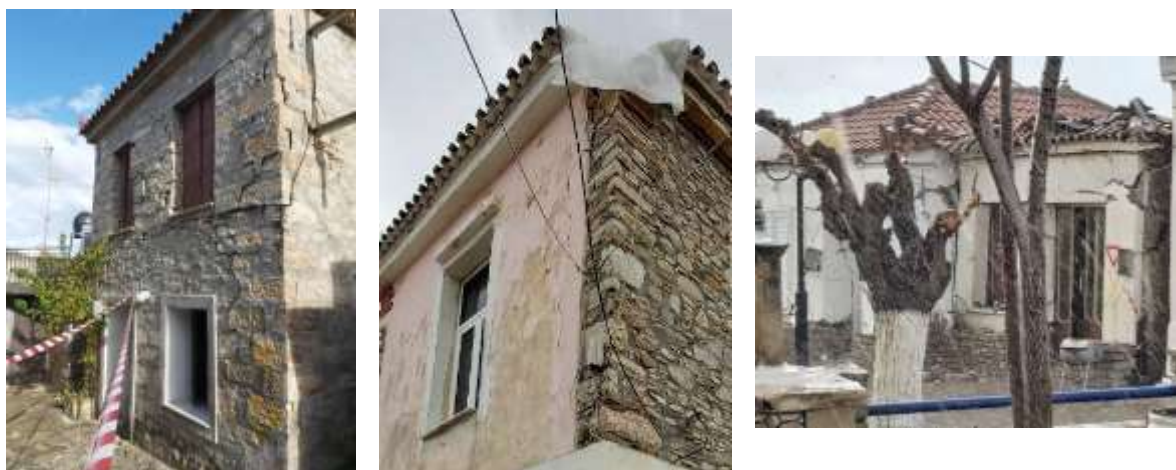


Figure 63: Corner failure in masonry buildings in Samos.



Figure 64: Damage in masonry buildings in Samos with horizontal cracks at floor level due to sliding (Photo credits to "Mikres diadromes" youtube channel)



Figure 65: Roof damage to masonry buildings in Samos.

Moreover, diagonal cracks along the walls (**Figure 66**), spandrels and piers (**Figure 67**) were another common damage pattern in masonry structures due to shear failure of the horizontal and vertical segments of the envelope. The crack width/extension varied, leading to diverse complex failure mechanisms, including out-of plane failure and partial collapse. In case of multi-leaf envelopes, the separation of the two wall wythes due to bad quality mortar was observed to lead to dislocation of the external wythe, and even to out-of-plane collapse (**Figure 67b**). Both partial and total collapse was mostly encountered in case of abandoned buildings with significant material deterioration and resulting overall structural delapidation prior to the earthquake (**Figure 68**).



Figure 66: Diagonal shear cracks to the walls with different widths.



Figure 67: (a) In plane cracks to spandrels and piers, (b) out of plane wall failure



Figure 68: Partially and totally collapsed buildings in rural localities and Samos town.

4.6.5. Damage Patterns to Cultural Heritage

Samos cultural heritage was severely hit by the earthquake on 30th October 2020. Both churches and monumental public buildings collapsed and/or heavily damaged so as to require demolition. Around 70 churches, chapels and monasteries were affected by the event (Naftemporiki 2020); moreover, according to the metropolitan Bishop of Samos and Icaria, around 80% of the clerical building stock in Samos were significantly damaged.

Heavy damage was observed to dome, roof and facades of several large churches (**Figure 69**). Few cases were damaged beyond repair (almost collapsed). The most notable heavy damage was observed to the roof and one façade of The Church of the Assumption of the Virgin Mary in Karlovasi (**Figure 70**). Small churches had a better performance (**Figure 71**) under the seismic actions.



Figure 69: (a) Panaghia Vrontiani, Konteika and (b) Agios Nikolaos, Kokkari (Photo credit: D.Malliaros, E.Giovani, A. Tatouris)



Figure 70: Koimisi Theotokou, Karlovasi (Samosvoice 2020)



Figure 71: (a) Agia Sofia, Chora; (b) Agios Georgios, Pyrgos; (c) Agios Konstantinos, Agios Konstantinos

Other historical structures suffered damage, including the Pythagoreio Castle ruins, town halls and the Old Tanneries in Karlovasi (Figure 72-73). The earthquake had also effects on museum contents. For example, at the Archaeological Museum at Pythagoreio, significant damage was observed to the pottery exhibition (Figure 74a) and at the Archaeological Museum of Vathy, a crack appeared at the gigantic foot of the man sculpture (“Kouros”) (Figure 74b). Moreover, several exhibits of choroplasty and ceramics broke when falling from the showcases in the Archaeological Museum of Chios.

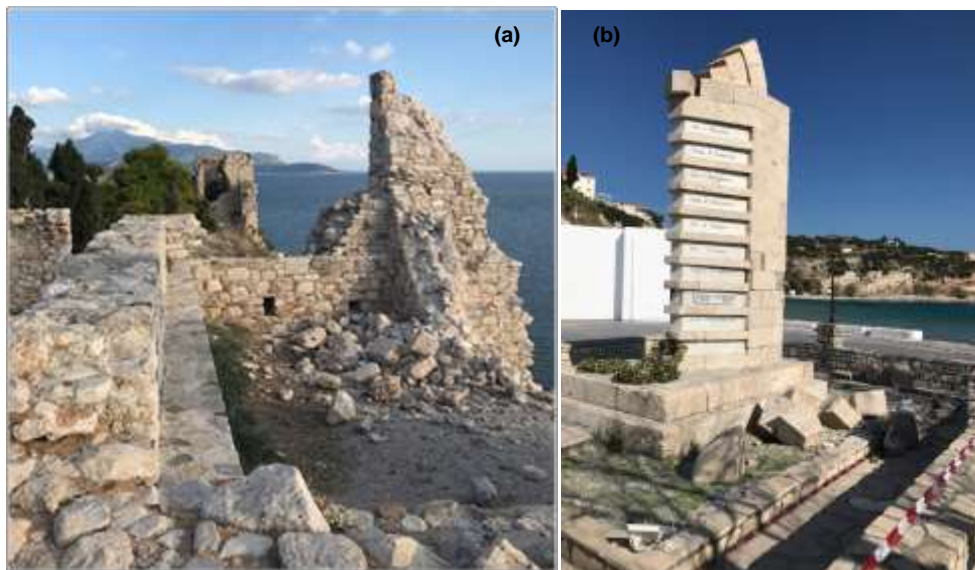


Figure 72: (a) Pythagoreio Castle and (b) Memorial at Pythagoreio (Photo credit: D.Malliaros, E.Giovani, A. Tatouris)



Figure 73: Severely damaged historical building of the town hall of Vathy (photo credit: Facebook page - Kathimerini)



Figure 74: (a) Damage to pottery exhibition at Archaeological Museum of Pythagoreio and (b) crack at the male sculpture at the Archaeological Museum of Vathy (Skai 2020)

4.7. Damage Observations: Izmir

(Authored by MA, ME, II & YDA)

4.7.1. Building Stock and Code Evolution

Izmir is the third city in Turkey for population with more than four million. The high density of the city is demonstrated by the census data given in **Figure 75** that shows the number of new buildings in Izmir per year of construction/permit as well as per use/function. According to the census results (TUIK, 2020), the majority of the buildings in Izmir are residential houses and/or complexes. A significant increase (around 40%) was observed in 2013-2014 for both commercial and industrial activities in the city. The most common structural typology is low- to mid-rise RC structures with infill walls (**Figure 76**), designed according to 1975 Turkish seismic design code (MRR 1975). Another typical structural system is confined masonry, comprised of load bearing masonry tie with reinforced concrete beams and columns, and unreinforced masonry structures (**Figure 77**) with various materials (brick, concrete block and stone).

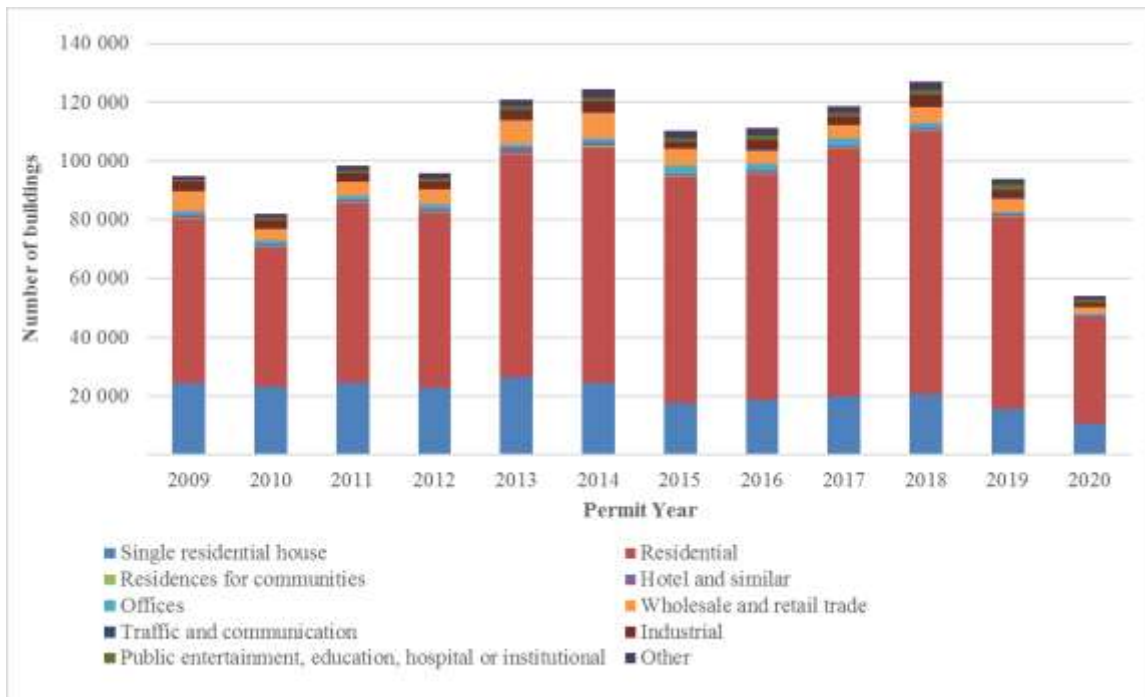


Figure 75: Number of buildings according to construction permits in Izmir (TUIK, 2020)



Figure 76: Street view from Izmir – reinforced concrete first and second extension under construction



Figure 77: Street view from Izmir Two storey load bearing masonry buildings

Since 1940, the seismic code in Turkey included procedures for calculating earthquake loads on buildings (Sezen et al., 2001). This first code was developed following the devastating 1939 Erzincan Earthquake, and was annexed in 1942 by a zonation map (Sezen et al., 2001, Ilki and Celep, 2012). since then, there have been six different versions of the Turkish Earthquake Code with the following main updates.

- In 1968 a new version of the code was released with spectral shape and dynamic response concepts introduced for the first time (Sezen et al., 2001).
- The 1975 version used the further improved 1972 zonation map with 4 seismic zones and some special reinforcing details for ductile design were introduced for the first time. However, these rules had little implementation in practice as demonstrated by most of the existing buildings built between 1975 and 1998 (Elyamaç and Erdoğan, 2005). This version is also significant for including the first, albeit undetailed, definition of irregularity and its effect on seismic performance.
- In 1998 a significant update of the code occurred. A detailed capacity design procedure was extensively included, with more emphasis on reinforcing details, ductile design and definition of seismic forces. Design earthquake was defined on a probabilistic basis (Ilki and Celep, 2012). Elastic design spectrum and nonlinear dynamic analysis were also covered in this version for the first time (Sezen et al., 2001).
- In 2008 important updates to the previous code were made with regards to the seismic safety assessment of existing structures with a performance-based design approach and seismic retrofitting, as well as the design of steel structures (Ilki and Celep, 2012). In 2019 a new was introduced a new interactive seismic hazard map (site-specific) as well as soil categorises (Guler and Celep, 2020). Concerning the structural design, the code provides new requirements about the design of tall buildings, seismic isolation and piled foundations. Structural analysis should be performed with non-linear analysis methods in some special cases. Quality control was enhanced by introducing a design supervision arrangement for specific applications.

4.7.2. Damage Statistics

As described in the above sections, the most common structural typology in Izmir is RC multi-storey frames with both commercial and residential use. The seismic event was recorded at 60km from the city and the recorded accelerations were in the range of the design values with the latest amendments in the design codes.

Figure 78a shows the map of Izmir with the field data and **Figure 78b** shows the assessed structures by the TMoEU (2020) with a severe damage level (DG4 or DG5). The comparison between the two data distribution justify the fieldwork itinerary as explained in Section 4.1. The overall response of the surveyed RC buildings in Izmir is shown in **Figure 79a** with 82% of the surveyed buildings to have sustained slight or no damage. However, most of the losses (deaths, injured people and need of demolishing) were recorded in RC multi-storey frames and all those buildings were located in three

neighbourhoods (Figure 79b) in Bayraklı (Adalet, Mansuroğlu and Manavkuyu). Figure 79c shows that the overwhelming majority (~73%) of the surveyed buildings in Turkey are RC.

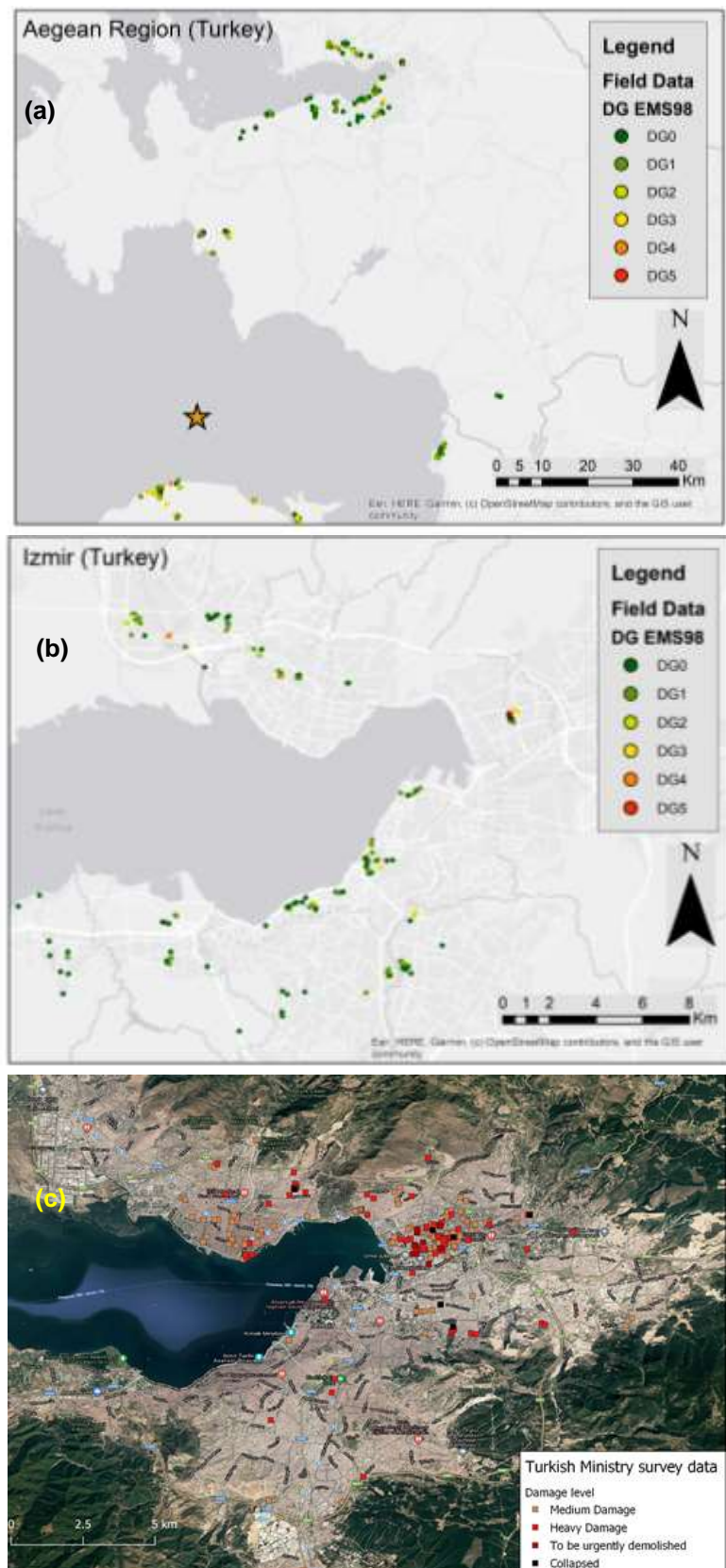
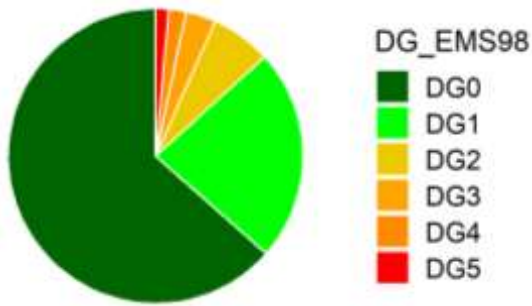


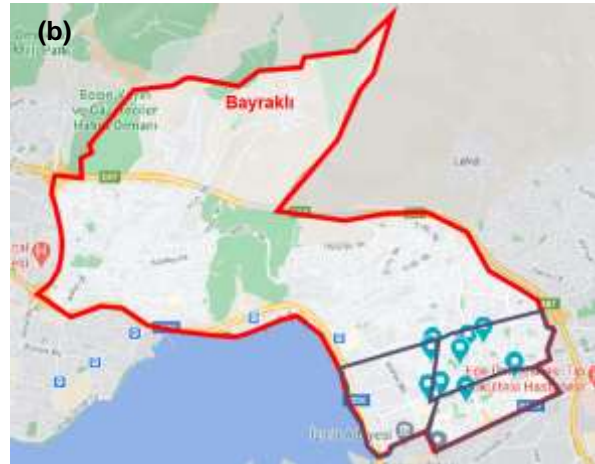
Figure 78: Map of the field assessment with damage grades (a) for the whole assessed area in Turkey and (b) for Izmir. and (c) map of the severely damaged structures by the TMOEU (2020)

EEFIT

(a)



(b)



(c)

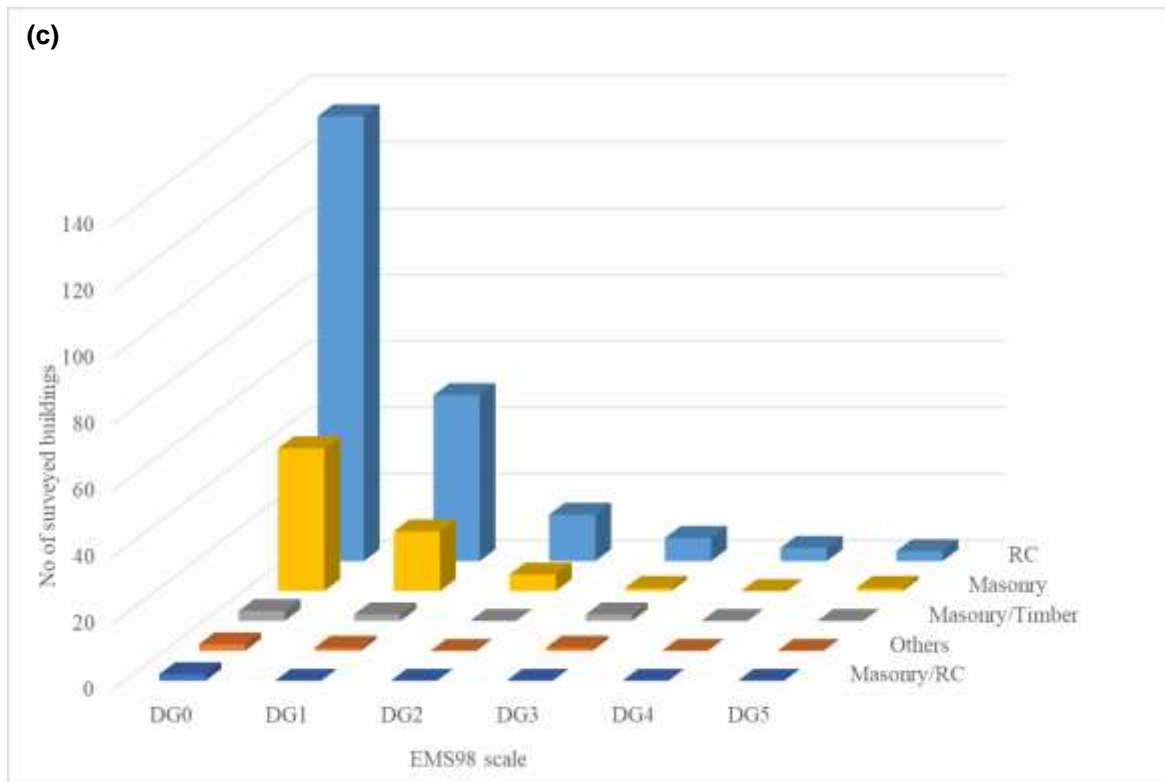


Figure 79: (a) Distribution of damage grade in Izmir, (b) location of collapsed buildings with casualties and/or significant losses, and (c) distribution of damage for the surveyed primary structural systems.

It is important to note that while the Turkish Seismic Design Code has been upgraded in certain time intervals, it is not possible to claim that buildings have been constructed following the codes valid in the time of their construction due to lack of sufficient enforcement of the code. Unfortunately, only a small portion of the existing buildings has been constructed in accordance with the Seismic Design Code until the 1999 Kocaeli earthquake, which has been a milestone in terms of public awareness. The state of degradation and or vulnerability of RC buildings was attributed to “inadequate material strength, extensive degradation in structural and non-structural components, inadequate ductility due to poor detailing in structural elements and insufficient stiffness of lower stories”, among others (Ilki and Celep, 2012). Many existing low-rise reinforced concrete frame buildings in Turkey can also be considered as confined masonry due to their weak reinforced concrete structural systems. In such cases, infill walls resist the seismic loads along with the weak reinforced concrete frames. Basic weaknesses of such buildings were identified as “low ductility of infill walls, lack of integrity of masonry units in walls” and large openings (Ilki and Celep, 2012). These basic weaknesses stemming from many different design and construction errors are main reasons of the catastrophic consequences experienced after earthquakes. These errors, which cause premature failures of structural members or structures, are

basically due to improper application practices on-site. The most common application errors in reinforced concrete structures include low-strength concrete, insufficient transverse bars, inadequate lap-splices of column reinforcement, insufficient bond between plain round bars and concrete, and deterioration of structural system by time due to low-quality materials and lack of maintenance. Most common problem related to design, especially due to architectural constraints, is irregularity of the structural system. Among other common reasons of damage are inadequate consideration of ground conditions in the layout and design of the structural system, addition of illegal stories to the existing structural systems without taking necessary measures, and unconsciously removing or damaging certain structural members (such as columns and beams in reinforced concrete structures or walls in masonry structures), which are not conveniently located or dimensioned for the occupants. It is worth noting that most of the low-rise buildings in cities are legally engineered structures. Normally, they are expected to be designed and constructed with proper engineering service. However, due to lack of a sufficient inspection mechanism, particularly a large number of buildings constructed before 1999 Kocaeli Earthquake, do not satisfy requirements of the related national codes and standards. Consequently, they cannot be classified as properly engineered buildings.

4.7.3. Damage Patterns to Reinforced Concrete Buildings (authored by ME)

Figure 80 shows some examples of good response by RC structures with residential/commercial and industrial use. The reported structures have the typical features of the buildings in this region: medium rise buildings with irregularities in elevation (mainly due to the opening layout at the ground floor). In several buildings the use of parts of the buildings changed during its lifetime; for example, most of the visited/assessed structures had balconies that were closed with infill walls to become proper internal floors (**Figure 80b**). This feature affected the regularity of the building in elevation at different storeys as well as the actions distributions and/or intensity.

A very good response was also observed in industrial structures (**Figure 80c**), typically consisting of RC precast buildings (one or two-storey). The field crew visited some of the factories in the Izmir Atatürk Organized Industrial Zone (IAOIZ) in Çiğli at north-east of the city. The assessed behaviour can be justified by two main reasons: (1) the industrial structures in this area are quite modern and they were built with the most current design codes; (2) these structures are very flexible and the recorded spectral accelerations did not achieve large values at high periods (larger than 2.0 seconds).



Figure 80: Good response of (a) – (b) RC frames with infill masonry walls and (c) RC precast industrial building

A limited percentage of RC structures were classified as DG3-DG4 by both the field crew and the TMoEU database. The more severe damage was mainly due to either poor design and the use of poor quality of structural material in their construction or to the failure of the non-structural components during the earthquake. **Figure 81** shows the case of an extensive degradation of structural materials (partly due to prolonged exposure to high humidity levels – interview with Eylem Ayatar, Chamber of Structural Engineers) as well as the poor quality of construction detailing in the element. **Figure 82** shows the failure of the masonry infill walls, typically adopted as non-structural components in most of the RC multi-storey structures that were assessed throughout this mission. The pictures show cases of a complete collapse of the walls all along the structure due to either the achievement of the shear strength in the panel or the out-of-plane failure due to the lack of constraints on the ex-balconies at the upper levels.



Figure 81: Degradation in structural material and poor detailing in an RC element



Figure 82: Infill walls damage in RC frames: (a) out of plane (Arda Savaşcıoğulları / Alamy Stock Photo) and (b) in-plane failure

4.7.3.1. Cases of Collapse

Based on the TMoEU database (<https://hasartespit.csb.gov.tr/#/>), 17 buildings collapsed after the earthquake in two Izmir's districts: Bayraklı and Bornova (**Figure 83a**). Among those cases, 9 were RC frame structures in three neighbourhoods in Bayraklı (**Figure 83b**) where most of the casualties and losses were recorded. This section aims to present the most peculiar cases to stress their similarities as well as to contribute to the discussion about the possible causes. The first common features are:

- built in the 1990s
- designed according to outdated 1975 earthquake resistant design code
- designed with poor code compliance
- built with poor construction quality
- modified to accommodate commercial use in the ground floors



Figure 83: Map of collapsed buildings in Bayraklı and Bornova (21) and (b) location of the RC frame buildings in Bayraklı

Figure 84 shows the case of the Doğanlar apartment: an RC 8-storey frame built in 1990 and designed according to the 1975 earthquake regulations. This building collapsed, killing 14 people (12 people escaped death, including a mother and her four kids who were saved from the debris after 23 hours following the event; see “Son dakika: Tek kelimeyle rezalet! İzmir'deki deprem bölgesine gelen 9 kişi yakalandı”, 2020 and “23 saat sonra gelen mucize kurtuluş: İzmir'deki depremde yıkılan Doğanlar Apartmanı enkazından anne ve 3 çocuğu çıkarıldı”, 2020). The collapse can be explained based on the combined impact of the amplification of the seismic action due to the soil properties in the area as well as pre-existing damage due to past earthquakes (1992 İzmir Earthquake with Mw=6.1 and in 2005 with Mw=5.9). Other buildings around Doğanlar apartment demonstrated a much different response during this event despite their similar age, structural system and number of storeys.

Very similar conclusions can be drawn in the case of both the Rıza Bey Apartments (**Figure 85**) and the Karagül Apartments (**Figure 86**), which are both 8/9 storey RC frame structures built in the 90s based on the 1975 regulations. While a 70 and 3-year old was saved from under the debris after 33 and 91 hours, respectively (“Ayda Gezgin 91. saatte kurtarıldı”, 2020), 34 people died in the Rıza Bey Apartments, including the latter’s mother; whereas all residents were able to be evacuated from the Karagül Apartments on time.

The reports prepared by the Bayraklı Municipality Earthquake Study Center indicated problems with all these three apartment buildings (“CHP’nin İzmir raporu: Fay kanunu teklifi bir an önce kanunlaştırılmalı”, 2020): in 2018 for Doğanlar apartment door jams and floor level irregularities on the ground floor attributed to liquefaction and earthquakes, as well as visible deformations on the balconies were noted, and a thorough soil survey and performance analysis was recommended. In a 2012 report, the issues flagged for the Rıza Bey Apartments on the other hand included inadequate rebar detailing, soft ground floor due to commercial use, heavy overhangs, cosmetic repair of the cracks induced by the 2005 earthquake, humidity induced material degradation, low concrete class and flat bar reinforcements, recommending similarly a thorough soil survey and performance analysis. However, in both cases, despite the municipality reports deeming the buildings unsafe, it was claimed that the ministry was never informed about this (Gurcaner and Torlak, 2020).



Figure 84: Doğanlar apartment: (a) before (Google Maps) and (b) after the earthquake (photo courtesy of Mauricio Morales-Beltran)



Figure 85: Riza Bey Apartments: (a) before (Google Maps) and (b) after the earthquake (<https://www.haberler.com/riza-bey-apartmani-nerede-riza-bey-apartmani-13705665-haberi/>)



Figure 86: Karagül Apartments: (a) before (<http://puzzleyapi.com/karagul-apt-bayrakli-izmir/>) and (b) after the earthquake (<https://www.birgun.net/haber/coken-karagul-apartmani-na-da-10-yil-once-rapor-verilmis-321551>)

The collapse of the other two RC buildings can also teach another important lesson on seismic vulnerability in existing structures. The Yılmaz Erbek Apartments (**Figure 87**) consisted of two twin structures built in 1992 with 11-storey RC frames. Both structures were damaged, but only one of them collapsed with a local mechanism (soft storey) involving the first two floors, killing 9 people out of 22 who were in the building at the time of the event (Yılmaz Erbek Apartmanı'nda acı bilanço!, 2020). It was claimed that the supermarket under the building cut the columns to make space, although this has not been verified. A similar example was the collapse of three out of the four buildings in the Barış Sitesi complex (**Figure 88**), built in 1999 and sadly allocated for the survivors of the Gölcük earthquake in 1999, relocated in Izmir. The 7-storey RC frame collapsed with soft storey mechanisms (involving different number of storeys at different levels), killing seven of the eleven people who are known to be in the building when the earthquake hit (Barış Sitesi'nde arama-kurtarma durduruldu! Enkazda 2 kişi var!, 2020). The different behaviours of the structures with the same design in the same location can be attributed to the fact that different contractors were involved during the construction as well as to the post-construction modifications during the last 20 years (change of actions, openings layout and ground floor use).



Figure 87: Yılmaz Erbek Apartments (<https://www.tr724.com/savcilik-raporu-bimin-oldugu-apartmanda-kolonlar-kesildi/>)



Figure 88: Barış Sitesi Apartments (<https://www.egetelgraf.com/izmirdeki-depremde-hayatini-kaybeden-nurcan-hicyilmaz-tosun-topraga-verildi/>)

4.7.4. Damage Patterns to Masonry Cultural Heritage Structures (Authored by DC and ME)

An overall good response was recorded in the case of masonry buildings (**Figure 89**). Most of the structures were classified as DG0 and few cases were DG1 because of pre-existing damage. The structures were usually well-maintained in both cases of public and residential. Cultural heritage buildings appear to have suffered very little, if any, damage at all. Low and medium rise load bearing masonry churches, mosques and minarets are visibly intact with no cracking. Industrial heritage buildings, including the historic gasworks and tall slender masonry chimneys are similarly unaffected (**Figure 90**). Other tall and slender historic buildings are similarly undamaged. For example, the 58 m high famous Asansör in Izmir (**Figure 91**), an historic lift built in 1907 to connect two roads at different elevations, is completely intact. An important landmark for the city of Izmir, Saat Kulesi in Konak was also untouched by the event.



Figure 89: Good response of masonry buildings: (top row) monumental examples in central Izmir; (bottom row) vernacular typologies in Seferihisar



Figure 90: Industrial heritage buildings



Figure 91: Asansör in Izmir

4.8. Masonry/Timber Vernacular Typology Common to Turkey and Greece

(Authored by YDA)

The area affected by the 30 October 2020 Earthquake is also home to diverse vernacular typologies. One of the most common typologies that are common in Turkey, Greece and part of the Balkans is composite structures with a masonry ground floor and timber frame upper storeys (except for the facades with services, e.g. fireplace, which carries on as masonry throughout the building height). These are commonly known as *himiş*, or post-Byzantine structures. The overall constructive and material characteristics of both masonry and timber frame components show a high variability depending on the region: brick, stone (or brick and stone), or adobe masonry with or without tie beams or timber posts, and single or double layered timber framing with masonry infill or cladding. The main façade of these buildings may incorporate a jetty, built in a simple cantilever form or with braces of different geometries, to have a wider view of the street, and, in case of narrow/irregular ground floor geometries, to complete the upper floor plan scheme into a full quadrangle (Aktas, 2017; Sahin Guchan, 2007).

Past reconnaissance studies concluded that these typologies were overall rather resistant to seismic events (Ambraseys and Jackson, 1981). This inherent seismic resilient behaviour of *himiş* structures has also been confirmed through experimental (Aktas et al, 2014) and analytical (Aktas and Turer, 2016) work, and has been explained by the following main factors: (1) High ductility and energy dissipation levels owed to (mostly) nailed connections, (2) High lateral load bearing capacity due to diagonal braces within the frames (**Figure 92a**). (3) Lightweight: This is especially the case with the cladded more than infilled typologies (**Figure 92b**). One of the most common cladding types is known as *bağdadi*, where 2-4 cm wide laths are nailed onto the frame with around 1 cm gap in between, resulting to a system which is very lightweight and with an efficient diaphragm action.

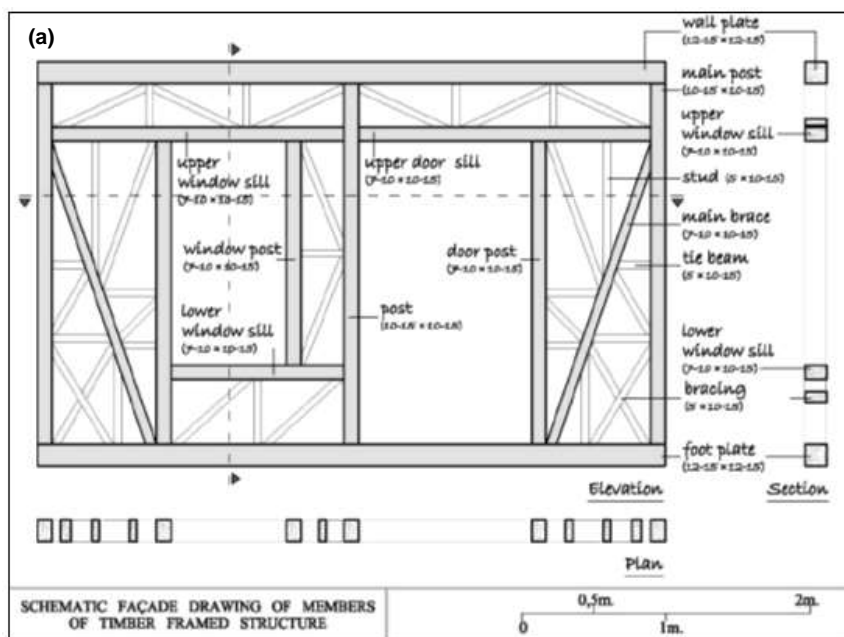


Figure 92: (a) Schematic representation of a timber frame (after Diri, 2010) and (b) two buildings with stone infill (the building in the middle) and *bagdadi* cladding (the building on the right) (from "Mikres diadromes" youtube channel)

The examples observed on site for both Samos and Turkey seem to be dominated by examples with *bagdadi* cladding (**Figure 93**). In case of Turkey, no or little damage is observed to this typology, while in Samos there are a few heavy damage cases, where the observed failure mechanisms are in broad agreement with those reported in previous post-earthquake studies, including out-of-plane failure of masonry infill (**Figure 94a**) and out-of-plane failure of upper floor masonry service walls (**Figure 94b**). There are also cases where the damage is limited to loss of plaster, which is particularly common in already dilapidated facades (**Figure 94c**). Other failure modes common to this typology include global failure due to collapse of the masonry ground floor and loss of the box action in the upper floors due to poor/deteriorated connections failing under elevated drift.

The discrepancy between the seismic performances of Turkey and Samos vernacular masonry/timber hybrid structures can be explained by the level of maintenance and occupancy status: the Samos examples seem to be relatively more poorly maintained and in certain cases abandoned.



Figure 93: Some examples of *hımsı* structures in the affected areas (top row) in Turkey and (bottom row) in Samos



Figure 94: Examples to damage in *hımsı* structures

4.9. Conclusions

- Samos and affected areas in Turkey have different building stocks: in Samos vernacular typologies constitute a significant portion of the stock, while in Turkey mid-rise RC dominate.
- The damage levels are more even in Samos and are mostly attributed to age and poor maintenance/abandonment. The mostly low-rise nature of the building stock led to much lower casualties in Samos.
- In Turkey, on the other hand, the damage is very concentrated to a small portion of mid-rise RC buildings which we understand were built using noncompliant design, material and workmanship. These factors were further exacerbated through site amplification in 0.8-1.4 s period range increasing seismic demand in mid-rise buildings especially in Bayraklı beyond their capacity, leading to high damage levels or collapses with a significant death toll.

- In Turkey, the lack of more operational quality assurance protocols for construction practices is considered to be the main barrier to pulling the overall seismic performance of the built environment.
- The discrepancy between the damage levels observed in buildings in the two countries comparable in terms of the primary structural system and age, for instance masonry and masonry/timber vernacular structures, highlight the importance of good upkeep for a desired seismic impact.
- The field surveys for this mission was carried out during the ongoing COVID pandemic. To ensure the safety and security of our field crew, buildings were always assessed from outside unless there were collapsed in such a way to expose the indoors. This might have led to the underestimation of damage levels.
- Data availability and content for a remote assessment of the impact of the event on buildings and other structures, seems to be country-dependent. This may be down to different cultures of engaging with social media in a given context, or how informed citizens are regarding the disaster risk. In case of the Aegean Mission we were able to find a higher amount of data from a wider set of sources for Greece than for Turkey thanks to a few comprehensive data sources on Youtube and Facebook.
- Another important factor governing the availability of data representative of the overall damage levels seems to be how dispersed damage is: in case of localised dramatic damage (Turkey), the damage bias in remote data sources is much higher than when the damage levels are more even and more scattered across the affected area (Samos).

References

- 23 saat sonra gelen mucize kurtuluş: İzmir'deki depremde yıkılan Doğanlar Apartmanı enkazından anne ve 3 çocuğu çıkarıldı. (2020, October 31) Retrieved from Yeni Safak: <https://www.yenisafak.com/gundem/23-saat-sonra-gelen-mucize-kurtulus-izmirdeki-depremde-yikilan-doganlar-apartmani-enkazindan-anne-ve-3-cocugu-cikarildi-3573093>
- Aktaş, Y.D., Türer, A. (2016) Seismic Performance Evaluation of Traditional Timber *Hımiş* Frames: Capacity Spectrum Method Based Assessment, Bulletin of Earthquake Engineering 14(11), pp. 3175-3194
- Aktaş, Y.D. (2017) Seismic Resistance of Traditional Timber Frame *Hımiş* Structures: A Brief Overview, International Wood Products Journal 8, pp. 21-28
- Aktaş, Y.D., Akyüz, U., Türer, A., Erdil, B., Şahin Güçhan, N. (2014) Seismic Resistance Evaluation of Traditional Ottoman Timber-Frame *Hımiş* Houses: Frame Loadings and Material Tests, Earthquake Spectra 30(4), pp. 1711-1732
- Ambraseys, N. N. and Jackson, J. A. 1981. Earthquake hazard and vulnerability in the northeastern Mediterranean: The Corinth earthquake sequence of February-March 1981. Disasters 5(4): 355–368.
- Ayda Gezgin 91. saatte kurtarıldı (2020, November 4) Retrieved from NTV: https://www.ntv.com.tr/galeri/turkiye/ayda-gezgin91-saatte-kurtarildideprem-enkazinda-zamana-karsi-buyuk-yaris.5A_G0qWvpESAPowArOwENA/F-ztDMzB-keoxZ-r8Rkwgg
- Barış Sitesi'nde arama-kurtarma durduruldu! Enkazda 2 kişi var! (2020) Retrieved from Ege Telgraf: <https://www.egetelgraf.com/baris-sitesinde-arama-kurtarma-durduruldu-enkazda-2-kisi-var/>
- CEN (1994). EUROCODE 8: Design Provisions for Earthquake Resistance of Structures.
- Diri, F. (2010) Construction Techniques of Traditional Birgi Houses. Ankara: Middle East Technical University, Msc Thesis. Retrieved from <http://etd.lib.metu.edu.tr/upload/12612632/index.pdf>
- EAK 2000 (2003). Greek National Building Code, Earthquake Planning and Protection Organization of Greece, EPPO Publications, Greece.
- EKOS (2000). National Code for Concrete Building Structures of Hellas.
- EL.STAT. (2011). Population and building census 2011. Hellenic Statistical Authority.
- Elyamac, K E and Erdogan A S (2005) Gecmisten Gunumuze Afet Yonetmelikleri ve Uygulamada Karsilasilan Tasarim Hatalari; in: *Deprem Sempozyumu Kocaeli 2005*, 23-25 March 2005 Kocaeli, Turkey
- Gazette Gs (1959). Royal Decree on the Seismic Code for Building Structures. Issue A, No. 36, Greece.
- Grünthal G (1998). European Macroseismic Scale 1998 (EMS-98) European Seismological Commission, sub commission on Engineering Seismology, Working Group Macroseismic Scales,

- Conseil de l'Europe, Cahiers du Centre Européen de Géodynamique et de Séismologie, Vol. 15, Luxembourg.
- Guler K, Celep Z (2020). On the general requirements for design of earthquake resistant buildings in the Turkish Building Seismic code of 2018,. IOP Conf. Ser.: Mater. Sci. Eng. 737 012015.
- Gurcaner, E, Torlak, C (2020) SON DAKİKA... İzmir'de Rızabey ve Doğanlar Apartmanı'nda rapor skandalı! Belediye bildiği halde Bakanlığa bildirmemiş, Retrieved from Sabah: <https://www.sabah.com.tr/gundem/2020/11/02/son-dakika-izmirde-rizabey-ve-doganlar-apartmaninda-rapor-skandalı-belediye-bildigi-halde-bakanliga-bildirmemis>
- Ilki A, Celep Z (2012). Earthquakes, Existing Buildings and Seismic Design Codes in Turkey. Arab J Sci Eng, 37: 365-380.
- Lekkas E, Mavroulis S, Gogou M, Papadopoulos GA, Triantafyllou I, Katsetsiadou K-N, Kranis H, Skourtsos , E., Carydis P, Voulgaris N, Papadimitriou P, Kapetanidis V, Karakonstantis A, Spingos I, Kouskouna V, Kassaras I, Kaviris G, Pavlou K, Sakkas V, Evelpidou N, Karkani E, Kampolis I, Nomikou P, Lambridou D, Krassakis P, Foumelis M, Papazachos C, Karavias A, Bafi D, Gatsios T, Markogiannaki O, Parcharidis I, Ganas A, Tsironi V, Karasante I, Galanakis D, Kontodimos K, Sakellariou D, Theodoulidis N, Karakostas C, Lekidis V, Makra K, Margaris V, Morfidis K, Papaioannou C, Rovithis E, Salonikios T, Kourou A, Manousaki M, Thoma T , Karveleas N (2020). The October 30, 2020 Mw 6.9 Samos (Greece) earthquake. Newsletter of Environmental, Disaster and Crises Management Strategies, 21: 2653-9454.
- Son dakika: Tek kelimeyle rezalet! İzmir'deki deprem bölgesine gelen 9 kişi yakalandı.* (2020, November 1) Retrieved from Milliyet: <https://www.milliyet.com.tr/galeri/son-dakika-tek-kelimeyle-rezalet-izmirdeki-deprem-bolgesine-gelen-9-kisi-yakalandi-63439677>
- MOD84 (1984). Amendments and Additions to the RD of 26/2/59. Ministry of Public Works, Decree 239B/6-4-1984(4, Athens, Greece).
- MRR (1975). Specification for Structures to be Built in Disaster Areas, . Ministry of Public Works and Settlement Government of Republic of Turkey.
- Naftemporiki (2020). Samos: significant damage to dozens of churches and monasteries. <https://www.naftemporiki.gr/story/1653430/samos-simantikes-zimies-se-dekades-ekklisies-mones>.
- NEAK (1995). Greek Earthquake Resistant Design Code. Ministry of Environment, Planning and Public Works, Decree 534B/20-6-1995: Athens, Greece.
- Şahin-Güçhan, N (2007) Observations on earthquake resistance of traditional timber framed houses in Turkey. Building and Environment 42: 840–851.
- Samos24 (2020). The destruction of the historical tanneries. Available at: <https://samosvoice.gr/2020/11/02/oldtanneries/>
- Samosvoice (2020). Available at: <https://samosvoice.gr/>
- Sezen H., Elwood K. J., S. WA, <http://geopubs.wr.usgs.gov/open-file/of01-163/web/publication.htm> (2001). Evolution of Building Design and Construction Practice in Turkey. USGS Open-File Report 01-163.
- Skai (2020). Samos – earthquake: damage to museums and monuments at Samos, Icaria and Chios. <https://www.skai.gr/news/greece/samos-seismos-zimies-se-mouseia-kai-mnimeia-se-samo-ikaria-xio>
- TMoEU (2020). Turkish Ministry of Environment and Urbanization. <https://hasartespit.csb.gov.tr/#/>.
- TMoEU (2020) 30 Ekim 2020 İzmir Depremi Afeti; TMoEU.TUIK (2020) Completed or Partially Completed New Buildings and Additions by Use of Building, (New Classification) (According to New Classification and Method) Since 2009. (2020, November 17) Retrieved from: <https://data.tuik.gov.tr/Kategori/GetKategori?p=insaat-ve-konut-116&dil=2>
- Vadaloukas G, Vintzileou E, Ganas A, Giarelis C, Ziotopoulou K, Theodoulidis N, Karasante I, Margaris B, Mylonakis G, Papachristidis A, Repapis C, Psarropoulos PN, Sextos AG (2020). Samos Earthquake of 30th October. Preliminary Report of the Hellenic Association for Earthquake Engineering.
- Yılmaz Erbek Apartmanı'nda acı bilanço! (2020, November 3) Retrieved from Hürriyet: <https://www.hurriyet.com.tr/gundem/yilmaz-erbek-apartmaninda-aci-bilanco-41652800>

5. TSUNAMI

(Authored by MB)

This chapter describes the characteristics and effects of the tsunami that inundated the coast of Turkey and Samos island and on 30th October 2020. The tsunami impact is assessed using information that was collected both in the field and remotely. The findings of the field survey conducted by the EEFIT crew in the coastal areas impacted by the tsunami are discussed, together with the evidence provided by numerous online resources and the considerable work carried out by other international reconnaissance missions. It is noted that considerations on tsunami economic impact, response and preparedness are presented in Chapter 7.

5.1. Tsunami Terminology

For earthquake-generated tsunami, the amount of seafloor displacement determines the *amplitude* of the tsunami. Similarly, the *wavelength* and period of the tsunami are determined by the size and shape of the underwater disturbance. Once a tsunami has reached the shoreline, it will continue to propagate onshore, possibly by several hundred metres (*inundation extent*). The vertical height of the maximum onshore *inundation extent* above the tidal level at the time of the event is called the *run-up height*. The *inundation height* and *inundation depth* are the vertical measure of the wave at a particular location with respect to the tide level and to the local ground elevation, respectively. These standard terms are shown graphically in **Figure 95**.

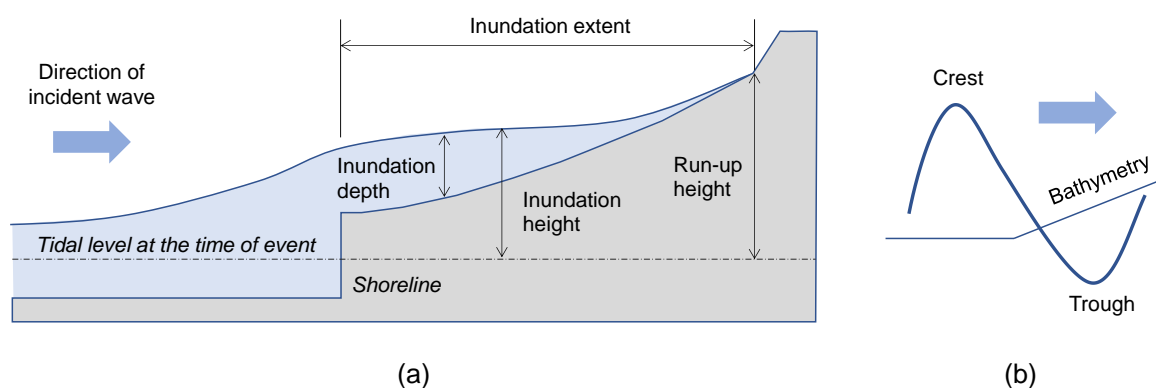


Figure 95: Definition of main onshore tsunami inundation parameters (after Fraser et al., 2013).

5.2. Past Tsunamis in the Aegean Sea

Historically there have been large tsunamis across the Eastern Mediterranean region (Papadopoulos and Chalkis, 1984). Major events include the tsunami triggered by earthquakes off Crete island (in 365 and 1303) and Amargos island (in 1956), as well as by the volcanic activity of the Thera (Santorini) island complex (in 1650) (Papadopoulos et al., 2007). More recently, on 20 July 2017 a Mw 6.6 earthquake generated a tsunami that inundated the coastal city of Bodrum in Turkey and the island of Kos (Greece). The impact was moderate, with maximum run-up heights of 1.9 m (Papadimitriou et al., 2018). However, there is little evidence of large tsunami triggered in the eastern Aegean Sea, despite the fact that the entire region is under tectonic tension (see Chapter 2). Over the last two centuries, only two events of small intensity have been recorded. In 1856, a 6.6-Mw-earthquake with epicentre off Chios island generated a tsunami of small intensity. More recently, on 12 June 2017 a Mw-6.3-earthquake off the island of Lesbos triggered a small tsunami. **Figure 96** illustrates the location of the abovementioned tsunamigenic earthquakes and volcanic source.

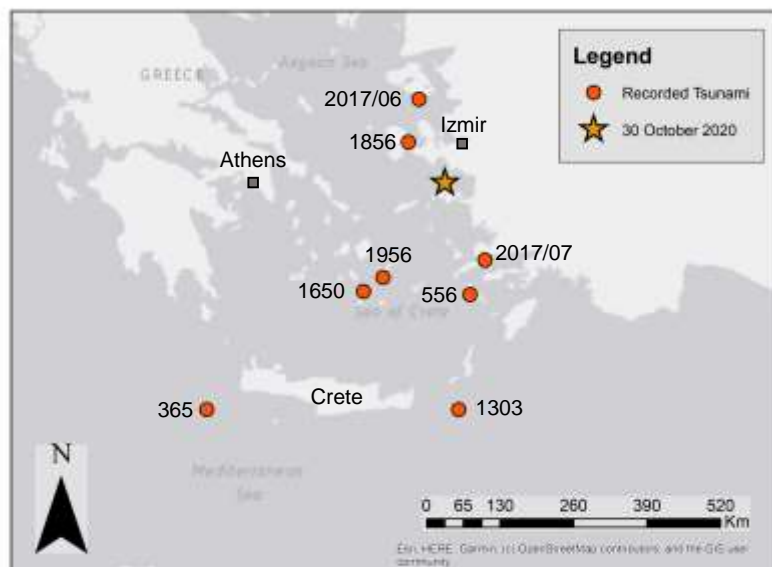


Figure 96: Recorded major tsunami events in the Aegean Sea.

5.3. The 30th October 2020 tsunami characteristics

As described in Chapter 2, the 30 October 2020 event (11:51:27 UTC) was a submarine normal fault earthquake under the shallow waters between the Greek island of Samos and the coast of the Aegean region of Turkey. The downward slip of the seafloor on one side of the fault and the upward movement on the other side triggered the setup of a tsunami wave. The wave travelled quickly towards the shoreline. It took just a few minutes for the tsunami wave to reach the coast of Samos Island near Karlovasi, and less than half an hour to inundate the towns of Vathy (Greece) and Sığacık (Turkey). **Figure 97** shows the arrival times based on video recordings published online and a recent study (Triantafyllou et al., 2021).



Figure 97: Tsunami arrival times on Samos island and Turkey. Note: AT = Arrival Time. YouTube Video frames: [1] https://youtu.be/_el3NfEJJKQ; [2] <https://youtu.be/9wcz1p9cKt4>; and [3] <https://youtu.be/bxar6B2ysFA>;

A CCTV installed at a house along the Ayios Nikolaos beach (coordinates: 37.8126747, 26.7422152), provided an extremely valuable recording of the onshore tsunami inundation. This location is at approximately 5 km distance from Karlovasi and very close to the earthquake epicentre (**Figure 97**). **Figure 98** illustrates the video frames of the tsunami inundation. It can be seen that only two minutes after the earthquake (11:53:37 UTC) the sea rapidly receded. Then, the water level increased to reach the house apron (11:54:33 UTC). These observations indicate that the tsunami was trough-led in this location (**Figure 95b**). In the next minute, the sea receded again, but this was followed by a much larger

EEFIT

wave that moved obliquely to the coast, eventually inundating the house (11:55:39 UTC) (**Figure 98**). There are two mechanisms suggested in Triantafyllou et al. (2021) to explain the nature and magnitude of this second wave, i.e. either a submarine landslide off this site or a near-field edge wave (waves trapped by refraction that propagate parallel to the shoreline; see Geist, 2012) phase. Eyewitnesses reported the arrival of a third small wave at around 12:15 UTC, which was not captured by the camera due to a power outage (Triantafyllou et al., 2021). The EEFIT Greek field crew visited the house and its surroundings on 8 December 2020 (**Figure 99**). The apron level was found 1.20 m above the sea level (asl). The water on the walls might have reached a depth in excess of 1.50 m above the apron, i.e. 2.80 m asl. Triantafyllou et al. (2021) estimated the splash might have inundated the house wall up to 2m. It is noted that, following the earthquake, the ground on Samos island experienced a coseismic uplift of around 20 cm (see Chapter 2). In the aftermath of the event, it is reported that the house owner observed a drop in the sea level of the same magnitude (Triantafyllou et al., 2021). The uplift certainly led to a reduction in the inundation measures recorded along the coast of Samos island.



Figure 98: Tsunami inundation in Ayios Nikolaos beach (coordinates: 37.8126747, 26.7422152; Samos Island, Greece).
YouTube Video frames: https://youtu.be/_eI3NfEJkQ.



Figure 99: House at Ayios Nikolaos beach: measurements by EEFIT Greek field crew.

EEFIT

Vathy (officially named as Samos Town) and its port, which are located at the edge of a shallow 5-km long bay (Cetin et al., 2021), were affected by the arrival of a first wave at 12:04 UTC. This was followed by a larger and more sustained wave at 12:24 UTC (Triantafyllou et al., 2021). Both waves inundated the esplanade facing the sea, while the second one reached the streets and buildings further inland. Cetin et al. (2021) mention reports of eyewitnesses that indicate the sea having receded in Vathy bay after the earthquake.

The tsunami inundation was significant along the Turkish coast. While the seaside city of Kuşadası within Aydın Province was affected by a small tsunami inundation, the coastal districts of the Izmir Province (highlighted in **Figure 100**) were more severely impacted. **Figure 101** shows the video frames of two tsunami waves arriving at a beach location south to Kuşadası, preceded in both occasions by the trough. Within the Seferihisar district, Akarca and Sığacık experienced large tsunami inundations. This appears due to their location near to the tsunami source. According to Triantafyllou et al., 2021, Akarca was inundated by the first wave at 12:03 UTC. The tsunami wave was amplified in Sığacık bay (Cetin et al., 2021) and reached Sığacık Marina at approximately 12:14 UTC, based on video recordings (see **Figure 97b**). The video frames recorded in Akarca (**Figure 102a**) confirm that the wave arrival was preceded by sea recession (i.e. trough-led tsunami). In Sığacık, the tsunami flow was channelled through the narrow streets of the historical centre. Several videos taken from this location showing sustained flooding and debris impacting shops and houses were circulated via social media (see **Figure 102b**). Other locations that experienced considerable tsunami inundation include Demircili, Tepecik and Port Alaçatı (Cetin et al., 2021).

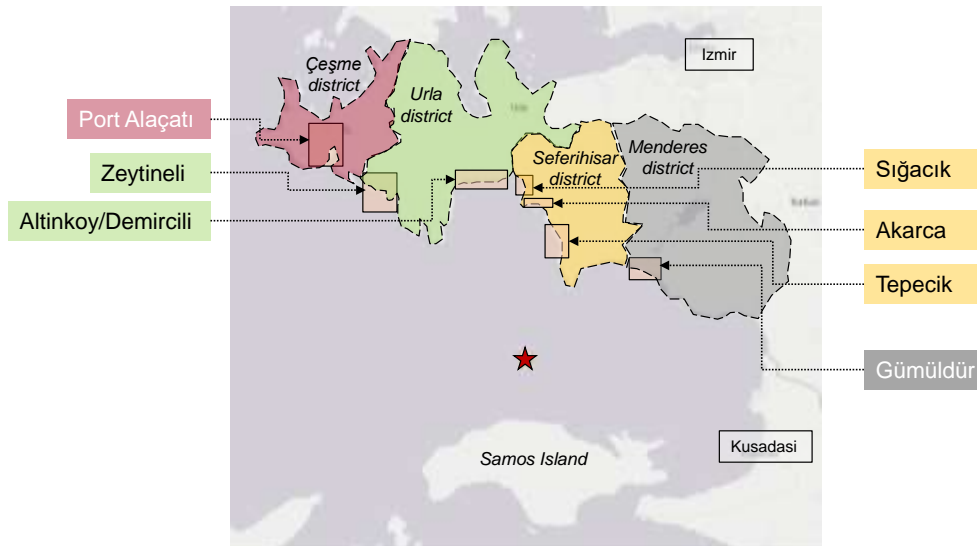


Figure 100: Coastal districts in Izmir province (Turkey) affected by the 30th October 2020 tsunami

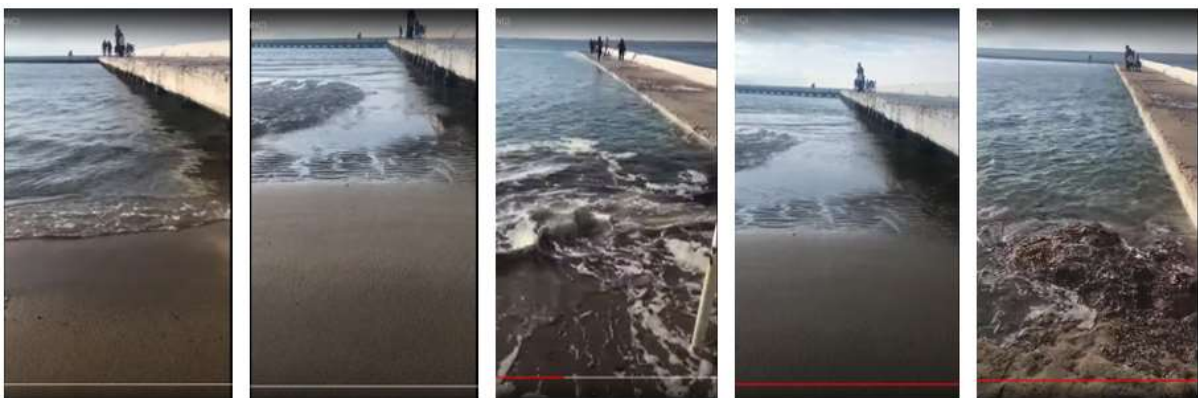


Figure 101: Video frames showing tsunami waves arrival in Kuşadası, Aydın Province (coordinates: 37.800806, 27.268718). YouTube video: <https://youtu.be/2w3qvNPJQgg>.



Figure 102: Tsunami inundation video frames recorded in Seferihisar district: (a) Akarca (source: <https://youtu.be/Fl-QDMXALTA>) and (b) Siğacık (source: <https://youtu.be/XJzIRNYvoiU>).

5.4. International tsunami surveys

In the aftermath of the 30th October 2020 event, two international teams led by Greek and Turkish researchers visited the areas affected by the tsunami, undertaking runup and inundation measurements. Detailed description and discussion of these post-event field survey data are presented in Cetin et al. (2021) and Triantafyllou et al. (2021). **Figure 103** shows the maximum run-up heights recorded in the locations surveyed by the international teams along the coast of Izmir Province and Samos Island. It can be seen that maximum run-up heights are in the region of 1.5-2 m in Siğacık, Vathy and Karlovasi. These coastal locations were the most affected by the tsunami, where substantial non-structural damage to properties, shops, offices, cars, boats was reported. However, initial findings did not indicate the occurrence of structural damage to buildings.

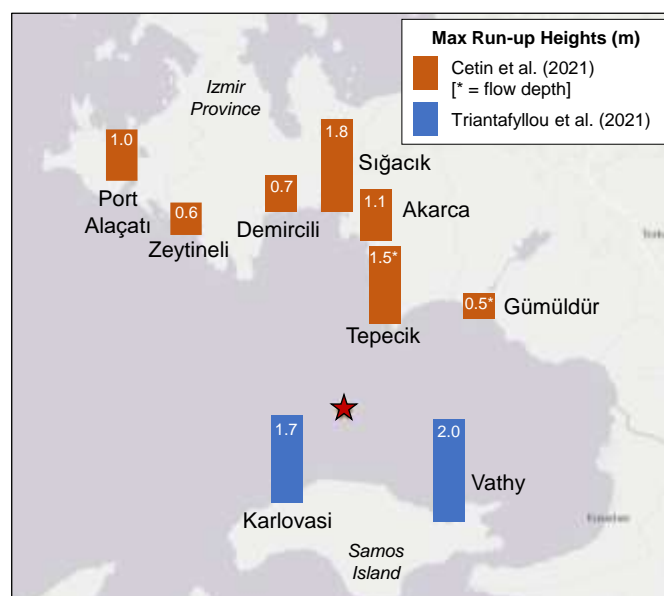


Figure 103: Measurements of maximum tsunami run-up heights in m for the most-affected locations by the tsunami along the coast of Izmir Province and Samos Island, according to Cetin et al. (2021) and Triantafyllou et al. (2021).

5.5. General observations obtained through field survey

The EEFIT field crews visited numerous locations along the coast of Izmir province and Samos island, conducting damage surveys of buildings for earthquake and tsunami effects. The initial evidence from news outlets and interim international mission reports indicated that the most tsunami affected areas were Siğacık and Akarca in Turkey, and Karlovasi and Vathy (and surrounding areas) along the northern coast of Samos. The crews were deployed in those locations at least one month after the event. For this reason, the main aim of the field survey was to collect more in-depth data of any visible structural or non-structural damage to buildings. However, it should be noted that, since such activity was conducted several weeks after the tsunami, non-structural damage was often already being repaired and any debris cleared away.

5.6. EEFIT Mobile App

The EEFIT Mobile App deployed during the mission is designed to allow for both earthquake and tsunami data collection. In fact, this required a specific update of the App, which has been mainly developed for earthquake data collection. Additional attributes have been included to reflect typical damage mechanisms due to tsunami hydrodynamic effects on buildings, such as: the number and types of openings, particularly at ground floor level; the presence of basement; assessment of surroundings, including perimeter walls and presence of debris; details of foundation type and damage (if that is visible); evidence of water marks on the building. Some of these attributes were included in the damage assessment form developed in the 2018 EEFIT mission in Palu (Rossetto et al., 2019), which has been adopted for the damage assessment carried out in this mission.

5.7. Observations from Siğacık and Akarca

In Siğacık, the field visit mainly focused on the historical centre that was affected by the sustained tsunami flow. Damage to shops, properties, cars and boats was substantial (Cetin et al., 2021). **Figure 104** illustrates the location and damage grade of the buildings surveyed by the EEFIT Turkish crew team. One month after the event, the town was in good conditions. All debris was cleared and no visible structural and non-structural damage was observed for most of the historical masonry buildings (DG0). On a few buildings, water marks could still be observed, indicating some minor damage to external walls (DG1) – see **Figure 105**. Despite being relatively close to the epicentre, buildings did not suffer any significant damage due to the earthquake. The survey did not cover Teos Marina, a large private marina, where extensive damage was reported to numerous boats and yachts. Chapter 6 will present data about the economic impact of tsunami damage occurred in ports and marinas in Turkey.

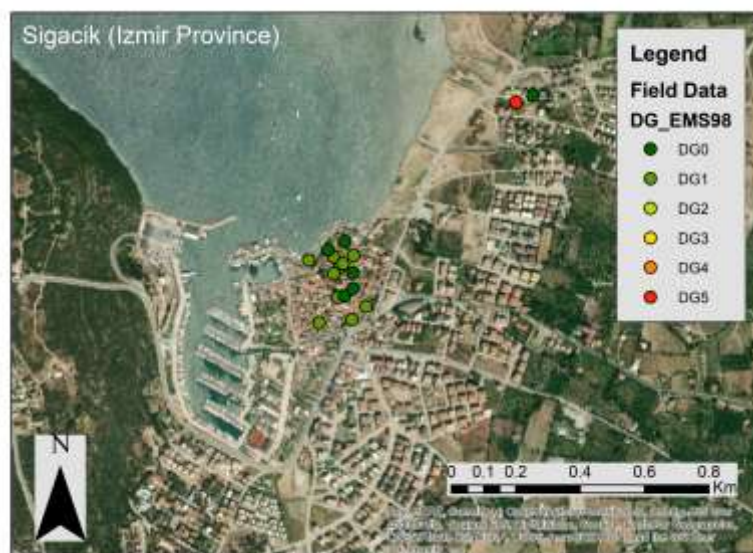


Figure 104: Damage assessment data for surveyed buildings in Siğacık.



Figure 105: Buildings surveyed in Sığacık (coordinates: 38.1944937, 26.7854733).

The field crew also visited an area on the northern outskirts of the town that experienced extensive tsunami inundation. **Figure 106** shows the video frame sequence of the overturning of a perimeter wall due to the effects of the tsunami flow. A close inspection of the wall indicates that the wall was made of a single layer of bricks, probably with very weak foundation supports. This wall is marked as a red dot (DG5) on the map in **Figure 104**. However, it is noted that the rest of the assessment records are for buildings. The satellite imagery (**Figure 104**) clearly shows that this wall and the surrounding urbanised area sits in fact on what used to be a river inlet. This clearly allowed the tsunami inundation to extend much further inland and with considerably sustained flow velocity.



Figure 106: Perimeter wall overturning due to tsunami hydrodynamic effects in Sığacık (coordinates: 38.1982930, 26.7902697). Video frames (on top) from YouTube video: <https://youtu.be/n93puRYKhs0>

Akarca is the second and last location in Seferihisar district (see **Figure 102**) that was visited by the EEFIT crew for tsunami damage assessment. In this coastal town, the building portfolio is different from Sığacık town and is made mainly of reinforced concrete structures. As reported in Cetin et al. (2021), tsunami impacted more significantly the southern coast. It appears that the configuration of the bay (see **Figure 102**) had a sheltering effect for the northern part of Akarca. Boats and cars were damaged, as well as fishery port piers, while very limited non-structural damage was recorded in the aftermath of the event (Cetin et al., 2021). At the time of the visit, there was still some evidence of the tsunami inundation,

with some rubble and debris still to clear. No structural damage was observed on the most exposed buildings along the beach that were surveyed (**Figure 107**).



Figure 107: Tsunami effects in Akarca (coordinates: 38.166245, 26.810087).

5.8. Observations from Samos island

The EEFIT Greek crew visited numerous locations along the coast of Samos that were impacted by the earthquake and tsunami. The seismic damage was more substantial on the Greek island. Several shops, houses, cars and boats were damaged in Vathy, Kokkari and Karlovasi (Triantafyllou et al., 2021). Structural damage assessment for Samos island is discussed in more detail in Chapter 3, as it combines key seismic observations. **Figure 108** shows two sample buildings from Karlovasi and Vathy, which had suffered damage due to the preceding earthquake (DG1) but no substantial damage due to the tsunami flow. Typically, it can be difficult to establish if the cause of damage is due to the earthquake only or tsunami at some degree. Nevertheless, no distinct tsunami structural damage mechanism was observed in the surveyed structures. The house located along Ayios Nikolaos beach (**Figure 99**) did not report any structural damage, despite having experienced very sustained tsunami flow that inundated the rooms at the ground floor up to 2.15m above grade (Triantafyllou et al., 2021).



Figure 108: Buildings affected by earthquake and tsunami: Karlovasi (coordinates: 37.800145, 26.704959) and Vathy (coordinates: 37.751835, 26.976584).

5.9. Summary

The 30th October 2020 earthquake and tsunami affected the eastern Aegean Sea, which has not been frequently affected by tsunami in recent history. The tsunami waves rapidly reached the coast of Samos island, with the closest location to the source being inundated in less than 2 minutes after the earthquake. The two major towns of the island and Izmir province were impacted by the tsunami in less than half an hour. Maximum measured run-up heights were between 1.5-2 m, causing substantial damage to shops, properties, cars, boats and coastal infrastructure. However, even in those locations where the tsunami waves were sustained, no visible structural damage was observed in the aftermath

of the event and one month later, when the EEFIT field crews carried out damage surveys to buildings affected by both earthquake and tsunami. A bespoke survey mobile App was used to provide an effective evaluation of damage to buildings that experienced both the earthquake and tsunami hazards. The damage scale is based on EMS-98 and was already used in the TDMRC-EEFIT mission for the 2019 Sulawesi event.

References

- Cetin, K. O., Mylonakis, G., Sextos, A., & Stewart, J. P. (2020). Seismological and Engineering Effects of the M 7.0 Samos Island (Aegean Sea) Earthquake. HAAE 2020/02, Earthquake Engineering Assoc of Turkey, Earthquake Foundation of Turkey, EERI, GEER-069. doi: <https://doi.10.18118/G6H088>
- Fraser, S., Raby, A., Pomonis, A., Goda, K., Chian, S.C., Macabuag, J., Offord, M., Saito, K. and Sammonds, P., (2013) Tsunami damage to coastal defences and buildings in the March 11th 2011 M w 9.0 Great East Japan earthquake and tsunami. *Bulletin of earthquake engineering*, 11(1), pp.205-239.
- Geist, E.L. (2013) Near-Field Tsunami Edge Waves and Complex Earthquake Rupture. *Pure Appl. Geophys.* 170, 1475–1491 <https://doi.org/10.1007/s00024-012-0491-7>
- Papadimitriou, P., Kassaras, I., Kaviris, G., Tselentis, G.A., Voulgaris, N., Lekkas, E., Chouliaras, G., Evangelidis, C., Pavlou, K., Kapetanidis, V. and Karakonstantis, A., 2018. The 12th June 2017 Mw= 6.3 Lesvos earthquake from detailed seismological observations. *Journal of Geodynamics*, 115, pp.23-42.
- Papadopoulos G.A., Chalkis B.J. (1984). Tsunamis observed in Greece and the surrounding area from antiquity up to the present times. *Marine Geology*, Volume 56, Issues 1-4.
- Papadopoulos G.A., Daskalaki E., Fokaefs A., Giraleas N. (2007). Tsunami hazards in the Eastern Mediterranean: strong earthquakes and tsunamis in the East Hellenic Arc and Trench system. *Natural Hazards and Earth System Science*, Copernicus Publications on behalf of the European Geosciences Union, 7 (1), pp.57-64.
- Rossetto T., Raby, A., Brennan, A., Lagesse, R., Robinson, D., Adhikari, R K., Rezki-Hr, M., Meilianda, E., Idris, Y., Rusydy, I, Kumala, I D. (2019). “The Central Sulawesi, Indonesia Earthquake and Tsunami of 28th September 2018 – A Field Report by EEFIT-TDMRC.” Earthquake Engineering Field Investigation Team (EEFIT), Institution of Structural Engineers, UK.
- Triantafyllou, I., Gogou, M., Mavroulis, S., Lekkas, E., Papadopoulos, G. A., & Thravalos, M. (2021). The Tsunami Caused by the 30 October 2020 Samos (Aegean Sea) Mw7. 0 Earthquake: Hydrodynamic Features, Source Properties and Impact Assessment from Post-Event Field Survey and Video Records. *Journal of Marine Science and Engineering*, 9(1), 68.

6. RELIEF, RESPONSE AND RECOVERY OBSERVATIONS

6.1. Methods and Sources of Information

(Authored by JC)

This section considers the relief, response and recovery (RRR) of Samos and the region of Izmir through the lens of the human and economic aftermath of the Oct 30, 2020, Aegean earthquake and tsunami. The RRR team developed a series of interviews and a public survey to understand the first-hand experience of residents and professionals involved in RRR operations. Other critical sources of information include press releases, Relief Web, and government and NGO reports.

The RRR team conducted eight interviews in Izmir and four in Samos to date (**Table 5**). The interviewees include government officials, educational and medical staff, volunteers and members of NGOs. Interviewees provided 'on-the-ground' perspectives of stresses, challenges and successes. This included the impact of COVID-19, the efficacy of early warning systems, and tsunami responses.

Table 5: List of interviewees in Turkey and Greece

Name/Surname	Role/Affiliation	Type of the Institute	Interview Date
Healthcare Professional (anonymous)	Doctor/Ege University Hospital	Health Service – Public/National	25.11.2020
Sude KILIÇ	Volunteer/World Human Relief	Relief Organization - NGO/International	26.11.2020
İlker KAHRAMAN	Head/Chamber of Architects Izmir Branch	Professional Chamber – Public/National	26.11.2020
Mehmet SARICA	Field Director/IDEMA	Relief Organization - NGO/National	01.12.2020
Eylem U. AYATAR	Head/Chamber of Structural Engineers Izmir Branch	Professional Chamber - National	01.12.2020
Ferdi GÖLCÜK	Fire Brigade Sergeant/Fire Department of Izmir Metropolitan Municipality	Local Government – Public/Local	02.12.2020
Mert U. AKSOY	Fund-Raising Manager/Lokman Hekim Sağlık Vakfı	Relief Organization - NGO/National	04.12.2020
Atilla ALTUNBULAK	Division Manager/AFAD	SAR – Public/National	04.12.2020
Dimitrios MALLIAROS	Head/Civil Protection Directorate of North Aegean Region	Disaster Management – Public/Regional	23.11.2020
Alexandros TATOURIS	Head/Civil Protection Department of Regional Unit of Samos	Disaster Management – Public/Local	25.11.2020
Thoma THEKLA	Head/Preparedness and Aid Provision Department, Earthquake Planning and Protection Organization	Damage and usability assessment – Public/National	04.12.2020
Ioannis STAMOULIS	Head, in general command of response operations/Regional Fire Service of North Aegean	SAR – Public/Regional	04.12.2020

The public surveys were translated into Greek and Turkish and distributed through local newspapers and social media networks. Within 72 hours, 270 and 860 respondents completed the surveys in Samos and the Izmir region, respectively. The surveys addressed the perceptions and behaviour towards seismic and tsunami risk; actual response to the events; capacity to respond; and impact and sustained losses.

6.2. Economic Aftermath

6.2.1. Turkey

(Authored by ATO)

The data sources used to investigate economic losses in Turkey from the 30 October 2020 Aegean Earthquake & Tsunami include DASK (Turkish Natural Catastrophe Insurance Pool), AFAD (the Disaster and Emergency Management Authority), newspapers and social media.

Although there has not been an official gross economic impact statement yet, the final statement of DASK released on the 7th of February (2021) (<http://www.dask.gov.tr>, **Figure 109**) states that 24,518 building damage claims have been received for Compulsory Earthquake Insurance policies from İzmir and surrounding provinces, and approximately **₺224M** (Turkish Liras) (£22.9M) were paid.



Figure 109: Official statement of DASK giving the latest numbers of damage notices and payouts as of 7 January 2021 (<http://www.dask.gov.tr>)

However, DASK states that the earthquake insurance is either not compulsory or cannot be purchased for the following buildings (<https://www.dask.gov.tr/tcip/zorunlu-deprem-sigortasi-teminat-ve-kapsami.html>):

- Buildings which belong to public institutions and organizations
- Buildings which are built in the villages
- Buildings which are fully used for commercial and industrial purposes (Office Block / Business Centre / Administrative Service / Training Centre, etc.)
- Buildings whose construction is still incomplete
- Buildings constructed without engineering principals
- Building whose main bearing structure has been weakened
- Buildings bearing structures designed and constructed against the building codes
- Buildings required to be demolished by the public offices and those with insufficient quality for living and obsolete condition

Therefore the statement about the amount of payouts for the insured losses in **Figure 109** *only* covers buildings in urban areas and the residential building types which fit to the insurance coverage policies. The extensive exemption list above makes it difficult to estimate the true cost of losses without looking to private insurance payouts as well. Moreover, public building damages can be estimated by only public institutions (particularly by the Environment and Urbanization Ministry units), which makes it even more difficult to come up with a total estimate.

We do know that the breakdown of the total financial aid allocated to the disaster region by various public institutions for relief, response and recovery efforts are as follows: AFAD (₺33M), the Ministry of Family, Labour and Social Services (₺28M), and the Ministry of Environment and Urbanization (TMoEU) (₺8M), amounting to **₺69M** (~£7M). Further we learn from Doğan (2020) that **₺120M** (~£12.3M) was paid to policyholders by private insurance and reinsurance firms.

DASK insurance coverage extends to marine risks, machinery, and equipment on board as well, and reported claims following the Aegean earthquake included tsunami damage for the first time¹. The total cost of boat damages in Izmir is reportedly about **€2.5-3M** (£2.2-2.6M) (“İzmir’de tekne hasarının toplam maliyeti 2,5-3 milyon euro”, 2020). According to the official numbers by AFAD related to tsunami impacts on boats, a total of 28 boats sank and 43 boats ran aground and 26 and 41 of these were rescued, respectively (AFAD Report no 67-81). The Turkish P&I Insurance Damage Group Manager Captain Kaan Özerk states that 250-300 boats were affected by the tsunami following Aegean Earthquake of October 30, 2020. According to Özerk, the tsunami affected 5 marinas in Izmir region which hosted 1,750 boats in total during the event, and damaged 250-300 boats in these marinas.

Based on these figures and in conjunction with the DASK’s reported payout, the total losses amount to approximately **₺415M** (~£42.5M). This figure however remains way below the **₺1.8B** (~£184M) insured losses reported by Doğan (2020).

6.2.2. Samos

(Authored by DK-F)

According to the Governmental Gazette (5293/1-12-20) the following financial impact estimations for both the earthquake and tsunami are made: (1) Provision of Free State Aid and the travel expenses of the engineers who will perform inspections amounting to €72.1M and (2) Coverage of interest on loans granted amounting to around €9M. This leads to a total economic loss equal to **€81M** (~£70.9M).

It is noted that for the buildings affected by both the earthquake and the cascading tsunami, additional Free State Aid is anticipated. In the above estimates the following state expenses have not been considered and should be added to the state’s total expenditures (samos24, 2021):

- Rent subsidies: This is granted to homeowners or tenants whose homes are damaged until these are repaired or reconstructed. The amount depends on the number of members of the household and can last up to 2 years for homeowners and up to 6 months for tenants. Reported total amount: **€17.5M**.
- One-time financial aid to cover the first needs of disaster victims up to € 586.94. Reported total amount: **€3.3M**.
- Reconstruction/repair for infrastructure. Reported total amount: **€10M**.
- Rehabilitation of monuments. For the moment, guaranteed **€600k** for bell towers retrofit and strengthening, and more to be expected.
- Expenditure on demolition, consolidation of damaged buildings, guaranteed **€700k**
- Additional **€4M** have been guaranteed for the municipalities of Samos to be used for other expenses.
- Additional expenditure not included to the abovementioned is expected to cover at least the following:
 - Financial support of affected businesses
 - Agricultural compensation
 - One-time monetary compensation of permanently injured people and to families with human losses

Overall, the announced state expenses so far are estimates as **€117.2M** (~£102.6M). This amount is expected to increase as coverage of different needs has not been yet officially announced.

6.3. Risk Transfer Mechanism

6.3.1. Turkey

(Authored by ATO)

In Turkey following the Kocaeli Earthquake on August 17, 1999 and Düzce Earthquake on November 12, 1999, the Compulsory Earthquake Insurance System (CES) was developed and launched on 27 September 2000 under the Disaster Insurances Law no 6305 put into effect in 2012 (Resmi Gazete,

¹ Following the 1999 Earthquake (August 17) of East Marmara Earthquake, sea level rise and sea surge due to tsunami impact was observed (BU-KRDAE BDTIDM, 2017) but their economic impacts were not assessed.

2012). The Disaster Insurance Institution (DASK) was established in the same year (<https://www.dask.gov.tr/hakkinda.html>). A non-profit institution, the DASK has a unique organizational structure based on the cooperation of public and private sectors.

As of January 2021, there were over 10 million insurance policies (known as *Yaşayan Poliçe* in Turkish) and over 17.5 million insured housing units with a 56.7% insurance rate in Turkey (**Figure 110** left). This ratio is slightly higher for Izmir with 61.6% (**Figure 110** right).



Figure 110: Insurance numbers for Turkey (left) and Izmir (right) in January 2021 (<https://www.dask.gov.tr/toplumsal-paylasim-etkilesimli-deprem.html>)

According to DASK, the ratio of households with CES before the Aegean earthquake was 54% along the coastline in Turkey, while for Izmir only this rate was 56%. Following the event, an 118%, 169% and 37% of increase in the insurance applications was observed in the Aegean Region, in Izmir and in the whole of Turkey, respectively (“1 milyon evin yarısı sigortalı”, 2020; “İzmir depremi DASK’a olan talebi patlattı”, 2020).

CES provides a maximum sum of insurance for residential buildings, determined every year as per the increase in the construction costs. The maximum sum insured by the CES is ₺268k for one housing unit for all building types as of January 1, 2021 (<https://www.dask.gov.tr/zorunlu-deprem-sigortasi-teminat-ve-kapsami.html>). If one prefers to buy a higher coverage in sum or the house’s value is much higher than the CES coverage, one needs to buy a private complementary insurance (**Table 6**).

Table 6: Coverage limit of CES and state and private insurance policy for residential buildings in urban areas of Turkey

	Insurance Value of the Housing	Max. Insurance coverage of the CES	Uninsured Amount	Private Policy Needed?	Number of Earthquake Policies
Example 1	220000 TL (30550 USD)	268000 TL (37.220 USD)	-	No	1 (State CES)
Example 2	500000 TL (69400 USD)	268000 TL (37.220 USD)	232000 TL (32.220 USD)	Yes	2 (State CES + Private)

6.3.2.Samos

(Authored by DK-F)

According to the official announcements, the repair and reconstruction costs based on the current price list granted to beneficiaries with damaged properties (e.g. for reconstruction of residences: €1000/m² for up to 150 m² and for repair of structural elements: €300/building m²), are covered by 80% by the Free State Aid and by 20% by interest free loan by local banks. The interest for the banks is covered by the State. The different expenses mentioned in Section 6.2.3 will be covered by the budget of different line ministries.

Moreover, in Greece only 15% of the building stock is privately insured against natural disasters. More specifically, in the affected islands of Samos, Chios, Icaria and Fournoi, 2900 buildings (residential, commercial, industrial) were insured, according to the report of the Hellenic Association of Insurance Companies (HAIC, 2020). Among them, 180 damages to buildings were declared to hold an insured value of €114.3M (total insured capital of the areas €614M) with initially estimated amount of compensation (without exemptions) equal to €3.46M. The mean declared damage is estimated at €19,238 per claimed asset and is disaggregated as following: €176.872 for industrial, €17.424 for commercial and €8.385 for residential. As expected, the majority of the damage is concentrated in Samos, with 150 buildings (5 industrial, 58 commercial and 87 residential).

As far as insurance of cars are concerned, from a total insured capital of €64,800,11 damages were declared with first estimated amount of €21,300. This corresponds to a mean declared amount of damage equal to €1,936 (HAIC,2020). No reference on possibly damaged and insured boats was found.

6.4. Casualties

6.4.1. Turkey

Casualties in Turkey due the 30 October Aegean Earthquake were reported as 116 and 1 due to earthquake and tsunami impact, respectively. In addition, a total of 1035 injuries were reported, 999 of whom were discharged within the first 5 days following the event (AFAD Report no 67).

According to an interview which was conducted with a healthcare professional from the Ege University Hospital who was in service when the earthquake hit, most of the casualties were women and children. This probably because most collapsed or heavily damaged buildings were residential, where at the time of the event were mainly occupied by children and their carers due to COVID related closures at schools. This elevated mother and child, and casualties (*interview with anonymous health professional, Ege University Hospital*).

6.4.2. Samos

Two adolescents were instantly killed by a wall of an old abandoned building that collapsed in a narrow street in Vathy. The total number of hospitalised injuries was nine, most of them elderly. 3 were transferred from the western part of the island. A 14-year old boy needed to be air-transferred by C-130 to Athens as he has suffered severe bone fractures. A 63 years old lady was also air-transferred to Athens with cheek fracture and partial rupture of spleen. At the Health Center of Karlovasi 10 people reached out for first aid.

No injuries were reported in other islands.

6.5. Emergency Response: Search and Rescue (SAR)

6.5.1. Turkey

Response to earthquake in Turkey in terms of Search and Rescue (SAR) operations, coordination of relief organizations and temporary housing is primarily organized by AFAD in line with the TAMP (Türkiye Afet Müdahale Planı - Turkey Disaster Response Plan) – the main official framework which applies to public institutions, private sector, civil society organizations and professionals to be called to duty for disaster response to regulate all disaster response operations (<https://www.afad.gov.tr/turkiye-afet-mudahale-planı>). Within this framework, AFAD, Local Governments, NGOs and other volunteers worked jointly in disaster area following the Aegean Earthquake and Tsunami for search and rescue operations. The following notes on these operations have been collated based on data collected from various web sources, interviews and the public survey.

Although AFAD is the main responsible body for SAR Operations, Izmir Fire Brigade Department was one of the most active participants of the SAR activities (*interview with Ferdi Gölcük, Fire Brigade*). The SAR operations ended by the 4th of November (*“İzmir depremi: Arama kurtarma çalışmaları sona erdi, can kaybı 114’e yükseldi”*, 2020). Turkey has a lot of experience SAR Operations from different past disaster events. One of the failures in SAR operations experienced during the 1999 East Marmara Earthquake was insufficient trained SAR staff and vehicles. During the 30 October 2020 Aegean Earthquake, about 8000 SAR staff, most of whom came from different cities and regions of Turkey, participated in the operations in the disaster-stricken area (Mazi, 2020). 17 buildings which completely collapsed during the earthquake were the focus of most of the S&R staff. Those teams worked for 5 days to save trapped people under ruins of collapsed buildings (Askin, 2020). S&R operations were well organized in comparison to 1999 earthquakes. Some other critical points related to S&R operations and experiences in Izmir can be given as follows:

- Although central government and AFAD are the main responsible bodies for S&R Operations, it is inevitable that local forces and teams will be the first responders in a disaster. Therefore, the capacity of local teams should be enhanced and more preparedness efforts, practices are needed (*interview with Ferdi Gölcük, Fire Brigade*).
- The total number of people (professional and trained staff) who took part in the S&R operations (from both public institutions and private teams) is around 8000. An additional 144 staff from Fire Brigade Department of Izmir worked for S&R Operations during the earthquake (*interview with Ferdi Gölcük, Fire Brigade*).
- AFAD has the INSARAG certificate which is very important for S&R efforts (<https://www.insarag.org/>). The Izmir AFAD S&R unit and Izmir Fire Brigade Department are currently HUSAR certification candidates (Yıldırım, 2017).
- A total of 2151 AFAD staff from different provinces of Turkey took part in disaster areas.
- This earthquake did not lead to secondary hazards such as fire (*interview with Ferdi Gölcük, Fire Brigade*).
- Following the earthquake, crowds flooded the S&R areas with the intensions of support, which soon started to pose a risk to the safety of the S&R staff and themselves due to risk of collapse and increased likelihood of COVID transmission. Similarly large numbers of people visiting hospitals to see the situation and check on their family/friends increased the COVID transmission propensity and made it hard for the health professionals to do their jobs (*interview with Ferdi Gölcük, Fire Brigade; interview with the healthcare professional, Ege University Hospital*).

6.5.2.Samos

Twenty minutes after the main shock, the General Secretariat of Civil Protection issued an early warning SMS to the citizens of Samos and some surrounding islands, informing them of a potential tsunami and to move away from coastal areas. Meanwhile, the Major General of the Fire Service, operational coordinator of the fire service of North and South Aegean and Crete, was informed directly by the Deputy Minister of Civil protection and Crisis management about the arrival of the tsunami. The police and fire brigade immediately moved to evacuate the port of Vathy. The primary challenge in the operation was traffic congestions. The coordination centre of the fire brigade in Samos requested that all the local fire stations, town mayors and military outposts provide situation updates.

Without receiving any call for rescue, the Fire Service pre-emptively led patrols to the upper old part of the city (Ano Vathy) as it was considered a vulnerable area. The first calls received by the fire service were from stores and houses along the coast as a result of the tsunami inundation (*interview with M.G. I. Stamoulis, Fire Service*).

The armed forces were immediately mobilized: a warning NAVTEX for tsunami in the Aegean was immediately issued. The army offered logistical support to the Region and municipalities. Air force helicopters provided situational awareness and rapid damage assessment minutes after the earthquake. A special rescue unit with rescue dogs was also deployed.

A few hours after the earthquake, the Minister of Civil Protection and Crisis Management was transferred to Samos alongside the General Secretariat of Civil Protection response team, search and rescue teams of the Fire Service, paramedics, engineers, and public servants of the relevant line ministries and organizations. Engineers under the coordination of the municipalities immediately started the 1st phase of damage inspection. The survey teams first assessed critical infrastructure, including the hospital, health centres, and care homes, as well as the fire service and police headquarters. The police headquarters were deemed damaged and unsafe for use. In addition, public buildings that were affected by both the earthquake and tsunami were also amongst the first to be assessed (*interview with T. Thoma, engineer EPPO*).

Within the first hour, under the command of the Major General of Fire Service, who has the general command during the response phase, a trans-organization operations centre was deployed, with the aid of the Army, in a tent in front of the damaged town hall (**Figure 111**). Representatives of the Fire Service, Police, Emergency Medical Service, the Army, the Municipality and Regional authorities participated in coordination meetings, together with the governmental members and crisis management experts. The next day, the prime minister also visited Samos and chaired a coordination meeting with

all local stakeholders, as well as disaster management representatives at central level. After request of the mayors, command of Deputy Minister and final decision of the Secretary General of Civil Protection, the Municipalities of West and East Samos have been declared in emergency state of civil protection for 6 months. This will enable fast compensations for recovery.

Figure 112 depicts the evacuated hazard zones that were deemed unsafe due to the potential collapse of buildings or structures or landslides. Hazard zones were identified as 1 seashore district at Samos, 2 districts of the old town of Vathy, 3 districts of Kokkari close to the coast, and 3 locations in Chora. First responders from the local fire service, strengthened by the search and rescue team with dogs from Athens, performed inspections in different areas with reports of collapsed buildings. They also designated dangerous areas and, in collaboration with the police, supported the evacuation from these areas. In collaboration with the volunteering groups, they coordinated the propping of buildings close to collapse, as well as the removal of precious ornaments from heavily damaged cultural buildings (**Figure 113**) (interview with M.G. I Stamoulis, Fire Service).



Figure 111: Images from the mobile coordination centre that was deployed at the town hall square of Samos (Samos24, 2020a; Eurokinissi-D.Papamitsos)



Figure 112: Evacuated zones at Samos town and Vathy (top) and Kokkari (bottom) (Municipality of East Samos)



Figure 113: Removal of precious ornaments from Karlovasi church (left; Samosvoice, 2020) and the historical town hall of Vathy (right; Municipality of Easter Samos Facebook page)

6.6. Medical Response

6.6.1. Turkey

The casualties were sent to Ege University Hospital which was the closest to the most adversely affected neighbourhoods, i.e. Bayrakli and Bornova. According to an interviewee who works in this health care facility, the hospital's disaster plan was put into effect immediately after the earthquake. Necessary task distributions were made in line with this plan amongst 70 assistants and specialist doctors in the emergency department. The capacity of Ege University Hospital was sufficient to deal with all of the 1035 injuries for being the largest hospital in the Aegean Region with >1800 beds capacity in addition to an emergency service which can be extended for service for approximately 175 people ("Ege Tıp, 64 yıldır hem şifa dağıtıyor hem de hekim yetiştiriyor", 2018). With the urgency of the event however the COVID measures were somewhat overlooked. There were also COVID positive people among the incoming patients, which in conjunction with overlooking the requirement to wear masks, resulted in an increase in COVID cases in the medical staff at the hospital (*interview with an anonymous health professional, Ege University Hospital*).

Some additional information regarding medical response are summarised below:

- In total, 31 health facilities were damaged by the 30 October Aegean Earthquake (**Figure 114**):
 - One state hospital, Buca Seyfi Demirsoy Training and Research Hospital, was damaged so heavily that it is inoperable. All staff and patients were directed to other health facilities, and the building will be demolished.
 - 10 state hospitals were slightly damaged but remained operational.
 - 20 family health centres were slightly damaged and remained operable.
- All 1035 injuries were directed to the Ege University Hospital (Ege Üniversitesi Hastanesi) which is located very close to disaster-stricken area in Bornova, Izmir. The hospital building, constructed in 1955, was only slightly damaged and remained fully operable.
- The UMKE (National Medical Teams) and 112 Acil Yardım Hizmetleri (112 Emergency Aid Service) under the General Directorate of Emergency Health Services, Ministry of Health had the responsibility for the first aid activities. More than 1100 UMKE emergency health staff worked in the disaster area (<https://www.afad.gov.tr/duyurular>).

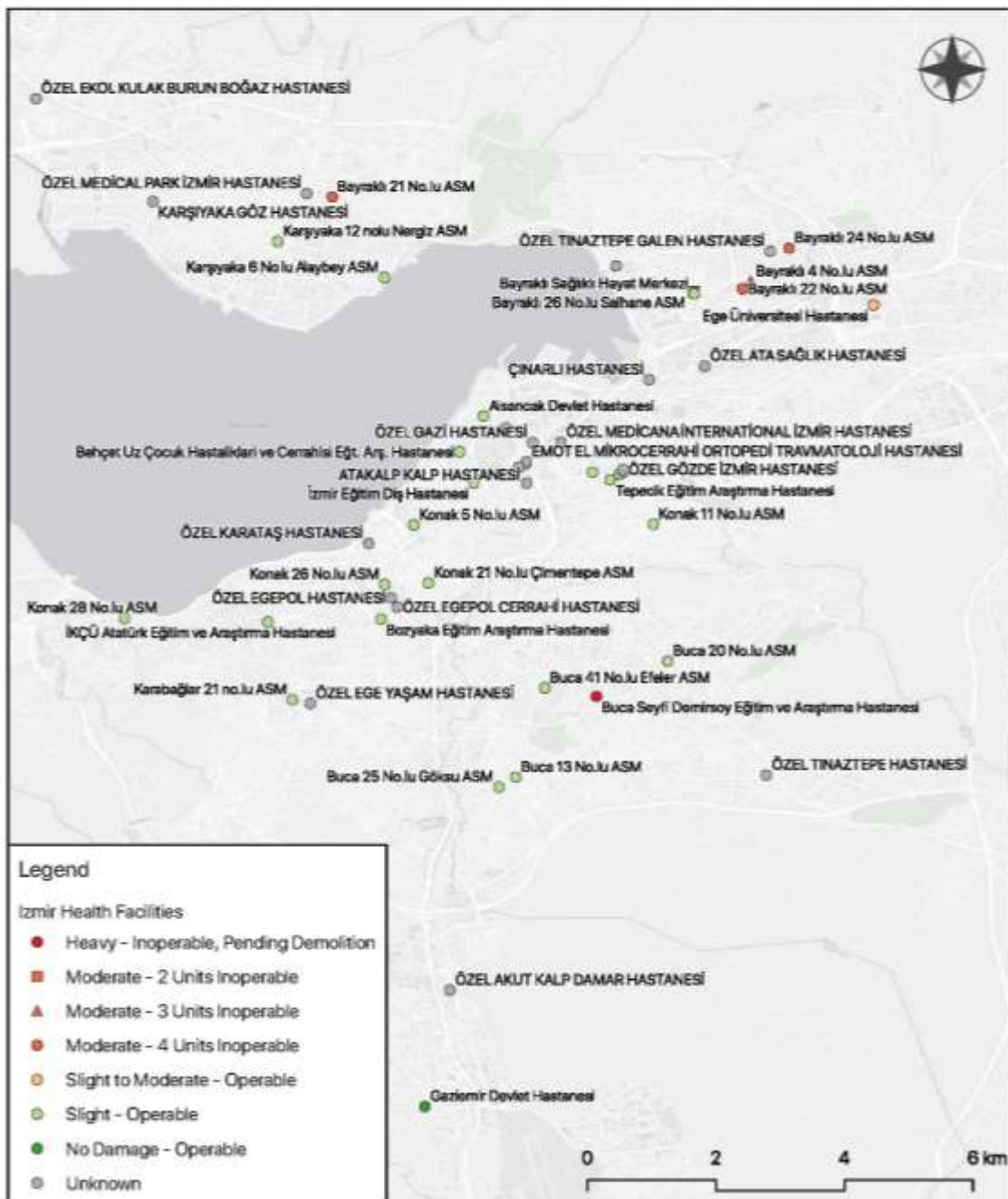


Figure 114: İzmir health facilities damage levels following the Aegean Earthquake

6.6.2. Samos

The healthcare system was not particularly heavily loaded in the earthquake aftermath. There was a total of 9 hospitalisation cases, most of them elderly. The two casualties were transferred from the western part of the island to the Hospital of Samos. Ten people received first aid treatment at the Karlovasi Health Center. The two injured people from Karlovasi were transferred to Vathy by the secondary road as the main artery was blocked, and then by military planes to Athens for specialised treatment.

Although no major problems were reported to the healthcare sector of Samos, healthcare facilities listed in **Table 7** have been reported to have been assessed, and some of them were deemed temporarily unusable. **Figure 115** maps the health facilities around Samos city and their damage levels.

Table 7: Damaged healthcare facilities (data collected and provided by Mr A. Pomonis)

Facility	Usability description
General Hospital of Samos	All buildings assessed as operational; in the main building there is need for the restoration of effects on rendering (coating)
Centre for The Education of Social Support and Training of Persons with Disabilities (CESSTP)	Assessed as operational
Public Institute of Vocational Nursery Training, Samos	Assessed as temporarily unusable and transferred to the facilities of the CESSTP
Centre of Physical/Psychological Health (CPH-KΨY), Samos	Assessed as operational
Infirmary /doctor's office of Pyrgos	Temporarily unusable
Infirmary /doctor's office of Kokkari	A container has been placed for relevant services

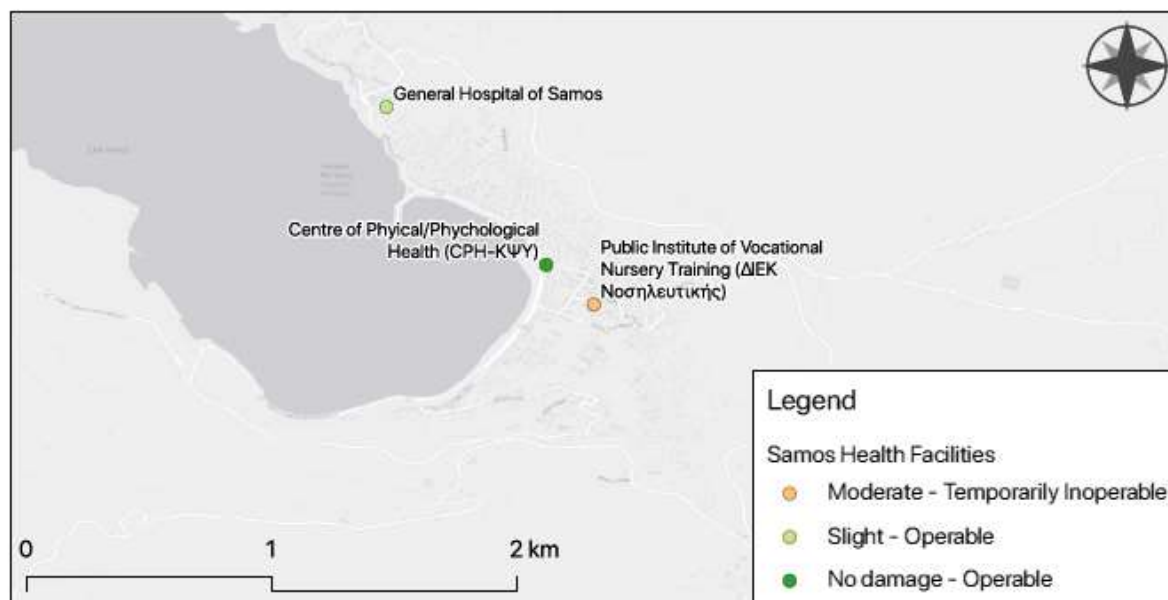


Figure 115: Samos City health facilities damage levels following the Aegean Earthquake

6.7. Temporary Shelters and Aid Distributions

6.7.1. Turkey

3120 tents (2334 tents by AFAD and 786 tents by İzmir Metropolitan Municipality) in total were installed in 18 different locations (**Figure 116**). While there is no explicit data on how many people these tents hosted, based AFAD's reported 1791 people living in 786 tents on 20 November. The total number of displaced persons is estimated at 7100 sheltered in 3120 tents. The number of tents in Izmir on 4 November was 2921, while this number dropped to 272 on 26 November (AFAD). Within central Izmir twenty temporary shelter facilities were set up. The largest of which was the Âşık Veysel Recreation Area, which initially hosted over 800 tents. The second largest temporary shelter site was Smirnia Area, which hosted 300 tents at its peak.

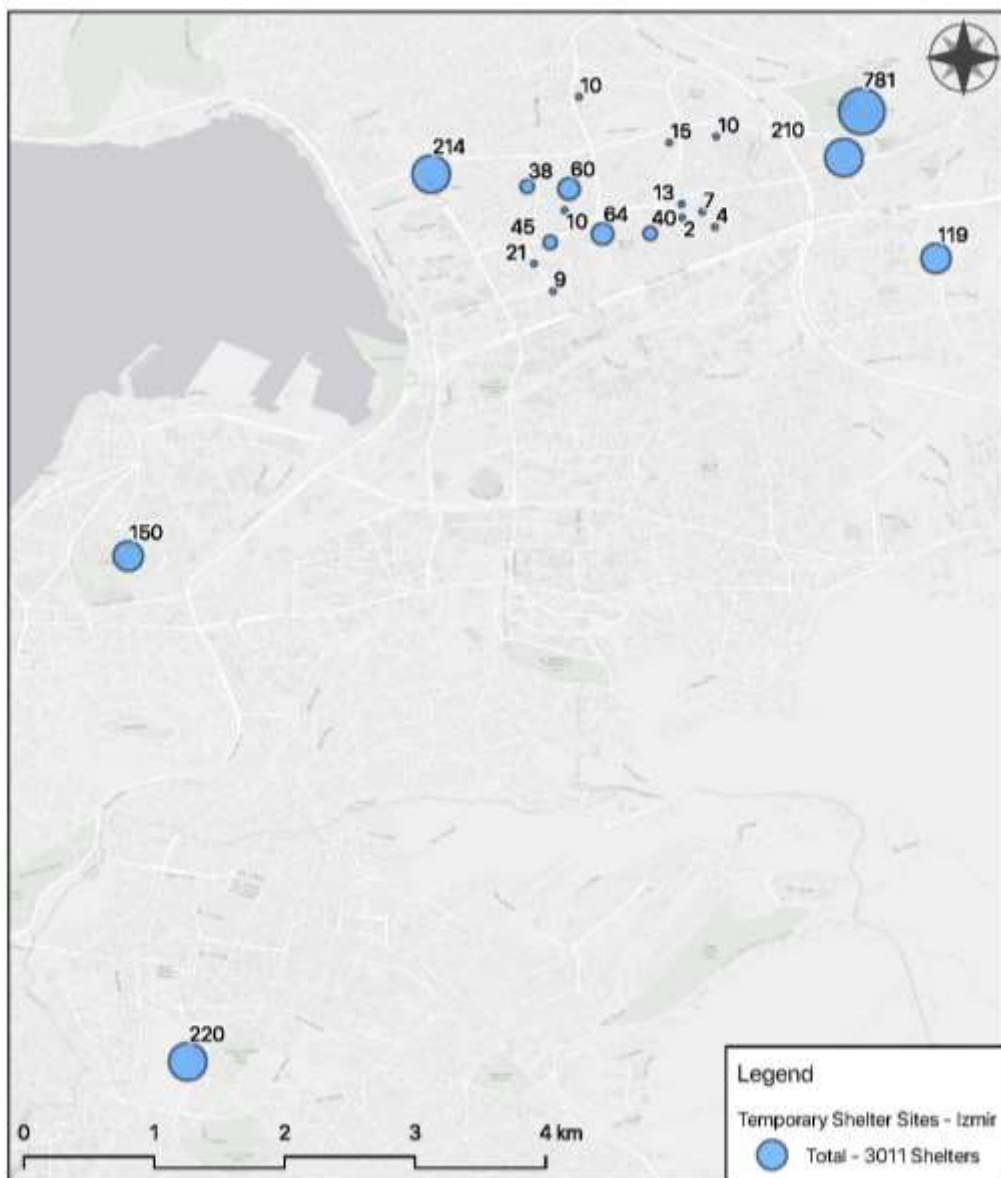


Figure 116: Shelters areas with the number of tents in İzmir as of 3 November based on data by İzmir Tabip Odası (2020)

AFAD aimed to phase out the use of tents as temporary shelters as quickly as possible. To this effect AFAD began construction of a neighbourhood for displaced persons in the Salhane in Bayraklı districts (**Figure 117**) consisting of 493 1-bedroom containers. Construction was set for completion on 04.11.2020 and displaced persons started to move into the containers twenty days after the earthquake. At the time of writing, 526 people live in 171 containers. An empty warehouse was provided to those who could not find a place immediately for storing their furniture and other belongings.



Figure 117: Temporary housing (photographs from <https://twitter.com/AFADBaskanlik/status/1329360425616617472>)

Further, to help meet housing needs, the "One Rent One Nest" campaign was launched in Izmir for private donors to provide rent support by for up to 5 months, or by granting access to an unoccupied property they own. This campaign was run in conjunction with the Needs Map Project which has been co-developed by IDEMA (<https://idema.com.tr/>).

Table 8: One Rent One Nest campaign in numbers as of 12 December 2020

Number of reported housing need	Number of people who donates rent	Total amount of donation	Number of unoccupied homes allocated to victim families	Number of families who have relocated using rent donations
8436	4643	₺42.6M (~£4.4M)	231	147

A warehouse of 11.500 m2 area in Kültür Park of Izmir was used to store aid materials. Hot meals, clothes, blankets and hygiene packages were distributed continuously. Over a million packages of hot meals were distributed from 51 distribution points (<https://www.afad.gov.tr/duyurular>). While Twitter and other social media were very helpful for communicating needs of the earthquake victims, they often provide inaccurate impression of critical needs, leading to an accumulation of unnecessary aid materials in the disaster area (*interview with Mert Aksoy, Lokman Hekim Sağlık Vakfı*). The clothing needs of the earthquake victims were met by the aids donated to the area. Second hand clothing aids were not accepted (*interview with Mehmet Sarıca, IDEMA*).

Further, psychosocial support was provided in the shelter areas under the organization of Ministry of Family, Labor and Social Services from the very first moment (*interview with Sude KILIÇ, World Human Relief*). Internet infrastructure was established for students living in the container city. Computer and tablets were provided by the Ministry of National Education.

Communication points were developed within neighbourhoods where representatives from AFAD and District Governorship collected demands and wishes from victims.

Following the 30 October 2020 Aegean Earthquake we overall observe a strong civic action and good cooperation between NGOs and public bodies for recovery beyond the immediate physical needs - an approach first used at the 24 Jan 2020 Elazığ Earthquake, and further developed at the 26 March 2020 Van Earthquake and refugee crises in March and April 2020. This cooperation was excelled in this particular event (interview with Mehmet Sarıca, IDEMA).

6.7.2. Samos

According to initial estimates, the earthquake and tsunami displaced over 400 families across Samos, pending a secondary inspection of their homes. A 40-tents camp was set up by the army in the stadium of Vathy (**Figure 118**). From the first day, some hotels were employed as emergency shelters. Several people initially used their own tents as makeshift shelters (**Figure 118**) or slept in cars until they found other arrangements. The Ministry of Migration and Asylum offered; 20 tents, 1000 blankets, 500 sleeping bags and 265 camp beds. The Hellenic Red Cross and UNHCR Greece provided 100 tents. A navy ship was made available for emergency sheltering but was not used. The army set up additional camps in Karlovasi, Pythagoreio, Kokkari and Chora (**Figure 119**).

The first day after the earthquake, the Ministry of Migration and Asylum issued 21 containers to be used as temporary shelters to the West and Eastern Municipalities of Samos (**Figure 120**). These containers were transferred from the refugee camp of Zervos (Samos). The containers were distributed to different communities along the island; Konteika, Platanos, Koumeika, Leka, Kontakeika, Ydroussa, Karlovassi, Kokkari, Mavratzaioi, Pagondas and Vathy. They were primarily used to shelter mostly elderly people that did not wish to move away from their homes (especially at Konteika and Platanos). Some of the containers were used as a warehouse or infirmary (*Interview by A. Tatouris, Head of CP R.U. Samos*). The municipalities expect to receive more containers to be used as classrooms.



Figure 118: Tent camp in Vathy deployed by the army the first day (skai news, 2020) and improvised tent at Koumeika

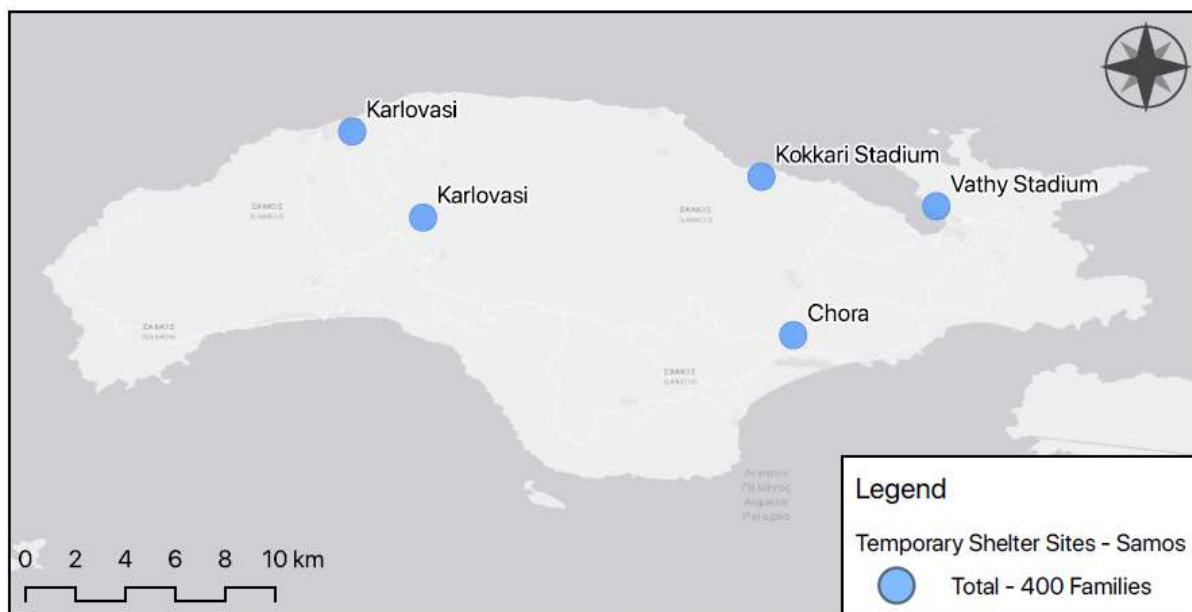


Figure 119: Location of emergency temporary shelters throughout the island



Figure 120: Container used as infirmary at Kokkari (samos2000goal, 2020); settlement of containers at Konteika

Organized camps lasted less than 10 days (*Interview by A. Tatouris, Head of CP R.U. Samos*). The general guidelines are to keep the duration of the camps as short as possible and due to the ongoing pandemic, this need was even more urgent. Food and non-food items were distributed to those affected by the Hellenic Red Cross and other Non-Governmental organizations with an established presence in Samos (**Figure 121**). The primary responsibility of aid provision rests with the municipality which was responsible for the coordination of aid.



Figure 121: Food distribution by the Army (skainews, 2020) and managing of the humanitarian aid received in Samos by the Hellenic Red Cross (achaianews, 2020)

6.8. Recovery

6.8.1. Turkey

(Authored by ATO)

- The TMOEU was the only institution who took part in the building damage assessment: other organisations were not called to duty (*Interview with Eylem Ayatar, Chamber of Structural Engineers Izmir Branch*). The TMOEU categorised damage under five levels; undamaged, slightly damaged, moderately damaged, heavily damaged and collapsed buildings. Earthquake victims, whose homes were categorised as undamaged and slightly damaged were authorised to reoccupy their homes. Moderately damaged households were asked to retrofit their homes before reuse within 1 year. The heavily damaged buildings will be demolished by the ministry, and the owners of these will be moved to a different home within a year. Following the removal of debris of collapsed buildings, it is not clear what will be planned for the empty areas.
- The Chambers of Structural Engineers, Architects and Geomatic Engineers offered detailed technical consultation on the damage levels, both upon direct requests from the earthquake victims themselves and invitation from the Izmir Metropolitan Municipality (*Interview with Eylem Ayatar, Chamber of Structural Engineers Izmir Branch; interview with Ilker Kahraman, Chamber of Architects*). These Chambers forming the Izmir Provincial Coordination Board initiated an open data platform to crowd-source information of damage (*interview with Ilker Kahraman, Chamber of Architects*).
- Homeowners who lost their homes during the earthquake were offered ₺5000 for moving costs and ₺8000 for other needs. Each homeowner and tenant within moderately damaged buildings were paid ₺5000 and ₺2500, respectively. The Social Security Foundation (*Sosyal Guvenlik Kurumu* in Turkish) offers an additional of ₺30k TL through using AFAD's aid list to those who cannot get their belongings from heavily damaged or collapsed buildings. A total number of 4.600 residences and 419 workplaces benefitted from these payments.
- Lack of a detailed building inventory emerges as a critical issue to be addressed in the coming periods (*Interview with Eylem Ayatar, Chamber of Structural Engineers Izmir Branch*).

6.8.2. Samos

(Authored by DK-F)

As presented in Section 6.2, the government will provide financial aid for buildings repair or reconstruction (residential, commercial, industrial, public). Owners or tenants of the buildings have requested funds proportional to the extent of damage incurred by their property. Additionally, funds have been pledged to the municipalities for the repair of damaged infrastructure, including ports. Funds have also been set aside for shoring works of hazardous bell towers of multiple churches in Samos.

Following the death of two adolescents, killed by a collapse wall while walking past an abandoned building, the government launched an initiative to address the issue of dilapidated buildings posing hazardous conditions. A new legal framework to encourage the rehabilitation or demolition of buildings was announced, which includes the registration and marking of dilapidated buildings throughout the country. Municipalities will undertake the demolition of dilapidated buildings with financing secured by the state. Incentives and subsidies have been announced to encourage the maintenance and rehabilitations of derelict buildings. The demolition of the most dangerous buildings started one month after the earthquake with the building that killed the two adolescents (**Figure 122**).



Figure 122: Shoring of near collapse buildings (“Mikres diadromes” you tube channel) and demolition of dangerous buildings (“Agakliazo ti Samo” facebook page)

The municipality has prioritised the rehabilitation of schools to ensure the rapid resumption of classes upon the lifting of lockdown restrictions. The president and other representatives of the Earthquake Planning and Protection Organization (EPPO) performed meetings with directors of local schools and other stakeholders to provide training on safe response during an earthquake in the school environment. The president of EPPO in collaboration with the Heads of Health Education and the Heads of School Activities of Primary and Secondary Education (Samos24,2020b) announced supplementary earthquake and tsunami awareness programs.

In Samos and Icaria, schools remained closed from Oct 31, 2020. The country entered lockdown due to the COVID pandemic on Nov 7. Primary schools opened again Jan 11, 2021 while schools of higher grades have remained closed up to the time of writing. According to the municipality of Samos, the primary school of Vathy and the Nursery of Palaiokastros are being relocated. The Pagonda and Mitilinioi (**Figure 123**) primary schools will be reopened after rehabilitation works are completed. The Chora primary school and Nursery will both temporarily continue to operate in containers. Agios Konstantinos primary school and the 3rd Primary school will open normally. Repair and retrofitting works have been undertaken at some other schools to render them safe to use.



Figure 123: Primary school of Mitilinioi, confinement of the walls with external straps (left); repair works at Agios Konstantinos Primary School, so that their function can be resumed (Municipality of Eastern Samos Facebook page, 16.01.20)

6.9. Compound disasters - impacts of the COVID-19 pandemic

(Authored by JC, DK-F and ATO)

Neither Turkey, nor Greece had specific protocols for response to earthquakes during a pandemic.

No statistical observations relating to COVID-19 caseloads following the earthquake can be made for the region of Izmir as only national figures are published. However, two first-hand accounts obtained

through the interviews highlight some of the compound effects COVID-19 on the earthquake. The first observation from a health professional (*anonymous*) at Ege University Hospital relays that there was a surge in COVID-19 cases amongst hospital staff in the days immediately following the earthquake. The second relates to an interview with the head of the fire service of Izmir province who expressed that training drills had to be cancelled in the half year preceding the earthquake due to the high number of COVID-19 cases amongst the ranks of firefighters. Additionally, a number of firefighters were tested positive with COVID-19 during the earthquake and could therefore not participate in the emergency response.

As Greece entered a period of lockdown a week following the earthquake, the region of Samos was exempted from complete lockdown to facilitate aid and emergency support. During the emergency response, the authorities took special precautions to minimise the coronavirus contagion risk among the first responders, relief workers, engineers and the affected population. Social distancing had to be maintained while relief items distribution was taking place (Thoma, 2020). Sheltering of displaced persons in temporary shelters and camps was therefore minimised phased out as rapidly as possible. Moreover, people seeking treatment at hospitals were tested for COVID-19 upon arrival (Thoma, 2020).

The first 15 days following the earthquake no significant increase in COVID cases were observed. On 10/12 the Municipality of Eastern Samos requested the central government adopt stricter COVID-19 measurements due to an increase in registered cases. This surge in cases may be correlated to the influx of response personnel to the island. However, no conclusive trends can be drawn owing to a lack of data and due to a general surge in COVID-19 cases in Greece overall.

Due to limited data, the extent to which COVID-19 hampered the response to the Aegean earthquake and tsunami in both Greece and Turkey remains unclear. The next section describes how lockdown restrictions in place at the time of the earthquake significantly altered the occupation rates of different building types, thereby affecting morbidity rates.

6.10. Public Survey

(Authored by JC)

We highlight a selection of key findings from the public survey below, highlighting community building stock, preparedness, and response to the actual events. Results are non-exhaustive but indicative of predominant themes that surfaced when analysing the survey data.

6.10.1. Residential building stock and impact of damage

The survey questioned respondents on their home's properties, to better understand how these relate to their experience/perception of the event in Samos and Turkey. In Turkey, most respondents lived in reinforced concrete homes that were between 20-50 years old. The floors varied – most commonly 1 (likely single home) or 5-10 (like multi-family homes, such as apartment buildings). In Samos, reinforced concrete homes of 20-50 years were also most common (though only marginally more than homes age 10-20 years). The majority of respondents lived in structures between 2-4 floors (**Figure 124-125**).

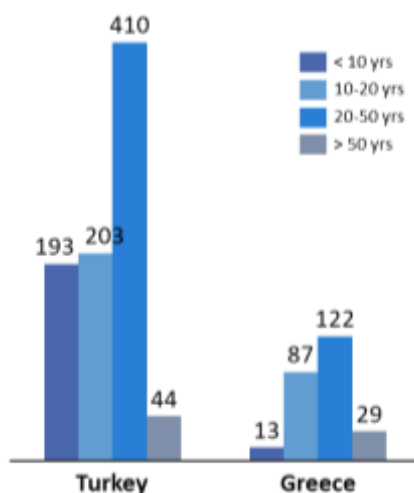


Figure 124: Overview of the residential building stock in Samos (Greece) and Izmir (Turkey) – building age

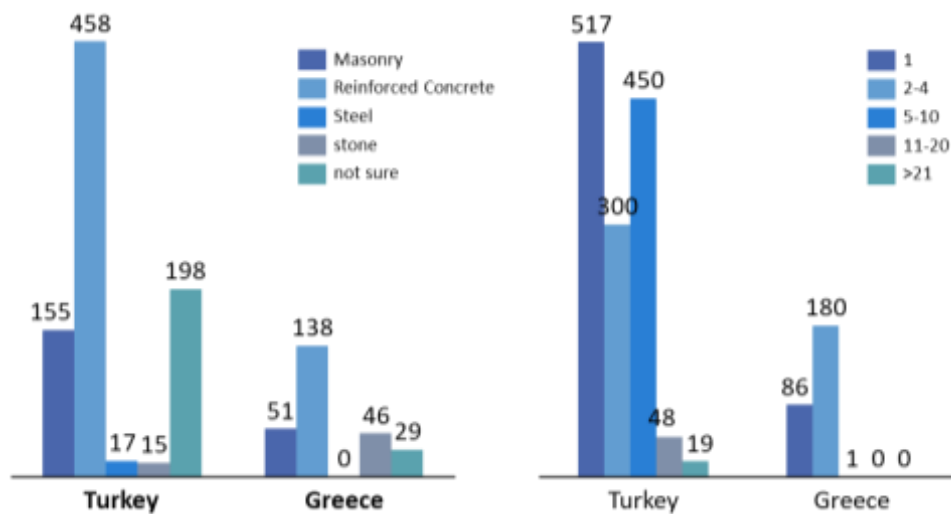


Figure 125: Overview of the residential building stock in Samos (Greece) and Izmir (Turkey) – primary structural material (left), number of floors (right)

6.10.2. Occupancy rates at the time of the event

Time of event and occupancy rates are critical in seismic and tsunami casualty estimation. The surveys provide valuable insight into Samos and Izmir's occupancy rates and the effects of local COVID-19 lockdown measures on occupancy rates. The earthquake occurred in the middle of the day on a Friday (14:51 Turkish time), a time when home occupancy rates would typically be lower, as more people would be in schools or workspaces. However, in Turkey, schools were fully closed due to COVID-19 lockdown measures; 59% of respondents were at home and only 17% at work. On the other hand, Greek schools were open, and a lower figure (47%) of respondents were at home, and 33% at work. See **Figure 126** for the occupancy distribution.

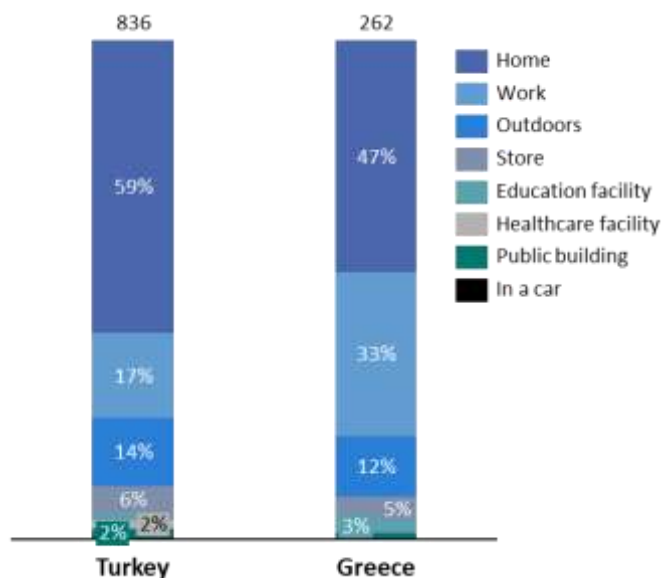


Figure 126: Occupancy rates

6.10.3. Risk perception and risk transfer

Respondents from Turkey reported a high level of seismic hazard awareness before the Aegean earthquake, **Figure 127** Only 4% said they were not aware that their region was prone to earthquakes, compared to 33% of Greek respondents. Turkish respondents also attributed a much higher level of seismicity. Regarding tsunami awareness, 57% of Greeks were aware of a tsunami's possibility compared to only 35% of Turkish respondents. **Figure 128** depicts the respondents' post-event perception of seismic hazard within their lifetime. Turkish respondents appear to have a significantly

higher perception of a seismic risk than their Greek counterparts, also feeling less safe in their current homes.

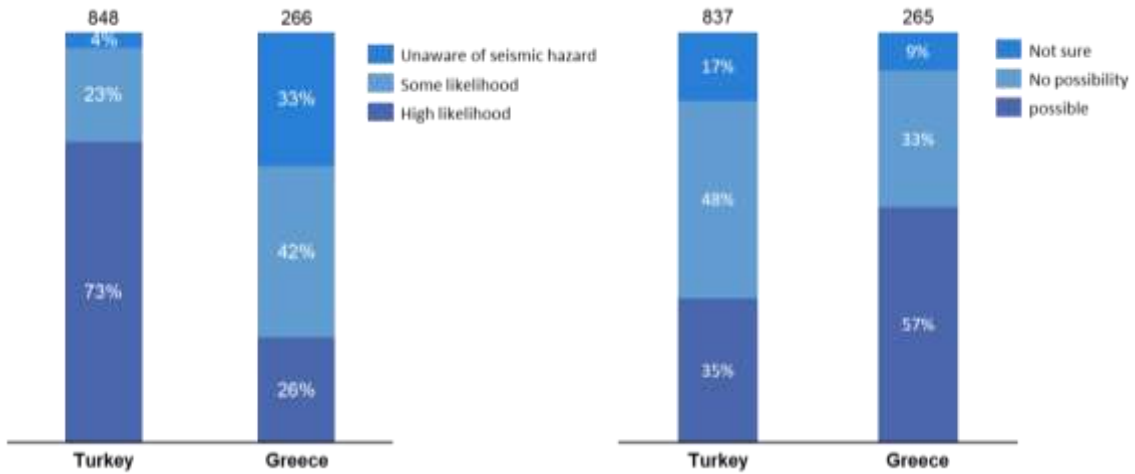


Figure 127: Pre-event knowledge of earthquake likelihood (left) and the possibility of a tsunami in each region (right)

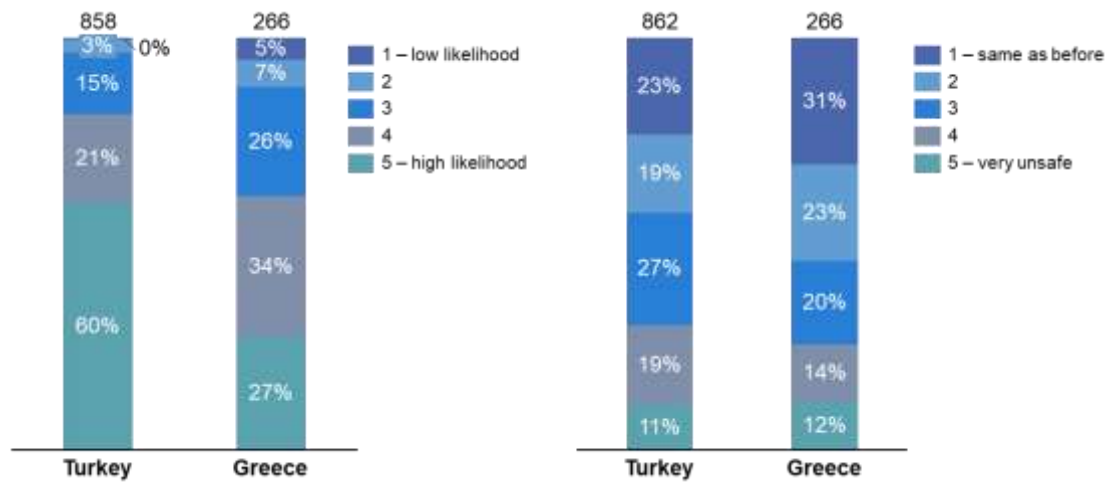


Figure 128: Likelihood of the region being affected by another earthquake equal or greater in size than the Aegean earthquake (left) feeling of safety in their current home (right)

51% of Turkish respondents reported having earthquake insurance. In Greece, where earthquake insurance is not mandatory, only 12% did (Figure 129). For many Turkish respondents, this insurance was likely DASK, which is the mandatory earthquake insurance provided by the Turkish Catastrophe Insurance Pool (TCIP). The official DASK insurance rate up-take for the Izmir region of 57%, equating to 635,600 residential properties (see Section 6.2.3).

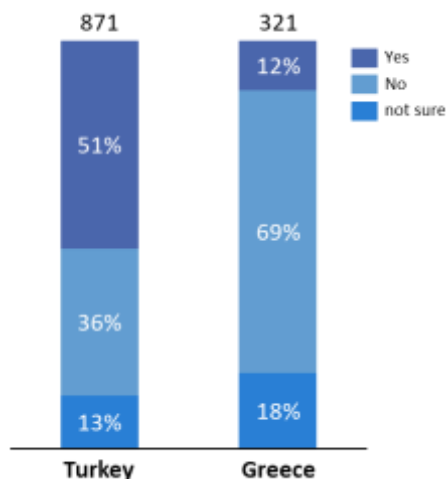


Figure 129: Earthquake insurance rate up-take

6.10.4. Preparedness for a seismic event or tsunami

Despite having a higher perception of seismic risk than their Greek counterparts, fewer Turks felt prepared for them. 44% were unsure what to do during an earthquake, compared to only 8% of Greeks, **Figure 130**. A smaller subset of both populations felt prepared for a tsunami, 52% compared 82% for Turkey and Greece, respectively. Respondents reported that when alerted to the tsunami they either moved away from the coast to higher ground (mostly by car), or to the highest level of a nearby building.

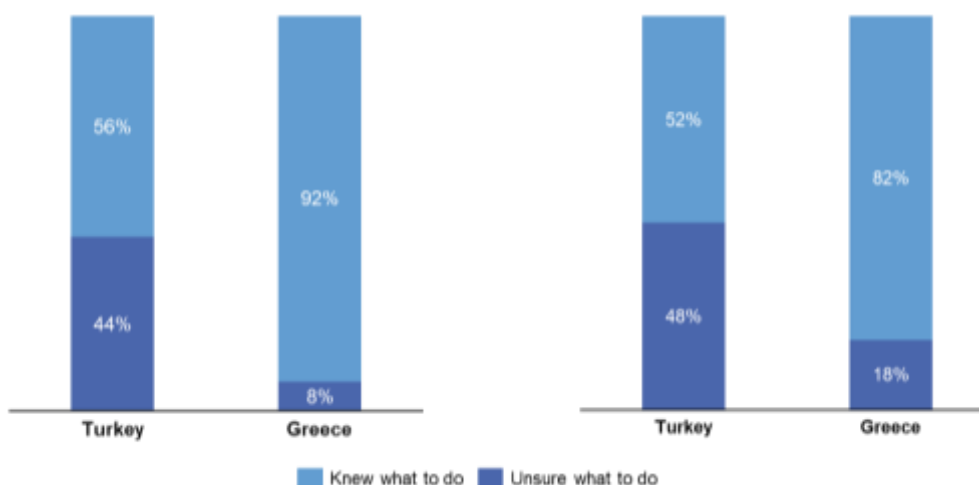


Figure 130: Levels of perceived preparedness for seismic (left) and tsunami events (right)

This disparity can be related to where respondents get their information. Greek respondents commonly learned about earthquake preparedness in school, 50%, whereas 53% of Turkish respondents said they used media sources (i.e. news, social media, internet), as shown in **Figure 131**. This suggests that school-level training plays a significant role in helping Greeks' appropriate response measures. In Turkey, while media is a popular channel to learn about preparedness, it does not appear as practicable as formal training. Further research is required to determine the most impactful ways of delivering preparedness training at a community-wide level. Many Turkish respondents expressed a desire to obtain more information on preparedness (see section 6.10.8).

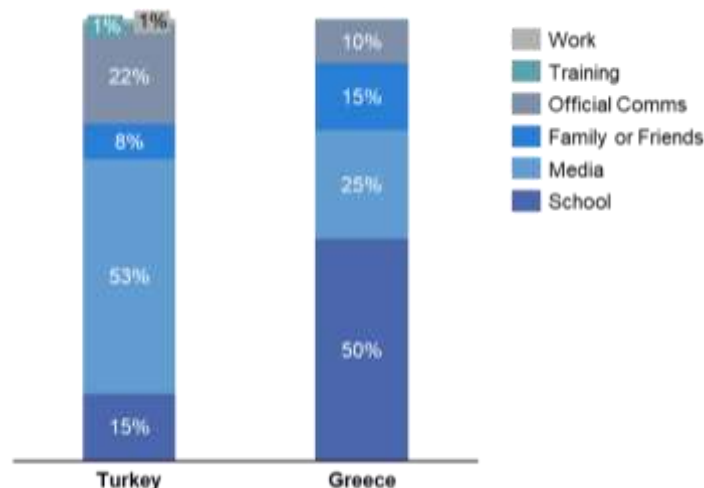


Figure 131: Sources of pre-existing knowledge of earthquakes and preparedness

6.10.5. Earthquake response

The surveys questioned respondents how they first responded to the ground shaking. In both Greek and Turkish surveys, roughly half of the respondents reported calling family or friends. The other half reported running outdoors. Several respondents mentioned packing or grabbing emergency packs or turning off the gas before heading outside. Others describe helping to evacuate buildings. In Samos, multiple respondents reported rushing to the schools to pick up their children.

Particularly in Izmir, people's outpour into the streets created a general sense of chaos. It led to severe traffic, compounded by debris that fell onto the roads. The traffic blockages slowed emergency response services. In Izmir, the experience of our health professional interviewee was that the travel time for a usual 20 min car journey stretched to 2-hours that evening as they tried to reach the hospital. Multiple search and rescue personnel reported similar gridlocks, often opting to leave their car behind and proceeding on foot.

6.10.6. Tsunami response and early warning

The Aegean tsunami was the first time the Greek Civil Protection issued a tsunami early warning. The surveys provide insight into the efficacy of the tsunami early warning. Of the respondents within a tsunami-affected area, 61% of those from Turkey received no warning compared to 10% of Greeks. Half of the Greek respondents received the early warning through SMS, 6% heard alarms and sirens, and 13% saw the sea receding. In Turkey, those that received warning either saw the sea receding (11%) or were given a warning by others (17%). Nine respondents reported receiving an early warning SMS but were not near an affected area (**Figure 132**).

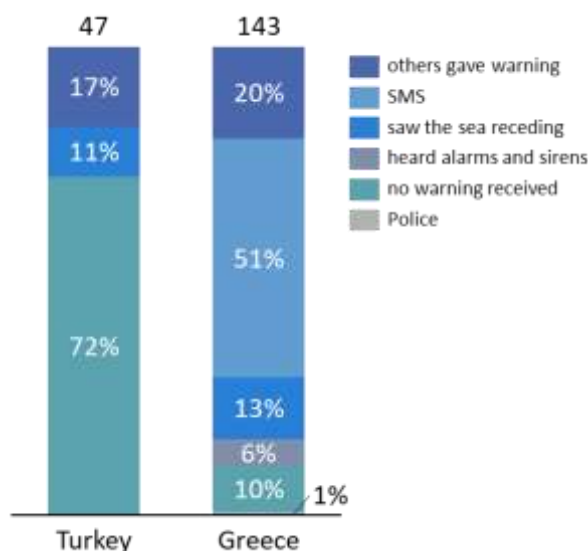


Figure 132: Method of tsunami early warning (% of respondents who lived or were in a tsunami-affected area)

6.10.7. Disaster causes and preventability

High rates of Greek (~77% total) and Turkish respondents (~95% total) believed that the disasters were preventable. Only 4% of Turks and 10% of Greeks felt that events were out of control. 94% of Turkish and 77% of Greek respondents attribute the disaster to poor construction practices or insufficient retrofitting (see **Figure 133**).

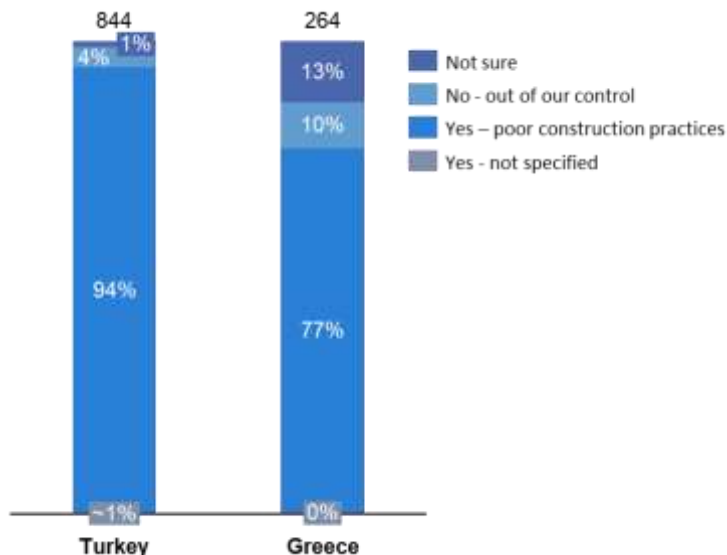


Figure 133: Disaster preventability

In terms of emergency services, however, respondents in both countries expressed favourable views. 67% of Turkish and 53% of Greek respondents rated emergency and services highly (**Figure 134**).

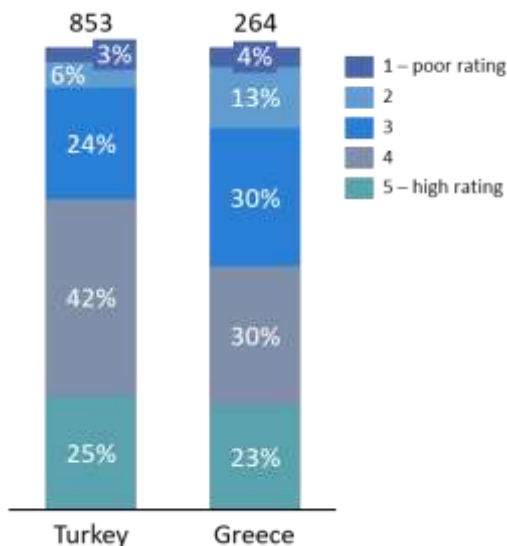


Figure 134: Assessment of emergency services

6.10.8. Additional respondent input

Respondent provided further observations concerning the event. Below are some of the reoccurring themes:

Turkey

- Causes of the disaster: Most attributed the causes of the disaster to poor planning and construction practices. There is a prevalent frustration with the lack of control and accountability over poor building quality, especially multi-storey rented apartment blocks

- **Traffic:** Multiple respondents highlighted traffic choking-up resulting from the general panic and chaos on the streets as people rushed outside. Several respondents recommended measures to unblock traffic and maintain traffic-free corridors for emergency services.
- **Preparedness:** Many highlighted the need for improved preparedness and education measures, including first aid training.
- **Communication channels:** Several wanted to see improved communication channels between government authorities and individuals to provide information on aid distribution provisions.
- **Poor ground conditions:** In addition to shoddy construction practices, many respondents identified the poor ground conditions (especially in the Bayraklı area) as amplifying seismic risk and being one of the primary causes of building damage.

Samos

- **Causes of the disaster:** In Samos, most respondents attribute the building damage to old and poorly retrofitted builds that are often dilapidated and abandoned. Multiple respondents highlighted the continuing risk these buildings posed in the event of aftershocks and recommended their demolition.
- **Preparedness:** Many would like more education/ training on what to do in the event of an earthquake.
- **Response-Relief-Recovery Communication:** There is a desire for more information regarding the authorities' plans and actions towards the response-relief-recovery.
- **Tsunami early warning:** The tsunami early warning SMSs reportedly caused widespread panic and confusion and resulted in traffic congestion, especially near the port.

References

- 1 milyon evin yarısı sigortalı. (2020, November 1). Retrieved from Sozcu: <https://www.sozcu.com.tr/2020/ekonomi/1-milyon-evin-yarisi-sigortalı-6106873/>
- Achaianews (2020). "Sending aid to the victims of the earthquake in Samos". Available at: <https://bit.ly/3pX3HYe> (last accessed 23/01/21)
- Askin, N (2020) "Arama kurtarma ekipleri İzmir depreminde yoğun mesai harcadı" (2020, November 4) Retrieved from Ilkha: <https://ilkha.com/guncel/arama-kurtarma-ekipleri-izmir-depreminde-yogun-mesai-harcadi-142484><https://ilkha.com/guncel/arama-kurtarma-ekipleri-izmir-depreminde-yogun-mesai-harcadi-142484>
- BU-KRDAE BDTIDM. (2017). *Türkiye ve Tsunami Riski*. Retrieved from B.Ü. KRDAE Bölgesel Deprem-Tsunami İzleme ve Değerlendirme Merkezi: <http://www.koeri.boun.edu.tr/sismo/2/tsunami/turkiye-ve-tsunami-riski/>
- Doğan, N. (2020, November 10). *İzmir'de hasar ödemeleri başladı*. Retrieved from Hurriyet: <https://www.hurriyet.com.tr/yazarlar/noyan-dogan/izmirde-hasar-odemeleri-basladi-41657926>
- Ege Tıp, 64 yıldır hem şifa dağıtıyor hem de hekim yetiştiriyor (2018) Retrieved from: https://ege.edu.tr/a-2267/ege-tip-64-yildir-hem-sifa-dagitiyor-hem-de-hekim-yetistiriyor_.html#:~:text=Ege%20%C3%9Cniversitesi%20T%C4%B1p%20Fak%C3%BCitesi%20Hastanesi%20bin%20806%20yatak%20say%C4%B1s%C4%B1%20ile,birlikte%20100%20sedye%20say%C4%B1s%C4%B1na%20ula%C5%9Fabiliyor.
- Hellenic Association of Insurance Companies (2020). "Financial damage from the earthquake sequence of Samos, 30th October 2020" (in Greek).
- İzmir depremi DASK'a olan talebi patlattı. (2020, November 16). Retrieved from Sozcu: <https://www.sozcu.com.tr/2020/sigorta/izmir-depremi-daska-olan-talebi-patlatti-61>
- İzmir depremi: Arama kurtarma çalışmaları sona erdi, can kaybı 114'e yükseldi (2020, November 4). Retrieved from BBC: <https://www.bbc.com/turkce/haberler-turkiye-54810440>
- İzmir Tabip Odası (2020) İzmir Depremi Değerlendirme Raporu. Türk Tabipleri Birliği
- İzmir'de tekne hasarının toplam maliyeti 2,5-3 milyon euro. (2020, December 1). Retrieved from 7Deniz: <https://www.7deniz.net/mobil.php?islem=haber&id=36349>
- "Mikresdiadromes" youtube channel: <https://www.youtube.com/channel/UC2eraxpvAND7VFC6F7GEqGw>
- Mazi,I (2020) AFAD'ın 'kahramanları' İzmir depreminde hayat kurtaran faaliyetlerini anlattı (2020, November 12). Retrieved from AA: <https://www.aa.com.tr/tr/turkiye/afadin-kahramanlari-izmir-depreminde-hayat-kurtaran-faaliyetlerini-anlatti/2041165>

- NPHO (2020). Epidemiological surveillance report, National Public Health Organization. <https://eody.gov.gr/en/>
- Resmi Gazete. (2012, May 9). *Afet Sigortalari Kanunu*. Retrieved from Resmi Gazete: <https://www.resmigazete.gov.tr/eskiler/2012/05/20120518-4..htm>
- Samos24 (2020a). "Meeting of Regional Councilors of Samos Prefecture under the Regional Governor" (in greek). Available at: <https://bit.ly/2Oa0HJY> (last accessed 23/01/21)
- Samos24 (2020b). "Efthymios Lekkas on the Board of the Municipality of Eastern Samos: At 7 magnitude and not at 6.7 the earthquake in Samos" (in Greek) Available at: (last accessed 23/01/21).
- Samos24 (2021). "Additional funding of 10 million to Samos for infrastructure and ports" (in greek). Available at: <https://bit.ly/39POp1y> (last accessed 23/01/21)
- Samosvoice (2020). "The cleansing of the church Koimiseos Theotokou of Karlovasi began" (in Greek). Available at: <https://bit.ly/3rpOhfd> (last accessed 23/01/21)
- Skai news (2020). "Army assistance to Samos: Tents, food distribution, road network restoration" (in Greek). Available at: <https://www.skai.gr/news/greece/syndromi-tou-stratou-sti-samo-skinis-dianomi-fagitou-apokatastasi-odikou-diktyou> (last accessed 23/01/21)
- Samos2000goal (2020). "Prefabricated doctor's office in the Parking of the Municipal Community of Kokkari Samos to cover any emergencies", Blogspot. Available at: <https://samos2000goal.blogspot.com/2020/12/blog-post.html?sref=fb&m=1> (last accessed 23/01/21)
- Thoma, T. (2020). "Samos 30/10/2020 earthquake amid a pandemic", Webinar on EQ in the midst of the pandemic, Europa Major Hazards Agreement, Council of Europe, Earthquake Planning and Protection Organization, 19th November 2020. Available at: <https://rm.coe.int/presentation-by-the-earthquake-planning-and-protection-organisation-an/1680a07b72>
- Yıldırım, M. (2017) Arama Kurtarma Ekiplerinin Standartlaştırılması. 1st Disaster and Pre-Hospital Management in Middle East Congress, 8-11 October, 2017, İstanbul. Retrieved from: https://file.atuder.org.tr/_atuder.org/fileUpload/BXxiTEBgQjng.pdf

7. SOCIAL MEDIA ANALYSES

(Authored by DiC and SW)

In recent years, social media (SM) has become a valuable tool for quickly collecting large amounts of data relating to disasters. It offers first-hand data, observations, sentiments, and perspectives (Yan, Chen, & Wang, 2020). This data can range from photos, videos, and comments uploaded to various internet platforms and apps such as Facebook, Twitter, Instagram, and/or specialist disaster monitoring apps such as LastQuake app from EMSC or 'Did you Feel it' from the United States Geological Survey (USGS). We have used SM in this EEFIT mission as a complementary data source of damages in buildings and lifelines, post-disaster needs, preparedness, emergency response, and post-disaster recovery. Available data and its usefulness are a rapidly evolving field, and in this report, we present some of the methods we have used to collect information in this mission.

Earthquake detection and SM analysis is a current active field of study. Correlation between the number of tweets and the intensity of an earthquake was observed for the first time in 2010. During the Tohoku earthquake, researchers observed the high correlation between the number of tweets and the earthquake's intensity in some locations (Doan, Vo, & Collier, 2012; Murakami & Nasukawa, 2012). The correlation between the number of tweets and Mercalli intensity was demonstrated in the earthquakes of California, Japan, and Chile by Kropivnitskaya, Tiampo, Qin, & Bauer, (2017). Later, Mendoza, Poblete, & Valderrama (2019) confirmed that high-intensity earthquakes produce a greater number of Mercalli reports and, therefore, consider SM a valid source of spatial information rapid estimation of earthquake damages. Furthermore, the extraction of sentiments during a disaster contributes to a vital situational awareness of the disaster zone dynamics. For example, Wu and Cui (2018) used SA to measure each tweet's emotion or mood and classified it as positive, negative, or neutral and confirmed that the severity of damage in one area is correlated with the disaster-related activity. Social media provides opportunities for engaging citizens in emergency management by disseminating information to the public and provide them access to it (Simon, Goldberg, & Adini, 2015). The SM is useful to mobilise the population and provide them with the most up-to-date information, which might not be available through alternative official channels (Lerman & Ghosh, 2010).

In this chapter we investigate if we can extract from SM meaningful information from image and text data related to the event. We believe that there will be a positive correlation between general earthquake impacts, and the number of tweets and intensity reports with negative polarity, while on the other side, there will be a positive correlation between the distance to the epicentre and the number of reports with positive polarity also identified in text and image data extracted from SM. Although we do not test this in this report, we investigate the sort of messages that are tweeted, whether we can ascertain their polarity and their location as well as what other useful information can be extracted, with the aim of identifying learning points which can inform the use of SM for future Missions.

On October 30, 2020 EEFIT members were alerted to the seismic event through posts on Twitter that later were forward to them by the community manager of the project's Twitter account: Learning from earthquakes: Dr Diana Contreras. This initial Twitter information and the links to videos, pictures, and preliminary reports of the event were major sources of information for EEFIT to decide to deploy a mission. Data extracted from SM aids in the selection of the areas to deploy the missions on-site.

7.1. Data Sources

This report contains two primary social media data sources: 1) LastQuake app and 2) Twitter. LastQuake is a crowdsourced-based earthquake information app developed by the European-Mediterranean Seismological Centre (EMSC). This Centre, provided the data for free through personal contacts, while the Twitter data was purchased from TweetBinder, a third-party vendor. This app allows eyewitnesses to share information about earthquakes they have felt, combined with seismic data. LastQuake app users report these data expressed in Modified Mercalli Intensity (MMI) through selecting one of the images included in the app that best resembles the effects of the earthquake on-site (Bossu et al., 2020; Fallou et al., 2020); its interface is depicted in **Figure 135**. The European-Mediterranean Seismological Centre provided us with 3,028 Intensity reports from LastQuake app users. After processing the initial dataset, we eliminated reports and reports without a meaning (Eg. Û†Ø¹Û... Ø§Û†Ø§ Ø-Ø³ÛŠØª Û• ÛŠØ§) or reports coming from outside the affected area. Eventually, we managed to analyse 2518 (84%) intensity reports with useful comments. It is important to note that the intensity reports were done through three different tools: 2,371 (94%) reports were done through the

LastQuake app, 123 (5%) through the mobile phone version, and only 24 (1%) from the Desktop version.



Figure 135: LastQuake app interface. Source: EMSC.

In the case of Twitter, several hashtags relating to the Aegean earthquake were detected through social media monitoring: #earthquake, #σεισμός, #Ierápetra, #Greece, #DodecaneseIslands, #Karlovasi, #quake, #depem, #Izmir, #Turkey, #Erdbeben #Ägäis #TurkeyEarthquake #izmirearthquake #izmirquake #Karabağlar #Terremoto #tsunami #Chios #Türkiye #TEWS #IzmirEarthquake #EarthquakeReport #TsunamiReport #Turkey #AegeanSea #Esmirna. An initial screening of a small set of tweets was performed, and we used these to select hashtags that frequently contained meaningful information such as #σεισμός #depem #Tsunami #Izmir #samos #TurkeyEarthquake, #izmirearthquake #izmirquake and #izmirdepeminde. Having selected our hashtags, we purchased from the third-party vendor: TweetBinder, 618,145 tweets posted from October 30 to November 30, 2020. In this dataset, there were 206,228 (33%) original Tweets and 411,914 (67%) retweets.

7.2. LastQuake App

The LastQuake app obtained reports from users mainly in Turkey and Greece (as was expected); however, there were 345 Intensity reports from Croatia (of these 44 were from Zadar – the location of the recent Croatia earthquake). Other intensity reports were uploaded from Bosnia and Herzegovina, Albania, Bulgaria, Romania, North Macedonia, and Serbia. The location of LastQuake app intensity reports can be observed in **Figure 136**.



Figure 136: LastQuake app intensity report location (source: authors)

7.2.1. Language

Most intensity reports with comments were written in Turkish, followed by English, Croatian, German, Bosnian and other languages listed in **Table 9**. Only four reports were written in Greek, other reports from Greece were written in English. Some LastQuake app users included punctuation marks such as suspension points, questions, and exclamation marks instead of words. Other users replaced words with numbers that we have assumed were related to the intensity they wanted to report. There were three user comments, whose language could not be identified.

Table 9: Users' comments languages

Languages	Number	Percentage
Turkish	1264	50%
English	898	36%
Croatian	255	10%
German	20	1%
Bosnian	11	0%
Slovenian	10	0%
Punctuation marks	10	0%
Albanian	9	0%
Numbers	9	0%
Romanian	7	0%
French	5	0%
Greek	4	0%
Italian	4	0%
Undefined	3	0%

Languages	Number	Percentage
Bulgarian	2	0%
Arabic	1	0%
Azerbaijani	1	0%
Czech	1	0%
Hungarian	1	0%
Latvian	1	0%
Polish	1	0%
Slovak	1	0%
Total	2518	100%

7.2.2. Intensity

As the Aegean mission's case study area is focused on Turkey and Greece, we concentrated on the intensities reported in these countries. A significant number of LastQuake app users reported intensities of III, II, and IV, followed by higher and lower intensities such as V, I, VI, and VII as measured by the Modified Mercalli Intensity scale (MMI). The exact number of reports per intensity is presented in **Table 10**. The location of intensities reported by LastQuake app users in the case study area can be observed in **Figure 137**, and with more detail in Izmir and Samos-Kuşadası in **Figure 138** and **139**.

Table 10: Intensities reported on the MMI scale by LastQuake app users

Intensity	Reports	Proportion
III	981	39%
II	617	25%
IV	417	17%
V	188	7%
I	146	6%
VI	116	5%
VII	36	1%
VIII	12	0
XI	4	0
X	1	0
Total	2518	100

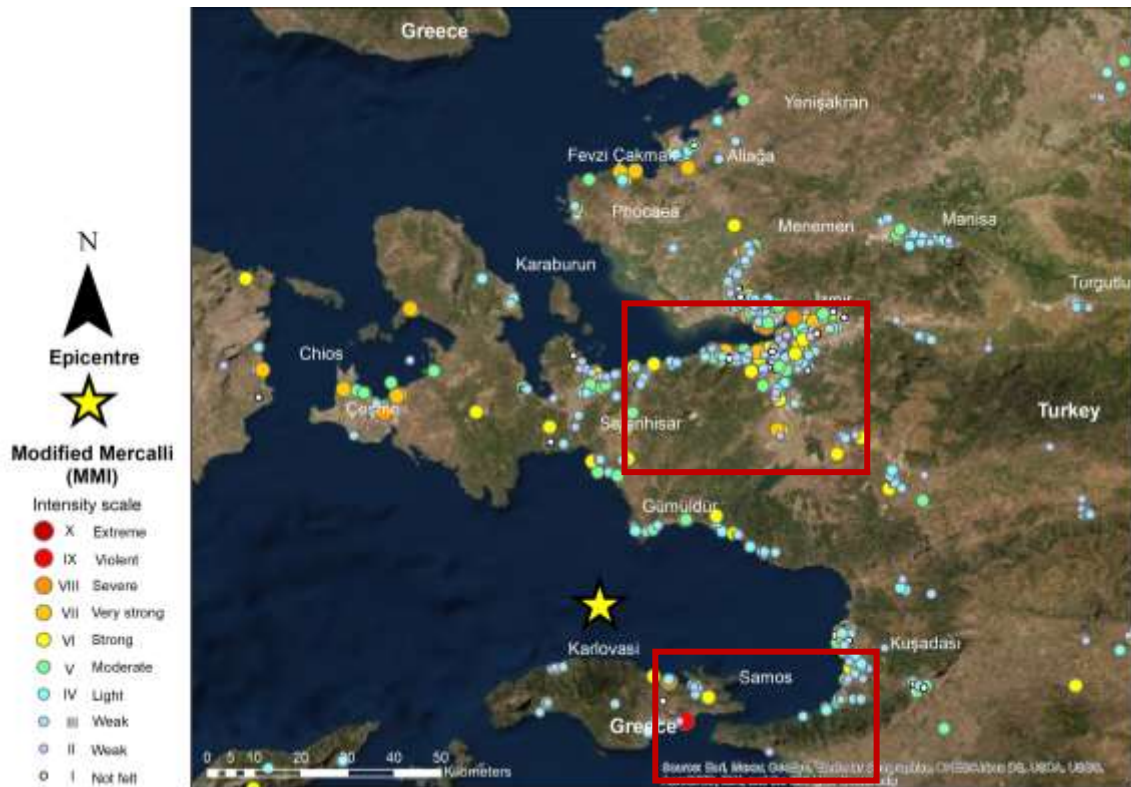


Figure 137: LastQuake app users intensity reports in the case study area (Source: Authors)

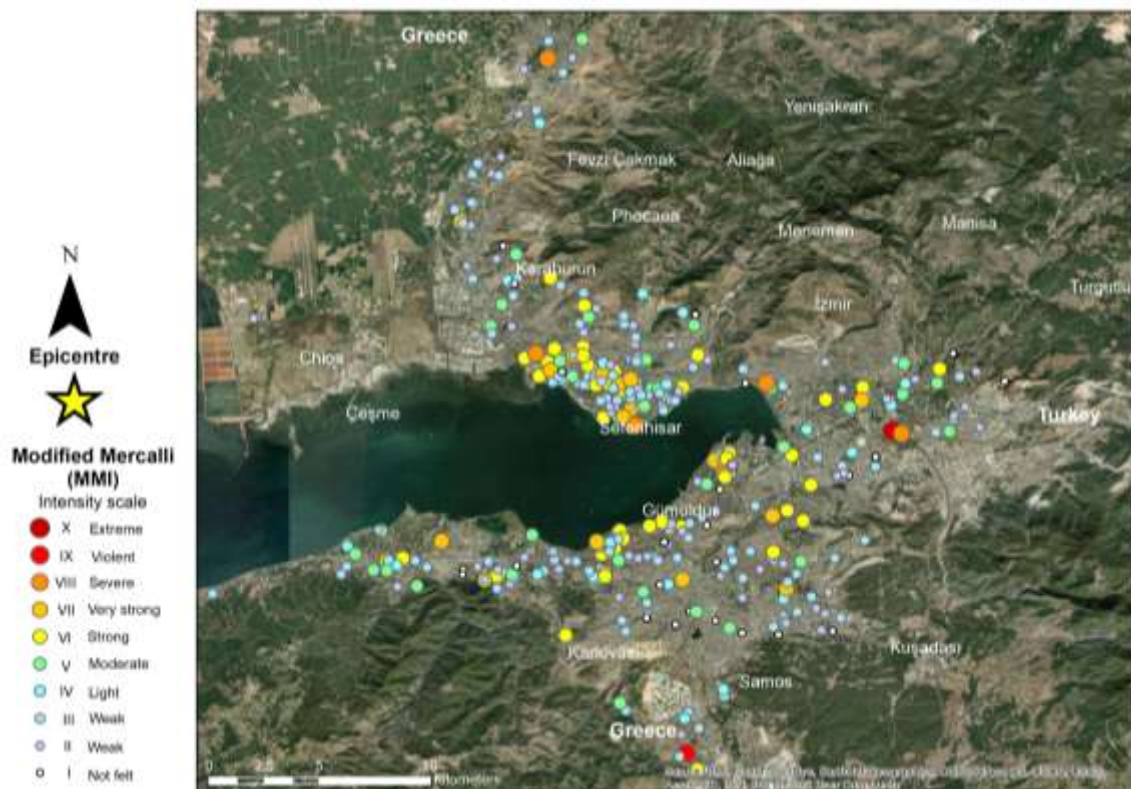


Figure 138: LastQuake app users intensity reports in Izmir (Sources: Authors)



Figure 139: LastQuake app users intensity reports in Samos and Kuşadası (Sources: Authors)

7.2.3.Sentiment Analysis (SA)

LastQuake app reports the intensity felt by the user and allows them to include comments and photos. These intensity measures, comments, and photographs are very valuable sources of data because they are geotagged, and therefore, intensity reports can be assigned an accurate location (GPS coordinates). This data is different from Twitter data, which no longer includes accurate location information but rather aggregates location into regions (such as Izmir). Therefore, we have taken these comments and performed a sentiment analysis (SA) on them, classifying them according to their polarity. Sentiment analysis is a natural language processing (NLP) technique applied to determine data polarity (positive, negative, neutral, or unrelated), as well as feelings and emotions, urgency, and intentions (interested v. not interested) (MonkeyLearn, 2020).

In this report, we have applied sentiment analysis (SA) (Mäntylä, Graziotin, & Kuutila, 2018), also known as opinion mining (OM) (Medhat, Hassan, & Korashy, 2014; Munir, 2019), as a method to extract information from the text data contained in the LastQuake Intensity reports provided by EMSC. This method has been mainly used before for customer reviews of products and places (restaurants and hotels), stock markets (Hagenau, Liebmann, & Neumann, 2013; Yu, Wu, Chang, & Chu, 2013), new articles (Xu, Peng, & Cheng, 2012), products, brands, services online feedback (MonkeyLearn, 2020) or political debates (Maks & Vossen, 2012). The project framework 'Learning from Earthquakes' uses SA for emergency management assessment (Contreras et al., 2021; So et al., 2020) and post-disaster recovery evaluation (Contreras, Wilkinson, Balan, Phengsuwan, & James, 2020). The aim of this analysis is to 1) collect the relative proportions of different sentiments for comparison with other future earthquakes, 2) to see if the proportion of different sentiments (positive, negative and neutral) vary with location and whether this can be used as an indication of the relative impacts at that location.

In case of an emergency due to an earthquake, most of the text data will have a negative polarity because it will contain words related to damage, fear, and anxiety. However, there will also be data that include words related to the event, such as magnitude, intensity, or the location of the epicentre, that will be considered neutral. Other data will contain solidarity messages, announcements of support with humanitarian aid, or descriptions of help. These are considered to be positive as they demonstrate instances of success. Our analysis employed a hybrid approach to classification, where both automatic and rule-based methods were used to make the classifications. The authors defined the rulesets used

EEFIT

in this classification based on their experience in disaster management and post-disaster recovery. The quantification of comments according to their polarity is listed in **Table 11**. Comments and location, including their polarity, are presented in **Figure 140**. Examples of comments classified as positive, negative, or Neutral reported from Samos islands can be read below, and its location is depicted in **Figure 141**.

Positive

- ✓ 'We felt it, but it was short'.
- ✓ 'Fast'

Neutral

- 'The epicentre is in Samos, Greece, not in Western Turkey'.
- 'Moment intensity VI'
- 'It is not Dodecanese islands. It is North Aegean Samos island'
- Samos island, GR

Negative

- ✗ 'Everything rattled for a few seconds. The cracks in our walls are getting bigger'
- ✗ 'House was shaking'
- ✗ 'Strong'
- ✗ 'Just felt it. Again and again. Make it stop'.
- ✗ 'With noise'
- ✗ 'Near Vathi Samos. Very loud and shaking'
- ✗ 'Very big and strong'
- ✗ 'Again and again!'
- ✗ 'The house was shaking, it woke us up'
- ✗ 'Pretty heavy vibration and chips of our walls falling off'
- ✗ 'I felt sudden shake'

Table 11: Topic classification of comments from LastQuake app users in their intensity reports

Polarity	Number	Percentage
Negative	1457	58
Neutral	542	22
Positive	519	21
Total	2518	100

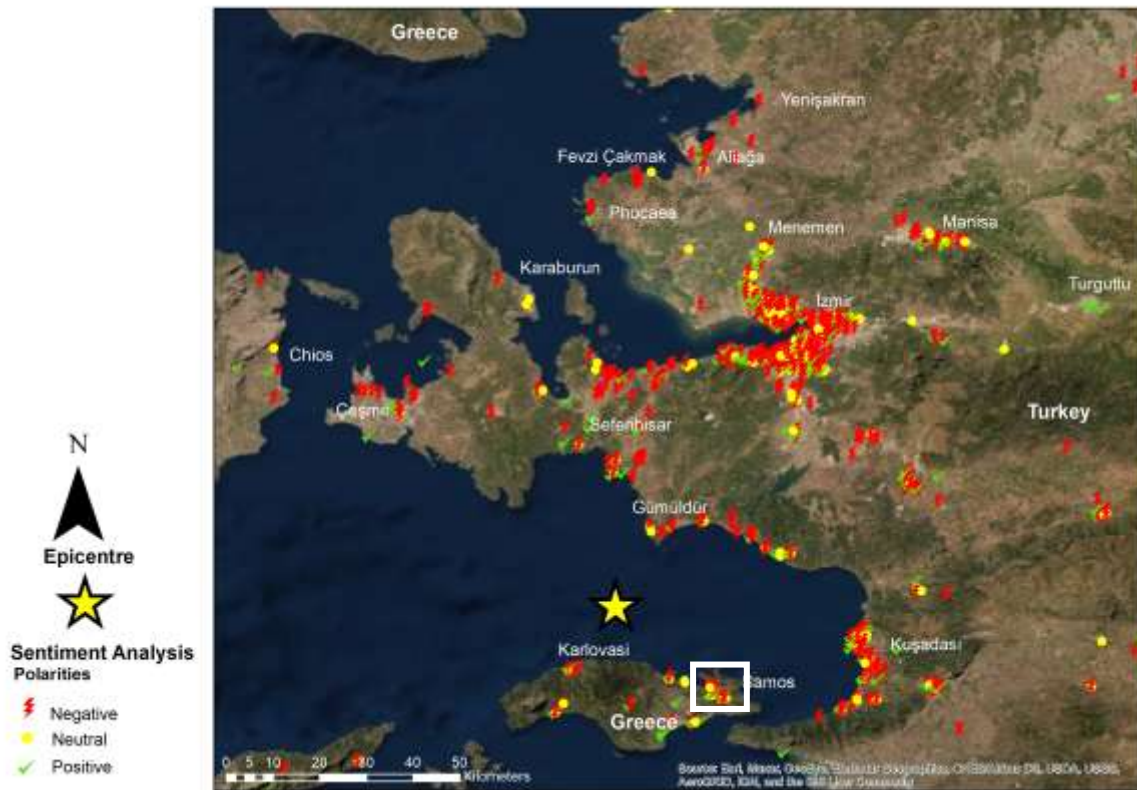


Figure 140: Location of LastQuake app users comments polarity.



Figure 141: Location of LastQuake app users comments polarity in Samos.

7.2.4. Topic Analysis

Topic analysis, also called topic detection, topic modelling or topic extraction, is another NLP technique to automatically extract meaning from text by identifying recurrent themes or topics. This technique uses machine learning to organise and understand large text-datasets (MonkeyLearn, 2020b), such as those coming from the LastQuake app users' comments, by assigning 'tags' or categories to each text's topic or theme. These categories can then be used to understand what impacts were most experienced, and potentially what resources should be deployed to help in the response and recovery, and where best to allocate those resources for maximum effect. Further categorisation is possible and these sub-categories may then be interrogated (either manually or automatically) to gather more specific and, therefore, potentially more actionable information. It may also be possible to use this technique to compare impacts between regions in a disaster or between disasters, but as this NLP technique and its application are so new, this has yet to be proven. The significant potential advantage in automatic topic detection is that it takes substantial amounts of data in the event's immediate aftermath. It quickly processes the information in this data, and potentially provides actionable information that can be implemented (e.g. can this method provide an initial needs assessment).

Based on the study of dataset related to the recent earthquakes in Albania (Andonov et al., 2020) (2019) and Croatia (So et al., 2020), we identified 12 topics addressed by LastQuake app users: building damage, tsunami effects, geotechnical effects, lifelines affected, injuries and casualties, emergency response, solidarity messages, preparedness, seismic information, intensity, early recovery and unrelated. However, the categories of injuries and casualties and early recovery were not applied in the Aegean mission because no comments that could have been classified under these categories were posted. Therefore only 10 topics were considered for the classification.

As the LastQuake app was designed to report intensities, 90% of the comments were related to this topic. After intensity, LastQuake app users tend to describe the sensed direction of the seismic movement, as both horizontal and vertical. They also sent solidarity messages, wishing that everyone 'will be safe'. Users shared the emergency response measures that they made (which was mainly the evacuation of homes). At least three users reported to have applied the theory of the triangle of life (we make no judgement on this theory here and only report that this is what three users applied). Additionally, one person who could not evacuate his/her home due to physical impediments, decided to turn off the natural gas tap to protect him or herself. Others describe the damages to buildings and the effects of the tsunami. People recommended to others that they ensure they have bottles of water, while others ask for advice on how to stay safe.

The user comments were also useful to identify georeferenced damages in phone lines and the possibility of damages in power lines. Examples of comments classified in the category of lifelines affected are:

- 📍 'It was the first time I saw the .300-ton transformers shaking like a cradle, which was shifted in Aliagada. God bless us all'.
- 📍 'Very powerful and long lasting. All neighbours are on the street. No visible damage although telephone poles sway and a line broke. Many smaller quakes within the last 45 minutes or so'.

No comments reporting injuries and casualties among population were identified. The classification and quantification of the topic comments can be observed in **Table 12** and **Figure 142**.

Table 12: Topic classification of comments from LastQuake app users in their intensity reports

Topic	Number	Percentage
Intensity	2283	90.67
Seismic information	87	3.46
Solidarity messages	39	1.55
Emergency response	39	1.55
Unrelated	27	1.07
Building damage	24	0.95
Tsunami effects	9	0.36
Preparedness	5	0.20
Lifelines affected	3	0.12
Geotechnical effects	2	0.08
Total	2518	100

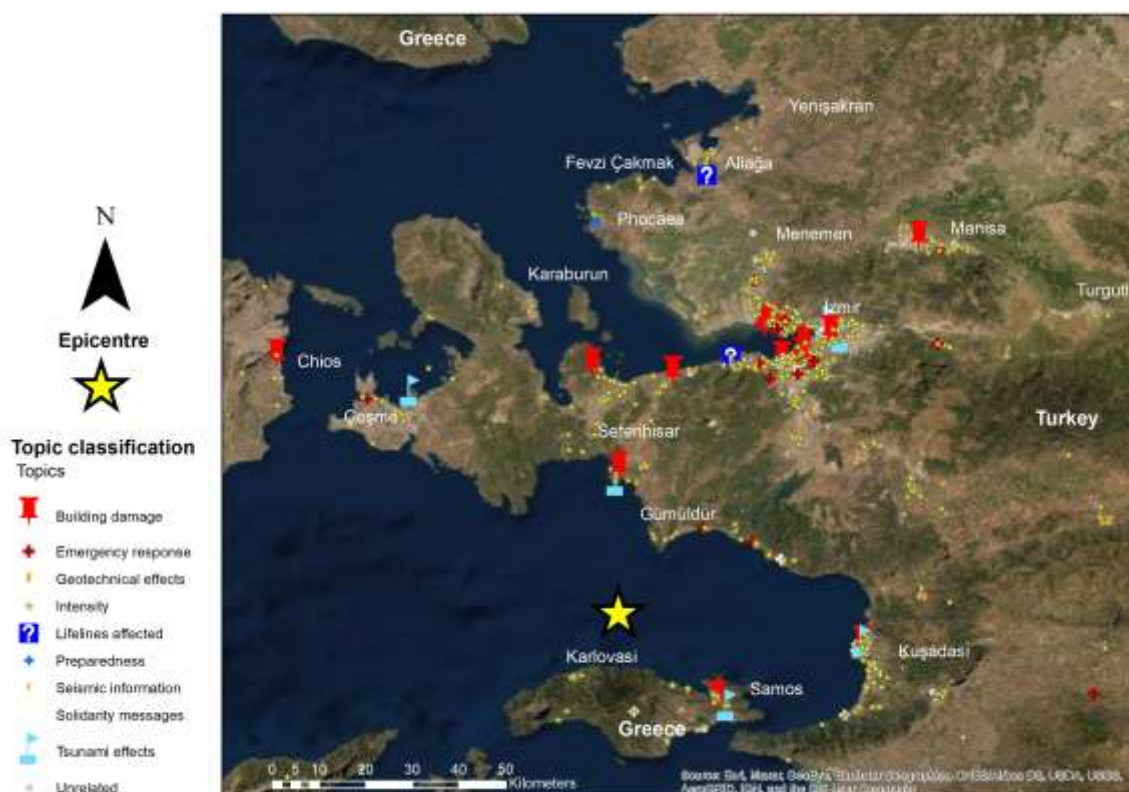


Figure 142: Topic classification of comments from LastQuake app users in their intensity reports.

From 2518 comments written by LastQuake app users, only 88 (3%) included georeferenced pictures. From those comments with pictures, we extracted 61 (69%), because some of the pictures were repeated, others were pictures of TV screens, and at least 4 did not include proper coordinates. The location of the georeferenced pictures and those with comments in the case study area are depicted in **Figure 143** and pictures without comments in **Figure 144**. However, approximately only 10% were useful for building damage assessment.



Figure 143: Georeferenced Pictures with comments taken by LastQuake app users (Source: Authors)



Figure 144: Georeferenced Pictures without comments taken by LastQuake app users.

EEFIT

These georeferenced pictures show the location and the degree of damage of buildings. This data can contribute to the planning and the deployment of the earthquake reconnaissance mission, especially in site planning and route selection. Examples of data and images obtained from LastQuake are depicted in **Figure 145** and **146**.



- Longitude: 27.1352
- Latitude: 38.3103
- Intensity: Not reported
- Distance to the epicentre: 51.5 Km

Figure 145: Data for earthquake reconnaissance mission planning in Izmir, Turkey. Source: EMSC



- Longitude: 26.9139
- Latitude: 37.6909
- Intensity: Not reported
- Distance to the epicentre: 25.2 Km

Figure 146: Data for earthquake reconnaissance mission planning in Samos, Greece. Source: EMSC

▪

7.3. Twitter

We have also analysed Twitter data. Twitter has the advantage of providing many more comments, comments from a more diverse range of people, and comments from a wider geographical area. However, it has the following disadvantages: 1) comments not necessarily being so relevant for earthquake reconnaissance, 2) comments being retweets instead of original comments, 3) location information being regional rather than a specific latitude and longitude and 4) the majority of users having less interest or experience in earthquake impacts in general. Looking at our Twitter data, we can observe the activity on Twitter related to the selected hashtags in **Figure 147**. Besides the main peak on the day of the earthquake: October 30, there can be seen two small peaks of Twitter activity, the first on November 11 and the second one on November 28, 2020 (see spike on **Figure 147**). In the first case a fire and explosions in the Vathy Reception and Identification Centre (RIC) (AP, 2020) were reported on Twitter with the hashtag #sam0s (one of the hashtags used also by us to collect data about the emergency management after the Aegean earthquake). In the second case, a minor earthquake M 2.0, depth 6 Km, 20 km NW of Bozkır (Central Turkey) 17:31:36 UTC was reported by EMSC on Twitter with the hashtag #deprem (another hashtag used by us to collect data about the emergency management after the Aegean earthquake).

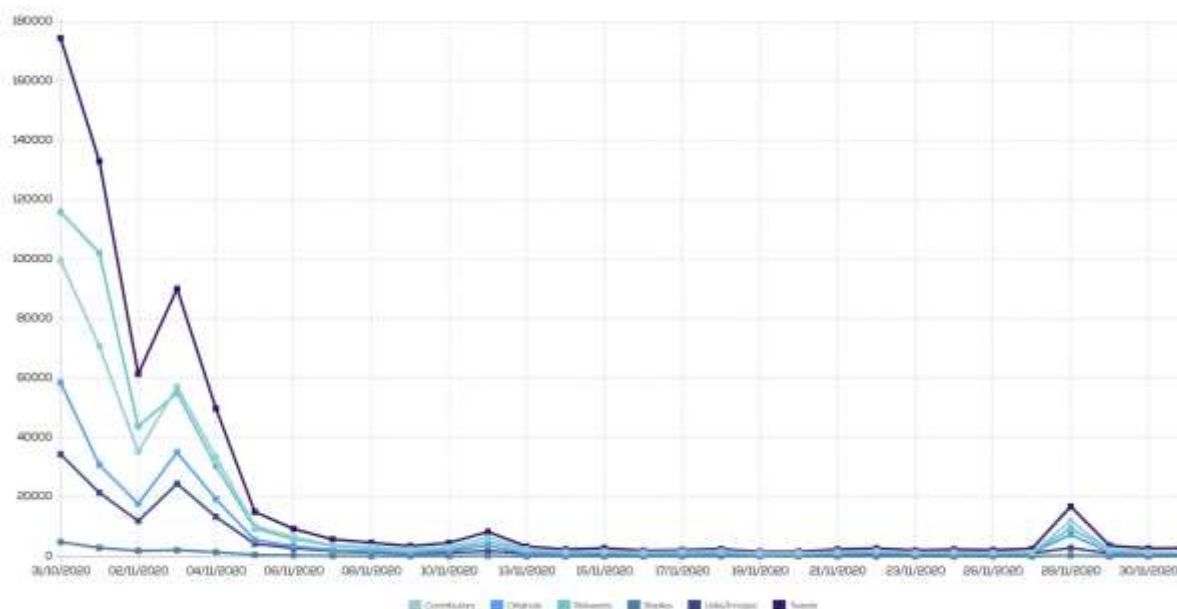


Figure 147: Activity on Twitter from October 31 to November 30, 2020. Source: Tweet Binder.

7.3.1. Sentiment Analysis

The polarity of the Tweets collected between the day of the earthquake and until one month later is depicted in **Figure 148**. The algorithms used by TweetBinder, could not define the polarity of the majority of the Tweets - 550,382 (89%); however, it did identify 46,176 (7%) as neutral, 13001 (2%) as negative and 8,587 (1%) positive. The estimated sentiment score was 56.16 in a score from 1 to 100, being neutral (TweetBinder, 2019). However further analysis is required using a customized SA model for emergency management. This customized SA model is currently on development based on the analysis of datasets for other case study areas, to ensure replicability and validity. This model must produce a more accurate classification of the text-data collected not only for emergency management but based on other dataset also for post-disaster recovery assessment.

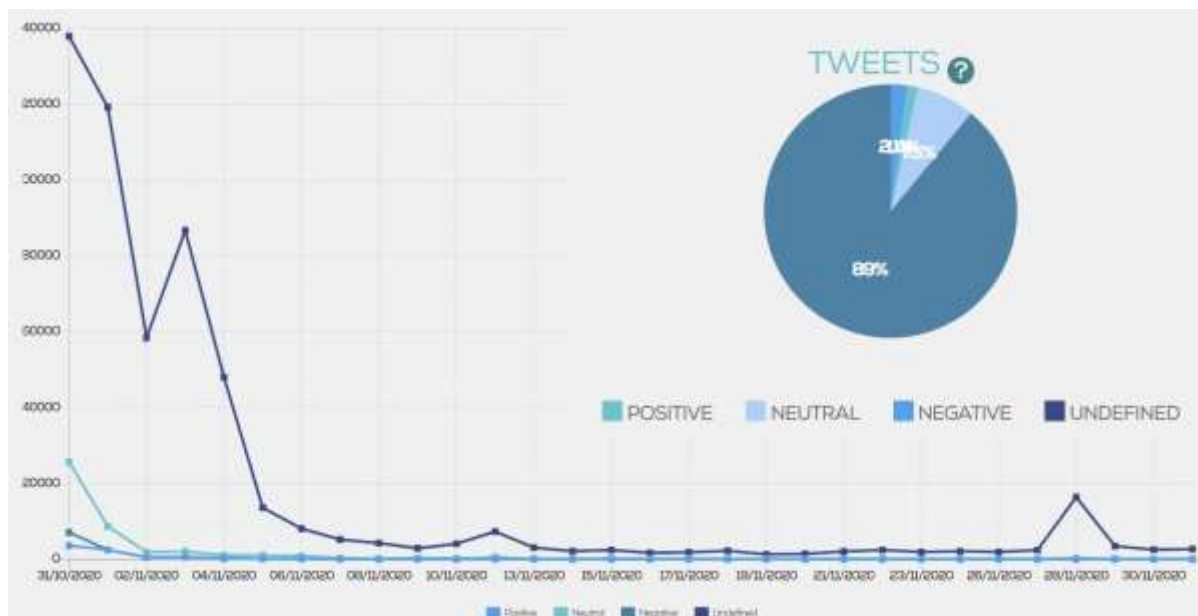


Figure 148: Tweets polarity with the selected hashtags from October 30 to November 30, 2000. Source: Tweet Binder





7.3.2. Most retweeted Tweets

Most retweeted tweets contained requests of help to find relatives, to express fear, to inform about people trapped under debris, to thank people and institutions involved in search and rescue (SAR) and to express solidarity. **Table 13** gives examples of the most retweeted tweets².

Table 13: Most retweeted tweets related to the Aegean earthquake (pictures accompanying tweets were excluded if they included people). Source: Tweet Binder.

Tweet	Translation from Turkish to English
 <p>7112 Retweets</p> <p>Babam ramazan bal a deprem olduğu andan itibaren ulaşamıyoruz gören veya herhangi bir bilgisi olan lütfen iletişime geçsin #deprem #depreyizmir #Tsunami https://t.co/DyZ0xkL1io</p>	<p>We cannot get in touch with my father, Ramazan Bal, since the earthquake hit. If somebody sees him or has any information about him, please contact us #earthquake #earthquakeizmir #Tsumami</p>
 <p>5640 Retweets</p> <p>İzlerken Tüylerim diken diken oldu #izmirinyanıdayız #deprem #izmir #İyikiVarsınAFAD @Gazapizm https://t.co/TbLEofrJxA</p>	<p>I had goosebumps while watching #wearewithizmir #earthquake #izmir #LuckytoHaveYouAFAD</p>

² The picture and the Twitter handle of has been covered to protect the privacy of Twitter users. We did not do this in case of governmental and not governmental institutions, as these can be considered to be public information. Also note that translations of tweets to English do not include a translation of the hashtags included to extract the main message.






 <p>4264 Retweets</p> <p>283/1 Emrah apartmanı 1.kat teyzem enkaz altında tevhide akkuş lütfen yardımcı olun #deprem #izmirdeprem</p>	<p>My aunt, Tevhide Akkus, is under the debris in 283/1 Emrah apartment, 1st floor, please help #earthquake #izmirearthquake</p>
 <p>3490 Retweets</p> <p>Birgün için hesabınız Retweetlerle dolsa birşey olmaz lütfen destek verin enkaz altında kalan insanlara ses olun!! #EgeDenizi #izmir #buse #depreminutma #depreyizmir #deprem https://t.co/NOi22qMOXQ</p>	<p>It won't do any harm if your account is full of retweets for one day; please support and be the voice of those trapped under the rubble!! #AegeanSea #izmir #buse #don'tforgetearthquake #earthquakeizmir #earthquake</p>
 <p>3377 Retweets</p> <p>Mansuroğlu mahallesi 283/13 Sok Rıza Bey apt No 2 kat 4 Daire 16 Bayraklı izmir enkaz altında 3 kişi var 1 anne 2 küçük çocuk Emine Yücel Toklu acil rt leyin lütfen #Deprem #depreyizmir #Tsunami https://t.co/cMM2eZ4Wsu</p>	<p>Mansuroğlu Neighborhood 283/13 Street Rıza Bey Apt No 2 floor 4 Flat 16 Bayraklı Izmir. There are three people under the wreckage: a mother, Emine Yücel Toklu, and two small children. Retweet please #Earthquake #earthquakeizmir #Tsunami</p>
 <p>EmniyetGM 2 months ago 3141 Retweets</p> <p>Son kişi çıkarılana kadar hepimiz enkaz altındayız! #izmirinyanındayız #deprem #izmir https://t.co/wqNgg7dPWF</p>	<p>We are all under the wreckage until the last one is found! #wearewithizmir #earthquake #izmir</p>

7.3.3. Most liked Tweets

Most liked tweets by Twitter users' express messages of solidarity, fear, opinions, and support. **Table 14** lists examples of the most-liked tweets.

Table 14: Most liked tweets related to the Aegean earthquake (pictures accompanying tweets were excluded if they included people). Source: Tweet Binder.

Tweet	Translation from Turkish to English
 <p>EmniyetGM 2 months ago 3141 Retweets</p> <p>Son kişi çıkarılana kadar hepimiz enkaz altındayız! #izmirinyanındayız #deprem #izmir https://t.co/wqNgg7dPWF</p>	<p>We are all under the wreckage until the last one is found! #wearewithizmir #earthquake #izmir</p>
 <p>5640 Retweets</p> <p>İzlerken Tüylerim diken diken oldu #izmirinyanındayız #deprem #izmir #lykiVarsınAFAD @Gazapizm https://t.co/TbLEofrJxA</p>	<p>I had goosebumps while watching #wearewithizmir #earthquake #izmir #LuckytoHaveYouAFAD</p>

 <p>22963 Likes</p> <p>Şehirler gökyüzüne doğru değil enlemesine genişlemelidir! #deprem</p>	<p>Cities show grow expansively, not towards the sky! #earthquake</p>
 <p>20723 Likes</p> <p>Öldüm derken kurtulmak ve o şokun etkisi Allah yardım eden herkesten razı olsun #deprem #izmir https://t.co/UTCJwPB6nR</p>	<p>The shock of having dodged death at the very last minute. God bless everyone who helped #earthquake #izmir</p>
 <p>20673 Likes</p> <p>Praying for Turkey! 🙏 #TurkeyEarthquake https://t.co/KypYc2COKI</p>	
 <p>16001 Likes</p> <p>İyi ki canımıza koşan can dostlarımız var. #deprem #buse https://t.co/O6zqc85ceT</p> 	<p>We are lucky to have dear friends running for our lives #deprem #buse</p>
 <p>AKUT_Derneği 2 months ago 15711 Likes</p> <p>Biz sizin için hep canla başla çalıştık. Siz ise bizi hiçbir zaman yalnız bırakmadınız! Bu desteğe layık olmak için her zaman olduğu gibi özveriyle çalışmaya devam edeceğiz. Çünkü biz sizi çok seviyoruz... #Izmirinyanındayız #Deprem #Izmir https://t.co/nnpDbmQDHv</p>	<p>We have always worked heart and soul for you. And you have never left us alone! We will continue to work devotedly as always to deserve this support. Because we love you very much... #wearewithizmir #Earthquake #Izmir</p>



7.4. Conclusions and recommendations

Most reports come from Turkey, although Greece was also affected. This could be explained by the widespread use of the LastQuake app in Turkey and the degree of damage. EMSC is currently investigating if the intensity reports from Zadar, Croatia correspond to the Aegean earthquake or a parallel seismic event. We found that citizens prefer to use apps and mobile phone to submit their intensity reports, rather than desktops computers.

The number of reports from LastQuake users as well as the intensities reported, decline with the distance inland from the coast nearest to the epicentre. After intensity, LastQuake app users tend to include in their comments seismic information, solidarity messages, emergency response measures taken by them, building damages, tsunami effects, preparedness, lifelines affected and geotechnical effects. In the comments, the negative polarity in the case of the Aegean earthquake is mainly related to aftershocks, fear, and uncertainty. In contrast, positive polarity is related to light seismic movements without any possibility of damages, solidarity messages, and preparedness to face the emergency phase.

Tweets containing information about people trapped, including addresses are among those more retweeted. These tweets are potentially useful for the SAR teams and for the earthquake reconnaissance missions to know damaged structures' location. Tweets expressing solidarity, fear, opinions and support are among those more liked by other Twitter users. Tweets' usefulness is very variable and we agree with in needing to train and empower citizens as sensors (Cervone and Hultquist, 2018) to safely contribute to the emergency response with meaningful comments, tweets, and post on SM. These contributions should include the location of damaged buildings, injured and casualties, needs and damages, failures in lifelines, and pictures of damages (see **Figure 149** and **Table 15**).

Pictures of collapsed buildings are potentially useful for SAR teams in the immediate aftermath of the earthquake. Pictures of damaged buildings are useful to guide earthquake reconnaissance missions and needs assessments; however, they need accurate geotag information, and while this is currently available with LastQuake, it is not with Twitter. Earthquakes, as other natural phenomena, reveal the differences in vulnerability of some individuals in society. In this case, the intensity reports include comments from undocumented immigrants, pregnant women alone at home, and school teachers responsible for calming students during the earthquake. Social media shows the potential to highlight those who may not be willing to come forward with their experiences or whose experience may not be made readily available to others through traditional means such as traditional media. However, it is necessary to carefully consider how the hashtags chosen to monitor the event are selected, as there will always be tweets with the chosen hashtags that contain issues unrelated to the event and relevant information that is not uncovered with those hashtags that are chosen.

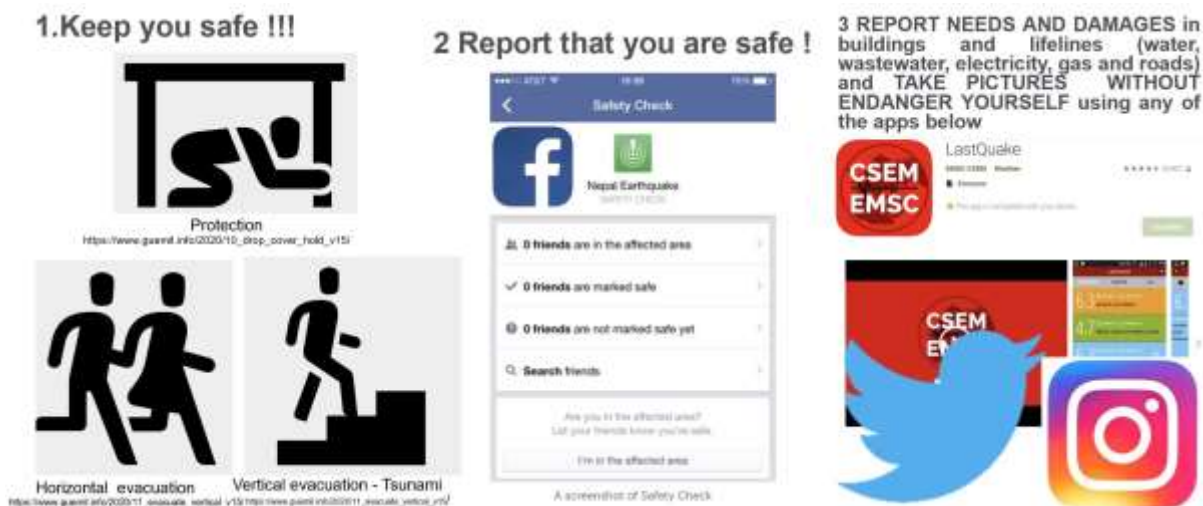


Figure 149: Citizens sensor recommended actions.

Table 15: Reports by relatives of injured people, including addresses

Tweet	Translation from Turkish to English
 <p>3377 Retweets</p> <p>Mansuroğlu mahallesi 283/13 Sok Rıza Bey apt No 2 kat 4 Daire 16 Bayraklı izmir enkaz altında 3 kişi var 1 anne 2 küçük çocuk Emine Yücel Toklu acil rt leyin lütfen #Deprem #depremir #Tsunami https://t.co/cMM2eZ4Wsu</p>	<p>Mansuroğlu Neighborhood 283/13 Street Rıza Bey Apt No 2 floor 4 Flat 16 Bayraklı Izmir. There are three people under the wreckage: a mother, Emine Yücel Toklu, and two small children. Retweet please #Earthquake #earthquakeizmir #Tsunami</p>
 <p>4264 Retweets</p> <p>283/1 Emrah apartmanı 1.kat teyzem enkaz altında tevhide akkuş lütfen yardımcı olun #deprem #izmirdeprem</p>	<p>My aunt, Tevhide Akkus, is under the debris in 283/1 Emrah apartment, 1st floor, please help #earthquake #izmirearthquake</p>

References

- Andonov, A., Andreev, S., Freddi, F., Greco, F., Gentile, R., Novelli, V., & Veliu, E. (2020). *The Mw6.4 Albania Earthquake on the 26th November 2019*. Retrieved from <https://www.istructe.org/IStructE/media/Public/Resources/report-eeffit-mission-albania-22102020.pdf>
- AP. (2020, The 11th November 2020). Migrants flee and workers evacuate amid large fire at camp in Samos, Greece. *The Telegraph*. Retrieved from <https://www.telegraph.co.uk/news/2020/11/11/migrants-flee-workers-evacuate-amid-large-fire-camp-samos-greece/>
- Bossu, R., Fallou, L., Landès, M., Roussel, F., Julien-Laferrrière, S., Roch, J., & Steed, R. (2020). Rapid Public Information and Situational Awareness After the November 26, 2019, Albania Earthquake: Lessons Learned From the LastQuake System. *Frontiers in Earth Science*, 8(235), 1-15. doi:10.3389/feart.2020.00235
- Contreras, D., Fallou, L., Landès, M., Wilkinson, S., Tomljenovich, I., Balan, N., . . . James, P. (2021). *Assessing Emergency Response and Early Recovery using Sentiment Analysis (SA). The case of Zagreb, Croatia (accepted)*. Paper presented at the 1st Croatian Conference on Earthquake Engineering (1CroCEE) 2021, Zagreb, Croatia. <https://crocee.grad.hr/event/1/>

- Contreras, D., Wilkinson, S., Balan, N., Phengsuwan, J., & James, P. (2020). *Assessing Post-disaster Recovery Using Sentiment Analysis. The case of L'Aquila, Haiti, Chile and Canterbury* Paper presented at the 17th World Conference on Earthquake Engineering (17WCEE), Sendai, Japan.
- Doan, S., Vo, B.-K. H., & Collier, N. (2012). *An Analysis of Twitter Messages in the 2011 Tohoku Earthquake*, Berlin, Heidelberg.
- Fallou, L., Bossu, R., Landès, M., Roch, J., Roussel, F., Steed, R., & Julien-Laferrière, S. (2020). Citizen Seismology Without Seismologists? Lessons Learned From Mayotte Leading to Improved Collaboration. *Frontiers in Communication*, 5(49), 1-17. doi:10.3389/fcomm.2020.00049
- Hagenau, M., Liebmann, M., & Neumann, D. (2013). Automated news reading: Stock price prediction based on financial news using context-capturing features. *Decision Support Systems*, 55(3), 685-697. doi:https://doi.org/10.1016/j.dss.2013.02.006
- Kropivnitskaya, Y., Tiampo, K., Qin, J., & Bauer, M. (2017). The Predictive Relationship between Earthquake Intensity and Tweets Rate for Real-Time Ground-Motion Estimation. *Seismological Research Letters*, 88, 840-850. doi:10.1785/0220160215
- Lerman, K., & Ghosh, R. (2010). *Information Contagion: an Empirical Study of the Spread of News on Digg and Twitter Social Networks*. Paper presented at the Fourth International AAAI Conference on Weblogs and Social Media. <https://arxiv.org/pdf/1003.2664.pdf>
- Maks, I., & Vossen, P. (2012). A lexicon model for deep sentiment analysis and opinion mining applications. *Decision Support Systems*, 53, 680–688. doi:10.1016/j.dss.2012.05.025
- Mäntylä, M. V., Graziotin, D., & Kuutila, M. (2018). The Evolution of Sentiment analysis—A Review of Research Topics, Venues, and Top Cited Papers. *Computer Science Review* 27, 16–32. Retrieved from <https://arxiv.org/ftp/arxiv/papers/1612/1612.01556.pdf>
- Medhat, W., Hassan, A., & Korashy, H. (2014). Sentiment analysis algorithms and applications: A survey. *Ain Shams Engineering Journal*, 5(4), 1093-1113. doi:https://doi.org/10.1016/j.asej.2014.04.011
- Mendoza, M., Poblete, B., & Valderrama, I. (2019). Nowcasting earthquake damages with Twitter. *EPJ Data Science*, 8(1), 3. doi:10.1140/epjds/s13688-019-0181-0
- MonkeyLearn. (2020). Sentiment Analysis. Retrieved from <https://monkeylearn.com/sentiment-analysis/>
- Munir, S. (2019). Basic Sentiment Analysis using NLTK. In *towards data science* (Vol. 2020).
- Murakami, A., & Nasukawa, T. (2012). *Tweeting about the tsunami?: mining twitter for information on the tohoku earthquake and tsunami*. Paper presented at the Proceedings of the 21st International Conference on World Wide Web, Lyon, France. http://delivery.acm.org/10.1145/2190000/2188187/p709-murakami.pdf?ip=128.240.225.56&id=2188187&acc=ACTIVE%20SERVICE&key=BF07A2EE685417C5%2E708BE730B8E35B42%2E4D4702B0C3E38B35%2E4D4702B0C3E38B35&__acm__=1560787316_bc1fd7cf5ea7ca9bc54e2e67ab6722b5
- Simon, T., Goldberg, A., & Adini, B. (2015). Socializing in emergencies—A review of the use of social media in emergency situations. *International Journal of Information Management*, 35(5), 609-619. doi:https://doi.org/10.1016/j.ijinfomgt.2015.07.001
- So, E., Babić, A., Majetic, H., Putrino, V., Verrucci, E., Contreras, D., . . . D'Ayala, D. (2020). *The Zagreb Earthquake of 22 March 2020* Retrieved from Newcastle, UK: https://research.ncl.ac.uk/learningfromearthquakes/outputs/So%20et%20al_2020_%20The%20Zagreb%20earthquake%20of%2022%20March%202020-compressed.pdf
- TweetBinder. (2019). Twitter sentiment analysis with Tweet Binder. Retrieved from <https://www.tweetbinder.com/blog/twitter-sentiment-analysis/>
- Wu, D., & Cui, Y. (2018). Disaster early warning and damage assessment analysis using social media data and geo-location information. *Decision Support Systems*, 111, 48-59. doi:https://doi.org/10.1016/j.dss.2018.04.005
- Xu, T., Peng, Q., & Cheng, Y. (2012). Identifying the semantic orientation of terms using S-HAL for sentiment analysis. *Knowl. Based Syst.*, 35, 279-289.
- Yan, Y., Chen, J., & Wang, Z. (2020). Mining public sentiments and perspectives from geotagged social media data for appraising the post-earthquake recovery of tourism destinations. *Applied Geography*, 123, 102306. doi:https://doi.org/10.1016/j.apgeog.2020.102306
- Yu, L.-C., Wu, J.-L., Chang, P.-C., & Chu, H.-S. (2013). Using a contextual entropy model to expand emotion words and their intensity for the sentiment classification of stock market news. *Knowledge-Based Systems*, 41, 89-97. doi:https://doi.org/10.1016/j.knosys.2013.01.001

EEFIT

Earthquake Engineering Field Investigation Team

EEFIT is a UK based group of earthquake engineers, architects and scientists who seek to collaborate with colleagues in earthquake prone countries in the task of improving the seismic resistance of both traditional and engineered structures. It was formed in 1982 as a joint venture between universities and industry, it has the support of the Institution of Structural Engineers and of the Institution of Civil Engineers through its associated society SECED (the British national section of the International Association for Earthquake Engineering).

EEFIT exists to facilitate the formation of investigation teams which are able to undertake, at short notice, field studies following major damaging earthquakes. The main objectives are to collect data and make observations leading to improvements in design methods and techniques for strengthening and retrofit, and where appropriate to initiate longer term studies. EEFIT also provides an opportunity for field training for engineers who are involved with earthquake-resistant design in practice and research.

EEFIT is an unincorporated association with a constitution and an elected management committee that is responsible for running its activities. EEFIT is financed solely by membership subscriptions from its individual members and corporate members. Its secretariat is generously provided by the Institution of Structural Engineers and this long-standing relationship means that EEFIT is now considered part of the Institution.

© All material is copyright of the Earthquake Engineering Field Investigation Team (EEFIT) and any use of the material must be referenced to EEFIT, UK. No material is to be reproduced for resale.

This report can be downloaded from www.eefit.org.uk

EEFIT
c/o The Institution of Structural Engineers,
47 – 58 Bastwick St, London EC1V 3PS
Tel: +44 (0)20 7235 4535
Fax: +44 (0)20 7235 4294
Email: mail@eefit.org.uk
Website: <http://www.eefit.org.uk>